THE UNIVERSITY
of EDINBURGH

Spontaneous Small Molecule Migration *via* Reversible Michael Reactions

by

Urszula Lewandowska

Degree of Doctor of Philosophy

School of Chemistry

The University of Edinburgh

February 2013

Table of Contents

Abstract and Layout of Thesis

Small molecule walkers developed to date take advantage of the reversibility of dynamic covalent bond formation to transport molecular fragments along molecular tracks using both diffusion processes and ratchet mechanisms. However, external intervention (the addition of chemical reagents and/or irradiation with light) is required to mediate each step taken by the walker unit in systems reported so far.

In this Thesis, the first synthetic small molecule able to walk back-and-forth upon an oligoethylenimine track without external intervention *via* intramolecular Michael and retro-Michael reactions is described. The 1D random walk is highly processive and exchange takes place between adjacent amine groups in a stepwise fashion. The walker is used to perform a simple task: quenching of the fluorescence of an anthracene group situated at one end of the track as a result of the walking progress. In the presence of excess of base, the molecule preferentially 'walks' towards the favoured final foothold of tracks of increasing length and it is possible to monitor the population of all or a few positional isomers over time. In each case the molar fraction of walkers reaching the final foothold is determined quantitatively by ^{1}H NMR. Control over the rate of exchange is achieved by varying the amount of base added. The dynamic migration of a small molecule upon the track is a diffusion process limited to one dimension and as such can in principle be described using the one dimensional random walk.

Chapter I identifies a set of fundamental walker characteristics and includes an overview of the DNA-based and small molecule transporting systems published to date.

Chapter II describes the inspiration for this work and model studies which lay the groundwork for the research presented in this thesis. The initial track architecture and optimisation of reaction conditions are demonstrated using a simple model compound which then led to the development and a detailed investigation of a first synthetic small molecule able to walk upon an oligoethylenimine track without external intervention.

Chapter III presents a modified synthetic route towards the desired walker-track architectures and a comprehensive investigation of the dynamic properties of a series of tracks of increasing length upon which the walker migrates in a unidirectional fashion.

The Outlook contains closing remarks about the scope and significance of the presented work as well as ideas for the design of novel small-molecule walkers, some of which are well under way in the laboratory.

Chapter II (with the exception of model studies included at the beginning of the chapter) is presented in the form of article that has recently been published. No attempt has been made to re-write this work out of context other than merging content of the article with the supplementary information published together with the article. Chapter II is reproduced in the **Appendix** in its published format.

Declaration

The scientific work described in the present thesis was carried out in the School of Chemistry at the University of Edinburgh between September 2009 and August 2012. Unless otherwise stated, it is the work of the author and has not been submitted in whole or in part in support of an application for another degree or qualification at this or any other University or institute of learning.

Signed:

Date:

Meetings Attended and Presentations Given

1. **Organic Research Seminars**, School of Chemistry, University of Edinburgh, UK, 2009–2011.
    a. Let's make it walk! Dynamic Covalent Rigid Energy Ratchet
    b. Molecular walkers – new mechanisms of moving around

2. **6th International Symposium on Macrocyclic and Supramolecular Chemistry (ISMSC)**, Brighton, July 2011
   Poster presentation: 'A Small Molecule that Walks Non-Directionally Along a Track Without External Intervention'

3. **40th Scottish Regional Meeting of the Organic Division of the Royal Society of Chemistry**, Glasgow, December 2011
   First prize for poster presentation: 'A Small Molecule that Walks Non-Directionally Along a Track Without External Intervention'

4. **School of Chemistry, Organic Section Firbush Symposium**, Firbush Point Centre, University of Edinburgh, UK, April 2012,
   Oral presentation: Molecular walkers – new mechanisms of moving around.

5. **13th Tetrahedron Symposium,** Amsterdam, 26–29 June 2012
   Poster presentation: A Small Molecule that Walks Non-Directionally Along a Track Without External Intervention'

6. **244th American Chemical Society Meeting and Exposition**, Philadelphia, 19–23 August 2012
   Oral presentation: A Small Molecule that Walks Spontaneously to a Specific Site Upon Tracks of Increasing Length '

Acknowledgments

First of all, I would like to thank my supervisor Prof. David Leigh for his support and supervision throughout my stay in his two world-class laboratories. It was a privilege to learn from him how to plan research and assess the results and to then format it into a top-class, well presented paper, filled with great and informative figures.

During my years in The Leigh Group I had the pleasure to learn from the best. I've been very fortunate to come across many excellent chemists who showed great support for my (successful in the end) work. Dr. Araceli Campaña-Gonzales, Dr. Max von Delius and Dr. Kathleen Mullen, who I had the pleasure to work with in Edinburgh, have introduced me to the group routine and shared my research efforts which have filled the pages of this thesis. When being in The Leigh group, one gets to know many stories… No story is interesting without its colourful heroes: Adam (aka Clint), Alan, Alina, Alex, Anneke, Antonio, Augustinas, Barry, Barney, Chris, Chris Martin, Daniel, Dave H, Francesca, Francesco, Guillaume, Jack, Jean-Francois, Jhenyi, John, Jon Beves, Jonathan, Jordi, Kathleen, Kevin, Louise, Malcolm, Marcus, Maria, Marius, Michael, Miguel, Mustafa, Patrick, Paul, Philipp, Stewart, Romen, Steffen, Steve, Tug, Vanessa, Valerie, Victor.

Special thanks go to everyone with whom I had the pleasure to work on various projects in Edinburgh: Angel, Armando, Bea, Craig, Daniela, Jordi, Leo. I would also like to thank Max von Delius, Dave Howgego and Augustinas Markevicius for keeping the HPLC and MS facilities in our group in good condition so they were always at my disposal. Adam Wilson, Bartosz Lewandowski, Miriam Wilson and Sonja Kuschel are acknowledged for maintaining the Leigh group NMR spectrometer and special gratitude goes to Miriam and Bartosz for their assistance with COUNTLESS kinetic experiments, crucial for this thesis. Big thanks to all my peers (Chris, Dave, Marcus and Patrick) who shared all stages of a postgraduate degree with me and special thanks to my bay-mates: Ara, Miriam, Alex, Mustafa, Barney, Armando, Dave, Craig, Jeff, Daniela and Victor for the good sense of humour and great, tidy work environment.

I would like to thank Sarah, Mary and Felicia for being our (un)official group members. Thanks to you, from day one, I felt very welcome in Edinburgh.

I would further like to thank several members of the School of Chemistry staff without who none of this work would have been possible: Annette and Amanda for their help with administrative queries, Martin and Manolo for keeping my claims processed and all the guys in the Stores for doing a terrific job (Derek, Tim, Raymond, John).

During my PhD I was privileged and lucky in many instances. I could work alongside Bartosz, who motivates, supports and understands me in professional as well as private matters. Thank you for these, sometimes intense, three years in Edinburgh. We did it!

Finally, I would like to thank my parents, Daria and Stefan Zomkowscy, who continued to support me on the path that I have chosen. It’s proven to be long but a beautiful one.

List of Abbreviations

AFM	atomic force microscopy
aq.	aqueous
ATP	adenosine-5'-triphosphate
Boc	*tert*-butoxycarbonyl
bp	base pair, base pairs
calcd.	calculated
Cbz	carboxybenzyl
CD	α-cyclodextrin
δ	chemical shift
E	(entgegen); opposite
ESI	electrospray ionisation
equiv.	equivalent
DCC	dynamic covalent chemistry, also dynamic combinatorial chemistry
DNA, DNAs	desoxyribonucleic acid, desoxyribonucleic acids
DMF	*N,N'*-dimethylformamide
DMSO	dimethylsulfoxide
h	hour, hours
HRMS	high resolution mass spectrometry
HS	high speed
HJ	Holliday Junction
LRMS	low resolution mass spectrometry
m.p.	melting point
MS	mass spectrometry
nm	nanometer, nanometers
NMR	nuclear magnetic resonance
PEG	polyethylene glycol
ppm	part per million
RNA	ribonucleic acid

RT	room temperature
STM	scanning tunnelling microscopy
THF	tetrahydrofuran
TLC	thin layer chromatography
UV	ultraviolet (light)
Z	(zusammen); together

Note: conventional abbreviations for units and physical quantities are not included.

Chapter I

Synthetic Molecular Walkers

ACKNOWLEDGMENTS

Dr. Bartosz Lewandowski is gratefully acknowledged for proofreading the entire manuscript.

Dr. Guillaume De Bo is gratefully acknowledged for proofreading **Chapter I**.

Dr. Araceli G. Campaña is gratefully acknowledged for proofreading **Chapter II** and **III**.

Miriam R. Wilson is gratefully acknowledged for inspecting the manuscript for formal mistakes.

1.1 Synopsis

In biology, molecular motors have evolved to overcome Brownian motion and perform specific tasks. Among cytoskeletal motor proteins, kinesins ensure directional transport of cargoes to the periphery of the cell by the means of taking steps upon microtubular tracks. In the past decade we have witnessed an increasing interest in the development of molecules which could mimic some aspects of their dynamics, which has become a starting point in the creation of artificial transport systems.

To date, both DNA and small molecule walkers have been developed, each taking advantage of the technology available to them. DNA strollers are based on the rules of base pairing and strand displacement reactions. They have evolved from systems in which sequential addition of fuel is required to perform walking to fully autonomous systems, capable of performing complex tasks as well as sequential chemical reactions. Small molecule walkers developed to date take advantage of the reversibility of supramolecular interactions as well as the variety of dynamic covalent bonds to transport molecular fragments along surfaces and molecular tracks using both diffusional processes and ratchet mechanisms.

1.2 Introduction

Since the advent of supramolecular chemistry there has been a keen interest in the fabrication of multicomponent systems capable of acting as molecular machines or motors. Utilizing fundamental concepts such as pre-organisation, molecular recognition [1] self-assembly[2] and template directed[3] synthesis has resulted in a dramatic increase in the variety of molecular devices[4] such as switches[5], rotors[6] and ratchets.[7] Nevertheless only a few artificial systems display characteristics that mimic the elegant complexity of motor proteins. Motor proteins are molecular machines which convert chemical energy obtained from the hydrolysis of ATP into mechanical work used to power cellular motility. [8] They participate in a wide range of processes that occur in cells, such as cell division, vesicle and organelle transport and organelle synthesis. [9] Particularly intensively studied are the families of cytoskeletal motor proteins: myosins, that act upon actin filaments, as well as kinesins and dyneins which can move along microtubules, transporting vesicles and organelles within cells. [10] Each of these superfamilies is populated with numerous distinct members that perform different cellular roles, and therefore have great diversity in their properties. The kinesin motor family is large, but it is kinesin I motor protein[11] that was found to move both unidirectionally and processively taking over 100 steps without detaching from the microtubule track. As this mode of action is reminiscent of a walking process, kinesin I may be called a 'molecular walker' and is therefore a direct inspiration for scientists attempting to create synthetic walking molecules.

1.2.1 Requirements for Walking Molecules

When designing a molecular walking system one has to consider many issues, including the structure of the walker and the track as well as their interactions at the points of contact (see Figure 1). For *processive* migration it is essential that the walker remains associated with the track at all times. This means that feet - track connection points need to be orthogonal or the structure of the walker unit must prevent it from diffusing away from the track. This processivity as well as the control over the direction of walking (*directionality*) are the key requirements that need to be fulfilled in the development of synthetic analogues of biological walking motors. Other requirements include *progressive* (work performed cannot be undone), *repetitive* operation (mechanical cycle can be repeated) ideally in an *autonomous* fashion (walking is taking place without external intervention as long as the fuel is available).[12] Constructing a synthetic molecular walker which fulfils all the above requirements is a challenging task. However, scientists have been successful in designing DNA and small

molecule systems which achieve several of these requirements. Several examples are presented below.

1.2.2 Mechanically Interlocked vs. Non-Interlocked Structures

When considering structural requirements for a system in which translocation of one component with respect to another could take place without losing its structural integrity (processivity), mechanically interlocked structures like rotaxanes or catenanes come to mind (Figure 1a, b, respectively). The possibility of restricting the degrees of freedom of relative motion by interlocking the components of a functional molecule has led to the development of many switches[5] and a few motors.[6,7]

A hypothetical system based on a track threaded through a walking unit consisting of two linked macrocyles in which the affinity of macrocycles to the consecutive complementary binding sites would be changed sequentially could achieve directionality while displaying the inherent processivity (Figure 1, c). The most obvious of the limitations of such systems is that a threaded ring cannot move upon branched structures thus selection between alternative pathways would be impossible (Figure 1d).

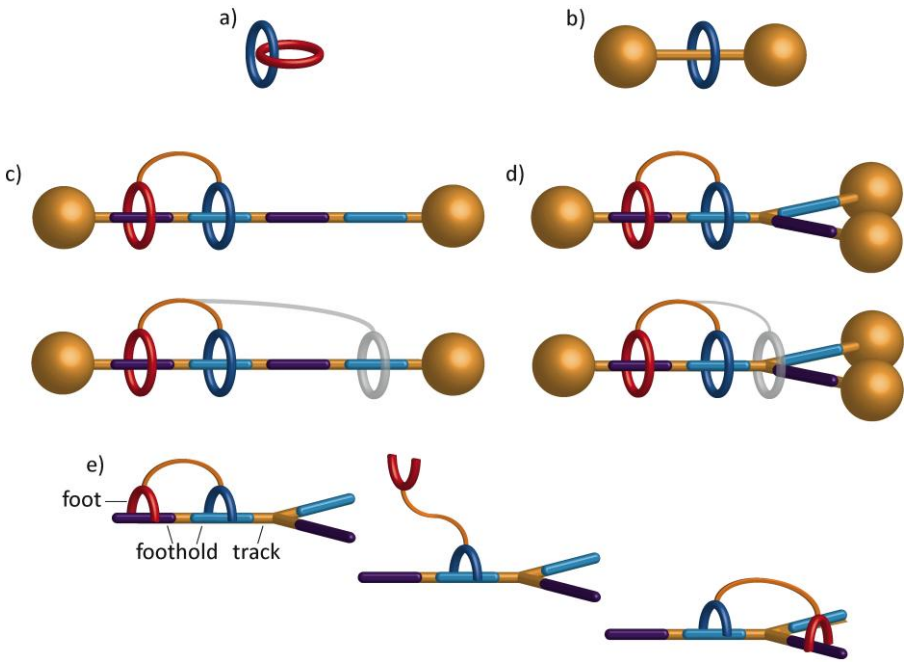

Figure 1. Schematic illustration of mechanically interlocked molecules: a) [2]catenane and b) [2]rotaxane. c) In a [3]rotaxane based walking molecule featuring complementary binding sites for rings on the thread an application of appropriate chemical or physical stimuli which would alter the chemical structure of the ring or thread can induce directional ring migration to the next binding site in a compartmentalised system. d) Ring in a branched [3]rotaxane based walking molecule cannot pass a junction. e) A molecular walker based on a non interlocked structure can, in principle, choose between alternative pathways.

Lack of an interlocked structure which restricts the degrees of freedom of a hypothetical macrocycle - based walker with respect to the threaded track brings new points for consideration as processivity needs to be carefully addressed. In the microscopic world molecular motors operate at low Reynold's number so motion is dominated by stochastic processes like random thermal motion and viscous forces.[13] Therefore, in the synthetic design we must include features of the architecture of the track which allow for the migration of the walking molecule (Figure 1e). Points of contact between a walker ('foot') and a track ('foothold') must be kinetically stable whilst being dynamic under operation conditions. Finally, the mechanism of migration and synthetic design of the walker - track conjugate must ensure that both components have at least one point of contact at all times which can be achieved by designing a walker with two (or more) orthogonal feet - track interactions. This way each of the feet could be addressed independently. Another possibility is to implement a walker design in which although the feet are identical, the detachment is mechanistically impossible or disfavoured.[12,14]

1.2.3 Mode of Migration

The migration of a bipedal walker may occur according to two fundamental mechanisms.[15] In an inchworm mode the leading foot detaches first from the track and steps forward. The trailing foot follows the leading foot at all times and the relative order of the feet during migration remains unchanged (Figure 2, left pathway). In passing leg, also known as hand over hand mode, the trailing foot detaches first from the track and steps forward, interchanging with the leading foot (Figure 2, right pathway). By carefully designing walker - track interactions both walking mechanisms could become a principle of a novel transport system.

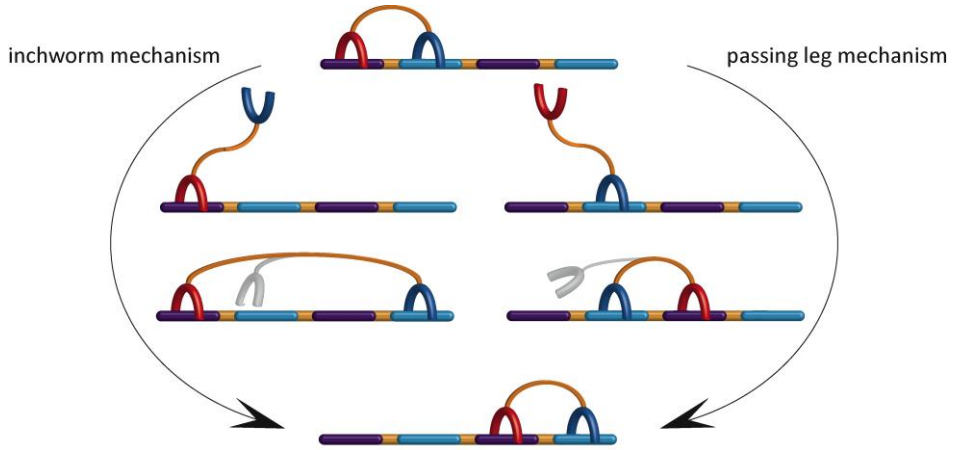

Figure 2. A molecular biped with two feet can walk along a track in two fundamental ways: inchworm, where one foot is always leading and hand-over-hand (also know as a passing leg gait), where feet exchange leading and trailing positions.

1.3 DNA Strand Displacement as a Tool for DNA Nanotechnology.

Since the advent of DNA-based walking molecules in 2004, strand displacement reactions and their cascades [16] have led to the development of non-autonomous and autonomous walking systems capable of performing complex tasks like cargo transportation [17] or sequential chemical synthesis.[18]

In a prehybridized DNA duplex the exchange of one strand with an external strand can be initialized by its hybridisation to a single stranded toehold region (Figure 3). The free energy of the formation of new base pairs makes the invading strand thermodynamically preferred. Let us imagine a system in which two DNA duplexes located on a rigid base are connected by an unreactive, flexible linker to form a large macrocycle. Using the toehold mediated strand displacement process it is possible to design an invading strand which reacts with only one of the duplexes (Figure 3). The exchanged single strand becomes a 'searching strand' ready to rebind at suitable position when an anchorage and an anchor strand is available but at the same time it remains attached to a rigid base by a linker through a stable holding duplex. Many walking devices have been designed based on such toehold initiated strand displacement processes.

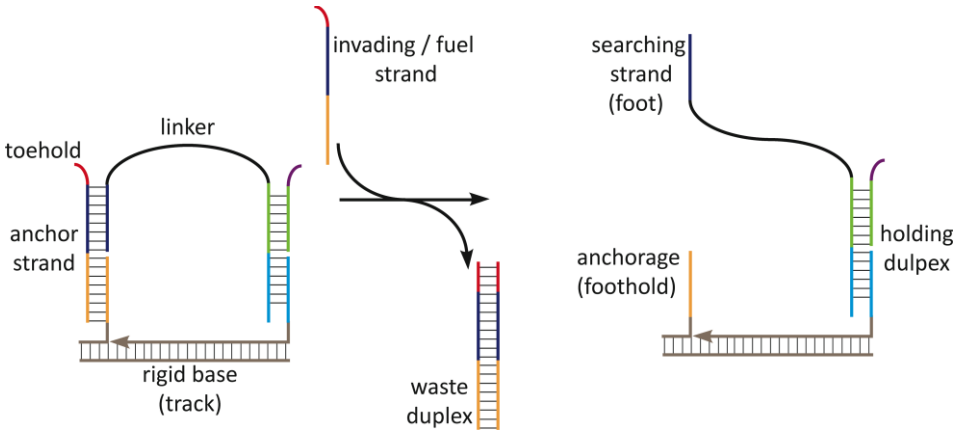

Figure 3. Schematic representation of a strand displacement process in which one of walker's feet is released from an anchor site by an invading stand which first attaches to a toehold section to yield a waste DNA duplex and an unbound foot ready for the rehybridisation. Lines indicating base pairing do not represent a particular number of bases.

1.4 Non-Autonomous DNA Walkers

Fascinating examples of bipedal DNA-based walking systems developed in the last decade utilise the elegant idea of controllable and programmable complementarity. They include non-autonomous walkers which move according to an inchworm [19] or passing-leg mechanism[20] and use a sequential addition of invading and anchor strands in order to move directionally, processively and progressively along a short track.[12]

Recently, this toehold-mediated branch migration method has been extended by Seeman and co-workers beyond a biped to a walker with a single stranded stator foot as a part of a rigid triangular core which features three flexible four-arm junctions that provide additional six single stranded motifs (see Figure 4, a).[17] Three of them are 'feet' which bind to the track together with a stator 'foot' in order to adopt a conformation which allows the remaining three single stranded 'hands' to selectively pick up a cargo. Release of a gold nanoparticle onto a walker is only possible when they both reside in a suitable proximity and the DNA machine holding a cargo is in a deshielded 'ON' state (see Figure 4, b and c). This triangular walking molecule is designed to walk upon sequential addition of invading and anchor strands and turns 120° each time it takes a step (Figure 4, d). In this work, Seeman *et al*. have moved DNA walking devices away from a one dimensional track architecture and used the framework of a DNA origami tile.[21] This large surface (more than 100 nm x 200 nm) allowed for precise spatial arrangement of 18 single stranded footholds serving as the track for the walker as well as the positioning of three slots in which three shielded cassettes (DNA machines) holding DNA bound gold nanoparticles were located (see Figure 4, b). Scientists have demonstrated the ability of selectively programming eight different products of cargo binding as well as good to excellent yields (up to >90%) of the designed operations.

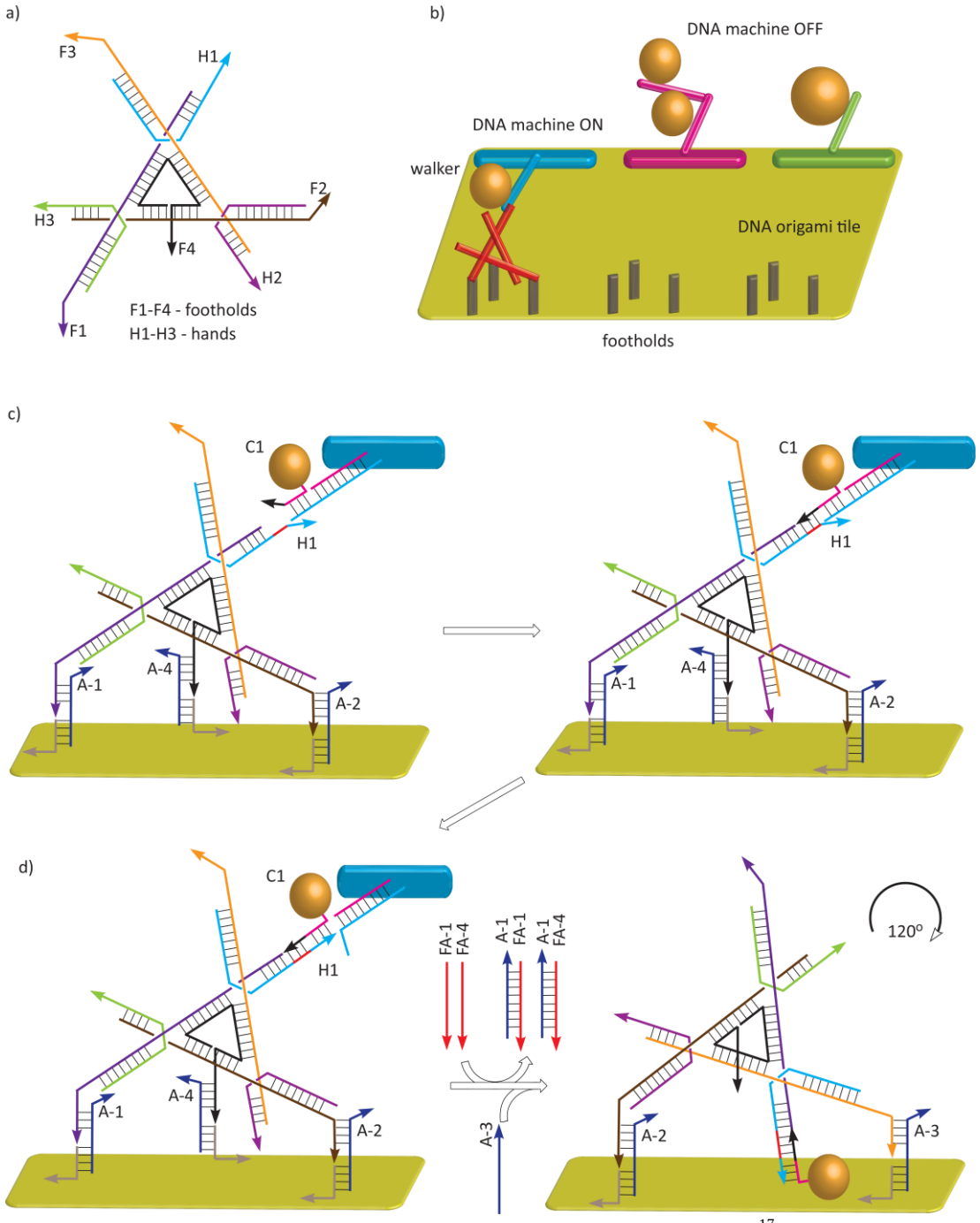

Figure 4. Details of DNA based system published by Seeman and coworkers.[17] a) Structure of the walker featuring seven single-stranded domains: four feet (F1 to F4) and three hands (H1 to H3). b) Basic components of the assembly line, consisting of a large DNA origami tile (track), three ON–OFF DNA machines which carry three different DNA-bound gold nanoparticle cargoes; triangular walker moiety. c) Cargo transfer and one 'stride' of the walker unit. The DNA machine in an ON state brings the arm (with a gold nanoparticle on) close to H1, allowing the black and red toeholds to bind together and d) branch migration transfers the cargo strand onto the walker (H1). The addition of two fuel strands (FA-1, FA-4) undoes binding of F1 and F4 and sequential addition of one anchor strand (A-3) induces rotation of the walker by 120° and rebinding on the track. Lines indicating base pairing do not represent a particular number of bases.

1.5 Autonomous Migration

A real breakthrough leading to the development of directional and autonomous DNA walkers came with an idea that toeholds needed to initialize the strand displacement process (Figure 3) could stay temporarily masked as loop domains, for example, in DNA hairpins[22] or two strand complexes[23] and be revealed gradually as a result of previous processes in the operation cycle.

In 2009, the introduction of sterically shielded regions[24] and the coordination of feet action by the use of signalling single strands[25] which provide an incoming fuel hairpin strand with an open binding site, allowed directionality to be achieved in the first autonomous walking systems based solely on a branch migration processes. Programmable, autonomous molecular device moving DNA fragments along a branched track have recently been described by Turberfield and co-workers [26] who have developed a system in which directionality is achieved by utilising the information embedded within fuel hairpins and the track's architecture (see Figure 5). F_x^y fuel hairpin holds an active anchorage address (X_1,X_2) from which the cargo is to be received, a sequestered fuel loop ($\bar{y}$) directing the cargo to the next anchorage **Y** and a $\bar{Y}_1$ domain (complimentary to the removal strand located on the adjacent anchorage, carrying both, y and Y_1 domain). First, a split toehold (a, X_1X_2) mediated hybridisation of a fuel hairpin leads to the formation and migration of a complete, four arm Holliday Junction (**HJ**) which reveals (masked in a fuel loop) the destination domain ($\bar{y}$) and forms a new split toehold ($\bar{y}$, c). Now a second four arm **HJ** is formed by the hybridisation of the matching single stranded domains on **X** and **Y** and after the second **HJ** migration the cargo strand is transferred to the **Y** anchorage while the removing strand has moved backwards, formed a duplex with a fuel hairpin and the **X** and deactivated both. Only after the first cargo transfer is complete, the new active address domain ($\bar{Y}_1\bar{Y}_2$), complimentary to F_y^z fuel hairpin is revealed and junction migration takes place again, uncovering the address domain $\bar{z}$ which can be used to move the cargo further from **Y**. Directional transport of DNA cargo is possible upon a sequential or simultaneous additions of F_x^y and F_y^z fuel hairpins. However, no hybridisation takes place when only F_y^z is present (Figure 5). This autonomous operation is possible by controlling the sequence in which split toeholds are released. It was possible to programme the movement of the DNA strand cargo along a branched track by a simultaneous addition of fuel hairpins containing information about the direction of transfer (left or right) between the alternative anchorages (see Figure 6). More recently, the same group has demonstrated the ability to signal (left or right) the direction of the DNA strand cargo movement by a small molecule (adenosine) which induces blocking or unblocking of available directions in a hairpin fuelled branched transport system.[27]

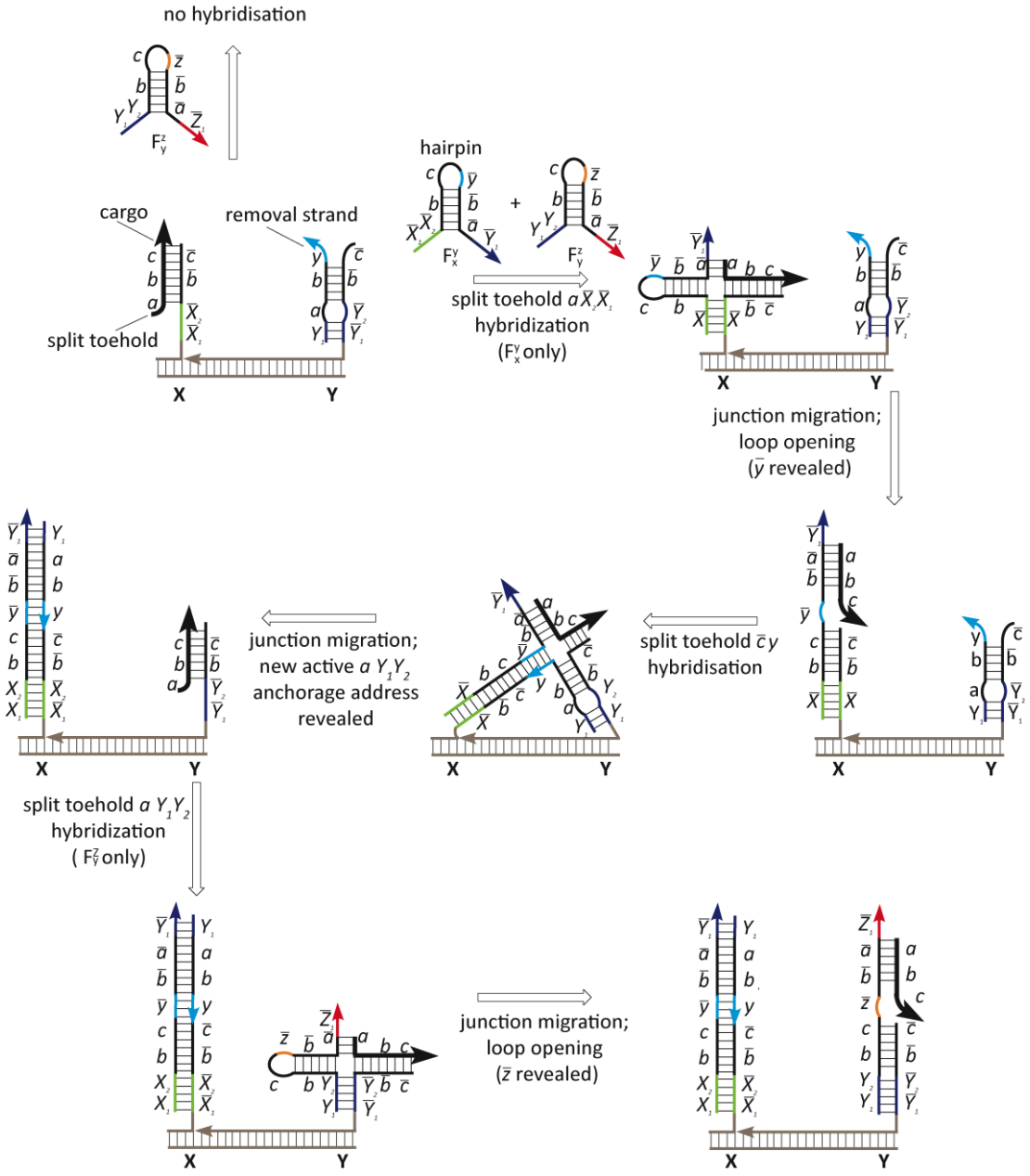

Figure 5. Autonomous cargo migration between adjacent anchorages.[26] The track consists of anchorages equipped with addressable domains. Anchor site bound with the cargo strand has an active address domain $\bar{\boldsymbol{X}}_\mathbf{1}\bar{\boldsymbol{X}}_\mathbf{2}$, while $\bar{\boldsymbol{Y}}_\mathbf{1}\bar{\boldsymbol{Y}}_\mathbf{2}$ in the adjacent anchorage is blocked with the removal strand. Out of two present fuel hairpins, only $\boldsymbol{F_x^y}$ and not $\boldsymbol{F_{\bar{y}}^z}$ binds to the split toehold created by the cargo-anchorage duplex, forming a four arm Holliday junction which after junction migration leads to the opening of the fuel hairpin loop and displacement of the cargo from source anchorage **X**, leaving it attached to the track through the fuel strand. The destination address domain $\bar{\boldsymbol{y}}$ is active after opening the fuel loop and an interaction between the fuel-cargo duplex and the split toehold on the adjacent destination anchorage **Y** forms a new Holliday junction. Junction migration effects transfer of the cargo to adjacent anchorage **Y**. A waste product, consisting of the fuel strand $\boldsymbol{F_x^y}$ and removal strand, is left on anchorage **X** and blocks backward motion. The new complex between cargo and anchorage **Y** displays the new source address $\bar{\boldsymbol{Y}}_\mathbf{1}\bar{\boldsymbol{Y}}_\mathbf{2}$. Fuel hairpin $\boldsymbol{F_{\bar{y}}^z}$ now binds to the split toehold created by the cargo-anchorage duplex, forming a four arm **HJ** capable of initiating the next step. Lines indicating base pairing do not represent a particular number of bases.

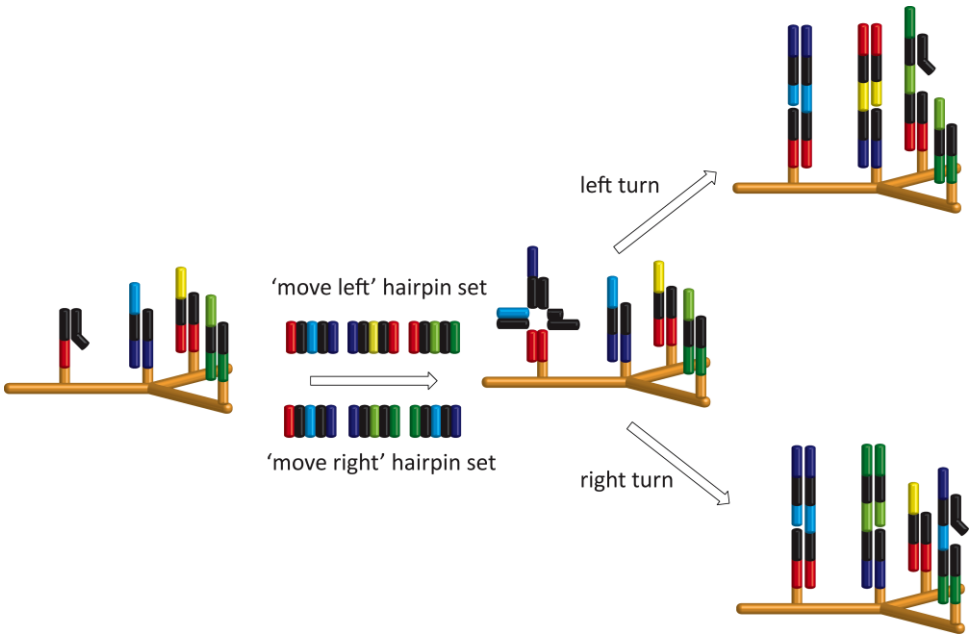

Figure 6. Programmed motion at a junction.[26] Depending on the selected set of fuel strands, the cargo can be sent to either left or right arm of the junction. All three fuels required for the desired migration direction across the junction are added simultaneously to the cargo-track conjugate. The cargo is first moved to the junction point and then beyond the junction, in either direction depending on the fuel hairpins selected.

1.5.1 Enzyme-Mediated Autonomous Migration

Directional, autonomous motion of DNA fragments was first achieved in 2004 by the use of restriction enzymes which could selectively recognise the position of the walker on the track and either detach the walker completely from one of two footholds[28] or cut off a short fragment of the walker-bound foothold, so the reattachment of the DNA fragment at the adjacent anchorage would become favourable and irreversible.[29] So far, the most advanced use of this methodology was unidirectional migration of a single strand of DNA (a cargo) upon a track consisting of 17 complimentary foothold strands separated by 6 nm from each other published by the Turberfield group.[30] The track was engineered diagonally on a DNA origami tile measuring approximately 100 nm x 70 nm and designed so the nicking restriction enzyme could recognise and cut the anchor single strand of the cargo-anchor duplex (Figure 7).

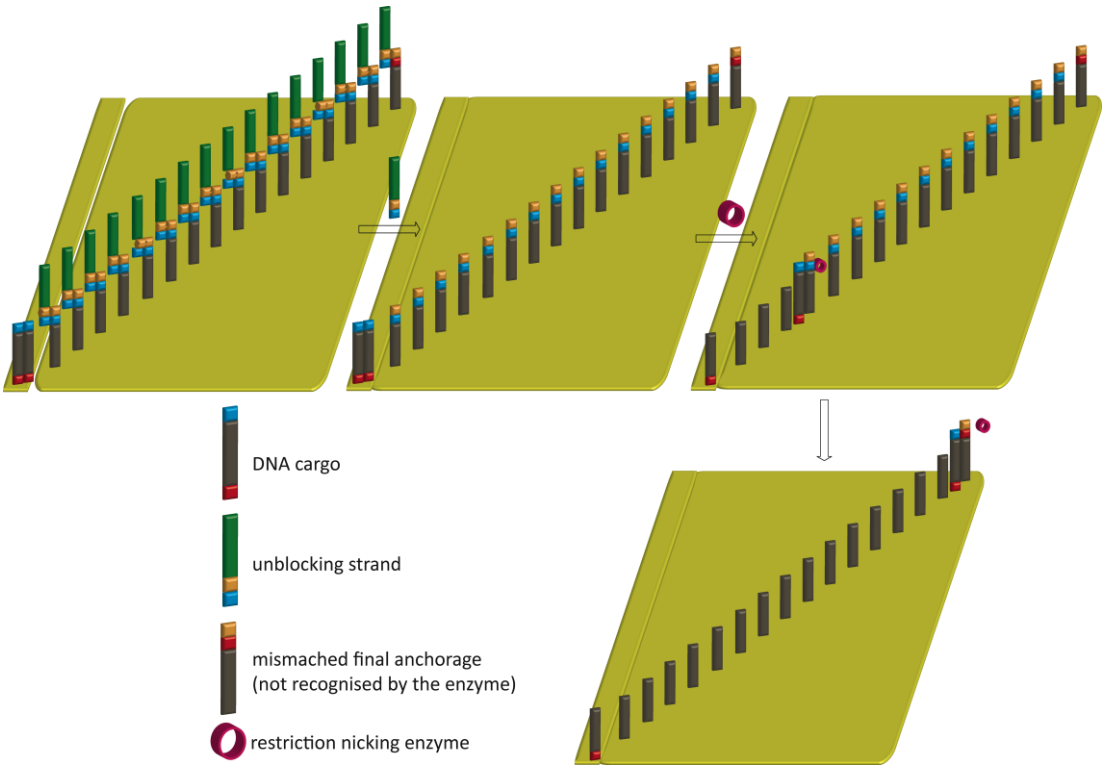

Figure 7. Schematic representation of the DNA cargo migration upon a DNA origami tile bearing single-stranded stators which form the track.[30] The cargo carrying duplex is precisely positioned on the origami tile thanks to its addition to the track in the last stage of the assembly process. Release strands remove the blockade and after incubation the nicking enzyme recognises and cuts the stator strand of the cargo-stator duplex. A toehold that facilitates strand transfer to the adjacent intact stator is now revealed and branch migration takes place in order to transport the cargo strand towards the last stator with modified sequence. Mismatch in the final duplex protects it from the enzyme and traps the DNA cargo at the end of the track.

To avoid spontaneous transport from occurring and to keep the integrity of the system before operation begins, a small piece of DNA origami tile with a cargo holding duplex (which contains two additional base pairs (bp)) was attached in the final stage of the assembly to a tile consisting of 16 anchorages protected with blocking strands. After unblocking the footholds with release strands, the walker-track conjugate was incubated with the enzyme and a unidirectional stepwise motion towards the end of the track was monitored with the use of fluorescence. In this system, the energy released during the consumption of the track drives the movement between the footholds. After the anchor is cut, moving backwards is disfavoured due to the irreversible changes in the track's structure which imposes the directionality and defines the mechanism as 'burnt bridges' walking.

Migration of a DNA cargo in a modified system was also monitored using high-speed atomic force microscopy (HS AFM).[31] In this case, blocking strands were not used before the assembly, therefore at the start of the operation only 45% of walker units were located at the first foothold while the rest were distributed along the track. After 3 h of

incubation the cargo strand was found predominantly bound to the last foothold (35%). The sequence of this final anchorage has been modified to create the mismatch in the duplex formed and prevent it from being recognized by the enzyme.

Incorporation of catalytic nucleic acids (DNAzymes) into the walker structure led to the development of autonomous bi- and tripedal walking systems which can move along a predefined track on a surface[32] and perform tasks, like a multistep organic synthesis.[18] The walking unit in such a system was shown to act like an enzyme and to sequence specifically cleave RNA nucleotides (Figure 8, blue dot). As the molecule destroys the track, it moves exclusively forward towards the more complimentary adjacent foothold *via* toehold-mediated branch migration (Figure 8).[33]

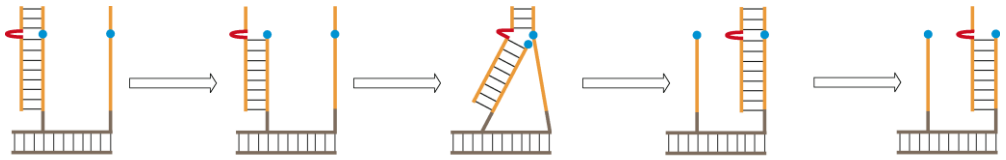

Figure 8. Operation principle of autonomous 'burnt-bridges' walking mediated by a DNAzyme (red loop) in the walker unit. The DNAzyme walker consumes all footholds carrying the recognition site (blue region) which it binds to. After cleavage, a short piece of the track dissociates and a toehold which mediates the walker's migration to the adjacent foothold is formed.[33] The final foothold is also hydrolysed. Lines indicating base pairing do not represent a particular number of bases.

Apart from simple single stranded walkers, more complex four-armed structures have been reported.[32,34] The spider walker with three single stranded DNAzyme legs and one arm used to precisely position the walker on the track all attached to an inert streptavidin core, it has been shown to walk along a surface of a DNA origami along a predefined trajectory and be able to follow turns in the track.[32] After being activated with the trigger strand, each of the 'spider' legs cleaves the foothold which it is associated with at an RNA base site (blue part of the foothold strand, Figure 9) incorporated into a DNA foothold. The walker binds significantly stronger and resides much longer on the substrate footholds (before RNA base cleavage) in comparison with the shorter product foothold which means that the three legged device achieves good processivity as the probability of at least one of the three legs being bound to the track is high. As a result, the walker's legs move preferentially towards the area of the track rich in non-cleaved footholds until the molecule reaches the footholds in which the RNA site is not incorporated. The spider's DNAzyme legs cannot cleave such substrates (Figure 9, red part of the foothold strand) so the walker unit is thermodynamically trapped at the end of the track.

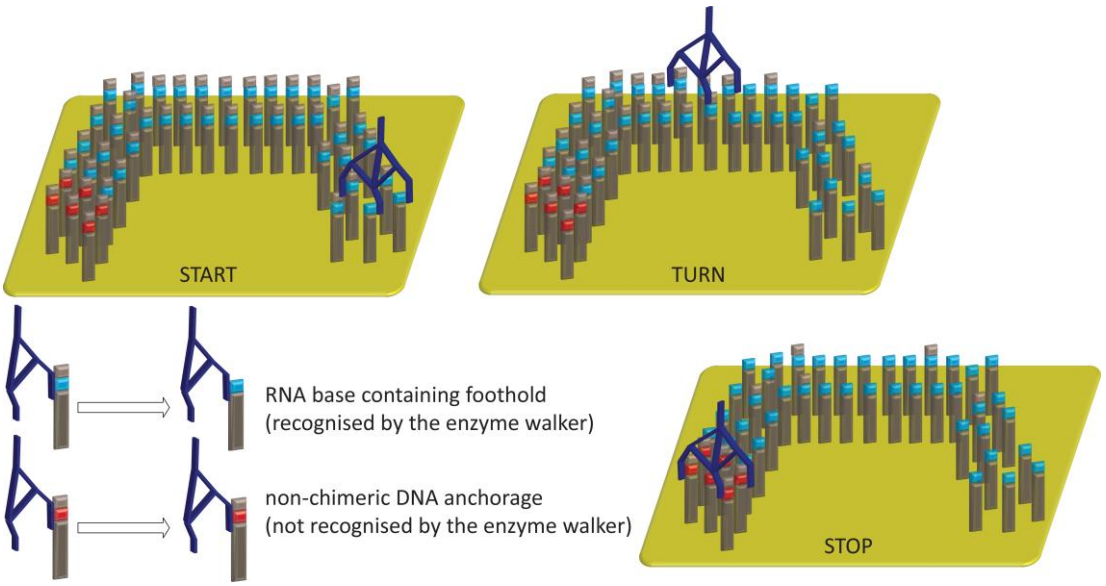

Figure 9. A walking spider with three DNAzyme legs that displays autonomous migration on a DNA origami landscape.[32] A molecular spider built from an inert streptavidin body, three DNAzyme feet that can cleave RNA substrates and one capture leg which is used to position the spider on the origami tile cleaves foothold strands of a foot-foothold duplex at an RNA base (blue). The spider walker follows the path as determined by the foothold sequence (including turns) and reaches 'STOP'-footholds lacking the RNA base (shown in red) which are not recognised (not cleaved) by DNAzyme.

Moving directionally along predefined surfaces was not the only task performed using autonomous walking systems. One of the most challenging tasks which chemists and biologists try to mimic is the ability of natural molecular machines to manufacture other molecules.[35] An autonomous walker able to move along the track and perform sequential amine acylations by reading the information embedded in the track has been reported by the Liu group.[18] A DNAzyme walker equipped with a free amine is bound to the first out of four spatially separated footholds in the track. Three footholds are loaded with unnatural amino acids (yellow, green and purple sphere) activated as *N*-succinimide esters (Figure 10). After the walker's migration to the adjacent foothold due to the close proximity of both substrates, acyl transfer of a first (yellow) amino acid building block onto the amine occurs. Next, hydrolysis of the RNA site of the foothold by the DNAzyme walker occurs. The cleavage step was designed to be much slower than the acyl transfer to ensure sequence selectivity of the synthesis. After dissociation of the short, hydrolysed fragment of the second foothold, the device carrying one amino acid building block can move to the third foothold *via* strand displacement. This migration - acylation - foothold cleavage - dissociation sequence is repeated two more times leaving walker which has synthesised a triamide attached to the fourth foothold.

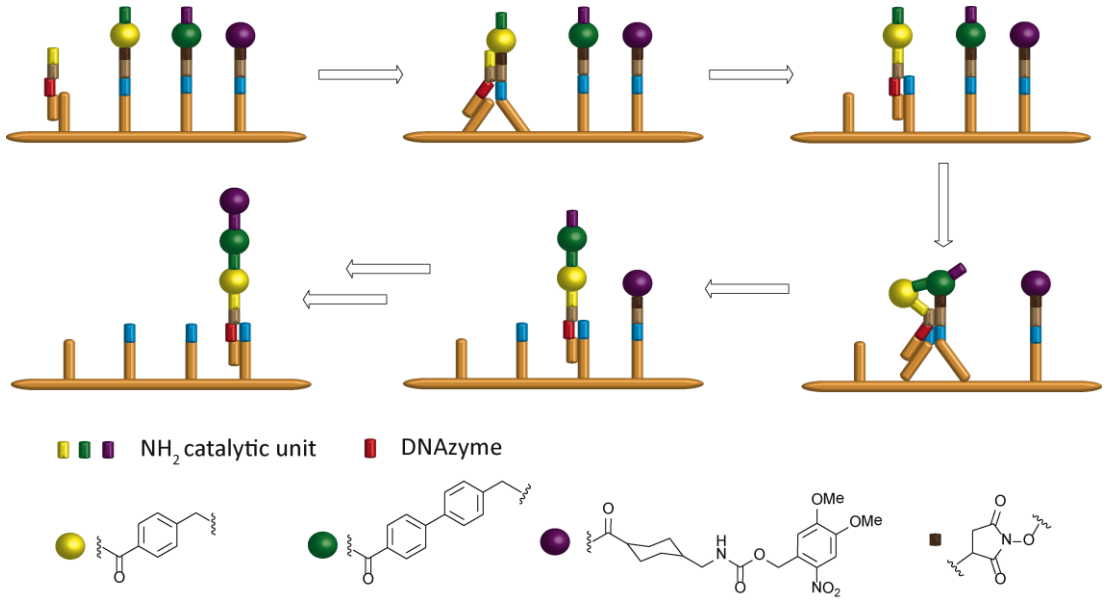

Figure 10. An autonomous molecular walker capable of performing consecutive intramolecular acylation reactions.[18] Schematic illustration of the operation sequence of the device. DNAzyme walker equipped with an amino group migrates between adjacent footholds and due to the close proximity of the substrates the transfer of acyl building blocks occurs. DNAzyme mediated hydrolysis of the track forms a short toehold region which mediates the walker migration to the adjacent foothold.

1.6 Light Induced Chemical Processes in DNA Walkers

DNAs offer programmability and robustness which allowed for the design of many impressive walking devices capable of moving upon branched tracks, performing synthesis and transporting cargoes. However, autonomous walking devices often face a limited degree of control. Once triggered, they usually cannot be stopped and either lack directionality[34] or move only in one direction as a result of consuming the track behind them.[18,30,33]

In 2012 a simple example of incorporation of a chemical reaction into a DNA walking device in order to regulate an autonomous migration was presented.[36] It utilises a pyrene moiety incorporated into a walker unit and four identical foothold strands which are built from two segments connected by a disulfide bond (Figure 11). The formation of a walker-foothold duplex brings the pyrene moiety and the disulfide bond close together. Irradiation at 350 nm triggers pyrene sensitised photolysis of only the neighbouring disulfide, followed by dissociation of the cleaved foothold segment, leaving the walker bound to a shorter anchor site. As a result, the walker migrates to the adjacent, longer foothold *via* a toehold-mediated branch migration process and remains bound there until the next sensitised disulfide photolysis takes place. Upon continuous irradiation less than 40% of walkers reached the end of the four foothold track according to the 'burnt bridges' mechanism.

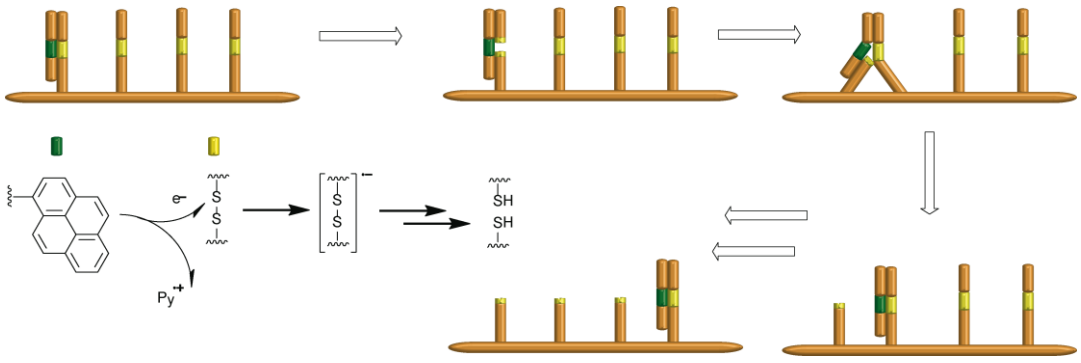

Figure 11. Schematic representation of an autonomous molecular walker which enables pyrene-assisted photolysis of a disulfide bond incorporated into a foothold strand of a walker-foothold duplex. Dissociation of a short piece of the track forms a short toehold region which mediates migration of the walker unit (which carries the pyrene moiety) to the adjacent foothold.[36]

Another example of a controllable autonomous walking device able to walk up and down a track as a result of a chemical process is a system in which a walker unit is hybridised to the first out of three adjacent footholds of increasing complementarily (Figure 12).[37] However, the second and third footholds have azobenzene moieties incorporated into the DNA sequence which lowers the binding affinity and makes duplex formation disfavoured when in the *Z* conformation. Upon visible light irradiation (ca. 465 nm) *Z*→*E* isomerisation takes place, spatial hindrance between the complimentary base pairs is removed and the migration of the walkers towards the longest complimentary anchor site (third footohold) can take place. As the azobenzene isomerisation is reversible and no damage to the track is imposed by the walker migration, upon UV light irradiation (ca 365 nm) *E*→*Z* isomerisation takes place and the walker is able to reuse the track and move back to the starting and now least disfavoured position. Directionality in this system depends on the photostationary states of azobenzene isomerisation and as such walking backwards (from third to first foothold) after more troublesome *E*→*Z* isomerisation is less efficient than the forward walking (after *Z*→*E* isomerisation).

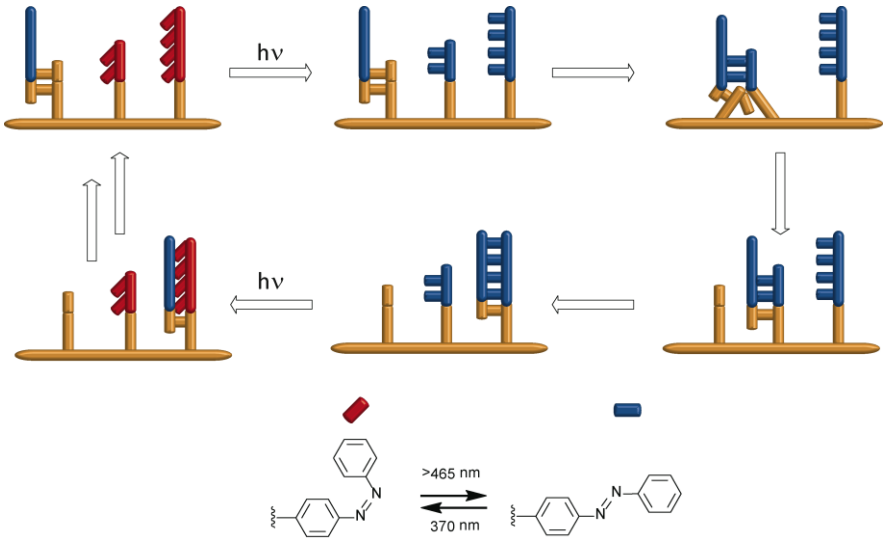

Figure 12. An autonomous migration of a DNA walker in both directions upon a three foothold track depends on the conformation of azobenzene moieties incorporated into DNA foothold strands.[37] Upon visible light irradiation, ***Z*→*E*** isomerisation removes the spatial hindrance between the complimentary base pairs and the walker migrates to the third foothold based on a toehold mediated strand displacement. After ***E*→*Z*** isomerisation the reverse process takes place.

1.7 Synthetic Small Molecule Walkers

Although there are a number of chemical reactions featuring migration of intact molecular fragments, only a few allow for the development of reaction cycles on which processive migration of molecules along tracks or surfaces could be based.[12] In purely synthetic walking devices no technology like programmable complementarily is available, therefore the dynamic foot-track interactions, processivity and directionality must be inferred by the designed, orthogonal processes and/or reactions which, when brought together, yield a stimuli responsive, functional, intact structure.

1.7.1 Diffusion as a Mechanism for Small Molecule Migration

In 2004, the Bartels group used scanning tunnelling microscopy (STM) techniques for the investigation of the diffusion of a small molecule upon a Cu(111) surface restricted only to the high symmetry [$\bar{1}$10] axes. First, 9,10 dithioanthracene (DTA) was shown to migrate linearly in a fashion reminiscent of a biped gait.[38] In the initial position (Figure 13, left), the aromatic core of DTA is perfectly parallel to the high symmetry direction, maximising interactions of the π system with the surface. As a result of the walker's geometry as well as the periodic character of the surface, both feet occupy different adsorption sites. Foot **A** resides in a high energy close-to-top position while the **B** foot occupies a more favoured site, where a sulfur atom bridges two copper atoms. At 50-70 K a small twist around **B** (residing

in a low energy site) brings both feet to a favourable near bridge position while the aromatic core is forced out of the favourable, parallel to [$\bar{1}$10], alignment. This movement can take place either back or forward and lacks directionality, but if at random the next step sees the sulfur feet again transferred forward, we can observe directional diffusion of a small molecule upon a Cu(111) surface.

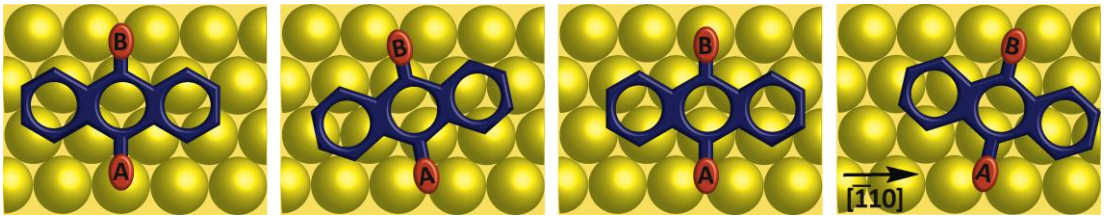

Figure 13. A proposed one-dimensional non-directional diffusion migration mechanism of DTA upon a high symmetry Cu(111) surface at 50 K based on DFT calculations.[38] Rotation around a sulfur atom which occupies a low energy site (bridging two copper atoms) brings both feet into favourable positions. The aromatic core however is forced out of a perfect alignment with a high symmetry direction. This orientation is only observed in experiments conducted at 10 K, where thermal movement of DTA is not observed.

The migration of an antraquinone (AQ) molecule [39] (following a mechanism analogous to DTA) along a high symmetry direction upon a Cu(111) surface was also investigated using STM. AQ was shown to reversibly attach and carry a CO_2 molecule which exhibits surface-mediated attractive interactions with the walker's oxygen atoms (Figure 14). While upon binding of the first cargo the diffusion velocity decreases by more than half (diffusion barrier increases from 23 meV to 57 meV), the second cargo attachment process slows the walking only by additional 20% (diffusion barrier rises to 73 meV).

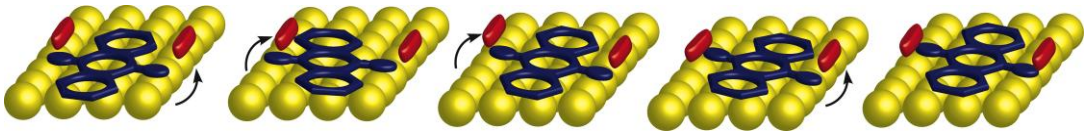

Figure 14. Schematic representation of the attachment of a CO_2 molecule during the diffusion of an AQ molecule along the substrate high-symmetry direction by means of individual steps taken by sequentially moving either one of the two oxygen feet.[39]

This methodology was extended to a pentaquinone (PQ) and pentacenetetrone (PT) molecules which have been investigated in sequences of STM measurements. [40] They revealed that with the increasing number of aromatic rings and/or oxygen feet, the rate of diffusion decreases but the direction of migration is still indicated by the elongated aromatic core. More insights into the mechanism of migration were provided, proving that pacing (moving two feet located on the same side of the aromatic core at once) is the mode of walking for the quadrupedal PT.

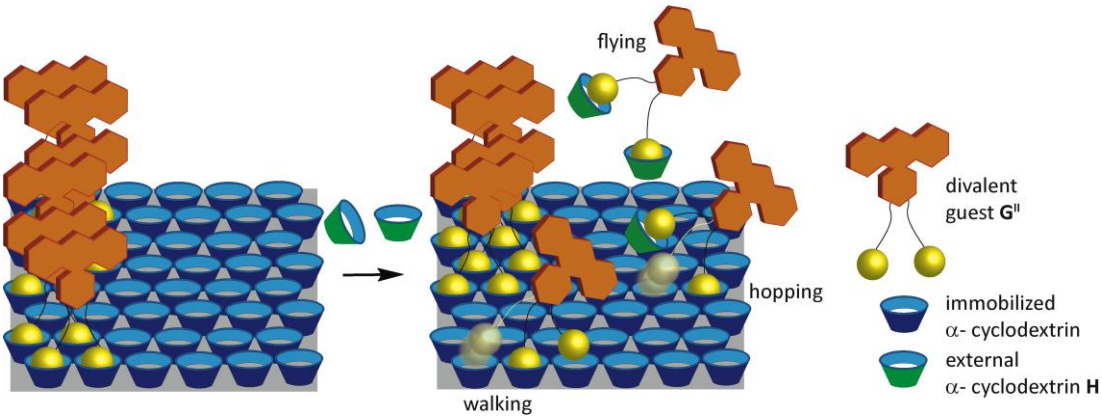

Figure 15. Cartoon representation of the basic mechanisms involved in the divalent surface diffusion.[41] The divalent, adamantane functionalised guests were assembled onto a α-cyclodextrin (CD) functionalised monolayer *via* microcontact printing. Spreading rates of 'bipedal' guests were then followed using fluorescence imaging in pure water (spreading mainly due to walking events) and in water with the increasing concentration of competitive CD hosts (by interacting with the adamantane guests increase hopping and flying events' contribution to the diffusion mechanism).

Walking was one of the three processes (together with hopping and flying, Figure 15) observed by Huskens and co-workers during the investigation of gradient driven surface diffusion of divalent guest molecules decorated with adamantane (Ad) 'legs' along the monolayer of α-cyclodextrin (CD) hosts deposited on glass.[41] Divalent guest molecules ($\mathbf{G^{II}}$) were functionalised with a probe for fluorescence microscopy imaging purposes and assembled *via* microcontact printing[42] to form sharp strips across the CD surface. Then, in the presence of an increasing concentration of external CD host molecules (**H**, green rings, Figure 15) the diffusion of $\mathbf{G^{II}}$ towards the non-printed (rich in empty CD) area of the surface was investigated using fluorescence microscopy imaging. As expected, the spreading rate of $\mathbf{G^{II}}$ has increased from 0.02 nms^{-1} when observed in pure water to almost 4 nms^{-1} in 7 mM solution of **H**. In pure water, lack of external hosts which could mediate adamantane leg transfer to a neighbouring CD strongly suggests that diffusion in these conditions is predominantly due to walking events. With the increase of **H** concentration, rates of spreading increase as a result of first hopping and later flying dominating over the walking pathway of diffusion (see cartoon representation of above processes in Figure 15).

1.7.2 Dynamic Covalent Chemistry (DCC) Based Walking Systems

The stimuli responsive and dynamic character of some covalent bond forming reactions[43] offers a robust tool for the development of small molecule transport devices. Molecules which rapidly change back and forth between numbers of constitutional isomers through low-energy intermediates have fascinated chemists due to their potential to adopt particular structures in response to their environment[44] or to act as prototypical molecular transport systems.[45] A very minimalistic representation of a spontaneous (under reaction conditions) intramolecular (*i.e.* processive) exchange of an imine derived from salicylaldehyde published by the Lehn group[46] showed that the rate of exchange between two ethylene-spaced primary amine groups can be very easily affected by varying the substituents in the aldehyde aromatic ring (Scheme 1).

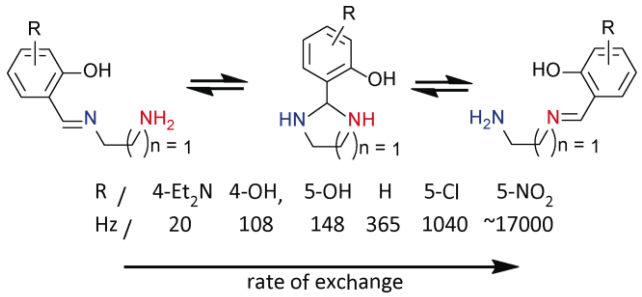

Scheme 1. Mechanism of the intramolecular exchange displayed by the monoimines formed by differently substituted *o*-hydroxybenzaldehydes with aliphatic ethylenediamine and influence of the aldehyde substitution on the rate of end-to-end migration.[46]

Other typical features for DCC-based systems, like strong solvent, temperature and concentration dependence of the exchange processes, were demonstrated. A significant decrease in the rate of exchange was observed as a result of increasing the spacer length between footholds (from 365 Hz for n = 1 to 10 Hz for n = 3, Scheme 1). Due to the difficulty with detection of exchange between secondary amines, a four foothold track was synthesised with outer primary amines functionalised as imines and two inner footholds in a form of an aminal (Figure 16a). Methoxyamine triggered selective displacement of one imine induced an intramolecular migration of the aminal aldehyde towards the periphery of the track to form more stable, symmetrical diimine compound. Hydrogen atoms allowing for the quantification of migration by extensive proton NMR studies are highlighted and a representation (mapped from Ref. 46) of signal intensity plotted against time is shown in Figure 16a and b, respectively.

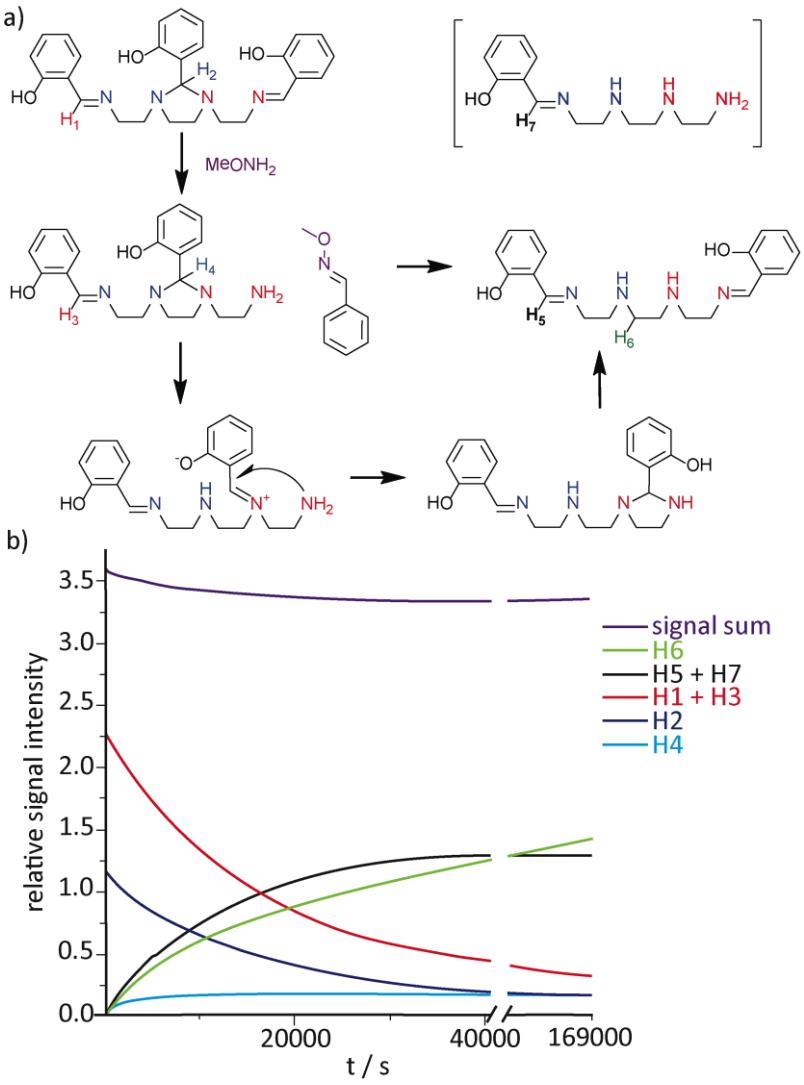

Figure 16. a) Mechanism of the dynamic intramolecular motion of a salicylidene aminal residue along an amine chain towards the periphery of the track induced by unblocking of the preferred, primary foothold by the addition of an external reagent (methoxyamine). b) Mapping of kinetic data for the reaction depicted (and signals highlighted) in a). Signal H7 corresponds to the side product formed due to relatively slow reaction between the substrate and methoxyamine. Signals were integrated with respect to an internal standard of *n*-butanol.[46]

The Leigh group has also reported a series of DCC based walkers. In this case, they were molecules with two chemically different, dynamic covalent feet connected to a track in such a way that each foot could act as a temporarily fixed pivot while the other was engaged in a dynamic covalent exchange reaction.[47] Under acidic conditions ((i) Figure 17) the disulfide linkage between the $\mathbf{C}_5$ walker (where $n = 5$ is the length of the carbon spacer that separates the feet) and the track remains kinetically locked while the hydrazone unit that joins the other foot to the track is labile allowing for the foot to select between a 'forward' and 'backward' foothold through hydrazone exchange (top process in Figure 17). Under

basic conditions (ii) the disulfide foot samples two possible binding sites on the track while the hydrazone foot is locked in place (see Figure 17). Upon oscillation of acid/base conditions, the walker molecule randomly and processively takes zero or one steps along the track using primarily a 'hand-over-hand' mode. After three such cycles (i+ii), an identical steady-state distribution of walkers on the four-foothold tracks is reached (table in Figure 17) regardless of which end of the track the walker starts from. This mode of operation is not directional as at the steady state, the probability of a forward step is equal to that of a backward step. Replacing the basic step with a redox-mediated disulfide exchange reaction (iii) carried out under kinetic control, however, leads to a different population distribution of the sulfur foot between the footholds and a moderate directional bias after 1.5 operation cycles of i+iii (table in Figure 17).

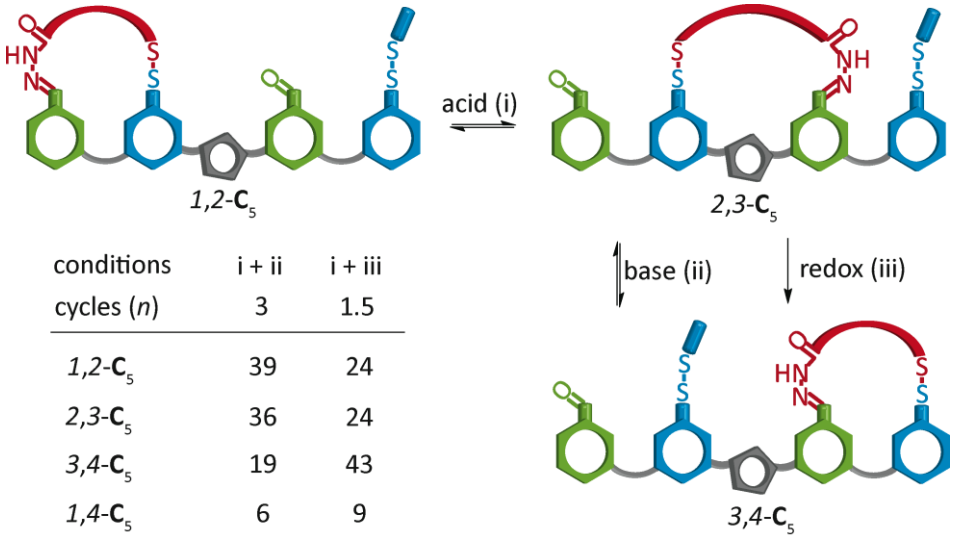

conditions	i + ii	i + iii
cycles (*n*)	3	1.5
1,2-$\mathbf{C}_5$	39	24
2,3-$\mathbf{C}_5$	36	24
3,4-$\mathbf{C}_5$	19	43
1,4-$\mathbf{C}_5$	6	9

Figure 17. Oscillation of acid/base conditions induces the migration of a walker molecule (shown in red) along a four-foothold track (footholds shown in green and blue; linker groups shown in grey). Replacing the reversible base-induced disulfide exchange reaction with an irreversible two-step redox process transports the walker predominantly to the right hand side of the track (away from the minimum energy distribution of walkers). Product distribution after: three cycles of a non-biased acid–base operation and 1.5 cycles of a biased acid-redox operation (both starting from pristine *1,2*-$\mathbf{C}_5$). Note: the minor isomer *1,4*-$\mathbf{C}_5$ results from folding of the track.[47]

An investigation of a series of walker–track conjugates, differing in the length of the carbon spacer separating the feet in the walker was also performed[48] and revealed that internal footholds are too far apart for the walker unit to be able to form *2,3*-$\mathbf{C}_2$ and *2,3*-$\mathbf{C}_3$ positional isomers (where n = 2 and 3, respectively). On the other hand, walkers with linkers > n = 5 achieved no significant directional bias, which indicated that a certain amount of ring strain in *2,3*- positional isomer is crucial for the emergence of directionality. Therefore, the replacement of a triazole linker with a double bond linkage between the internal aldehyde

and disulfide footholds of the track (Figure 18) was an important improvement over previous systems. It allowed for a light driven, reversible introduction of significant ring strain in the *2,3*- positional isomer through *Z*→*E* double bond isomerisation (effectively *Z*→*E* stilbene isomerisation) and directional transport of the walking unit away from the stilbene spacer in either direction as determined by operation conditions applied (Figure 18, ii or iv).[49]

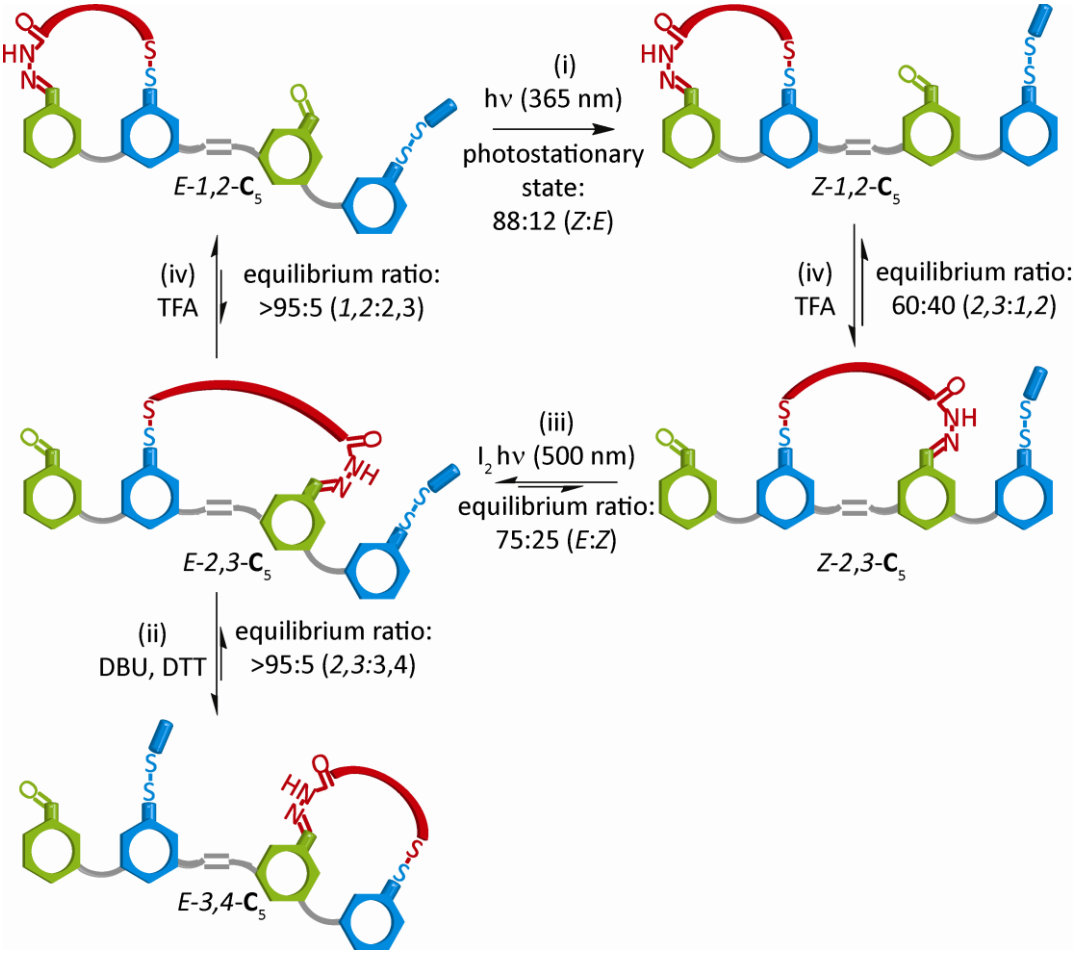

Figure 18. Light driven directional walker migration in either direction upon a four foothold track. For clarity reasons only the major isomer is shown after each stilbene isomerisation or dynamic covalent exchange process.[49]

1.8 Conclusions

Fascinating bipedal motor proteins able to walk along cellular tracks, carrying out essential tasks, such as vesicle transport and muscle contraction have inspired numerous mimics based on DNA as well as synthetic small-molecule analogues that exhibit some of the most important characteristics of the biological walkers. Although the complexity of operations performed by non-autonomous DNA walkers is truly impressive, the autonomous systems, which execute still challenging but simpler tasks, suffer from limited controllability. Therefore the implementation of chemical processes (like reversible $Z \rightarrow E$ isomerisations) and reactions into the operation cycles of DNA walkers is an interesting and promising direction for the development of this research. Steady but limited progress in the area of synthetic small molecules able to perform translational motion shows how difficult it is to design sets of reactions on which processivity of such devices could be based.

It is important however to develop new small molecule analogues based on novel reaction cycles and to expand the analytical toolbox which can be used for the monitoring of motion and task performance at the molecular level.

1.9 References

[1] a) Lehn, J.- M.; *Supramolecular Chemistry*. Weinheim: Wiley-VCH. **1995**; b) Gellman, S. H. *Chem. Rev.* **1997**, *97*, 1231–1232.

[2] a) Whitesides, G. M.; Boncheva, M. *Proc. Natl. Acad. Sci. U.S.*. **2002**, *99*, 4769–4774; b) Whitesides, G. M.; Grzybowski, B. *Science* **2002**, *295*, 2418–2421.

[3] a) Aucagne, V.; Berná, J.; Crowley, J. D.; Goldup, S. M.; Hänni, K. D.; Leigh, D. A.; Lusby, P. J.; Ronaldson, V. E.; Slawin, A. M. Z.; Viterisi, A.; Walker, D. B. *J. Am. Chem. Soc.* **2007**, *129*, 11950–11963; b) Goldup, S. M.; Leigh, D. A.; Long, T.; McGonigal, P. R.; Symes, M. D.; Wu, J. *J. Am. Chem. Soc.* **2009**, *131*, 15924–15929; c) Barran, P. E.; Cole, H. L.; Goldup, S. M.; Leigh, D. A.; McGonigal, P. R.; Symes, M. D; Wu, J.; Zengerle, M. *Angew. Chem. Int. Ed.* **2011**, *50*, 12280–12284.

[4] Kay, E. R.; Leigh, D. A.; Zerbetto, F. *Angew. Chem. Int. Ed.* **2007**, *46*, 72–191.

[5] Feringa, B. L.; van Delden, R. A.; Koumura, N.; Geertsema, E. M. *Chem. Rev.* **2000**, *100*, 1789–1816.

[6] a) Kelly, T. R.; De Silva, H.; Silva, R. A. *Nature* **1999**, *401*, 150–152; b) Koumura, N.; Zijlstra, R. W. J.; van Delden, R. A.; Harada, N.; Feringa, B. L. *Nature* **1999**, *401*, 152–155; c) Browne, W. R.; Feringa, B. L. *Nat. Nanotechnol.* **2006**, *1*, 25–35; d) Wang, J.; Feringa, B. L. *Science* **2011**, *331*, 1429–1432; e) Kudernac, T.; Ruangsupapichat, N.; Parschau, M.; Macia, B.; Katsonis, N.; Harutyunyan, S. R.; Ernst, K.- H.; Feringa, B. L. *Nature* **2011**, *479*, 208–211.

[7] a) Serreli, V.; Lee, C.- F.; Kay, E. R.; Leigh, D. A. *Nature* **2007**, *445*, 523–527; b) Alvarez-Pérez, M.; Goldup, S. M.; Leigh, D. A.; Slawin, A. M. Z. *J. Am. Chem. Soc* **2008**, *130*, 1836–1838; c) Carlone, A.; Goldup, S. M.; Lebrasseur, N.; Leigh, D. A.; Wilson, A. *J. Am. Chem. Soc.* **2012**, 134, 8321−8323.

[8] Howard. J. *Mechanics of Motor Proteins and the Cytoskeleton*, Sinauer Associates, Inc. **2001**.

[9] a) Hirokawa, N. *Science* **1998**, *279*, 519–526; b) Vale, R. D.; Milligan, R. A. *Science* **2000**, *288*, 88–95; c) Schliwa, M.; Woehlke, G. *Nature* **2003**, *422*, 759–765; d) Mallik, R.; Gross, S. P. *Curr. Biol.* **2004**, *14*, 971– 982; e) Amos, L. A. *Cell. Mol. Life Sci.* **2008**, *65*, 509–515.

[10] Hoyt, M. A.; Hyman, A. A.; Bähler, M. *Proc. Natl. Acad. Sci. U S A* **1997**, *94*, 12747–12748.

[11] a) Woehlke, G.; Schliwa, M. *Nature Rev.* **2000**, *1*, 50–58; b) Vale, R. D. *Cell* **2003**, *112*, 467–480; c) Yildiz, A.; Tomishige, M.; Vale, R. D.; Selvin, P. R. *Science* **2004**, *303*, 676–678.

[12] von Delius, M.; Leigh, D. A. *Chem. Soc. Rev.* **2011**, *40*, 3656–3676.

[13] a) Astumian, R. D. *Phys. Chem. Chem. Phys.* **2007**, *9*, 5067–5083; b) Astumian, R. D. *Biophys. J.* **2010**, *98*, 2401–2409; c) Astumian, R. D. *Nat. Nanotechnol.* **2012**, *7*, 684–688.

[14] Hugel, T.; Lumme, C. *Curr. Opin. Biotechnol.* **2010**, *21*, 683–689.

[15] a) Asbury, C. L.; Fehr, A. N.; Block, S. M. *Science* **2003**, *302*, 2130–2134; b) Yildiz, A.; Selvin, P. R. *Trends in Cell Biol.* **2005**, *15*, 112–120; c) Clancy, B. E.; Behnke-Parks, W. M.; Andreasson, J. O. L.; Rosenfeld S. S.; Block, S. M. *Nat. Struct. Mol. Biol.* **2011**, *18*, 1020–1027.

[16] Zhang, D. Y.; Seelig, G. *Nat. Chem.* **2011**, *3*, 103–113.

[17] Gu, H.; Chao, J.; Xiao, S.- J.; Seeman, N. C. *Nature* **2010**, *465*, 202–205.

[18] He, Y.; Liu, D. R. *Nat. Nanotechnol.* **2010**, *5*, 778–782.

[19] Sherman, W. B.; Seeman, N. C. *Nano Lett.* **2004**, *4*, 1203–1207.

[20] Shin, J.- S.; Pierce, N. A. *J. Am. Chem. Soc.* **2004**, *126*, 10834–10835.

[21] Rothemund, P. W. K. *Nature* **2006**, *440*, 297–302.

[22] a) Dirks, R. M.; Pierce, N. A. *Proc. Natl. Acad. Sci. U S A* **2004**, *101*, 15275–15278; b) Green, S. J.; Lubrich, D.; Turberfield, A. J. *Biophys. J.* **2006**, *91*, 2966–2975; c) Yin, P.; Choi, H. M. T.; Calvert, C. R.; Pierce, N. A. *Nature* **2008**, *451*, 318–323.

[23] a) Turberfield, A. J.; Mitchell, J. C.; Yurke, B.; Mills, A. P.; Blakey, M. I.; Simmel, F. C. *Phys. Rev. Lett.* **2003**, *90*, 118102; b) Seelig, G; Yurke, B.; Winfree, E. *J. Am. Chem. Soc.* **2006**, *128*, 12211–12220.

[24] a) Green, S. J.; Bath, J.; Turberfield, A. J. *Phys. Rev. Lett.* **2008**, *101*, 238101(4); b) Bath, J.; Green, S. J.; Allen, K. E.; Turberfield, A. J. *Small* **2009**, *5*, 1513–1516.

[25] a) Omabegho, T. Sha R. Seeman, N. C. *Science*, **2009**, *324*, 67–71; b) Sherman, W. *Science* **2009**, *324*, 46–47.

[26] Muscat, R. A.; Bath, J.; Turberfield, A. J. *Nano Lett.* **2011**, *11*, 982–987.

[27] Muscat, R. A.; Bath, J.; Turberfield, A. J. *Small* **2012**, *8*, 3593–3597.

[28] Yin, P.; Yan, H.; Daniell, X. G.; Turberfield, A. J.; Reif, J. H. *Angew. Chem. Int. Ed.* **2004**, *43*, 4906–4911.

[29] Bath, J.; Green, S. J.; Turberfield, A. J. *Angew. Chem. Int. Ed.* **2005**, *44*, 4358–4361.

[30] Wickham, S. F.; Endo, M.; Katsuda, Y.; Hidaka, K.; Bath, J.; Sugiyama, H.; Turberfield, A. J. *Nat. Nanotechnol.* **2011**, *6*, 166–169.

[31] Ando, T. *Nanotechnol.* **2012**, *23*, 062001.

[32] Lund, K.; Manzo, A. J.; Dabby, N.; Michelotti, N.; Johnson- Buck, A.; Nangreave, J.; Taylor, S.; Pei, R.; Stojanovic, M. N.; Walter, N. G.; Winfree, E.; Yan, H. *Nature* **2010**, *465*, 206–210.

[33] Tian, Y.; He, Y.; Chen, Y.; Yin P.; Mao C. *Angew. Chem. Int. Ed.* **2005**, *44*, 4355–4358.

[34] Pei, R.; Taylor, S. K.; Stefanovic, D.; Rudchenko, S.; Mitchell, T. E.; Stojanovic, M. N. *J. Am. Chem. Soc.* **2006**, *128*, 12693–12699.

[35] Lewandowski, B.; De Bo, G.; Ward, J. W.; Papmeyer, M.; Kuschel, S.; Aldegunde, M. J.; Gramlich, P. M. E.; Heckmann, D.; Goldup, S. M.; D'Souza, D. M.; Fernandes, A. E.; Leigh, D. A. *Science* **2013**, *339*, 189-193.

[36] You, M.; Chen, Y.; Zhang, X.; Liu, H.; Wang, R.; Wang, K.; Williams, K. R.; Tan,W. *Angew. Chem. Int. Ed.* **2012**, *51*, 2457–2460.

[37] You, M.; Huang, F.; Chen, Z.; Wang, R.; Tan, W. *ACS Nano* **2012**, *6*, 7935–7941.

[38] Kwon, K.- Y.; Wong, K. L.; Pawin, G.; Bartels, L.; Stolbov, S.; Rahman, T. S. *Phys. Rev. Lett.* **2005**, *95*, 166101(4).

[39] Wong, K. L.; Pawin, G.; Wong, K.-Y.; Lin, X.; Jiao, T.; Solanki, U.; Fawcett, R. H. J.; Bartels, L.; Stolbov, S.; Rahman, T. S. *Science* **2007**, *315*, 1391–1393.

[40]Cheng, Z.; Chu, E. S.; Sun, D.; Kim, D.; Luo, M.; Pawin, G.; Wong, K. L.; Carp, R.; Marsella, M.; Bartels, L. *J. Am. Chem. Soc.* **2010**, *132*, 13578–13581.

[41] Perl, A.; Gomez - Casado, A.; Dam, H. H.; Jonkheijm, P.; Reinhoudt, D. N.; Huskens, J. *Nat. Chem*. **2011**, *3*, 317–322.

[42] Xia, Y.; Whitesides, G. M. *Angew. Chem.* **1998**, *110*, 568–594; *Angew. Chem. Int. Ed.* **1998**, *37*, 551–575; b) Gates, B. D.; Xu, Q. B.; Stewart, M.; Ryan, D.; Willson, C. G.; Whitesides, G. M. *Chem. Rev*. **2005**, *105*, 1171–1196; c) Perl, A.; Reinhoudt, D. N.; Huskens, J. *Adv. Mater.* **2009**, *21*, 2257–2268.

[43] a) Lehn, J.- M. *Chem. Eur. J.* **1999**, *5*, 2455−2463; b) Rowan, S. J.; Cantrill, S. J.; Cousins, G. R. L.; Sanders, J. K. M.; Stoddart, J. F. *Angew. Chem. Int. Ed.* **2002**, *41*, 898−952; c) Corbett, P. T.; Leclaire, J.; Vial, L.; West, K. R.; Wietor, J.- L.; Sanders, J. K. M.; Otto, S. *Chem. Rev.* **2006**, *106*, 3652−3711; d) Lehn, J.- M. *Chem. Soc. Rev.* **2007**, *36*, 151–160; e) Hunt, R. A. R.; Otto, S. *Chem. Commun*. **2011**, *47*, 847−858; f) Cougnon, F. B. L.; Jenkins, N. A.; Patoş Dan, G.; Sanders, J. K. M. *Angew. Chem. Int. Ed.* **2012**, *51*, 1443−1447; g) Belowich, M.; Stoddart, J. F. *Chem. Soc. Rev*. **2012**, *41*, 2003−2024; h) Miller, B. L.; *Dynamic Combinatorial Chemistry*; Wiley: Chichester, **2010**; i) Reek, J. N. H., Otto, S.; *Dynamic Combinatorial Chemistry*; Wiley-VCH: Weinheim, **2010**.

[44] a) Lippert, A. R.; Kaeobamrung, J.; Bode, J. W. *J. Am. Chem. Soc*. **2006**, *128*, 14738–14739; b) Lippert, A. R.; Keleshian, V. L.; Bode, J. W. *Org. Biomol.Chem*. **2009**, *7*, 1529–1532; c) Lippert, A. R.; Nagawana, A.; Keleshian, V. L.; Bode, J. W. *J. Am. Chem. Soc*. **2010**, *132*, 15790–15799; d) He, M.; Bode, J. W. *Proc. Nat. Acad. Sci. U S A* **2011**, *108*, 14752–14756.

[45] von Delius, M.; Geertsema, E. M.; Leigh, D. A. *Org. Biomol. Chem.* **2010**, *8*, 4617-4624.

[46] Kovaříček, P.; Lehn, J.- M. *J. Am. Chem. Soc*. **2012**, *134*, 9446–9455.

[47]von Delius, M.; Geertsema, E. M.; Leigh, D. A. *Nat. Chem.* **2010**, *2*, 96–99.

[48] von Delius, M.; Geertsema, E. M.; Leigh, D. A.; Tang, D. -T. D. *J. Am. Chem. Soc.* **2010**, *132*, 16134–16145.

[49] Barrell, M. -J.; Campaña, A. G.; von Delius, M.; Geertsema, E. M.; Leigh, D. A. *Angew. Chem. Int. Ed.* **2011**, *50*, 285–290.

Chapter II

A Small Molecule that Walks Non-Directionally Along a Track Without External Intervention

Published as *A Small Molecule that Walks Non-Directionally Along a Track Without External Intervention*,
Campaña, A. G.; Carlone, A.; Chen, K.; Dryden, D. T. F.; Leigh, D. A.; Lewandowska, U.; Mullen, K. M.
Angew. Chem. Int. Ed. **2012**, *51*, 5480–5483.
Selected highlight:
On the right track Cantrill, S. *Nat. Chem*. **2012** *4*, 430–431
Also published as a press report:
A Two-Legged Molecule Angew. Chem. Int. Ed., 24 April 2012

ACKNOWLEDGMENTS

Work presented in **Chapter II** is a joint effort of the author and Dr. Araceli G. Campaña. Synthesis of compounds **3**, **4**, **7**, **9**, their precursors and scale-up of synthesis of **11** and **12** was performed by Dr. A. G. Campaña. Dr. Kathleen Mullen is gratefully acknowledged for synthesis of **M**-*1*and **9**. Dr. David Dryden and Dr. Kai Chen have contributed by performing fluorescence lifetime measurements and dilution experiments and both are gratefully acknowledged for their assistance in static fluorescence measurements. Dr. Bartosz. Lewandowski is acknowledged for his assistance in acquiring ^{1}H NMR data for kinetic experiments.

2.1 Synopsis

Small molecule walkers developed to date take advantage of the reversibility of dynamic covalent bond formation to transport molecular fragments along surfaces and molecular tracks using both diffusional processes and ratchet mechanisms. However, external intervention (the addition of chemical reagents and/or irradiation with light) is required to mediate each step taken by the walker units in the non-DNA systems reported to date.

A first small synthetic molecule able to walk back-and-forth upon a five-foothold pentaethylenimine track without external intervention is described. The 1D random walk is highly processive (mean step number ~530) and exchange takes place between adjacent amine groups in a stepwise fashion. The walker is used to perform a simple task: quenching of the fluorescence of an anthracene group, sited at one end of the track, as a result of the walking progress.

2.2 Introduction

Kinesin, dynein, and some myosin motor proteins transport cargoes within the cell by 'walking' along polymeric filaments, *i.e.* carrying out successive, repetitive, mostly-directional changes of their point of contact with the molecular track without completely detaching from it.[1] These extraordinary biomolecules are inspiring scientists to mimic aspects of their dynamics in order to create artificial molecular transport systems.[2,3] Recently, the first small molecules that are able to walk down short molecular tracks were described.[2] However, external intervention (the addition of chemical reagents and/or irradiation with light) was required to mediate each step taken by the walker units in those sytems. Although migrations of submolecular fragments occur in many different types of chemical reactions,[4] few systems appear to offer the potential for multiple, successive and cumulative transport necessary for developing small-molecule walkers.[5] Interesting examples are the so-called equilibrium transfer alkylating cross-linking (ETAC) reagents introduced in the 1970s by Lawton and co-workers for the dynamic cross-linking of biomolecules (Scheme 2.1, a).[6,7]

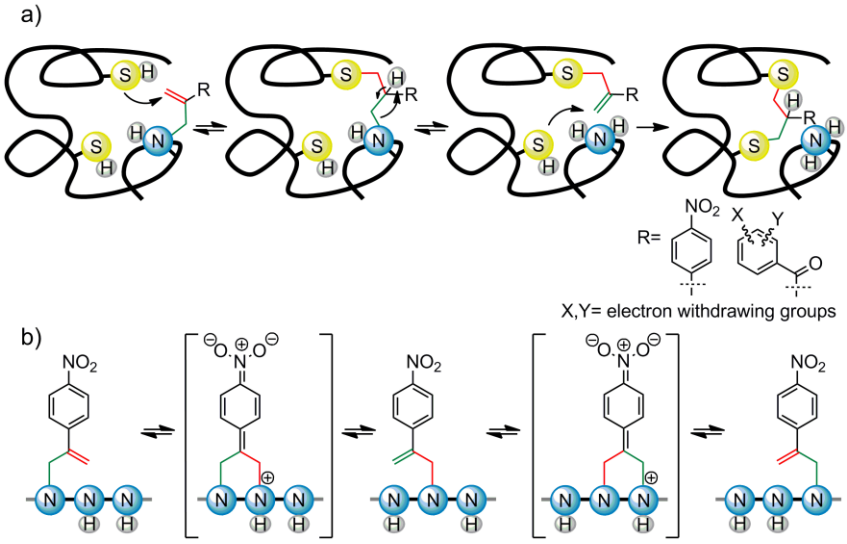

Scheme 2.1. a) The migration of an ETAC[6] reagent between nucleophilic sites of a protein *via* Michael/retro-Michael reactions towards the most thermodynamically stable cross-linked product. b) Processive (*i.e.* intramolecular) migration of α-methylene-4-nitrostyrene along a polyamine track. Michael addition of a track amine group to the olefin of the 'two-legged walker' results in a bridged intermediate (both 'feet' attached to the track, shown in square brackets) that can subsequently undergo a retro-Michael reaction to either side, unmasking the double bond and leaving the walker attached to the track through a single covalent linkage.

These reagents are known to reversibly form covalent bonds between pairs of accessible nucleophilic sites on proteins through a series of inter- and intramolecular Michael and retro-Michael reactions until the most thermodynamically-stable crosslink is located.[6a]

We wondered whether it would be possible to apply a similar concept, focusing instead on finding reaction conditions where the crosslinked products are less stable than those attached by a single covalent bond, in order to create synthetic small molecules that spontaneously migrate with a high degree of processivity[8] along a linear, molecular track (Scheme 2.1b).

2.3 Results and Discussion

2.3.1 Model Studies.

In order to be able to use the reagent, described by Lawton and co-workers for the dynamic cross-linking of biomolecules, as a walking unit, model studies including the attachment and subsequent intramolecular exchange of α-methylene-4-nitrostyrene between footholds had to be performed. For this reason, a model track **M**-*1*-Boc was synthesised according to literature procedure,[9] in one step from commercially available diethylenetriamine.

The walker unit **(W)** featuring an amonium salt as a leaving group was synthesised and attached to diethylenetrieamine according to published procedures,[6a] affording **M**-*1*-Boc. After Boc deprotection with CF_3CO_2H followed by addition of aqueous $NaHCO_3$ to reach pH 7, **M**-*1* was isolated and subjected to exchange conditions (Scheme 2.2) described by Lawton for intermolecular exchange of α-methylene-4-nitrostyrene between primary amines.[6a] The reaction was followed by ^{1}H NMR spectroscopy through the different chemical shift of vinyl protons ($H_{c/c'}$ and $H_{d/d'}$) of model compounds **M**-*1* and **M**-*2* (Scheme 2.2). Partial ^{1}H NMR spectra of the exchange between **M**-*1* and **M**-*2* in CD_3OD (6 equiv. ^{i}Pr$_2$NEt, 348 K, 10 mM) are shown in Figure 2.1. The reaction was also successful in milder conditions, namely [D_7]DMF in the presence of 6 equiv. ^{i}Pr$_2$NEt either at 40 °C (see Figure 2.2) or at room temperature resulting in approximately 80 % of the walker migrating to the outer amine after about 2 and 8 hours, respectively.

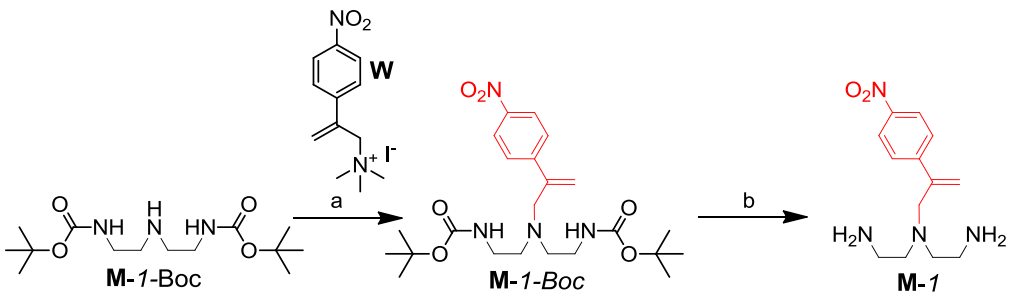

Scheme 2.2. Walker attachment followed by Boc deprotection of the track. Reaction conditions: a) $^{i}Pr_2NEt$, MeOH, 50 °C, 4 days, 83%, b) CF_3CO_2H, CH_2Cl_2, 1 h; $NaHCO_{3aq.}$, quant.

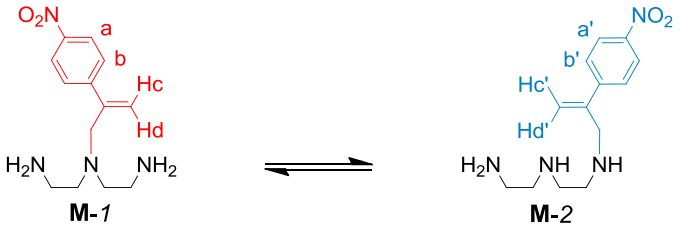

Scheme 2.3. Transfer of α-methylene-4-nitrostyrene from secondary amine group to a primary amine group through 1,4-*N*,*N*-migration.

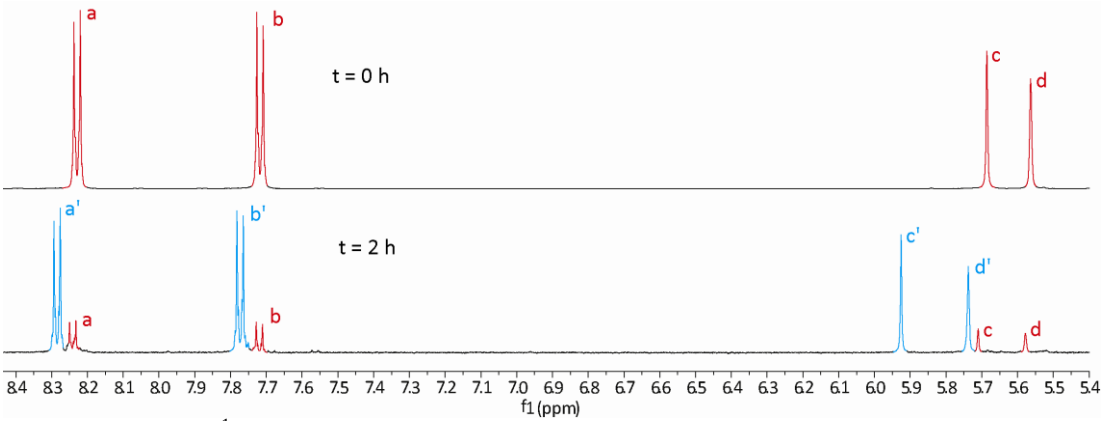

Figure 2.1. Partial ^{1}H NMR spectra (400 MHz, CD_3OD, 10 mM, 348 K) of exchange between **M**-*1* and **M**-*2* in the presence of 6 equiv. $^{i}Pr_2NEt$ at: given times. At t = 2 h **M**-*1*: **M**-*2* ratio 1:4. The lettering corresponds to the proton labelling shown in Scheme 2.3.

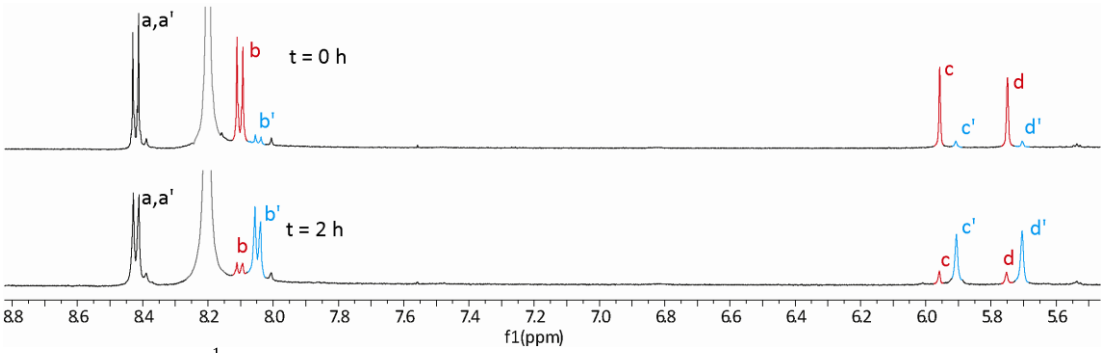

Figure 2.2. Partial ^{1}H NMR spectra (400 MHz, $[D_7]DMF$, 10 mM, 338 K) of exchange between **M**-*1* and **M**-*2* in the presence of 6 equiv. $^{i}Pr_2NEt$ at: given times. At t = 2 h **M**-*1*: **M**-*2* ratio 1:5. The lettering corresponds to the proton labelling shown in Scheme 2.3.

2.3.2 Design and Investigation of a Three - Foothold Walker-Track Conjugate.

Based on model studies, walker-track conjugate **1**, in which *α*-methylene-4-nitrostyrene was attached to an outer amine group of a triamine track was synthesised and the dynamics of its subsequent migration between secondary amine footholds without fully detaching *via* a sequence of intramolecular Michael and retro-Michael reactions was investigated (Scheme 2.4, see Experimental Section for the synthetic route).[10] The reaction was followed by ^{1}H NMR spectroscopy through the different chemical shift of vinyl protons ($H_{c/c'}$ and $H_{d/d'}$) of isomers **1** and **2** (Scheme 2.4). Partial ^{1}H NMR spectra of the exchange between **1** and **2** in [D_6]DMSO (298 K, 5 mM) are shown in Figure 2.3.

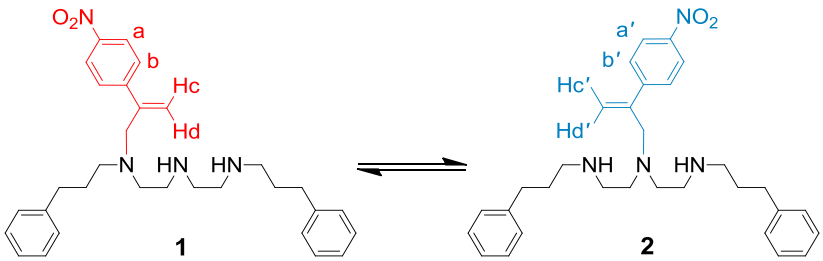

Scheme 2.4. Transfer of α-methylene-4-nitrostyrene between secondary amine groups through 1,4-N,N-migration

Upon investigation of reaction conditions, the dynamic character of the amine-to-amine migration of the *α*-methylene-4-nitrostyrene unit (‘walking’) was found to be highly solvent dependent. A solution of **1** (5 mM) in various solvents ($CDCl_3$, CD_2Cl_2, CD_3CN, CD_3OD, [D_6]DMSO and [D_7]DMF) was monitored using ^{1}H NMR spectroscopy. No formation of **2** was observed in $CDCl_3$ or CD_2Cl_2 over 15 h at room temperature (see Figure 2.4) and the reaction only proceeded slowly in CD_3OD (<10% conversion over 15 h) or CD_3CN (<25% conversion over 15 h). However, the interconversion of **1** with **2** reached a close-to-1:1 steady-state ratio over 15 h in [D_7]DMF or 4.5 h in [D_6]DMSO (298 K, 5 mM). Polar, aprotic solvents like [D_6]DMSO and [D_7]DMF are able to stabilize charge-separated transition states (see Scheme 2.1b) due to their high dielectric constants. This stabilization, lowering the barrier of conjugate addition, renders the process rapid and reversible. Addition of $^{i}Pr_2NEt$ wasn’t necessary for the walking to occur in these solvents.

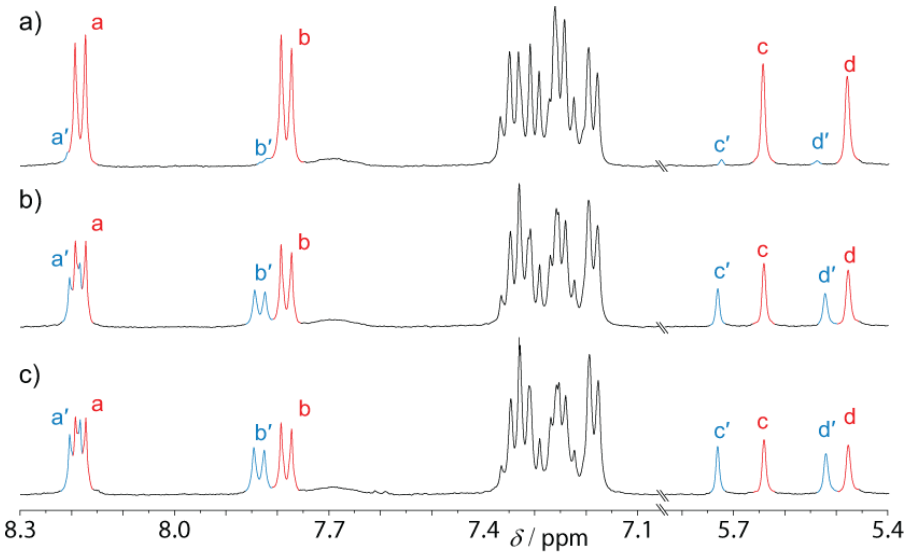

Figure 2.3. Partial ^{1}H NMR spectra (400 MHz, [D_6]DMSO, 5 mM, 298 K) of exchange between **1** and **2** at: a) t = 5 min, **1**:**2** ratio 1:0.06; b) t = 2 h, **1**:**2** ratio 1:0.6; c) t = 15 h, **1**:**2** ratio 1:0.9. The lettering corresponds to the proton labelling shown in Scheme 2.4.

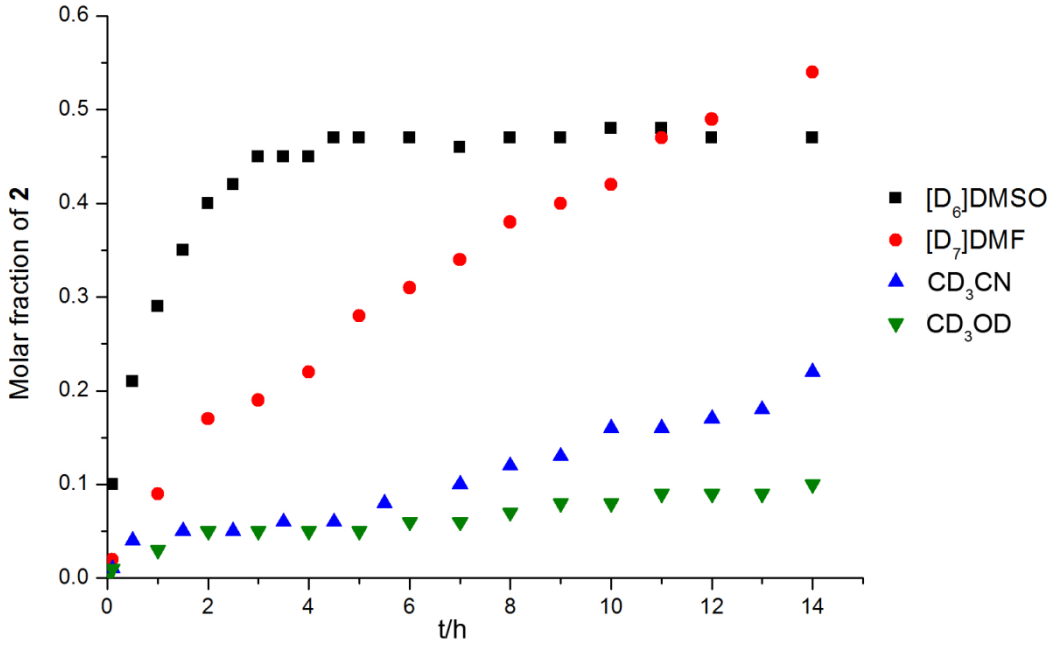

Figure 2.4. The formation of compound **2**, based on ^{1}H NMR (5 mM, 298 K) in different solvents over time.

A solution of **1** in [D_7]DMF at various concentrations (5 mM, 15 mM and 50 mM) was monitored using ^{1}H NMR spectroscopy. Formation of **2** during the exchange at different concentrations is shown in Figure 2.5. We observed that the change in concentration of **1** (three- and ten-fold increase) had a very small influence on the relative ratio of positional isomers **1**:**2** at given times. What is more, no additional vinyl signals

indicating the presence of two walker units attached to the same track were observed. This suggested that the exchange was predominantly due to the intramolecular process.

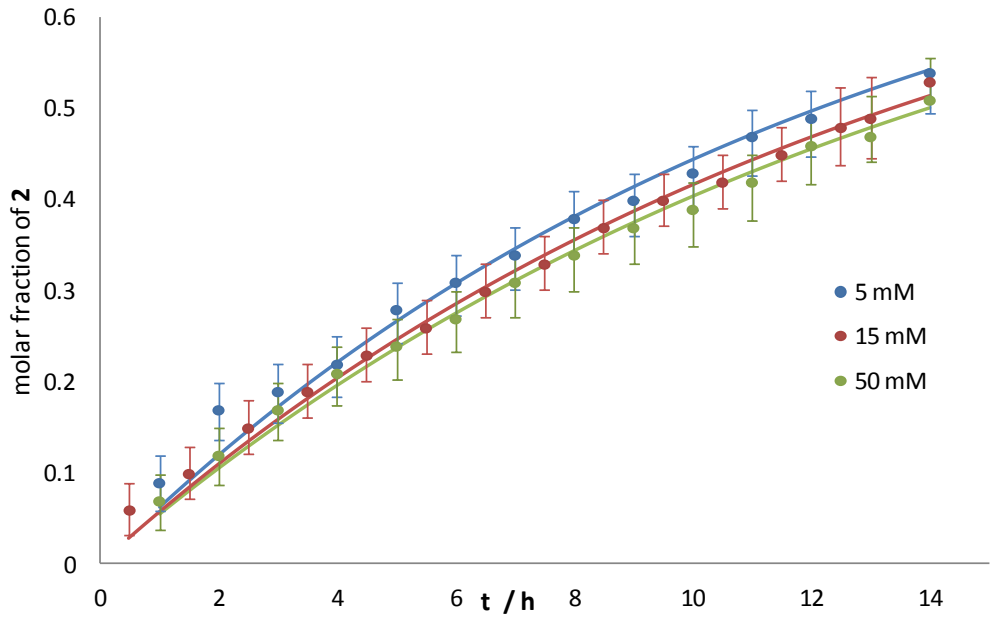

Figure 2.5. Molar fraction of **2** ([D_7]DMF, 298 K) at various concentrations (5, 15 and 50 mM). Solid lines represent the least-square fitting of the data using equation (8). Error bars represent the estimated ±3% error of ^{1}H NMR integration (the proton signals used for the integration are the equivalent ones in each positional isomer, see section 3.6.3.3 in Chapter III).

2.3.3 Description of the Walking Process as a Reversible First Order Reaction.

In order to further characterise the walking process, the concentration of **2** formed in the reaction (**1**, 5 mM, [D_6]DMSO at 298 K) was plotted against time (Figure 2.6). The experimental data were then fitted to reversible 1st order rate equations (as shown below), taking into account $[2]_{eq}$ = 2.375 mM. Rate constants for the forward k_1 = 1.19×10^{-4} s^{-1} and backward k_{-1} = 1.31×10^{-4} s^{-1} stepping were determined and an average half-life of this reversible process ($t_{1/2}$, half of the time needed to reach an equilibrium between **1** and **2**) of 1.54 h was calculated as an average of $t_{1/2}$ of forward and $t_{1/2}$ of backward process. In other words, under these conditions the walker unit needed on average 1.5 h to be found one position forward along the track.

$$\mathbf{1} \underset{k_{-1}}{\overset{k_1}{\rightleftharpoons}} \mathbf{2}$$

$$\frac{d[\mathbf{2}]}{dt} = k_1[\mathbf{1}] - k_{-1}[\mathbf{2}] \qquad (1)$$

we know that:

$$[\mathbf{1}] = [\mathbf{1}]_0 - [\mathbf{2}] \qquad (2)$$

where $[\mathbf{1}]_0$ is the concentration of the substrate at $t = 0$.
Putting that into the starting equation we get:

$$\frac{d[\mathbf{2}]}{dt} = k_1([\mathbf{1}]_0 - [\mathbf{2}]) - k_{-1}[\mathbf{2}] \qquad (3)$$

At the same time:

$$[\mathbf{1}]_0 = [\mathbf{2}]_{eq} + [\mathbf{1}]_{eq} \qquad (4)$$

And from the equilibrium constant equation we know that:

$$K_{eq} = \frac{k_1}{k_{-1}} = \frac{[\mathbf{2}]_{eq}}{[\mathbf{1}]_{eq}} \qquad (5), \text{ so:}$$

$$[\mathbf{1}]_{eq} = \frac{k_{-1}}{k_1}[\mathbf{2}]_{eq} \qquad (6)$$

Using this relationship in (4) we get:

$$[\mathbf{1}]_0 = [\mathbf{2}]_{eq} + \frac{k_{-1}}{k_1}[\mathbf{2}]_{eq} \qquad (7)$$

By inserting the above into (3) we obtain the following equations:

$$\frac{d[\mathbf{2}]}{dt} = k_1\left([\mathbf{2}]_{eq} + \frac{k_{-1}}{k_1}[\mathbf{2}]_{eq} - [\mathbf{2}]\right) - k_{-1}[\mathbf{2}]$$

$$\frac{d[\mathbf{2}]}{dt} = k_1\left(\frac{k_1[\mathbf{2}]_{eq} + k_{-1}[\mathbf{2}]_{eq}}{k_1} - [\mathbf{2}]\right) - k_{-1}[\mathbf{2}]$$

$$\frac{d[\mathbf{2}]}{dt} = k_1[\mathbf{2}]_{eq} + k_{-1}[\mathbf{2}]_{eq} - k_1[\mathbf{2}] - k_{-1}[\mathbf{2}]$$

$$\frac{d[\mathbf{2}]}{dt} = (k_1 + k_{-1})[\mathbf{2}]_{eq} - (k_1 + k_{-1})[\mathbf{2}]$$

$$\frac{d[\mathbf{2}]}{dt} = (k_1 + k_{-1})([\mathbf{2}]_{eq} - [\mathbf{2}])$$

Multiplying by dt and dividing by $([\mathbf{2}]_{eq} - [\mathbf{2}])$ we get:

$$\frac{d[\mathbf{2}]}{([\mathbf{2}]_{eq} - [\mathbf{2}])} = (k_1 + k_{-1})dt$$

$$\int_0^{[\mathbf{2}]} \frac{d[\mathbf{2}]}{([\mathbf{2}]_{eq} - [\mathbf{2}])} = \int_0^t (k_1 + k_{-1})dt$$

as $[\mathbf{2}]_0 = 0$,and $t_0 = 0$ that gives us:

$$-\ln \frac{|[\mathbf{2}]_{eq} - [\mathbf{2}]|}{[\mathbf{2}]_{eq}} = (k_1 + k_{-1})t$$

but as $[\mathbf{2}] < [\mathbf{2}]_{eq}$:

$$-\ln \frac{[\mathbf{2}]_{eq} - [\mathbf{2}]}{[\mathbf{2}]_{eq}} = (k_1 + k_{-1})t$$

$$\ln \frac{[\mathbf{2}]_{eq} - [\mathbf{2}]}{[\mathbf{2}]_{eq}} = -(k_1 + k_{-1})t$$

$$\frac{[\mathbf{2}]_{eq} - [\mathbf{2}]}{[\mathbf{2}]_{eq}} = e^{-(k_1 + k_{-1})t}$$

$$[\mathbf{2}]_{eq} - [\mathbf{2}] = [\mathbf{2}]_{eq} e^{-(k_1 + k_{-1})t}$$

and finally:

$$[\mathbf{2}] = [\mathbf{2}]_{eq}(1 - e^{-(k_1 + k_{-1})t}). \quad (8)$$

Based on (8) and (5)

$k_1 + k_{-1} = (2.5 \pm 0.11)\ 10^{-4}\ s^{-1}$

$$k_1 / k_{-1} = K_{eq} = [\mathbf{2}] / [\mathbf{1}] = 0.002375 / 0.002625$$

$$k_1 = 0.90476\ k_{-1}$$

$t_{1/2} = \ln 2 / k_1 \longrightarrow$ $k_1 = 1.19\ 10^{-4}\ s^{-1}$ $\longrightarrow$ $t_{1/2} = 5824$ s = 1.618 h

$t_{1/2} = \ln 2 / k_{-1} \longrightarrow$ $k_{-1} = 1.31\ 10^{-4}\ s^{-1}$ $\longrightarrow$ $t_{1/2} = 5291$ s = 1.469 h

$$t_{1/2} = (t_{1/2} + t_{1/2})/2 = 1.54 \text{ h}$$

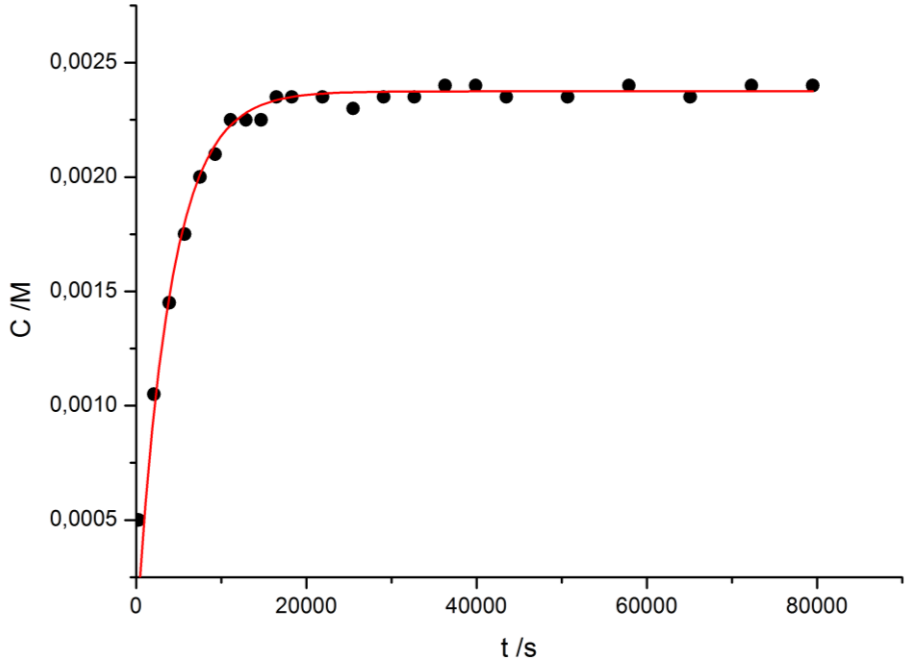

Figure 2.6. Concentration of **2** (mM) vs time (s). Experimental data are shown as black dots. The red line represents the best fit according to equation (8).

2.3.4 Overstepping Study.

To determine how likely the walker is to take a 'double' (1,7-) or 'triple' (1,10-) step while migrating along the track, diamine walker-track conjugates with five (**4**) or eight (**5**) methylene groups between the secondary amine sites were synthesised (Scheme 2.5) (See Experimental Section for further details).[11] One of the terminal sites of the track was deuterium labelled in order to distinguish the walker position (*i.e.* **3** or **4**; **5** or **6**) by ^{1}H NMR spectroscopy. Under conditions where single (1,4-) stepping occurs for **1**/**2** with a $t_{1/2}$ = 1.5 h, no reaction was observed for either **3** or **5** over 48 h. After 48 h under exchange conditions, compound **3** remained stable and the product of intramolecular exchange (**4**) was not observed (Figure 2.7). This suggests that a 'double' step (1,7-) is not favoured under these exchange conditions.

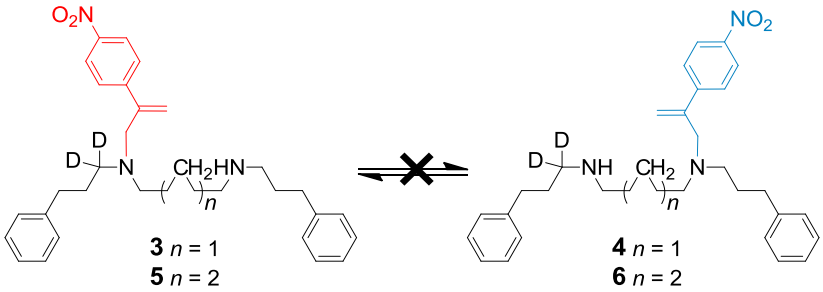

Scheme 2.5. The experimental results show that under conditions ([D_6]DMSO, 298 K, 5 mM) where $t_{1/2}$ = 1.5 h for **1**/**2** exchange, the double (1,7-) and triple (1,10-) 'overstepping' shown is not detectable over 48 h, suggesting that they would be rare events during walker migration along a poly(ethylenimine) track.

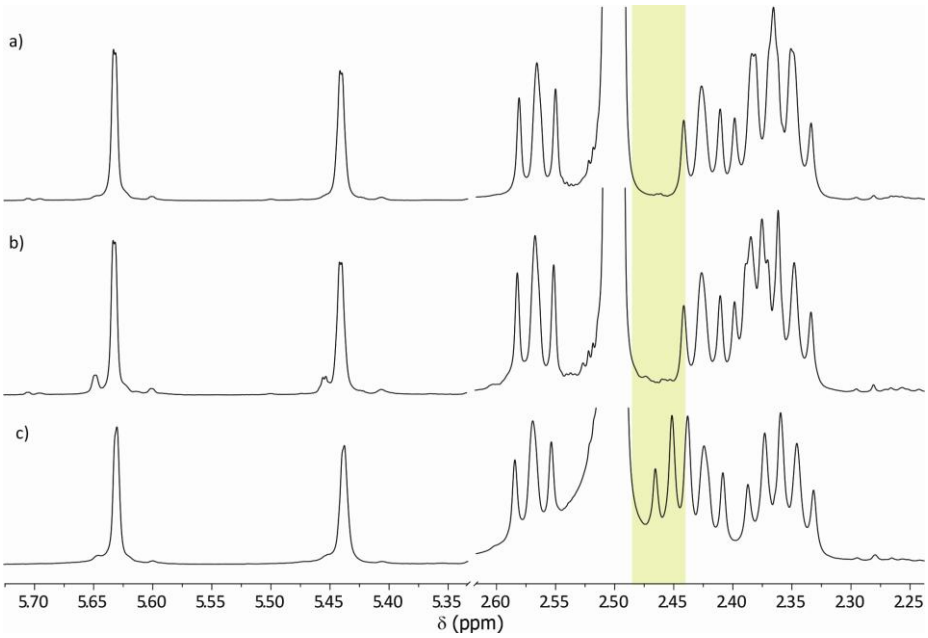

Figure 2.7 Partial ^{1}H NMR spectra (400 MHz, [D_6]DMSO, 5 mM, 298 K) of: a) **4** at t = 0 h; b) **4** after 48 h of exchange; c) reference compound **3**. The highlighted region (δ = 2.45–2.50 ppm) shows distinctive signals for the two positional isomers.

To determine how likely the walker was to take a 'triple' (1,10-) step while migrating along the track compound **5** was dissolved in [D_6]DMSO (5 mM) and the exchange process was monitored by ^{1}H NMR spectroscopy. The results obtained are shown in Figure 2.8. After 48 h under exchange conditions, compound **5** remained stable and product of intramolecular exchange (**6**) was not observed. This suggests that a 'triple' step (1,10-) is not favoured under these exchange conditions.

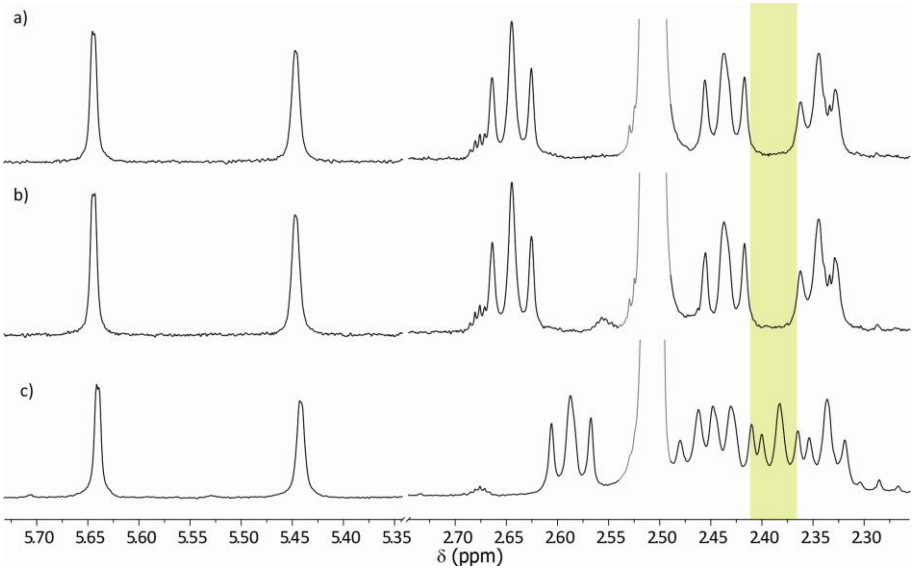

Figure 2.8 Partial ^{1}H NMR spectra (400 MHz, [D_6]DMSO, 5 mM, 298 K) of (from the bottom to the top): a) spectrum of **5** at t = 0 h; b) compound **5** at t = 48 h; c) reference compound **6**. The expanded region (δ = 2.25–2.65 ppm) shows distinctive signals for the two positional isomers.

These results suggest that the walker should migrate predominantly through exchange between adjacent amine footholds on a longer, polyamine track. The large number of steps that the α-methylene-4-nitrostyrene walker takes on average before competing reactions occur (*i.e.* overstepping, complete detaching or exchange with other tracks) is presumably a consequence of the relatively low energy seven-membered ring transition state for 1,4-*N*,*N*-migration.

2.3.5 Processivity Study.

To determine the processivity of the migration reaction (in other words, the degree to which the reaction is intramolecular or intermolecular[8]), we performed a track-crossover study based on electrospray ionisation mass spectrometry (ESI-MS) analysis during the walking process (Scheme 2.6). The objective of this experiment was to determine how likely the walker unit is to step to another walker-free track. For this reason, the intramolecular exchange of **1** was performed in the presence of 1 equiv. of a five foothold, walker-free track **7**. Data analysis was carried out in analogy to previous processivity studies.[2] In the Scheme 2.6, structures **8** and **9** represent products contributing to the loss of processivity which can be quantitatively identified in the reaction mixture. Remaining products of intermolecular exchange (like **S1** and **S2,** Scheme 2.6) cannot be quantified in this experiment as their (relative to **1, 7, 8, 9**) ionization is unknown. In order to avoid overestimation of the intramolecular character of the exchange, the presence of structures which contribute to the processitity loss is estimated as a double of the measured value.

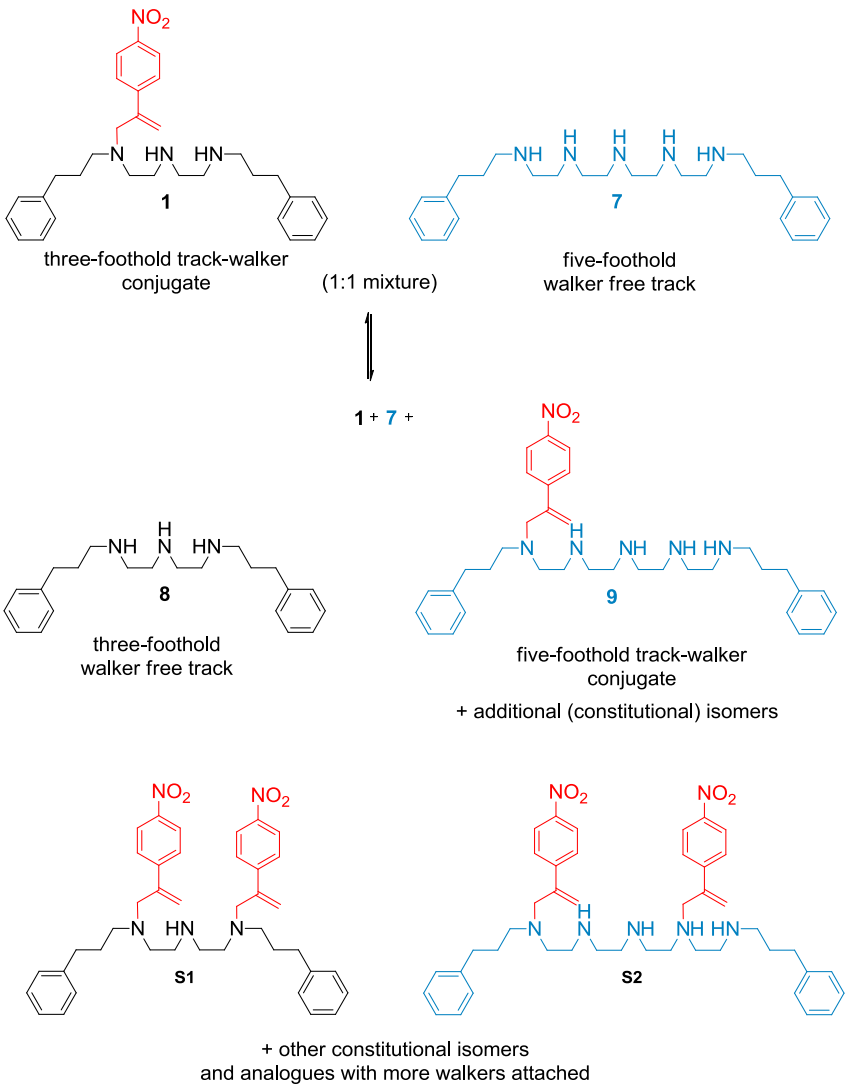

Scheme 2.6. Concept of track crossover experiment representing compounds contributing to the processivity loss.

2.3.5.1 MS Analysis of Reference Mixture of 1, 7, 8 and 9 in a 1:1:1:1 Molar Ratio.

A mixture of **1, 7**, **8**, and **9** in a 1:1:1:1 molar ratio was dissolved in [D_6]DMSO (20 mM) and immediately analysed by ESI-MS. The molar ratio of the mixture was confirmed by ^{1}H NMR spectroscopy. As shown in Figure 2.10, the four compounds showed very different relative ionization. Therefore a correction factor for the abundance of each compound was determined (Table 2.1).

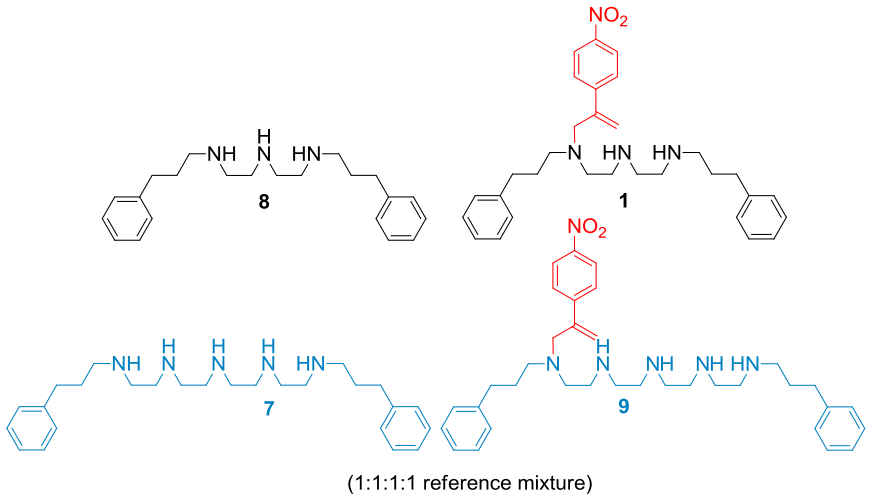

Figure 2.9. Components of the reference mixture consisting of compounds **8**, **1**, **7** and **9** in 1:1:1:1 molar ratio used for the determination of the relative ionisation of compounds investigated in processivity studies.

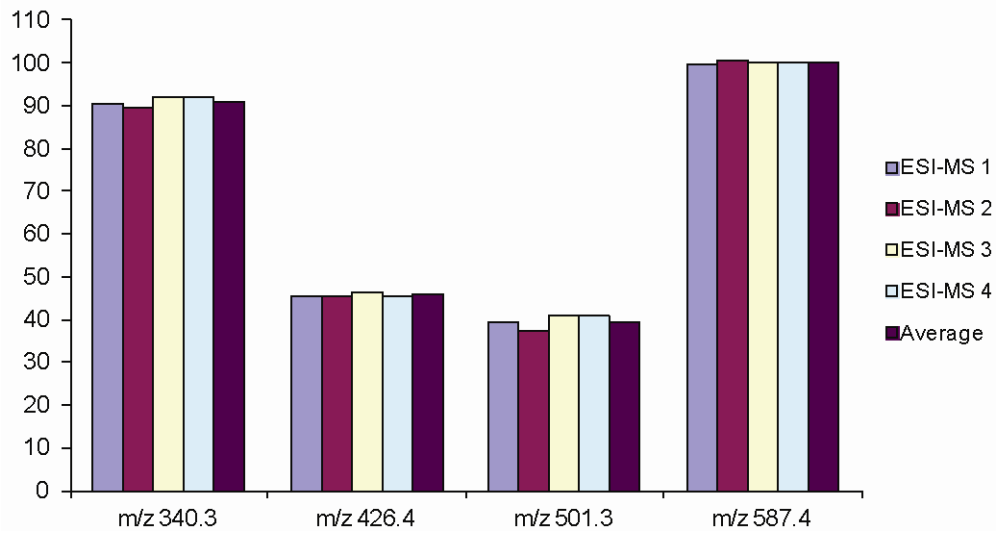

Figure 2.10. Chart of found and average signals of the reference mixture of compounds **8** (m/z = 340.3 $[M+H]^+$), **7** (m/z = 426.4 $[M+H]^+$), **1** (m/z = 501.3 $[M+H]^+$) and **9** (m/z = 587.4 $[M+H]^+$) in a 1:1:1:1 molar ratio.

Table 2.1. Abundances of the signals for each compound observed in the ESI-MS spectrum shown in Figure 2.9. Four separate measurements are shown. The correction factors were determined from the average intensity of four measurements.

Compound	m/z $[M+H]^+$	ESI-MS 1	ESI-MS 2	ESI-MS 3	ESI-MS 4	Mean	Correction Factor
8	340.3	90.62	89.37	91.87	91.87	90.9325	**0.7597**
7	426.4	45.62	45.62	46.25	45.62	45.7775	**1.5090**
1	501.3	39.37	37.50	40.62	40.62	39.5275	**1.7476**
9	587.4	99.37	100.62	100.31	100.00	100.075	**0.6902**

2.3.5.2 MS Analysis of a Mixture of 1 and 7 (1:1 molar ratio) After Operation.

A mixture of the three-foothold track-walker conjugate **1** and walker-free track **7** in a 1:1 molar ratio was subjected to walking conditions ([D_6]DMSO, 20 mM, 298 K). The mixture was analysed periodically by ESI-MS. The results after 3 days of exchange are shown in Figure 2.11. After 3 days at RT, scrambling compounds **8** and **9** were present as approximately 2.7% of the reaction mixture.[12] Double attachment of a walker to a single track could not be quantified but nevertheless had to be taken into consideration in order to estimate the overall loss of processivity (see Scheme 2.6). If we assume that products of an intermolecular exchange which cannot be quantified in this experiment contribute to the processivity loss equally as **8** and **9** (see section 2.3.4), the scrambling products would represent at most 5.5% of the reaction mixture after 3 days.

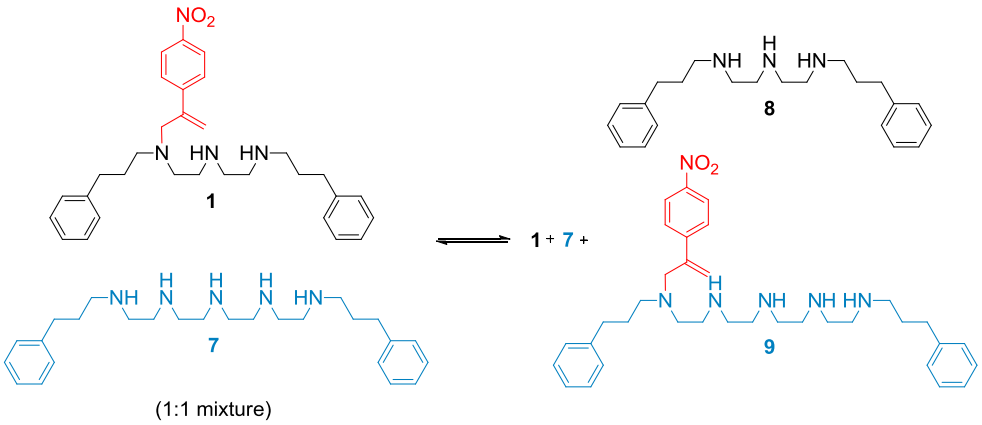

Scheme 2.7. Pathway of processivity loss of compound **1** *via* intermolecular Michael/retro-Michael reaction monitored in track crossover experiment.

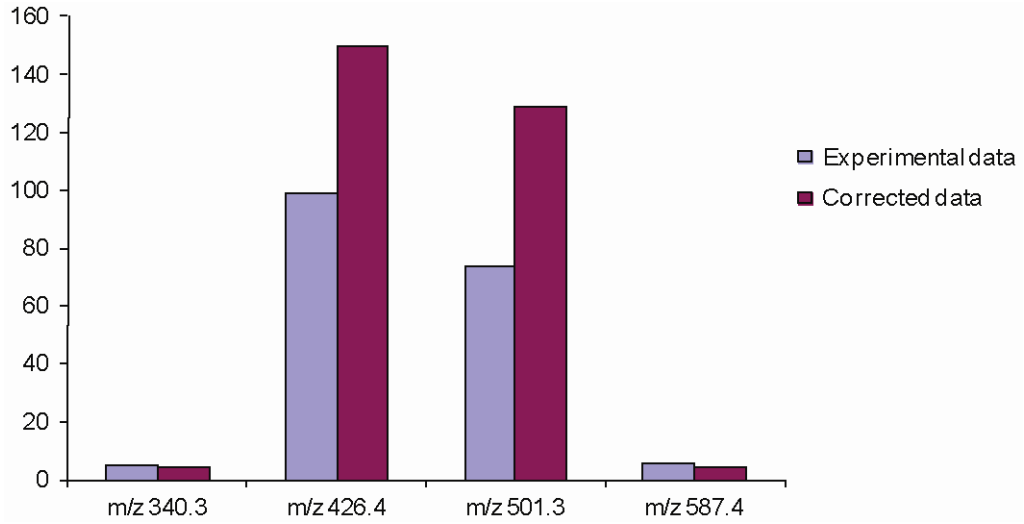

Figure 2.11. Chart of experimental and corrected data from the ESI-MS analysis of the mixture of compounds **7** (m/z = 426.4 $[M+H]^+$) and **1** (m/z = 501.3 $[M+H]^+$) in a 1:1 molar ratio after 3 days in DMSO (20 mM) at 298 K. Slowly appearing compounds **8** (m/z = 340.3 $[M+H]^+$) and **9** (m/z = 587.4 $[M+H]^+$) contribute to the processivity loss of at most 5.5%.

2.3.5.3 MS Analysis of Mixture of 8 and 9 (1:1 molar ratio) After Operation.

A mixture of five foothold track-walker conjugate **9** and walker-free track **8** in a 1:1 molar ratio (compounds were synthesised as reference materials for normalisation of the MS spectrum) was subjected to walking conditions ([D_6]DMSO, 20 mM, 298 K). The mixture was analysed periodically by ESI-MS. The results after 3 days of exchange are shown in Figure 2.12. After 3 days at 20 mM, scrambled compounds **7** and **1** accounted for approximately 2.1% of the reaction mixture. If we assume that products of an intermolecular exchange which cannot be quantified in this experiment contribute to the processivity loss equally as **1** and **7** (see section 2.3.4), the scrambling products would represent at most 4.2% of the reaction mixture after 3 days.

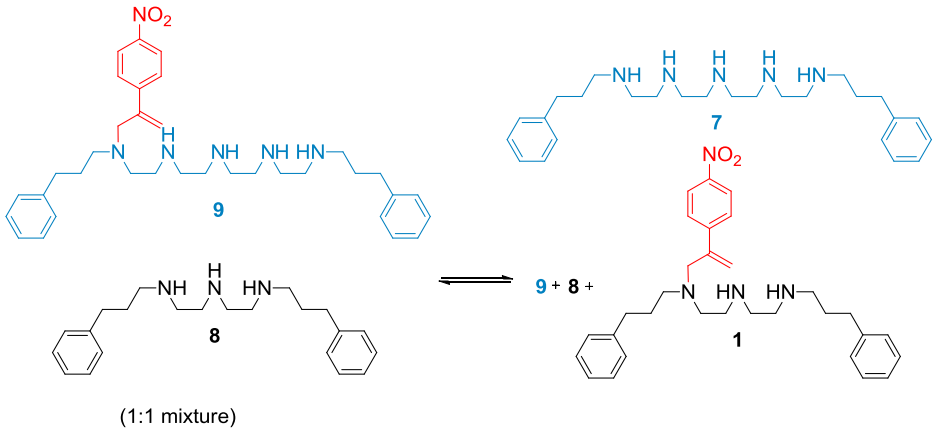

Scheme 2.8. Pathway of processivity loss of compound **9** *via* intermolecular Michael/retro-Michael reaction monitored in track crossover experiment.

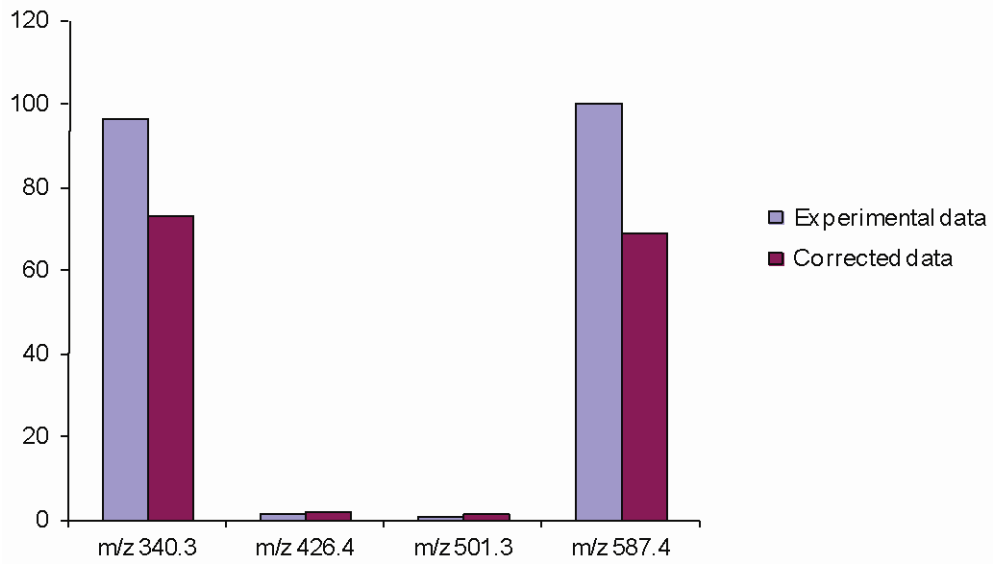

Figure 2.12. Chart of experimental and corrected data from the ESI-MS analysis of the mixture of compounds **8** (m/z = 340.3 $[M+H]^+$) and **9** (m/z = 587.4 $[M+H]^+$) in a 1:1 molar ratio after 3 days in DMSO (20 mM) at 298 K. Slowly appearing compounds **7** (m/z = 426.4 $[M+H]^+$) and **1** (m/z = 501.3 $[M+H]^+$) contribute to the processivity loss of at most 4.2%.

2.3.5.4 Mean Step Number Determination.

In both cases (the exchange of **1** or **9** in the presence of **7** or **8**, respectively) the system proved to be highly processive; during 3 days of exchange the walker takes an average of 48 steps (as $t_{1/2}$ = 1.5 h for one step) and during this time less than 6% of the walkers have detached from their original track or have been transferred to a different walker-track system.[2] The fraction of molecules in which the walker moiety is still connected to its original track, can be described by an exponential function (equation and graph shown in Figure 2.13). Accordingly, under these conditions each α-methylene-4-nitrostyrene unit has taken on average ~530 'steps' between amine groups before losing processivity (50 % of the walker units were no longer connected to the original track or were transferred to another walker-track conjugate), which is several times the processivity of most wild-type kinesin motor proteins (typical mean step number 75–175).[13]

Table 2.2. Summary of the key deductions drawn from the experimental data. The processivity loss of 6% during 3 days is the maximum amount of scrambling products, based on the experimental results. The processivity loss during one step results from division of the previous value by the number of steps taken on average by the walker in 3 days (48 steps). The exponential function for processivity decay describes the level of processivity in the system p after n steps, where p_0 is the level of processivity to start with (typically: p_0 = 1). The mean step number is calculated from the exponential function by equation in Figure 2.13 and returns the number of steps after which 50 % of the walker units are no longer connected to the original track or are transferred to another walker-track conjugate.

$t_{1/2}$ (h)	Number of steps taken in 3 days	Maximum processivity loss in 3 days (%)	Processivity loss during 1 step (%)	Function for processivity decay (p; n = steps)	Mean step number n_{mean}
1.5	48	6	0.125	$p = p_0(1\text{-}0.00125)^n$	532

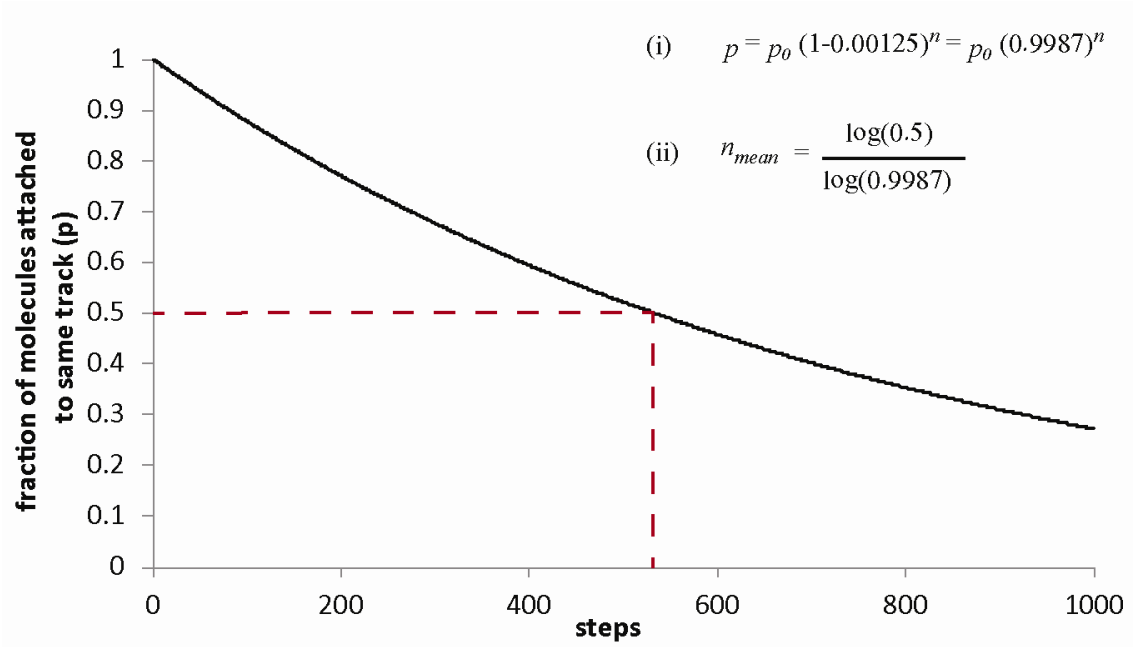

Figure 2.13. Decay of processivity as described by the exponential function (i). p = fraction of molecules attached to same track; p_0 = initial fraction of molecules connected to original track (in the graph p_0 = 1.0); n = number steps. Mean step number n_{mean} was calculated according to equation (ii).

2.3.6 Fluorescence Quenching as an indication of the Walker Migration

2.3.6.1 Fluorescence of Model Compounds.

Having established that an α-methylene-4-nitrostyrene walker can exchange between the amino groups of a di- or triamine track in a stepwise fashion with a high degree of processivity, we sought to demonstrate that the walker could migrate along a longer track through this mechanism and perform an observable task: quenching of the fluorescence of an anthracene group sited at one end of the track as a result of the walking progress. Compounds **10** and **11** provided some insights into the influence of the length of a polyamine tracks on the anthracene fluorescence.[14]

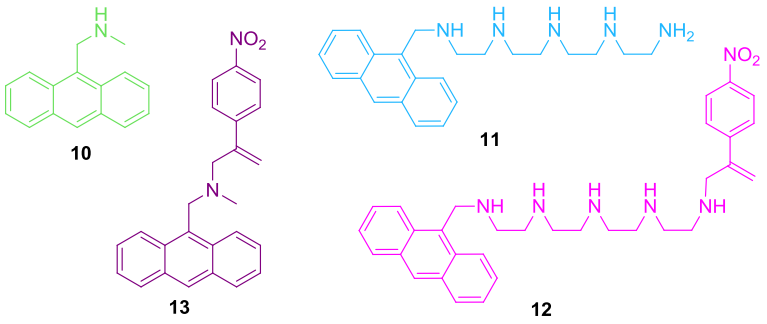

Figure 2.14. Model compounds used for fluorescence experiments

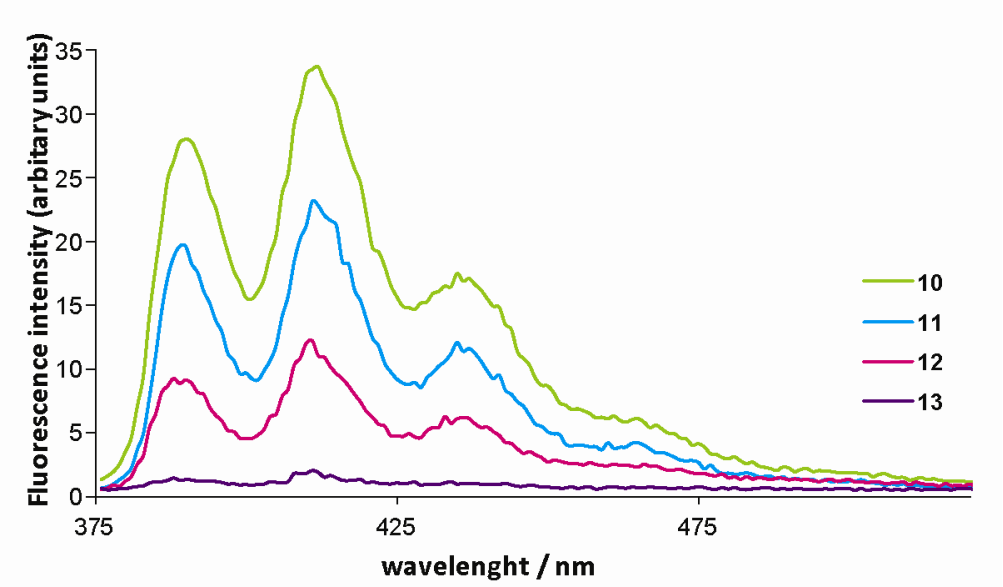

Figure 2.15. Fluorescence emission spectra of model compounds **10**–**13** in EtOH (1.0×10^{-5} M) (λ_{exc} = 366 nm, λ_{em} = 413 nm).

To determine if the distance between the walker unit and a fluorophore in the track influences its fluorescence, model compounds **12** and **13** were synthesised (see Experimental Section for details). The fluorescence intensity of the four model compounds (Figure 2.14) was measured and compared in EtOH (spectrophotometric grade) at 1.0×10^{-5} M. The results are shown in Figure 2.15. Fluorescence of **10** was the most intense, followed by compound **11** in which anthracene was linked to a pentaamine side chain.[15] Comparison of fluorescence intensity of compounds **11** and **12** showed that attachment of the walker unit at the far end of a pentamine track resulted in additional quenching of the fluorescence. Moreover, a drastic decrease of emission intensity was observed when the walker unit was attached close to the anthracene moiety as shown in the fluorescence spectrum of compound **13** in Figure 2.15.

This study proved that the inter-chromophoric distance between the walker unit and the anthracene moiety in the polyamine track very significantly influenced its fluorescence. When the walker unit was located close to the anthracene, the fluorescence quenching was very effective.

2.3.6.2 Fluorescence Lifetime Measurements.

To establish the mechanism involved in the fluorescence quenching, lifetime data were obtained in two solvents (EtOH and DMSO which was the solvent that walking process occurs in) on samples of compounds varying in the quencher (walker unit) presence and distance from the fluorophore. If a decrease in the fluorophore lifetime occurs in the series, quenching is an additional process which depopulates the excited state and therefore

decrease in fluorescence is due to dynamic quenching. In static quenching a complexed fluorophore forms a non-fluorescent species in the ground state. Therefore only the uncomplexed fluorophore is observed during the measurement and lifetime (τ) remains unchanged.[16] Fluorescence decays of **10**, **12** and **13** were fitted using a multiexponential decay equation (two or three distinct lifetimes) with the minimum number of decay components required to obtain a χ^2 value close to 1. The same fluorescence lifetimes of about 14 ns were observed for all three compounds in DMSO showing that static quenching occurs in this system (see Table 2.3).

Table 2.3. Fluorescence lifetime parameters τ, α χ^2 denote the lifetime, relative molecular population of the species and a nonlinear least-squares fitting analysis for compounds **10**, **12** and **13**. In all cases, three data sets were taken and the average values are given.

	τ (ns)	τ error (%)	α (rel. mol. population)	χ^2
EtOH	**12**			
τ1	2.17	2.7	0.57	
τ2	7.34	0.9	0.43	1.156
	10			
τ1	1.47	39.9	0.05	
τ2	7.09	0.4	0.95	1.294
	13			
τ1	2.31	3.2	0.67	
τ2	7.41	2.1	0.33	1.132
DMSO	**12**			
τ1	1.41	9.1	0.17	
τ2	8.94	1.3	0.76	
τ3	**12.01**	6.9	0.07	1.169
	10			
τ1	1.83	24.0	0.09	
τ2	7.03	3.2	0.85	
τ3	**14.00**	14.6	0.06	1.169
	13			
τ1	1.22	15.5	0.24	
τ2	6.61	7.1	0.55	
τ3	**15.65**	7.4	0.21	1.044

2.3.6.3 Influence of Concentration on the Fluorescence Intensity.

The fluorescence intensity of several solutions of compound **10** in EtOH at increasing concentrations was measured. Measurements showed a linear increase of fluorescence intensity with concentration. This showed that quenching was due to an intramolecular interaction. If quenching was due to intermolecular interactions (for example self-quenching by aggregation of fluorophores), increase in concentration would on average make quenching events more probable and result in a non-linear dependence of fluorescence on concentration.

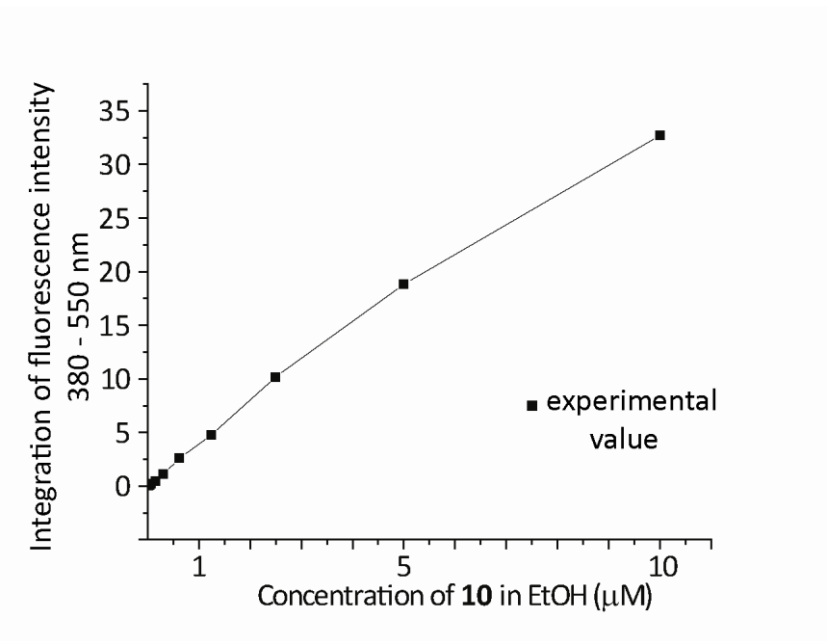

Figure 2.16. Graph showing a linear increase of fluorescence intensity (integration of fluorescence intensity (380–550 nm) after removing the background) with concentration of **10** in EtOH.

2.3.6.4 Walking Upon Five Foothold Track Monitored by ^{1}H NMR and Fluorescence Spectroscopy.

Having confirmed that the position of the walker does influence the fluorescence of an anthracene fluorophore located at the far end of the polyamine track and the fluorescence quenching is due to the intramolecular interaction, a five-foothold walker–track conjugate **14**, incorporating an anthracene group at the far end of the pentaethylenimine track from the initial site of the walker attachment, was prepared as shown in Scheme 2.9. Pentaamine **15** was desymmetrised *via* reductive amination with 3-phenylpropionaldehyde and subsequent reaction with 9-anthraldehyde to give **16**. The α-methylene-4-nitrostyrene walker unit (**W**) was introduced onto both unprotected secondary amine footholds. A single positional isomer with **W** on the amine furthest from the anthracene group was separated by chromatography. Subsequent CF_3CO_2H mediated Boc deprotection and neutralisation gave compound **14** in which the walker was free to migrate along the five-foothold track from its original position.

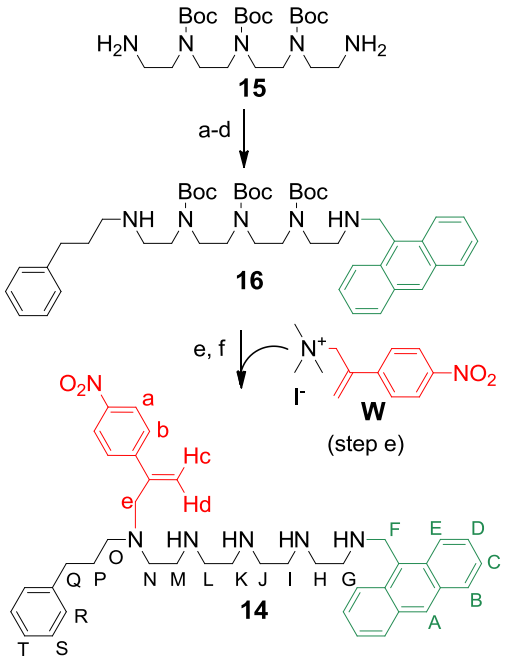

Scheme 2.9. Synthesis of five-foothold walker–track conjugate **14**. a) 3-phenylpropionaldehyde, EtOH, RT, 72 h; b) $NaBH_4$, RT, 24 h, 60 % (two steps); c) 9-anthraldehyde, EtOH, RT, 72 h; d) $NaBH_4$, RT, 24 h, 55 % (two steps); e) MeOH, $^iPr_2NEt$, 50 °C, 72 h, 30 %; f) CH_2Cl_2, CF_3CO_2H, 5 h, $NaHCO_{3aq.}$, quantitative.

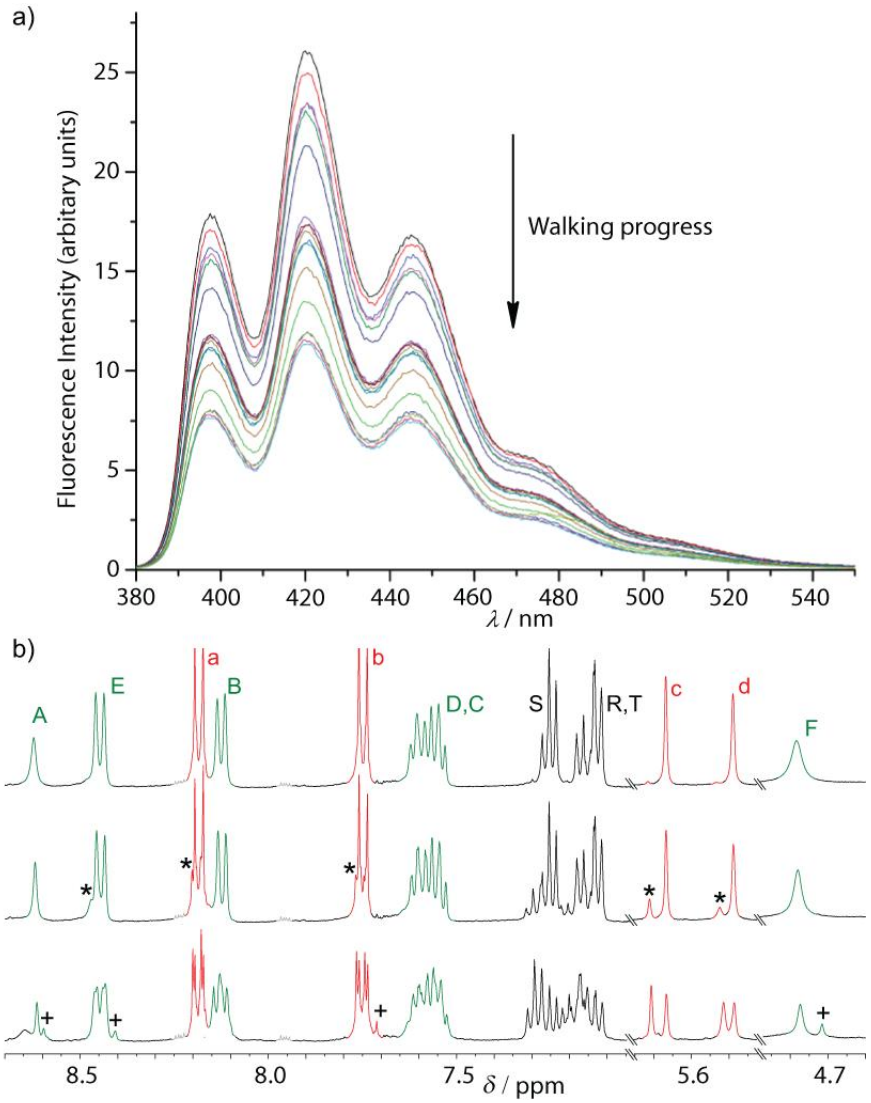

Figure 2.17. a) Fluorescence quenching (λ_{exc} = 366 nm, λ_{em} = 413 nm) in **14** (DMSO + 0.25% CF_3CO_2H, 1.78 × 10^{-5} M) as a result of migration of α-methylene-4-nitrostyrene along the oligoamine track. b) Partial ^{1}H NMR spectra (400 MHz, [D_6]DMSO, 20 mM, 298 K) of the reaction mixture at: *t* = 5 min (top); *t* = 1 h (middle); *t* = 6.5 h (bottom). The key signals are indicative of the walker position: * walkers attached to the inner three amine footholds. + walkers close to the anthrylmethylamine group. The lettering and colouring corresponds to the proton labelling shown in Scheme 2.9.

Molecular walker-track conjugate **14** was submitted to walking conditions (DMSO, 7.14 × 10^{-5} M, 298 K) and its fluorescence emission spectrum recorded periodically.[17] The fluorescence intensity diminished by 54% over 6.5 h after which time the fluorescence intensity became almost invariant (Figure 2.17a). The walker migration in **14** was also monitored by ^{1}H NMR spectroscopy, albeit under more concentrated conditions to give a suitable signal-to-noise ratio ([D_6]DMSO, 20 mM, 298 K, Figure 2.17b). The reaction was monitored every 0.5 h. Signals indicating walker unit migration along the track have appeared instantly. Quantification of each positional isomer was not possible due to the

chemical similarity of inner footholds, however after 3 h it was possible to identify that a proportion of walker units reached final footholds in the track due to the shift of the methylene protons H_f (δ_{Hf} = 4.76 ppm) close to the anthracene unit, caused by the presence of the α-methylene-4-nitrostyrene walker ($\Delta\delta_{Hf}$ = 0.06 ppm). After 6.5 h no further changes were observed in the ^{1}H NMR spectrum until signals attributed to degradation of the anthracene moiety started to appear.[18]Accordingly, both ^{1}H NMR and fluorescence measurements indicated that the walking of the *α*-methylene-4-nitrostyrene unit proceeded back-and-forth along the pentaethylenimine track producing a steady distribution of walkers over the five-foothold track after 6.5 h.

2.4 Conclusions

In conclusion, we have described a system in which a small synthetic molecular walker migrates along oligoamine tracks without external intervention moving towards an equilibrium distribution of walkers on the track. In terms of synthetic molecular machine properties, this walker-track system is reminiscent of a rotaxane-based molecular shuttle with degenerate stations:[19]

The walker-track system uses a transferable covalent linkage between the *α*-methylene-4-nitrostyrene and the oligoethylenimine to ensure processivity and determine the preferred positions of the substrate on the track; in a rotaxane-based molecular shuttle a mechanical linkage confers the former property and attractive non-covalent interactions between a macrocycle and specific sites on the thread can be used to achieve the latter.

The small-molecule walker migration is processive and takes place predominantly in a stepwise fashion *via* a Michael-retro-Michael addition mechanism between adjacent amines. The position of the walker can be precisely determined on short tracks by ^{1}H NMR spectroscopy and on longer tracks the progress of walker migration can be inferred by performance of a simple task: quenching of the fluorescence of an anthracene group at one end of the track by the walker.

2.5 Experimental Section

2.5.1.General Remarks on Experimental Data.

Unless otherwise stated, all reagents were purchased from commercial sources and used without further purification. Dry CH_2Cl_2, $CHCl_3$ and THF were obtained by passing the solvent (HPLC grade) through an activated alumina column on a PureSolv™ solvent purification system (InnovativeTechnologies, Inc., MA). Dry DMF, EtOH and MeOH were purchased from Sigma-Aldrich. Flash column chromatography was carried out using Kieselgel C60 (Merck, Germany) as the stationary phase. Analytical TLC was performed on precoated silica gel plates (0.25 mm thick, 60 F254, Merck, Germany) and observed under UV light or visualised using ninhydrin dip/heating. All ^{1}H and ^{13}C NMR spectra were recorded on Bruker AV 400, AV 500 (cryoprobe), at a constant temperature of 298 K. Chemical shifts are reported in parts per million and referenced to residual solvent. Coupling constants (*J*) are reported in Hertz (Hz). Standard abbreviations indicating multiplicity were used as follows: m = multiplet, p = pentet, q = quartet, t = triplet, d = doublet, s = singlet, b = broad. Assignment of the ^{1}H NMR signals was accomplished by two-dimensional NMR spectroscopy (COSY, NOESY, HSQC). All melting points were determined using a Sanyo Gallenkamp apparatus. Mass spectrometric analysis was carried out by the mass spectrometry services at the University of Edinburgh and by the EPSRC National Centre at the University of Wales, Swansea.

Steady-state fluorescence intensity measurements were performed on an Edinburgh Instruments FS900 spectrofluorometer (Edinburgh Instruments) with a 5 nm bandwidth. The cuvette path lengths were 10 mm. Time-correlated single-photon counting was performed with a time-resolved fluorimeter equipped with an Edinburgh Instruments TCC900 single photon counting card, 376 nm pulsed LED driven by a PDL 800-B pulsed diode laser driver (PicoQuant Gmbh) and a PMH-100-3 single photon counting photomultiplier tube (Becker & Hickl Gmbh). A 405 nm pulsed laser (Edinburgh Instruments) was also sometimes used. Emission wavelengths were selected with a monochromator. Polarisation was applied using quartz Glan– Thompson polarisers and the magic angle was used. Cuvette pathlengths were 10 mm and the emission bandpass was 20 nm. Fluorescence decays were fitted using a multiexponential decay equation with the minimum number of decay components required to obtain a $\chi 2$ value close to 1.

2.5.2 Synthesis Overview.

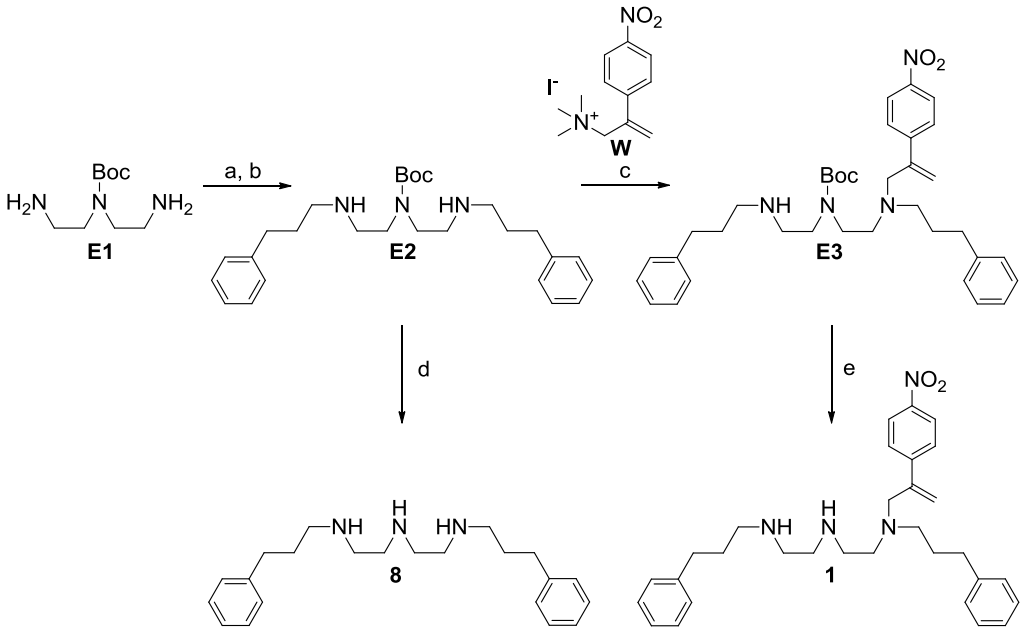

Scheme E2.1. a) 3-phenylpropionaldehyde, EtOH, RT, 72 h; b) $NaBH_4$, RT, 24 h, 23% (two steps); c) MeOH, $^{i}Pr_2NEt$, 50 °C, 72 h, 29%; d) CH_2Cl_2, CF_3CO_2H, 5 h, 98%; e) CH_2Cl_2, CF_3CO_2H, 5 h, 97%.

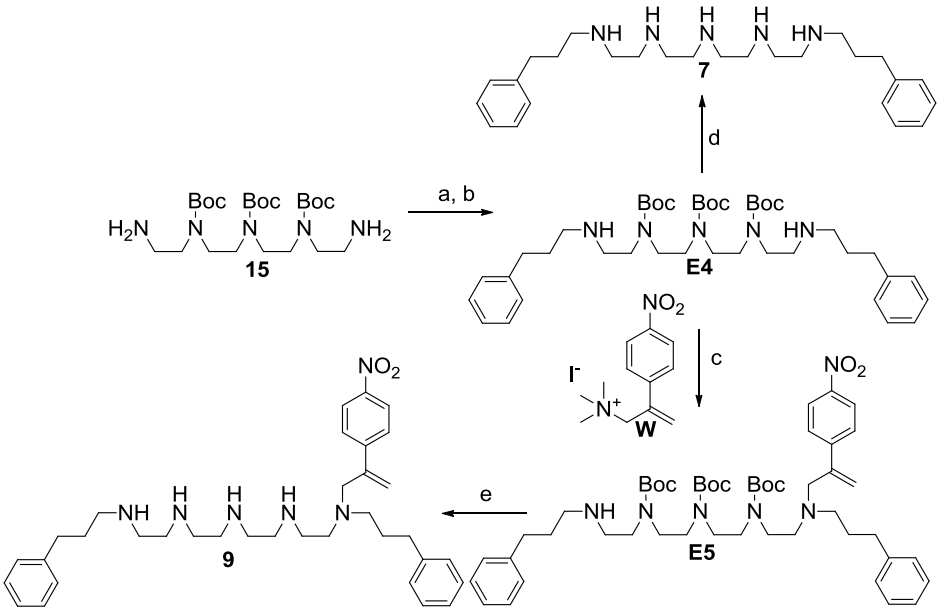

Scheme E2.2. a) 3-phenylpropionaldehyde, EtOH, RT, 72 h; b) $NaBH_4$, RT, 24 h, 21% (two steps); c) MeOH, $^{i}Pr_2NEt$, 50 °C, 72 h, 47%; d) CH_2Cl_2, CF_3CO_2H, 5 h, 85%; e) CH_2Cl_2, CF_3CO_2H, 5 h, quant.

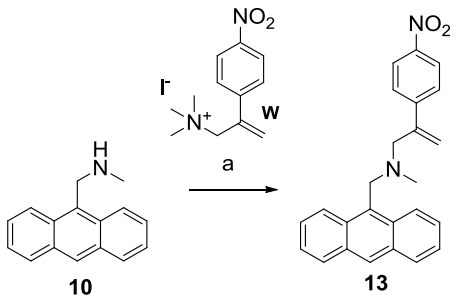

Scheme E2.3. a) MeOH, $^{i}Pr_2NEt$, 50 °C, 72 h, 79%.

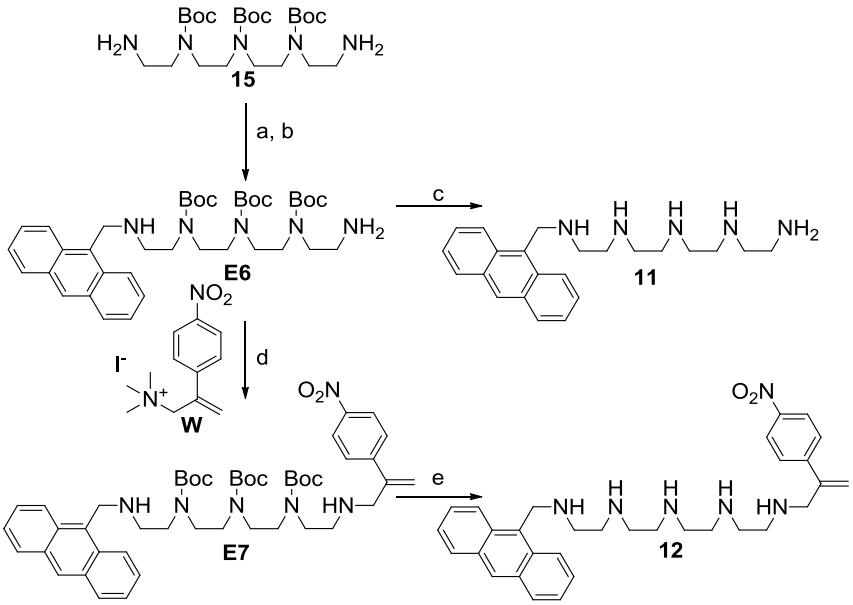

Scheme E2.4. a) 9-anthraldehyde, EtOH, RT, 72 h; b) $NaBH_4$, RT, 24 h, 21% (two steps); c) CH_2Cl_2, CF_3CO_2H, 5 h, 79%; d) MeOH, $^{i}Pr_2NEt$, 50 °C, 72 h, 20%; e) CH_2Cl_2, CF_3CO_2H, 5 h, 93%.

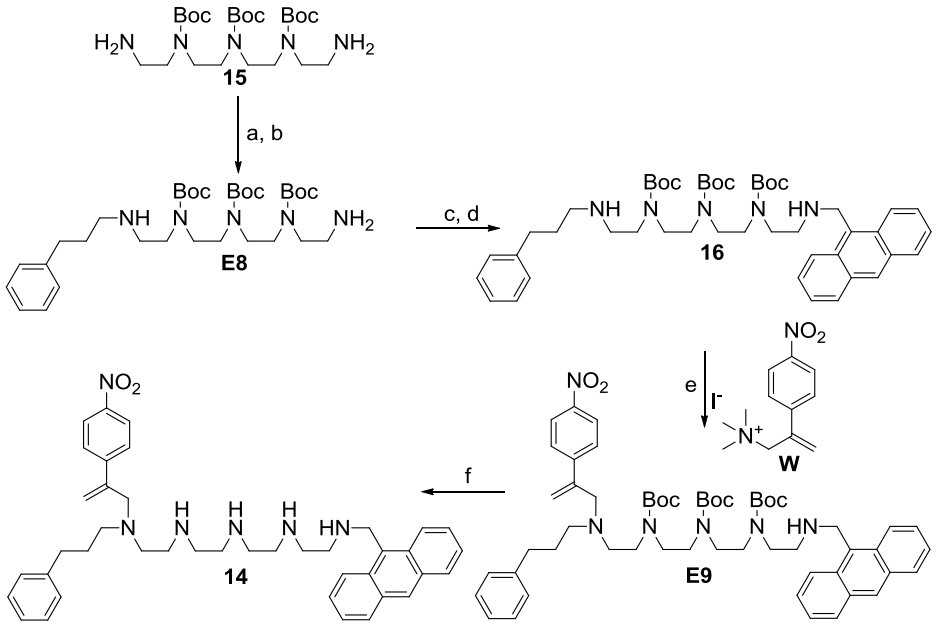

Scheme E2.5. a) 3-phenylpropionaldehyde, EtOH, RT, 72 h; b) $NaBH_4$, RT, 24 h, 38% (two steps); c) 9-anthraldehyde, EtOH, RT, 72 h; d) $NaBH_4$, RT, 24 h, 55% (two steps); e) MeOH, $^{i}Pr_2NEt$, 50 °C, 72 h, 42%; f) CH_2Cl_2, CF_3CO_2H, 5 h, quant.

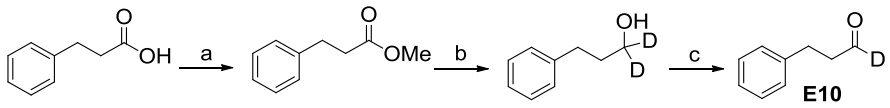

Scheme E2.6. a) $SOCl_2$, MeOH, RT, 15 h, quant. b) $LiAlD_4$, THF, RT, 15 h, 91%; c) DMP, CH_2Cl_2, RT, 16 h, 79%.

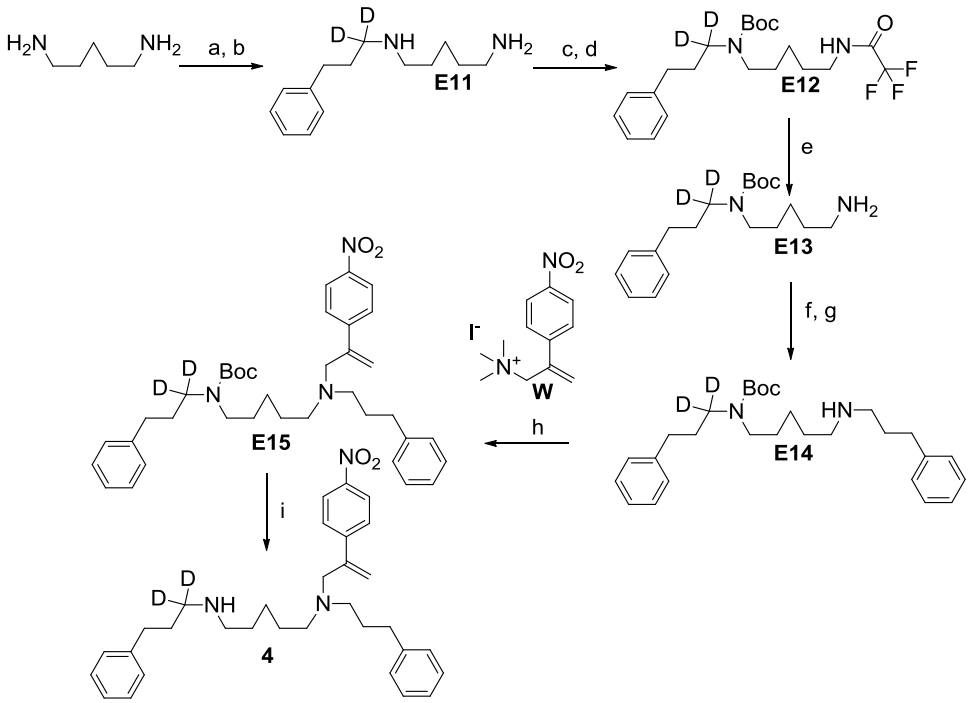

Scheme E2.7. a) 3-phenylpropionaldehyde-d, EtOH, RT, 72 h; b) $NaBD_4$, RT, 24 h, 44% (two steps); c) CF_3CO_2Et, CH_2Cl_2, 0 °C, 2 h; d) Boc_2O, Et_3N, RT, 12 h, 76% (two steps); e) $NaOH_{aq}$, MeOH, RT, 5 h; f) 3-phenylpropionaldehyde, EtOH, RT, 72 h; g) $NaBH_4$, RT, 24 h, 41% (two steps); h) MeOH, $^{i}Pr_2NEt$, 50 °C, 72 h, 88%; i) CH_2Cl_2, CF_3CO_2H, 5 h, 52%.

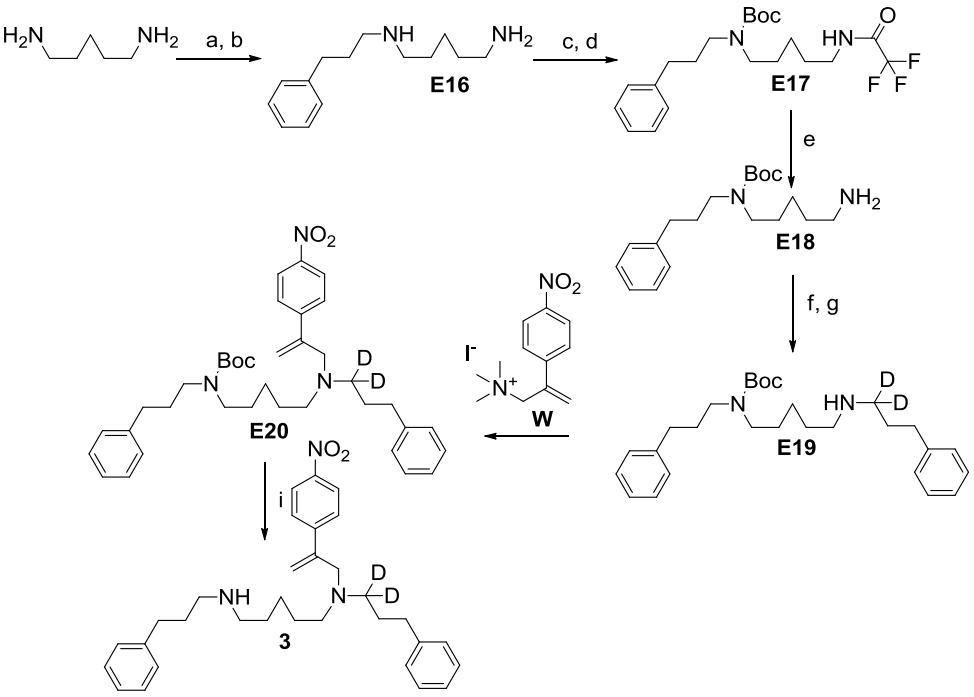

Scheme E2.8. a) 3-phenylpropionaldehyde, EtOH, RT, 72 h; b) $NaBH_4$, RT, 24 h, 35% (two steps); c) CF_3CO_2Et, CH_2Cl_2, 0 °C, 2 h; d) Boc_2O, Et_3N, RT, 12 h, 75% (two steps); e) $NaOH_{aq}$, MeOH, RT, 5 h, 71%; f) 3-phenylpropionaldehyde-*d*, EtOH, RT, 72 h; g) $NaBD_4$, RT, 24 h, 47% (two steps); h) MeOH, $^{i}Pr_2NEt$, 50 °C, 72 h, 77%; i) CH_2Cl_2, CF_3CO_2H, 5 h, 52%.

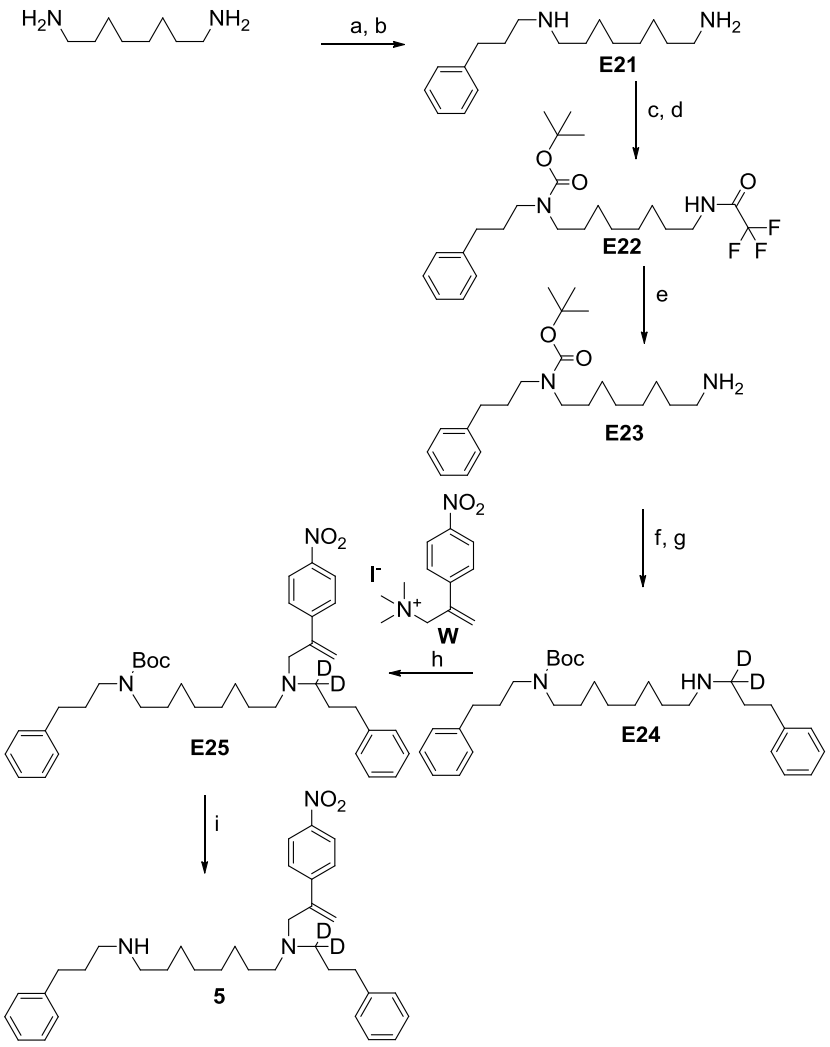

Scheme E2.9. a) 3-phenylpropionaldehyde, EtOH, RT, 72 h; b) $NaBH_4$, RT, 24 h, 40% (two steps); c) CF_3CO_2Et, CH_2Cl_2, 0 °C, 2 h; d) Boc_2O, Et_3N, RT, 12 h, 88% (two steps); e) $NaOH_{aq}$, MeOH, RT, 5 h, 67%; f) 3-phenylpropionaldehyde-*d*, EtOH, RT, 72 h; g) $NaBD_4$, RT, 24 h, 47% (two steps); h) MeOH, $^{i}Pr_2NEt$, 50 °C, 72 h, 76%; i) CH_2Cl_2, CF_3CO_2H, 5 h, 53%.

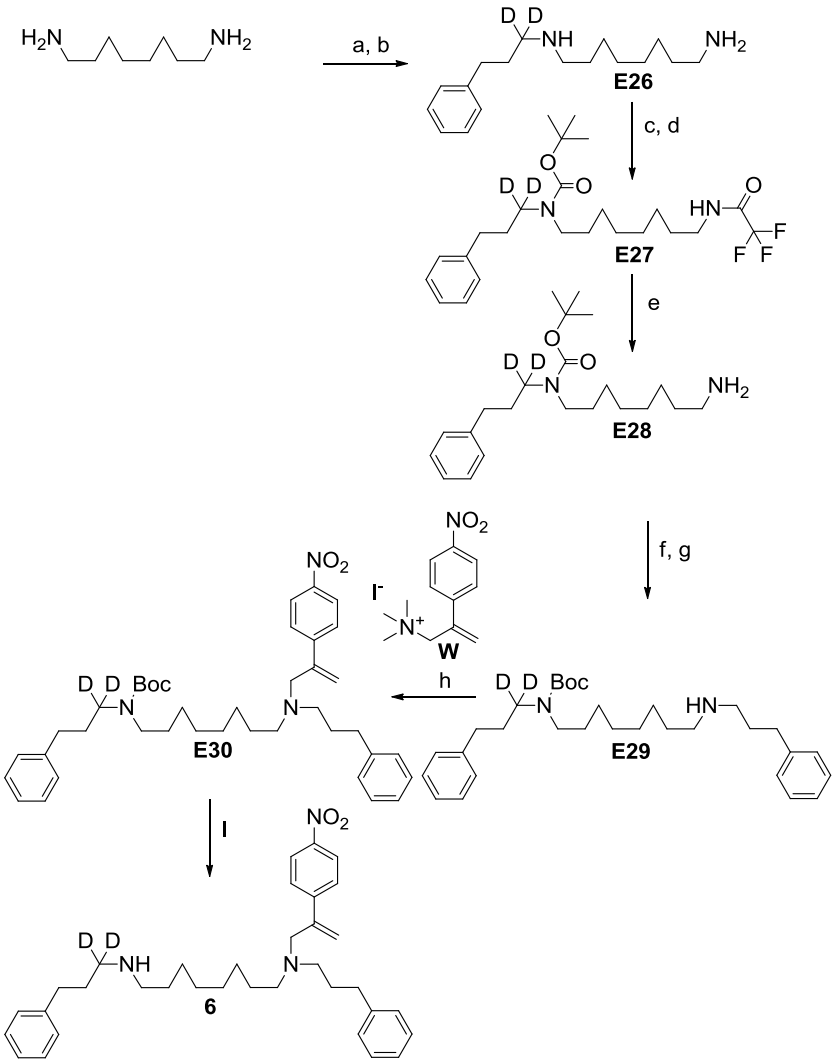

Scheme E2.10. a) 3-phenylpropionaldehyde-*d*, EtOH, RT, 72 h; b) $NaBD_4$, RT, 24 h, 33% (two steps); c) CF_3CO_2Et, CH_2Cl_2, 0 °C, 2 h; d) Boc_2O, Et_3N, RT, 12 h, 47% (two steps); e) $NaOH_{aq}$, MeOH, RT, 5 h, 20%; f) 3-phenylpropionaldehyde, EtOH, RT, 72 h; g) $NaBH_4$, RT, 24 h, 20% (two steps); h) MeOH, $^{i}Pr_2NEt$, 50 °C, 72 h, 80%; i) CH_2Cl_2, CF_3CO_2H, 5 h, quant.

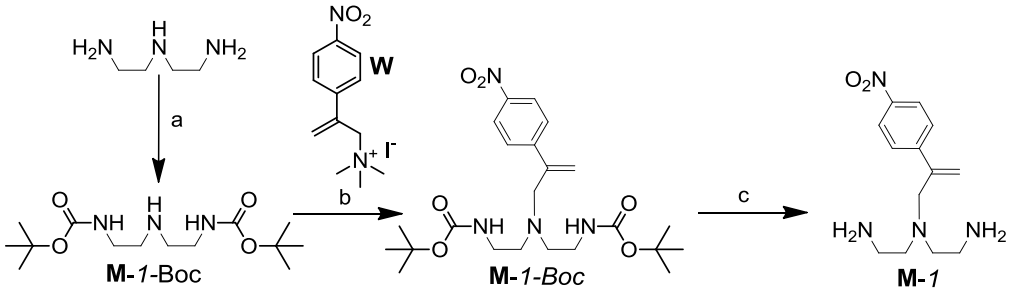

Scheme E2.11. Walker attachment followed by Boc deprotection of the track. Reaction conditions: a) Boc-ON, THF, 3 h, 0 °C→RT,99 %, b) $^{i}Pr_2NEt$, MeOH, 50 °C, 4 days, 83%, c) CF_3CO_2H, CH_2Cl_2, 1 h; $NaHCO_3$,

2.5.3 Synthetic Procedures and Characterization Data

Synthesis of (W)

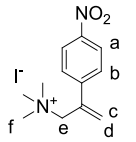

Synthesised according to a literature procedure.[6] Isolated as yellow solid. ^{1}H NMR (500 MHz, DMSO-d$_6$) δ = 8.35 – 8.17 (m, 2H, H$_a$), 7.98 – 7.81 (m, 2H, H$_b$), 6.14 (s, 1H, H$_c$), 5.98 (s, 1H, H$_d$), 4.61 (s, 2H, H$_e$), 2.97 (s, 9H, H$_f$). ^{13}C NMR (126 MHz, DMSO-d$_6$) δ = 147.70, 146.06, 136.42, 132.41, 128.43, 124.36, 66.83, 53.04. m.p. 219–220°C with decomp.

Synthesis of (E1)

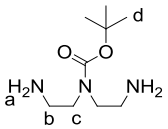

Synthesised according to a literature procedure.[20] Isolated as clear oil, used directly in the next step without further purification. ^{1}H NMR (400 MHz, CDCl$_3$): δ = 3.33 (t, J = 6 Hz, 4H, H$_c$), 2.92 (t, J = 5.8 Hz, 4H, H$_b$), 1.46 (s, 9H, H$_d$), 1.28 (bs, 4H, H$_a$).

Synthesis of (E2)

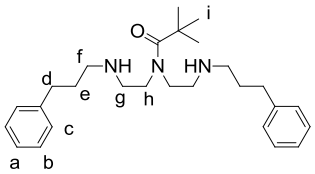

To a solution of tert-butyl *N*,*N*'-bis(2-aminoethyl)carbamate **E1** (863 mg, 4.25 mmol, 1.0 equiv.) in dry EtOH (250 mL), 3-phenylpropionaldehyde (1.00 mL, 7.65 mmol, 1.8 equiv.) was added in one portion. The reaction was stirred under N_2 for 24 h at room temperature. $NaBH_4$ (1.6 g, 42.3 mmol, 10 equiv.) was then added in portions and reaction was kept stirring under N_2 for another 24 h. After this time H_2O (100 mL) was added to the reaction mixture and product was extracted with CH_2Cl_2 (3 × 100 mL). The combined organic layers were washed with brine, dried over $MgSO_4$ and the solvent was removed under reduced pressure. Column chromatography (SiO_2, MeOH/CH_2Cl_2/NH_3 4:96:1) gave **E2** (411 mg, 23%) as a colourless oil. ^{1}H NMR (400 MHz, CDCl$_3$): δ = 7.36 – 7.21 (m, 4H, H$_b$), 7.22 – 6.99 (m, 6H, H$_{a,c}$), 3.54 – 3.22 (m, 4H, H$_h$), 2.95 – 2.76 (m, 4H, H$_g$), 2.68 (t, J = 7.5 Hz, 4H, H$_f$), 2.63 (t, J = 7.7 Hz, 4H, H$_d$), 1.84 (apparent as dt, J = 14.9, 7.7 Hz, 4H, H$_e$), 1.44 (s, 9H, H$_i$). ^{13}C NMR (101 MHz, CDCl$_3$) δ = 155.80, 141.39, 128.46, 128.34, 126.02, 80.18, 48.56,

47.88, 47.85, 33.38, 30.68, 28.45 (3C). HRMS ESI $[M+H]^+$ $C_{27}H_{42}O_2N_3$ calc. 440.3272, found 440.3268.

Synthesis of (E3)

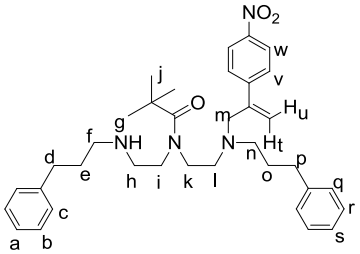

To a degassed solution of **E2** (156 mg, 0.35 mmol, 1.0 equiv.) in dry MeOH (30 mL), **W** (100 mg, 0.29 mmol, 0.82 equiv.) was added in one portion. Reaction mixture was kept stirring under N_2 at 50 °C for 72 h in the presence of $^{i}Pr_2NEt$ (183 µL, 1.05 mmol, 3 equiv.). After this time, reaction was cooled to room temperature and H_2O (30 mL) was added. Mixture was extracted with CH_2Cl_2 (2 × 30 mL), dried over $MgSO_4$ and the solvents were removed under reduced pressure. Column chromatography (SiO_2, MeOH/CH_2Cl_2, 2:98) gave **E3** (40 mg, 29%) as an orange oil. ^{1}H NMR (400 MHz, $CDCl_3$): δ = 8.17 (d, J = 8.6 Hz, 2H, H_w), 7.61 (d, J = 8.7 Hz, 2H, H_v), 7.33–7.24 (m, 4H, $H_{b,r}$), 7.24–7.17 (m, 4H, $H_{c,q}$), 7.16–7.10 (m, 2H, $H_{a,s}$), 5.55 (s, 1H, H_u), 5.43 (s, 1H, H_t), 3.51 (s, 2H, H_m), 3.37–3,11 (m, 4H, $H_{k,l}$), 2.86 – 2.42 (series of m, 12H, $H_{h,i,d,f,n,p}$), 1.90 – 1.74 (m, 4H, $H_{e,o}$), 1.45 (s, 9H, H_j). ^{13}C NMR (126 MHz, $CDCl_3$): δ = 156.03, 147.10, 146.67, 144.11, 141.84, 141.68, 128.43, 128.37, 128.35, 128.33, 127.26, 125.96, 125.88, 123.45, 118.84, 58.96, 53.54, 51.59, 48.34, 48.30, 33.54, 33.41, 31.42, 30.79, 29.72, 29.16, 28.46 (3C), 28.23. HRMS ESI $[M+H]^+$ $C_{36}H_{49}O_4N_4$ calc. 601.3748, found 601.3731.

Synthesis of (1)

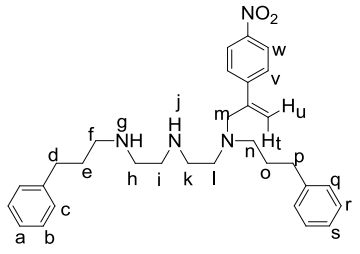

To a solution of **E3** (40 mg, 0.07 mmol, 1.0 equiv.) in CH_2Cl_2 (3 mL), trifluoroacetic acid (3 mL) was added dropwise. The reaction was left stirring open to air, at RT, and the disappearance of the substrate was monitored by ESI-MS. After 5 h, 5 mL of CH_2Cl_2 was added to the reaction mixture and solution was carefully neutralised using $NaHCO_3$ (sat). The layers were separated and the aqueous layer was extracted with CH_2Cl_2 (5 mL). The

combined organic layers were dried over $MgSO_4$ and the solvents were removed under reduced pressure to give **1** (32 mg, 97%) as an orange oil. ^{1}H NMR (500 MHz, $CDCl_3$): δ = 8.29 – 8.09 (m, 2H, H_w), 7.60 – 7.50 (m, 2H, H_v), 7.31 – 7.23 (m, 4H, $H_{b,r}$), 7.23–7.17 (m, 2H, $H_{a,s}$), 7.17 – 7.07 (m, 4H, $H_{q,c}$), 5.54 (s, 1H, H_u), 5.42 (s, 1H, H_t), 3.56 (s, 2H, H_m), 2.79 (apparent as s, 4H, $H_{h,i}$), 2.77 – 2.67 (m, 4H, $H_{k,l}$), 2.64 – 2.55 (m, 4H, $H_{d,f}$), 2.55 – 2.45 (m, 4H, $H_{p,n}$), 1.84 – 1.68 (m, 4H, $H_{o,e}$). ^{13}C NMR (126 MHz, $CDCl_3$): δ = 147.23, 146.42, 143.35, 141.41, 140.61, 128.61, 128.50, 128.29, 128.27, 127.35, 126.28, 126.13, 123.63, 119.96, 58.69, 52.93, 51.05, 48.05, 45.66, 45.52, 33.43, 32.95, 32.84, 29.85, 27.52. HRMS ESI $[M+H]^+$ $C_{31}H_{41}O_2N_4$ calc. 501.3224, found 501.3219.

Synthesis of (8)

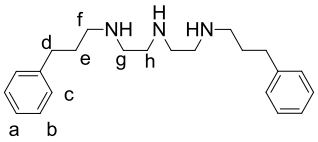

To a solution of **E2** (100 mg, 0.02 mmol, 1.0 equiv.) in CH_2Cl_2 (5 mL), trifluoroacetic acid (5 mL) was added dropwise. The reaction was left stirring open to air, at RT, and the disappearance of the substrate was monitored by ESI-MS. After 5 h, 5 mL of CH_2Cl_2 was added to the reaction mixture and solution was neutralised using $NaHCO_3$ (sat). The layers were separated and the aqueous layer was extracted with CH_2Cl_2 (10 mL). The combined organic layers were dried over $MgSO_4$, and the solvents were removed under reduced pressure to give **8** (75 mg, 98%) as colourless oil. ^{1}H NMR (500 MHz, $CDCl_3$): δ = 7.35 – 7.25 (m, 4H, H_b), 7.25 – 7.07 (m, 6H, $H_{a,c}$), 3.06 – 2.90 (m, 12H, $H_{f,g,h}$), 2.72 (t, J = 7.6 Hz, 4H, H_d), 2.14 (apparent as dt, J = 15.3, 7.7 Hz, 4H, H_e). ^{13}C NMR (126 MHz, $CDCl_3$): δ = 139.93, 128.62, 128.32, 126.34, 47.84, 47.79, 45.75, 32.57, 27.23. HRMS ESI $[M+H]^+$ $C_{22}H_{34}N_3$ calc. 340.2747, found 340.2750.

Synthesis of (15)

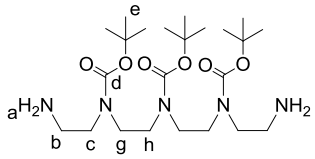

Synthesised according to a literature procedure.[20] Isolated as clear oil, used directly in the next step without further purification. ^{1}H NMR (400MHz, $CDCl_3$): δ = 3.34 (apparent as s, 8H, $H_{g,h}$), 3.26 (t, J = 5.4 Hz, 4H, H_c), 2.83 (t, J = 6.2 Hz, 4H, H_b), 1.46 (s, 27H, H_e), 1.16 (bs, 4H, H_a).

Synthesis of (E4)

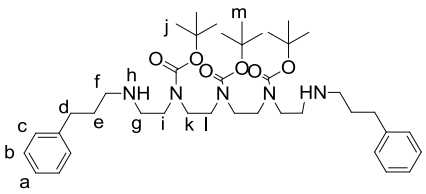

To a solution of **15** (190 mg, 0.388 mmol, 1.0 equiv.) in dry EtOH (50 mL), 3-phenylpropionaldehyde (0.776 mmol, 106 µL, 2.0 equiv.) was added in one portion. The reaction was stirred under N_2 for 24 h at room temperature. $NaBH_4$ (4.66 mmol, 176 mg, 12 equiv.) was then added in portions and reaction was kept stirring under N_2 for another 12 h. After this time H_2O (50 mL) was added to the reaction mixture and product was extracted with CH_2Cl_2 (3 × 100 mL). The combined organic layers were washed with brine, dried over $MgSO_4$ and the solvent was removed under reduced pressure. Column chromatography (SiO_2, MeOH/CH_2Cl_2 5:95) gave **E4** (61 mg, 21%) as a colourless oil. ^{1}H NMR (500 MHz, $CDCl_3$): δ = 7.30 (apparent as t, J = 7.3 Hz, 4H, H_b), 7.26 – 7.04 (m, 6H, $H_{a,c}$), 3.65 – 3.03 (m, 12H, $H_{i,k,l}$), 2.98 – 2.59 (m, 12H, $H_{d,f,g}$), 1.95 – 1.75 (m, 4H, H_e), 1.47 (s, 27H, $H_{j,m}$). ^{13}C NMR (126 MHz, $CDCl_3$): δ = 155.41, 141.96, 128.37, 128.36, 125.82, 79.87, 49.31, 48.37, 47.99, 45.67, 33.57, 31.83, 29.71, 28.49 (9C). $[M+H]^+$ $C_{41}H_{68}O_6N_5$ calc. 726.5164, found 726.5158.

Synthesis of (7)

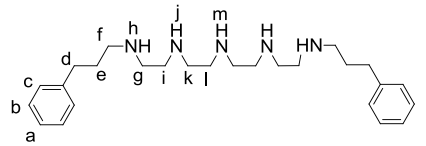

To a solution of **E4** (50 mg, 0.07 mmol, 1.00 equiv.) in CH_2Cl_2 (3 mL), trifluoroacetic acid (3 mL) was added dropwise. The reaction was left stirring open to air, at RT and the disappearance of the substrate was monitored by ESI-MS. After 5 h, 5 mL of CH_2Cl_2 was added to the reaction mixture and solution was neutralised using $NaHCO_3$ (sat). The layers were separated and the aqueous layer was extracted with CH_2Cl_2 (1 × 10 mL). The combined organic layers were dried over $MgSO_4$, and the solvents were removed under reduced pressure to give **7** (25 mg, 85%) as an orange oil. ^{1}H NMR (500 MHz, $CDCl_3$): δ = 7.33 – 7.23 (m, 4H, H_b), 7.23 – 7.18 (m, 2H, H_a), 7.18 – 7.08 (m, 4H, H_c), 3.17 – 3.08 (m, 4H, H_g), 3.08 – 2.82 (m, 16H, $H_{f,i,k,l}$), 2.66 (t, J = 7.6 Hz, 4H, H_d), 2.06 (apparent as dt, J = 15.7, 7.9 Hz, 4H, H_e). ^{13}C NMR (126 MHz, $CDCl_3$): δ = 140.21, 128.74, 128.42, 126.48, 48.02, 47.70, 47.12, 45.18, 45.02, 32.91, 27.48. $[M+H]^+$ $C_{26}H_{44}N_5$ calc. 426.3591, found 426.3591.

Synthesis of (E5)

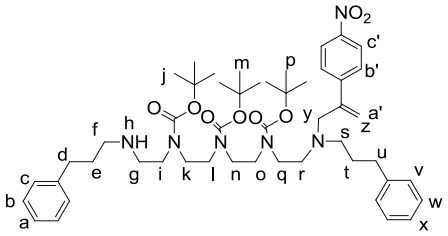

To a degassed solution of **E4** (110 mg, 0.15 mmol, 2.0 equiv.) in dry MeOH (30 mL), **W** (26 mg, 0.07 mmol, 1.0 equiv.) was added in one portion. The reaction mixture was kept stirring under N_2 at 50 °C for 72 h in the presence of $^{i}Pr_2NEt$ (36 µL, 0.21 mmol, 3 equiv.). After this time, the reaction was cooled to room temperature and H_2O (30 mL) was added. The mixture was extracted with CH_2Cl_2 (2 × 30 mL), dried over $MgSO_4$ and the solvents were removed under reduced pressure. Column chromatography (SiO_2, MeOH/CH_2Cl_2, 5:95) gave **E5** (29 mg, 47%) as an orange oil. ^{1}H NMR (400 MHz, $CDCl_3$): δ = 8.09 (d, J = 8.6 Hz, 2H, $H_{c'}$), 7.54 (d, J = 8.7 Hz, 2H, $H_{b'}$), 7.28 – 7.14 (m, 4H, $H_{b,w}$), 7.14 – 7.08 (m, 4H, $H_{c,v}$), 7.07 – 6.97 (m, 2H, $H_{a,x}$), 5.47 (bs, 1H, $H_{a'}$), 5.35 (s, 1H, H_z), 3.39 (s, 2H, H_y), 3.36 – 2.97 (m, 12H, $H_{i,k,l,n,o,q}$), 2.88 – 2.36 (m, 12H, $H_{d,f,g,r,s,u}$), 1.89 – 1.61 (m, 4H, $H_{e,t}$), 1.36 (s, 18H, $H_{j/m/p}$), 1.31 (s, 9H, $H_{j/m/p}$). ^{13}C NMR (126 MHz, $CDCl_3$): δ = 155.91, 155.23, 155.05, 147.04, 146.87, 146.67, 144.33, 144.12, 142.03, 141.80, 128.49, 128.36, 128.31, 128.28, 127.30, 126.13, 125.90, 123.43, 118.63, 80.27, 79.82, 79.52, 59.23, 59.12, 53.68, 53.54, 52.05, 51.61, 48.67, 48.29, 48.03, 46.09, 45.21, 33.58, 33.23, 29.70, 29.37, 28.45 (9C). $[M+H]^+$ $C_{50}H_{70}N_6O_8$ calc. 887.5641, found 887.5638.

Synthesis of (9)

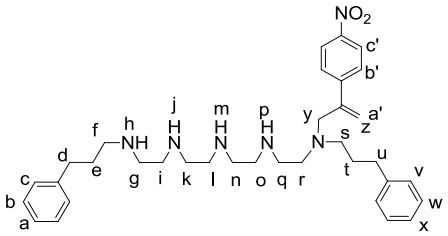

To a solution of **E5** (20 mg, 0.02 mmol, 1.00 equiv.) in CH_2Cl_2 (3 mL), trifluoroacetic acid (3 mL) was added dropwise. The reaction was left stirring open to air, at RT, and the disappearance of the substrate was monitored by ESI-MS. After 5 h, 5 mL of CH_2Cl_2 was added to the reaction mixture and solution was carefully neutralised using $NaHCO_3$ (sat). The layers were separated and the aqueous layer was extracted once with CH_2Cl_2 (5 mL). The combined organic layers were dried over $MgSO_4$ and the solvents were removed under reduced pressure to give **9** (13 mg, quant.) as an orange oil. ^{1}H NMR (400 MHz, $CDCl_3$): δ =

8.15 (d, J = 8.9 Hz, 2H, $H_{c'}$), 7.54 (d, J = 8.9 Hz, 2H, $H_{b'}$), 7.33–7.22 (m, 4H, $H_{b,w}$), 7.23–7.16 (m, 2H, $H_{a,x}$), 7.16 – 7.07 (m, 4H, $H_{c,v}$), 5.50 (s, 1H, $H_{a'}$), 5.34 (s, 1H, H_z), 3.38 (s, 2H, H_y), 2.98 (apparent as s, 4H, $H_{g,i}$), 2.93–2.77 (m, 10H, $H_{f,k,l,n,o}$), 2.76 – 2.57 (m, 6H, $H_{d,q,r}$), 2.48 (t, J = 8.0 Hz, 2H, H_u), 2.41 (t, J = 8.0 Hz, 2H, H_s), 2.04 (apparent as dt, J = 14.7, 7.7 Hz, 2H, H_e), 1.70 (apparent as dt, J = 15.2, 7.6 Hz, 2H, H_t). ^{13}C NMR (101 MHz, $CDCl_3$): δ = 146.95, 146.64, 143.91, 141.76, 140.13, 128.51, 128.29, 128.22, 127.23, 126.21, 125.79, 123.35, 118.96, 58.87, 53.25, 50.84, 48.05, 47.56, 47.14, 46.45, 46.39, 46.27, 45.57, 33.38, 32.66, 31.85, 29.63, 27.87 (2C). $[M+H]^+$ $C_{35}H_{50}N_60_2Na$ calc. 609.3887, found 609.3903.

Synthesis of (13)

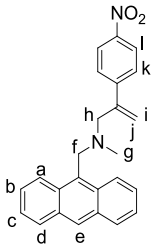

To a degassed solution of 9-(methylaminomethyl)anthracene **10** (50 mg, 0.22 mmol, 1.0 equiv.) in dry MeOH (30 mL), **W** (78 mg, 0.22 mmol, 1.0 equiv.) was added in one portion. The reaction mixture was kept stirring under N_2 at 50 °C for 48 h in the presence of $^{i}Pr_2NEt$ (117 µL, 0.813 mmol, 3.0 equiv.). After this time, a product has precipitated from the reaction mixture. The orange solid was filtered off and washed with MeOH to give **13** (68 mg, 79%) as an orange powder. ^{1}H NMR (500 MHz, $CDCl_3$): δ = 8.45 (s, 1H, H_e), 8.31 (d, J = 8.9 Hz, 2H, H_a), 8.02 (d, J = 8.4 Hz, 2H, H_d), 7.78 (d, J = 8.7 Hz, 2H, H_l), 7.47 (apparent as t, J = 7.4 Hz, 2H, H_b), 7.43 – 7.34 (m, 2H, H_c), 7.15 (d, J = 8.7 Hz, 2H, H_k), 5.51 (s, 1H, H_i), 5.37 (s, 1H, H_j), 4.47 (s, 2H, H_f), 3.42 (s, 2H, H_h), 2.34 (s, 3H, H_g). ^{13}C NMR (125 MHz, $CDCl_3$): δ = 146.87, 146.00, 144.23, 131.53 (3C), 131.50 (2C), 129.70, 129.20 (2C), 127.90, 127.38 (4C), 125.78 (2C), 125.08, 125.07, 123.09, 118.63, 61.39, 53.76, 42.39. HRMS ESI $[M+H]^+$ $C_{25}H_{23}O_2N_2$ calc. 383.1754, found 383.1757.

Synthesis of (E6)

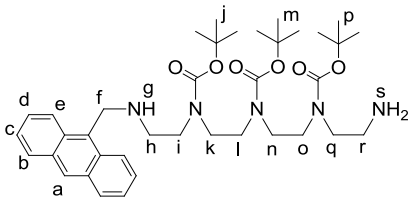

To a solution of **15** (550 mg, 1.2 mmol, 4.28 equiv.) in dry EtOH (150 mL), 9-anthraldehyde (58 mg, 0.28 mmol, 1.0 equiv.) was added in portions. The reaction was stirred under N_2 for

72 h at room temperature. $NaBH_4$ (68 mg, 1.68 mmol, 6.0 equiv.) was then added in portions and reaction was kept stirring under N_2 for another 24 h. After this time H_2O (100 mL) was added to the reaction mixture and product was extracted with CH_2Cl_2 (3 × 50 mL). The combined organic layers were washed with brine, dried over $MgSO_4$ and the solvent was removed under reduced pressure. Column chromatography (SiO_2, MeOH/CH_2Cl_2/NH_3 2.5:97.5:1.5) gave **E6** (135 mg, 71%) as an orange oil. ^{1}H NMR (400 MHz, $CDCl_3$): δ = 8.40 (s, 1H, H_a), 8.32 (apparent as t, J = 10.2 Hz, 2H, H_e), 8.00 (d, J = 8.1 Hz, 2H, H_b), 7.57 – 7.48 (m, 2H, H_d), 7.45 (apparent as t, J = 7.4 Hz, 2H, H_c), 4.74 (s, 2H, H_f), 3.45 (bs, 1H, H_g), 3.40 – 3.12 (m, 12H, $H_{i,k,l,n,o,q}$), 3.12 – 2.89 (m, 2H, H_h), 2.89 – 2.67 (m, 2H, H_r), 1.60 – 1.36 (m, 27H, $H_{j,m,p}$). ^{13}C NMR (101 MHz, $CDCl_3$): δ = 155.75 (3C), 131.78 (2C), 130.39 (2C), 129.24 (2C), 127.33, 126.27, 126.19, 125.05 (2C), 124.42, 124.20, 79.98 (3C), 51.18, 50.47, 48.99, 48.58, 47.22, 46.02, 45.79, 45.54, 41.06, 40.73, 28.55 (9C). HRMS ESI $[M+H]^+$ $C_{38}H_{58}O_6N_5$ calc. 680.4382, found 680.4879.

Synthesis of (E7)

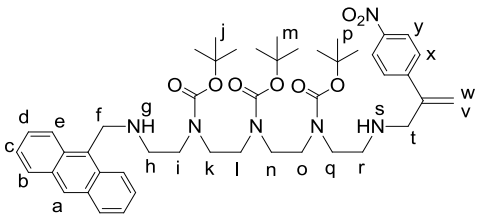

To a degassed solution of **E6** (80 mg, 0.12 mmol, 1.0 equiv.) in dry MeOH (10 mL), **W** (36 mg, 0.11 mmol, 0.9 equiv.) was added in one portion. The reaction mixture was kept stirring under N_2 at 50 °C for 72 h in the presence of ^{i}Pr$_2$NEt (62 µL, 0.36 mmol, 3.0 equiv.). After this time, the reaction was cooled to room temperature and H_2O (15 mL) was added. The mixture was extracted with CH_2Cl_2 (2 × 15 mL), dried over $MgSO_4$ and the solvents were removed under reduced pressure. Column chromatography (SiO_2, MeOH/CH_2Cl_2, 5:95) gave **E7** (32 mg, 20%) as an orange oil. ^{1}H NMR (400 MHz, $CDCl_3$): δ = 8.40 (s, 1H, H_a), 8.37 – 8.28 (m, 2H, H_e), 8.16 (d, J = 8.6 Hz, 2H, H_y), 8.00 (d, J = 8.3 Hz, 2H, H_b), 7.59 (d, J = 8.9 Hz, 2H, H_x), 7.56 – 7.49 (m, 2H, H_d), 7.49 – 7.41 (m, 2H, H_c), 5.53 (s, 1H, H_w), 5.42 (s, 1H, H_v), 4.76 (s, 2H, H_f), 3.66 (s, 2H, H_t), 3.51 – 3.12 (m, 13H, $H_{g,i,k,l,n,o,q}$), 3.11 – 3.85 (m, 2H, H_h), 2.77 (apparent as s, 2H, H_r), 1.51 – 1.30 (m, 27H, $H_{j,m,p}$). ^{13}C NMR (101 MHz, $CDCl_3$): δ = 155.61 (3C), 147.13, 144.74 (2C), 131.55 (3C), 130.35 (2C), 129.1 (2C), 127.33, 127.04, 126.17 (2C), 124.96, 124.19, 124.02, 123.64, 116.94, 79.82 (3C), 52.73, 48.72, 47.49 (2C), 45.60 (8C), 30.00, 28.43 (9C). $[M+H]^+$ $C_{47}H_{65}O_8N_6$ calc. 841.4858, found 841.4864.

Synthesis of (12)

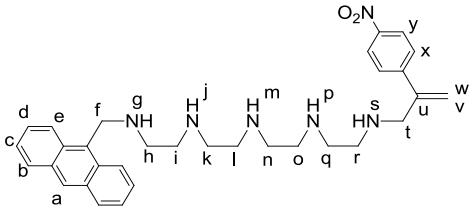

To a solution of **E7** (20 mg, 0.02 mmol, 1.0 equiv.) in CH_2Cl_2 (3 mL), trifluoroacetic acid (3 mL) was added dropwise. The reaction was left stirring open to air, at RT, and the disappearance of the substrate was monitored by ESI-MS. After 5 h, 5 mL of CH_2Cl_2 was added to the reaction mixture and solution was carefully neutralised using $NaHCO_3$ (sat). The layers were separated and the aqueous layer was extracted with CH_2Cl_2 (5 mL). The combined organic layers were dried over $MgSO_4$, and the solvents were removed under reduced pressure to give **12** (13 mg, 93%) as an orange oil. ^{1}H NMR (500 MHz, $CDCl_3$): δ = 8.39 (s, 1H, H_a), 8.33 (d, J = 8.8 Hz, 2H, H_e), 8.11 – 8.08 (m, 2H, H_y) 8.00 (d, J = 8.4 Hz, 2H, H_b), 7.54 (ddd, J = 8.9, 6.5, 1.4 Hz, 2H, H_d), 7.52 – 7.49 (m, 2H, H_x), 7.47 (ddd, J = 7.6, 6.5, 1.0 Hz, 2H, H_c), 5.51 (s, 1H, H_w), 5.39 (s, 1H, H_v), 4.82 (s, 2H, H_t), 4.73 (s, 2H, H_f), 3.08 – 3.01 (m, 2H, H_h), 2.93 – 2.87 (m, 2H, H_r), 2.85 – 2.66 (m, 12H, $H_{i,k,l,n,o,q}$). ^{13}C NMR (126 MHz, $CDCl_3$): δ = 147.12, 146.16, 143.95, 131.45(3C), 130.45(2C), 129.23(2C), 127.78(2C), 127.04(2C), 126.99(2C), 126.47, 125.15, 123.99, 123.61, 117.41, 52.66, 47.73, 47.35, 47.24, 46.90, 46.26, 46.11, 45.84, 45.53, 44.69, 29.72. $[M+H]^+$ $C_{32}H_{41}O_2N_6$ calc. 541.3286, found 541.3284. (for HRMS, the HCl salt was used for stability purposes).

Synthesis of (11)

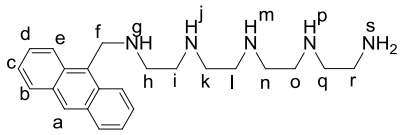

To a solution of **E6** (70 mg, 0.1 mmol, 1.0 equiv.) in CH_2Cl_2 (3 mL), trifluoroacetic acid (3 mL) was added dropwise. The reaction was left stirring open to air, at RT, and the disappearance of the substrate was monitored by ESI-MS. After 5 h the solvent was removed under reduced pressure and the residue was taken-up in 15 N NaOH. The aqueous layer was extracted with $CHCl_3$ (3 × 25 mL). The combined organic layers were dried over $MgSO_4$ and solvent was removed under reduced pressure to give **11** (30 mg, 79%) as an orange oil. ^{1}H NMR (500 MHz, $CDCl_3$): δ = 8.39 (s, 1H, H_a), 8.33 (d, J = 8.8 Hz, 2H, H_e), 8.00 (d, J = 8.4 Hz, 2H, H_b), 7.53 (ddd, J = 8.7, 6.5, 1.1 Hz, 2H, H_d), 7.49 – 7.41 (m, 2H, H_c), 4.73 (s, 2H, H_f), 2.96 (apparent as bs, 2H, H_h), 2.77 (apparent as bs, 2H, H_r), 2.73 – 2.48 (a series of m, 12H, $H_{i,k,l,n,o,q}$), 2.36 (bs, 6H, $H_{g,j,m,p\ s}$). ^{13}C NMR (126 MHz, $CDCl_3$): δ = 131.52 (3C), 130.29

(2C), 129.19 (2C), 127.29 126.23 (2C), 125.03 (2C), 124.08 (2C), 49.26, 49.05, 48.75, 48.48, 45.48, 31.94, 29.71, 22.71, 14.14. $[M+H]^+$ $C_{23}H_{34}N_5$ calc. 380.2809, found 380.2807 (for HRMS, the HCl salt was used for stability reasons).

Synthesis of (E8)

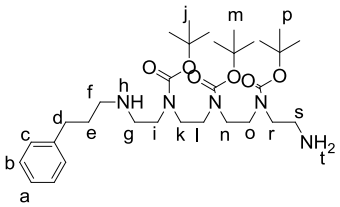

To a solution of **15** (1.5 g, 3.06 mmol, 2.00 equiv.) in dry EtOH (250 mL), 3-phenylpropionaldehyde (1.50 mmol, 205 µL, 1 equiv.) was added in one portion. The reaction was stirred under N_2 for 72 h at room temperature. $NaBH_4$ (9.1 mmol, 346 mg, 6 equiv.) was then added in portions and the reaction was kept stirring under N_2 for another 24 h. After this time H_2O (100 mL) was added to the reaction mixture and the product was extracted with CH_2Cl_2 (3 ×100 mL). The combined organic layers were washed with brine, dried over $MgSO_4$ and the solvent was removed under reduced pressure. Column chromatography (SiO_2, $MeOH/CH_2Cl_2/NH_3$ 25:75:2.5) gave **E8** (350 mg, 38%) as a colourless oil. ^1H NMR (400 MHz, $CDCl_3$): δ = 7.31 – 7.22 (m, 2H, H_b), 7.22 – 7.09 (m, 3H, $H_{a,c}$), 3.48 – 3.16 (m, 12H, $H_{g,i,k,l,n,o}$), 2.68 (apparent as bs, 4H, $H_{r,s}$), 2.65 (apparent as t, J = 7.5 Hz, 4H, $H_{d,f}$), 1.89 – 1.74 (m, 2H, H_e), 1.56 – 1.35 (m, 27H, $H_{j,m,p}$). ^{13}C NMR (101 MHz, $CDCl_3$): δ = 155.20 (3C), 142.74, 128.36 (2C), 128.35, 125.86 (2C), 79.97 (3C), 50.76, 49.17, 48.03(2C), 47.49, 45.49 (3C), 40.66, 33.46, 31.60, 28.33 (9C). HRMS ESI $[M+H]^+$ $C_{32}H_{58}O_6N_5$ calc. 608.4382, found 608.4376.

Synthesis of (16)

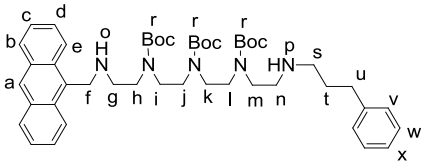

To a solution of **E8** (320 mg, 0.60 mmol, 1.0 equiv.) in dry EtOH (250 mL), 9-anthraldehyde (0.12 g, 0.60 mmol, 1.0 equiv.) was added in one portion. The reaction was stirred under N_2 for 72 h at room temperature. $NaBH_4$ (100 mg, 2.60 mmol, 4.5 equiv.) was then added in portions and reaction was kept stirring under N_2 for another 24 h. After this time H_2O (100 mL) was added to the reaction mixture and the product was extracted with CH_2Cl_2 (3 × 100 mL). The combined organic layers were washed with brine, dried over $MgSO_4$ and the

solvent was removed under reduced pressure. Column chromatography (SiO_2, MeOH/CH_2Cl_2 2.5:97.5) gave **16** (263 mg, 55%) as an orange oil. ^{1}H NMR (500 MHz, $CDCl_3$): δ = 8.40 (s, 1H, H_a), 8.42– 8.32 (m, 2H, H_e), 8.00 (d, J = 7.8 Hz, 2H, H_b), 7.58 – 7.53 (m, 2H, H_d), 7.51 – 7.45 (m, 2H, H_c), 7.31 – 7.22 (m, 2H, H_w), 7.20–7.16 (m, 3H, $H_{v,x}$), 4.75 (s, 2H, H_f), 3.52 – 3.11 (m, 12H, $H_{h,i,j,k,l,m}$), 3.11 – 2.94 (m, 2H, H_g), 2.75 (apparent as bs, 2H, H_n), 2.64 (apparent as t, J = 7.1 Hz, 4H, $H_{s,u}$), 1.86 – 1.74 (m, 2H, H_t), 1.50 – 1.37 (m, 27H, H_r). ^{13}C NMR (126 MHz, $CDCl_3$): δ = 155.70(3C), 142.25, 131.69(4C), 130.44, 129.28(2C), 128.50(2C), 128.48(2C), 127.39, 126.20, 125.93(2C), 125.07(2C), 124.52, 124.27, 79.90(3C), 49.45, 48.13(2C), 47.51(2C), 45.84, 45.50(4C), 33.71, 32.00, 28.59(9C). HRMS ESI $[M+H]^+$ $C_{47}H_{68}O_6N_5$ calc. 798.5164, found 798.5156.

Synthesis of (E9)

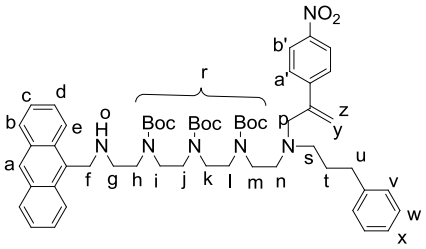

To a degassed solution of **16** (290 mg, 0.36 mmol, 1 equiv.) in dry MeOH (30 mL), **W** (63 mg, 0.18 mmol, 0.5 equiv.) was added in one portion. The reaction mixture was kept stirring under N_2 at RT for 72 h in the presence of ^{i}Pr$_2$NEt (189 µL, 1.08 mmol, 3 equiv.). After this time, another portion of the walker (32 mg, 0.09 mmol 0.25 equiv.) was added in one portion and the reaction was kept stirring for another 72 h. After this time, H_2O (30 mL) was added. The mixture was extracted with CH_2Cl_2 (2 × 30 mL), dried over $MgSO_4$ and the solvents were removed under reduced pressure. Column chromatography (SiO_2, MeOH/CH_2Cl_2, 5:95) gave **E9** (110 mg, 42%) as an orange oil. ^{1}H NMR (500 MHz, $CDCl_3$): 8.32 (s, 1H, H_a), 8.29 – 8.20 (m, 2H, H_e), 8.07 (d, J = 8.7 Hz, 2H, H_b), 7.92 (d, J = 8.3 Hz, 2H, $H_{b'}$), 7.51 (d, J = 8.4 Hz, 2H, $H_{a'}$), 7.44 (apparent as t, J = 7.7 Hz, 2H, H_d), 7.37 (apparent as t, J = 7.4 Hz, 2H, H_c), 7.17 (apparent as t, J = 7.4 Hz, 2H, H_w), 7.09 (apparent as t, J = 7.4 Hz, 1H, H_x), 7.03 (d, J = 7.4 Hz, 2H, H_v), 5.53 (bs, 1H, H_z), 5.41 (s, 1H, H_y), 4.76 (s, 2H, H_f), 3.55 – 2.87 (m, 16H, $H_{h,i,j,k,l,m,n,p}$), 2.65 – 2.39 (m, 6H, $H_{g,s,u}$), 1.81 – 1.70 (m, 2H, H_t), 1.50 – 1.29 (m, 27H, H_r). ^{13}C NMR (126 MHz, $CDCl_3$): δ = 155.24 (3C), 147.05, 144.31 (2C), 142.05, 131.56 (4C), 130.33 (2C), 129.16 (2C), 128.32 (4C), 127.29, 126.14 (2C), 125.82, 124.95, 124.33, 124.13, 123.43, 123.35, 118.58, 79.69 (3C), 59.09, 53.66 (4C), 51.64, 48.87, 48.42, 47.15, 45.65 (2C), 33.58, 28.66 (2C), 28.46 (9C). HRMS ESI $[M+H]^+$ $C_{56}H_{75}O_8N_6$ calc. 959.5641, found 959.5640.

Synthesis of (14)

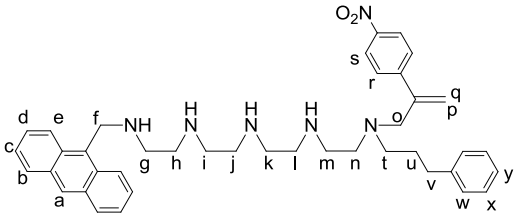

To a solution of **E9** (58 mg, 0.05 mmol, 1.0 equiv.) in CH_2Cl_2 (5 mL), trifluoroacetic acid (5 mL) was added dropwise. The reaction was left stirring open to air, at RT, and the disappearance of the substrate was monitored by ESI-MS. After 5 h, 10 mL of CH_2Cl_2 was added to the reaction mixture and solution was carefully neutralised using $NaHCO_3$ (sat). The layers were separated and the aqueous layer was extracted with CH_2Cl_2 (10 mL). The combined organic layers were dried over $MgSO_4$ and the solvents were removed under reduced pressure to give **14** (34 mg, quant.) as an orange oil. ^{1}H NMR (500 MHz, $CDCl_3$): δ = 8.44 (s, 1H, H_a), 8.34 (d, J = 8.8 Hz, 2H, H_e), 8.11 (d, J = 8.8 Hz, 2H, H_s), 8.01 (d, J = 8.4 Hz, 2H, H_b), 7.61 – 7.51 (m, 4H, $H_{d,r}$), 7.51 – 7.44 (m, 2H, H_c), 7.25 (apparent as t, J = 7.4 Hz, 2H, H_x), 7.17 (apparent as t, J = 7.4 Hz, 1H, H_y), 7.11 (d, J = 7.1 Hz, 2H, H_w), 5.53 (s, 1H, H_q), 5.38 (s, 1H, H_p), 4.90 (s, 2H, H_f), 3.46 (s, 2H, H_o), 3.05 (t, J = 5.7 Hz, 2H, H_g), 2.94 (t, J = 5.7 Hz, 2H, H_h), 2.88 (apparent as s, 4H, $H_{i/j/k/l}$), 2.84 (apparent as s, 4H, $H_{i/j/k/l}$), 2.79–2.73 (m, 2H, H_n), 2.73 – 2.67 (m, 2H, H_m), 2.57–2.50 (m, 4H, $H_{t,v}$), 1.79 (apparent as dt, J = 15.0, 7.6 Hz, 2H, H_u). ^{13}C NMR (126 MHz, $CDCl_3$): δ = 147.19, 146.73, 143.73, 141.89, 131.54 (2C), 130.74 (2C), 129.40 (2C), 128.51 (2C), 128.46 (2C), 128.30 (2C), 127.42, 126.76 (4C), 126.02, 125.31, 123.97 (2C), 123.58 (2C), 119.44, 59.16, 53.55, 49.48, 47.52 (2C), 46.96, 45.88, 45.86, 45.67, 44.72, 44.40, 33.56, 28.03. $[M+H]^+$ $C_{41}H_{51}O_2N_6$ calc. 659.4068, found 659.4066.

Synthesis of (E10)

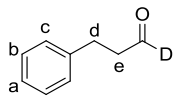

To a solution of hydrocinnamic acid (10 g, 66.6 mmol) in dry MeOH (200 mL), thionylchloride (10 mL) was added slowly at 0 °C. The reaction was allowed to warm to RT and stirred for 16 h after which the solvent was removed under reduced pressure. The crude material was dissolved in CH_2Cl_2 and washed with H_2O. The aqueous layer was extracted with CH_2Cl_2 (3 x 50 mL) and the combined organic layers were dried over $MgSO_4$. The solvent was removed under reduced pressure and 3-phenylpropionic acid methyl ester (10.9 g, quant.) was isolated. The crude product was submitted to the next step without further

purification. ^{1}H NMR (400 MHz, $CDCl_3$): δ = 7.30–7.25 (m, 2H, H_{Ar}), 7.23–7.17 (m, 3H, H_{Ar}), 3.66 (s, 3H), 2.94 (t, J = 8.0 Hz, 2H), 2.62 (t, J = 8.0 Hz, 2H).

Under N_2, a solution of 3-phenylpropionic acid methyl ester (2 g, 12.2 mmol, 1.0 equiv.) in dry THF (20 mL) was added slowly to a solution of $LiAlD_4$ (1.02 g, 24.4 mmol, 2.0 equiv.) in dry THF (100 mL) at 0 °C. The mixture was stirred for 16 h at room temperature after which the reaction mixture was cooled to 0 °C and 1 mL of H_2O was added carefully, dropwise. After 30 min at 0 °C, 1 mL of NaOH (aq, 15%) was added slowly and the mixture was stirred at 0 °C for another 30 min. 3 mL of H_2O were then added slowly and after 30 min at 0 °C, $MgSO_4$ was added. The mixture was filtered over celite and washed with THF and EtOAc. The solvents were removed under reduced pressure and 3-phenylpropan-1-ol-d_2 (1.52 g, 91%) was isolated. The crude product was submitted to the next step without further purification. ^{1}H NMR (400 MHz, $CDCl_3$): δ = 7.34–7.28 (m, 2H, H_{Ar}), 7.25–7.19 (m, 3H, H_{Ar}), 2.72 (t, J = 8.0 Hz, 2H), 1.89 (t, J = 8.0 Hz, 2H). ^{13}C NMR (101 MHz, $CDCl_3$): δ = 141.93, 128.49, 128.46, 125.92, 61.46, 34.05, 32.08.

3-Phenylpropan-1-ol-d_2 (1.52 g, 11.01 mmol, 1.0 equiv.) was dissolved in CH_2Cl_2 (75 mL). Dess-Martin periodinane (4.67 g, 11.04 mmol, 1.0 equiv.) was added and the reaction was stirred for 16 h at room temperature. The reaction mixture was filtered, dried over $MgSO_4$ and the solvent removed under reduced pressure. Column chromatography (SiO_2, EtOAc:Pet 93:7) gave **E10** (1.18 g, 79%) as a colourless oil. ^{1}H NMR (400 MHz, $CDCl_3$): δ = 7.34–7.28 (m, 2H, H_{Ar}), 7.25–7.19 (m, 3H, H_{Ar}), 2.97 (t, J = 7.5 Hz, 2H, H_e), 2.79 (t, J = 7.7 Hz, 2H, H_d). ^{13}C NMR (101 MHz, $CDCl_3$): δ = 201.4 (t, J = 26.4 Hz, C-D), 140.50, 128.62, 128.34, 126.32, 45.31, 28.15.

Synthesis of (E11)

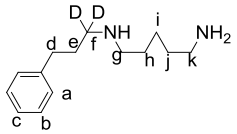

To a solution of 1,5-pentanediamine (524 mg, 5.13 mmol, 1.2 equiv.) in dry MeOH (60 mL), 3-phenylpropionaldehyde-d_1 **E10** (577 mg, 4.27 mmol, 1.0 equiv.) was added in one portion. The reaction was stirred under N_2 for 72 h at room temperature. $NaBD_4$ (360 mg, 8.55 mmol, 2.0 equiv.) was then added and the reaction was kept stirring under N_2 for 15 h. After this time H_2O (30 mL) was added to the reaction mixture and product was extracted with CH_2Cl_2 (3 x 50 mL). The combined organic layers were washed with brine, dried over $MgSO_4$, and

the solvent was removed under reduced pressure. Column chromatography (SiO_2, MeOH:CH_2Cl_2:NH_3 (aq. 10%) 20:80:1.5) gave **E11** (502 mg, 44%) as a colourless oil. ^{1}H NMR (400 MHz, $CDCl_3$): δ = 7.30 – 7.25 (m, 2H, H_b), 7.20 – 7.15 (m, 3H, $H_{a,c}$), 2.71 – 2.57 (m, 6H, $H_{d,g,k}$), 1.84 – 1.78 (m, 2H, H_e), 1.53 – 1.47 (m, 4H, $H_{h,j}$), 1.37–1.31 (m, 2H, H_i). ^{13}C NMR (126 MHz, $CDCl_3$): δ =142.11, 128.35, 128.33, 125.78, 49.78, 48.72 (p, J = 20.5 Hz, C-D), 42.00, 33.67, 33.47, 31.42, 29.89, 24.62. $[M+H]^+$ $C_{14}H_{23}{}^2H_2N_2$ calc. 223.2138, found 223.2135.

Synthesis of (E12)

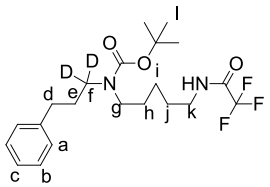

Synthesised according to a modified literature procedure.[20]

Under N_2, **E11** (475 mg, 2.14 mmol, 1.0 equiv.) was dissolved in CH_2Cl_2 (30 mL) and cooled to 0 °C. Ethyl trifluoroacetate (0.28 mL, 2.35 mmol, 1.1 equiv.) was added dropwise over 30 min to protect the primary amine. This mixture was then stirred for 30 min at 0 °C and then at room temperature for an additional 1 h. To the resulting mixture, a solution of Boc_2O (700 mg, 3.21 mmol, 1.5 equiv.) in CH_2Cl_2 (10 mL) was added dropwise. Dry Et_3N (0.45 mL, 3.21 mmol, 1.5 equiv.) was then added and the solution was stirred for 15 h at RT. The reaction mixture was then washed with $NaHCO_3$ (sat). The organic layer was separated, washed with water, dried over $MgSO_4$, and the solvent removed. Column chromatography (SiO_2, MeOH:CH_2Cl_2 2.5:97.5) afforded **E12** (678 mg, 76%) as a colourless paste. ^{1}H NMR (400 MHz, $CDCl_3$) δ 7.32 – 7.24 (m, 2H, H_b), 7.20 – 7.15 (m, 3H, $H_{a,c}$), 3.37–3.21 (m, 2H, H_k), 3.25 – 3.07 (m, 2H, H_g), 2.59 (t, J = 8.0 Hz, 2H_d), 1.83 (t, J = 8.0 Hz, 2H, H_e), 1.65 – 1.55 (m, 2H, H_j), 1.55 – 1.38 (m, 11H, $H_{h,l}$), 1.35 – 1.24 (m, 2H, H_i). ^{13}C NMR (126 MHz, $CDCl_3$): δ =157.30 (q, J = 36.7 Hz, C-F), 157.45, 141.64, 128.4, 128.42, 125.90, 115.90 (q, J = 287.8 Hz, C-F), 79.36, 46.36 (apparent as broad, due to C-D coupling), 46.20, 39.85, 33.21, 30.03, 28.48 (3C), 28.42, 27.72, 23.66. $[M+H]^+$ $C_{21}H_{30}{}^2H_2F_3O_3N_2$ calc. 419.2485, found 419.2488.

Synthesis of (E13)

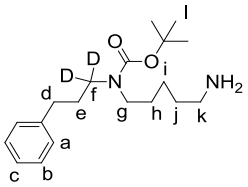

To a solution of **E12** (655 mg, 1.56 mmol, 1.0 equiv.) in MeOH (10 mL), NaOH (313 mg, 7.82 mmol, 5.0 equiv.) in H_2O (7 mL) was added. The mixture was stirred at RT for 15 h. After this time, methanol was removed, the residue was dissolved in CH_2Cl_2, washed with H_2O and extracted with CH_2Cl_2 (3 x 20 mL). The combined organic layers were dried over $MgSO_4$, and the solvent was removed under reduced pressure to afford **E13.** The crude material (497 mg) was used in the next step without further purification. ^{1}H NMR (400 MHz, $CDCl_3$): δ = 7.29 – 7.23 (m, 2H, H_b), 7.20 – 7.13 (m, 3H, $H_{a,c}$), 3.20–3.06 (m, 2H, H_g), 2.66 (t, J = 7.0 Hz, 2H, H_k), 2.58 (t, J = 8.0 Hz, 2H, H_d), 1.82 (t, J = 8.0 Hz, 2H, H_e), 1.53 – 1.37 (m, 13H, $H_{h,j,l}$), 1.30 – 1.23 (m, 2H, H_i). ^{13}C NMR (126 MHz, $CDCl_3$): δ = 155.70, 141.83, 128.45, 128.36, 125.92, 79.17, 47.01, 46.30 (p, J = 20.5 Hz, C-D), 42.15, 33.45, 33.30, 30.16, 28.56, 28.51 (3C), 24.21. $[M+H]^+$ $C_{19}H_{31}{}^2H_2O_2N_2$ calc. 323.2662, found 323.2667.

Synthesis of (E14)

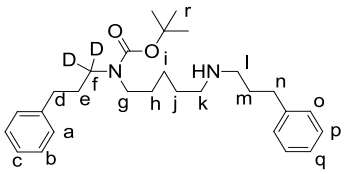

To a solution of **E13** (467 mg, 1.45 mmol, 1.0 equiv.) in dry MeOH (50 mL), 3-phenylpropionaldehyde (214 mg, 1.59 mmol, 1.1 equiv.) was added in one portion. The reaction was stirred under N_2 for 72 h at room temperature. $NaBH_4$ (164 mg, 4.35 mmol, 3.0 equiv.) was then added and the reaction was kept stirring under N_2 for another 4 h. After this time H_2O (50 mL) was added to the reaction mixture and the product was extracted with CH_2Cl_2 (3 x 30 mL). The combined organic layers were washed with brine, dried over $MgSO_4$ and the solvent was removed under reduced pressure. Column chromatography (SiO_2, MeOH/CH_2Cl_2 5:95) gave **E14** (260 mg, 41%) as a colourless oil. ^{1}H NMR (400 MHz, $CDCl_3$): δ = 7.30–7.25 (m, 4H, $H_{b,p}$), 7.21–7.15 (m, 6H, $H_{a,c,o,q}$), 3.22–3.05 (m, 2H, H_g), 2.68–2.63 (m, 4H, $H_{d,n}$), 2.63–2.56 (m, 4H, $H_{k,l}$), 1.89 – 1.80 (m, 4H, $H_{e,m}$), 1.55 – 1.40 (m, 13H, $H_{h,j,r}$), 1.32–1.22 (m, 2H, H_i). ^{13}C NMR (126 MHz, $CDCl_3$): δ = 155.68, 142.15, 141.87, 128.45, 128.44, 128.41, 128.37, 125.92, 125.86, 79.17, 49.85, 48.74 (apparent as

broad, due to C-D coupling), 47.11, 46.93, 33.71, 33.34, 31.43, 30.17, 29.83, 28.56 (3C), 28.29, 24.72. $[M+H]^+$ $C_{28}H_{41}{}^2H_2O_2N_2$ calc. 441.3445, found 441.3444.

Synthesis of (E15)

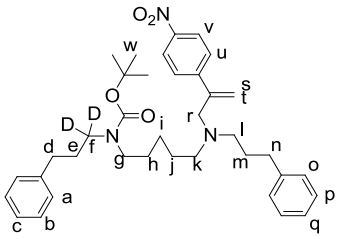

To a degassed solution of **E14** (200 mg, 0.46 mmol, 1.0 equiv.) in dry MeOH (30 mL), **W** (190 mg, 0.92 mmol, 1.2 equiv.) was added in one portion. The reaction mixture was kept stirring under N_2 at 40 °C for 65 h in the presence of $^{i}Pr_2NEt$ (240 µL, 1.36 mmol, 3.0 equiv.) After this time, the reaction was cooled to room temperature and H_2O (30 mL) was added. The mixture was extracted with CH_2Cl_2 (3 x 30 mL), dried over $MgSO_4$, and the solvent removed under reduced pressure. Column chromatography (SiO_2, MeOH:CH_2Cl_2, 1:99) gave **E15** (202 mg, 88%) as an orange oil. ^{1}H NMR (400 MHz, $CDCl_3$): δ = 8.16 (d, J = 12 Hz, 2H, H_v), 7.62 (d, J = 12 Hz, 2H, H_u), 7.31 – 7.22 (m, 4H, $H_{b,p}$), 7.22 – 7.15 (m, 4H, $H_{a,c,q}$), 7.15–7.08 (m, 2H, H_o), 5.53 (s, 1H, H_s), 5.40 (s, 1H, H_t), 3.42 (s, 2H, H_r), 3.18–3.04 (m, 2H, H_g), 2.59 (t, J = 8.0 Hz, 2H, H_d), 2.51 (t, J = 8.0 Hz, 2H, H_n), 2.48–2.37 (m, 4H, $H_{k,l}$), 1.82 (t, J = 8.0 Hz, 2H, H_e), 1.77–1.68 (m, 2H, H_m), 1.51 – 1.31 (m, 13H, $H_{h,j,w}$), 1.20–1.11 (m, 2H, H_i). ^{13}C NMR (101 MHz, $CDCl_3$): δ = 155.58, 147.06, 146.99, 144.57, 142.26, 141.77, 128.38, 128.31, 128.29, 127.31, 126.93, 125.86, 125.76, 123.70, 123.32, 118.37, 79.12, 59.02, 53.58, 52.27 (apparent as broad, due to C-D coupling), 47.11, 46.90, 33.62, 33.28, 30.34, 28.49 (3C), 28.17, 26.51, 24.79. $[M+H]^+$ $C_{37}H_{48}{}^2H_2O_4N_3$ calc. 602.3921, found 602.3919.

Synthesis of (4).

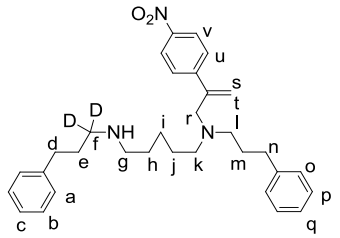

To a solution of **E15** (200 mg, 0.33 mmol, 1.0 equiv.) in CH_2Cl_2 (8 mL), trifluoroacetic acid (2 mL) was added dropwise. The reaction was left stirring open to air, at RT, and the disappearance of the substrate was monitored by ESI-MS. After 5 h, 15 mL of CH_2Cl_2 was

added to the reaction mixture and solution was carefully neutralised using $NaHCO_3$. The layers were separated and the aqueous layer was extracted with CH_2Cl_2 (2 x 15 mL). The combined organic layers were dried over $MgSO_4$ and the solvents were removed under reduced pressure to give **4** (87 mg, 52%) as an orange oil. ^{1}H NMR (400 MHz, $CDCl_3$): δ = 8.15 (d, J = 8.9 Hz, 2H, H_v), 7.62 (d, J = 8.9 Hz, 2H, H_u), 7.33 – 7.25 (m, 4H, $H_{b,p}$), 7.24 – 7.15 (m, 4H, $H_{a,c,q}$), 7.14–7.08 (m, 2H, H_o), 5.52 (s, 1H, H_s), 5.39 (s, 1H, H_t), 3.42 (s, 2H, H_r), 2.64 (t, J = 8.0 Hz, 2H, H_d), 2.57–2.36 (m, 8H, $H_{g,k,l,n}$), 1.80 (t, J = 8.0 Hz, 2H_e), 1.78–1.66 (m, 2H, H_m), 1.47–1.34 (m, 4H, $H_{h,j}$), 1.23–1.15 (m, 2H, H_i). ^{13}C NMR (101 MHz, $CDCl_3$) δ =147.03, 146.98, 144.61, 142.25, 141.79, 128.38, 128.35, 128.31, 128.29, 127.33, 125.87, 125.76, 123.31, 118.38, 59.11, 53.51, 53.11, 49.55, 48.42 (apparent as broad, due to C-D coupling), 33.67, 33.53, 30.81, 29.72, 28.43, 26.61, 25.15.. $[M+H]^+$ $C_{32}H_{40}{}^2H_2O_2N_3$ calc. 502.3397, found 502.3389.

Synthesis of (3).

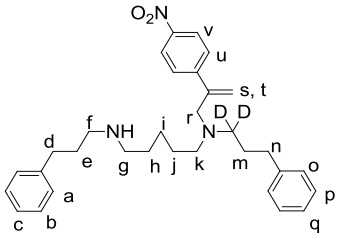

Compound **3** was synthesised according to Scheme E2.8. Experimental procedures are analogous to the ones described for the synthesis of compound **4**. Yields are shown in Scheme E2.8. ^{1}H NMR (400 MHz, $CDCl_3$): δ = 8.18 (d, J = 8.9 Hz, 2H, H_v), 7.65 (d, J = 8.9 Hz, 2H, H_u), 7.33 – 7.25 (m, 4H, $H_{b,p}$), 7.24 – 7.15 (m, 4H, $H_{a,c,q}$), 7.14 (d, J = 7.0 Hz, 2H, H_o), 5.55 (d, J = 0.9 Hz, 1H, H_s), 5.42 (d, J = 1.0 Hz, 1H, H_t), 3.45 (s, 2H, H_r), 2.70 – 2.62 (m, 4H, $H_{d,f}$), 2.58–2.50 (m, 4H, $H_{g,n}$), 2.43 (t, J = 8.0 Hz, 2H, H_k), 1.89–1.80 (m, 2H, H_e), 1.76–1.71 (m, 2H, H_m), 1.50–1.38 (m, 4H, $H_{h,j}$), 1.24–1.18 (m, 2H, H_i). ^{13}C NMR (101 MHz, $CDCl_3$) δ = 147.19, 147.11, 144.77, 142.42, 142.22, 128.50, 128.48, 128.44, 128.27, 127.47, 125.93, 125.89, 123.44, 118.50, 59.19, 53.62, 50.06, 49.66, 33.82, 33.75, 31.72, 30.08, 29.84, 28.28, 26.81, 25.35, (C-D not observed). $[M+H]^+$ $C_{32}H_{40}{}^2H_2O_2N_3$ calc. 502.3397, found 502.3390.

Synthesis of (E21)

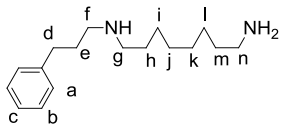

To a solution of 1,8-octanediamine (0.757 g, 5.20 mmol, 1.0 equiv.) in dry EtOH (100 mL), 3-phenylpropionaldehyde (685 µL, 5.20 mmol, 1.0 equiv.) was added in one portion. The reaction was stirred under N_2 for 72 h at room temperature. $NaBH_4$ (2.30 g, 62.0 mmol, 12 equiv.) was then added in portions and reaction was kept stirring under N_2 for another 12 h. After this time H_2O (50 mL) was added to the reaction mixture and product was extracted with CH_2Cl_2 (3 x 100 mL). The combined organic layers were washed with brine, dried over $MgSO_4$ and the solvent was removed under reduced pressure. Column chromatography (SiO_2, MeOH:CH_2Cl_2:NH_3(30% in H_2O) 10: 90:1.5) gave **E21** (550 mg, 40%) as a colourless oil. ^{1}H NMR (400 MHz, $CDCl_3$): δ = 7.33 – 7.23 (m, 2H, H_b), 7.22 – 7.14 (m, 3H, $H_{a,c}$), 2.70 – 2.61 (m, 6H, $H_{f,g,n}$), 2.58 (t, J = 7.4 Hz, 2H, H_d), 1.82 (apparent as dt, J = 14.6, 7.6 Hz, 2H, H_e), 1.56 – 1.37 (m, 4H, $H_{m,h}$), 1.35 – 1.23 (m, 8H, $H_{i,j,k,l}$). ^{13}C NMR (101 MHz, $CDCl_3$): δ = 141.75, 128.30 (4C), 125.74, 50.02, 49.58, 42.24, 33.81, 33.73, 31.70, 30.09, 29.52, 29.42, 27.33, 26.83.. $[M+H]^+$ $C_{17}H_{31}N_2$, calc. 263.2482, found 263.2478.

Synthesis of (E22)

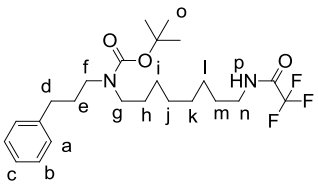

Synthesised according to the modified literature procedure.[20]

Under N_2, **E21** (550 mg, 2.09 mmol, 1 equiv.) was dissolved in CH_2Cl_2 (50 mL) and cooled to 0 °C. Ethyl trifluoroacetate (0.274 mL, 2.30 mmol, 1.1 equiv.) was added dropwise over 30 min to protect the primary amine. This mixture was then stirred for 30 min at 0 °C and at room temperature for additional 1 h. To the resulting mixture, a solution of Boc_2O (685 mg, 3.14 mmol, 1.5 equiv.) in CH_2Cl_2 (5 mL) was added dropwise. Dry Et_3N (0.438 mL, 3.144 mmol, 1.5 equiv.) was then added and the solution was stirred for 12 h at RT. The reaction mixture was then washed with $NaHCO_3$. The organic layer was separated, washed with water, dried over Na_2SO_4 and evaporated. Column chromatography (SiO_2, MeOH/CH_2Cl_2 4:94) afforded **E22** (960 mg, 88%) as a colourless paste. ^{1}H NMR (500 MHz, $CDCl_3$) δ = 7.32 – 7.24 (m, 2H, H_b), 7.23 – 7.12 (m, 3H, $H_{a,c}$), 6.33 (bs, 1H, H_p), 3.35 (apparent as q, J = 6.8 Hz, 2H, H_n), 3.29 – 3.04 (m, 4H, $H_{f,g}$), 2.59 (t, J = 8.0 Hz, 2H, H_d), 1.84 (apparent as dt, J

= 12.0, 8.0 Hz, 2H, H_e), 1.63 – 1.53 (m, 2H, H_m), 1.54 – 1.38 (m, 11H, $H_{h,o}$), 1.38 – 1.19 (m, 8H, $H_{i,j,k,l}$). ^{13}C NMR (126 MHz, $CDCl_3$): δ = 157.15 (q, J = 36.7 Hz, C-F), 155.78, 142.79, 128.37 (2C), 128.29 (2C), 125.99, 115.88 (q, J = 287.9 Hz, C-F), 79.24, 47.17, 46.99, 40.07, 33.29, 30.33, 29.03, 28.87, 28.49 (3C), 28.12 (2C), 26.66, 25.53. $[M+H]^+$ $C_{24}H_{38}F_3N_2O_3$, calc. 459.2829, found 459.2824.

Synthesis of (E23)

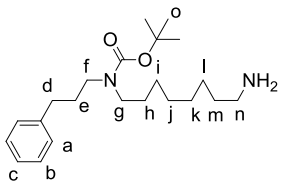

To a solution of **E22** (800 mg, 1.7 mmol, 1 equiv.) in MeOH (5 mL), NaOH (500 mg, 12.5 mmol, 13.6 equiv.) in H_2O was added. The reaction mixture was stirred at RT for 5 h. After this time the solvent was removed under reduced pressure, the residue was dissolved in H_2O, and extracted with CH_2Cl_2 (5 x 20 mL). The combined organic layers were dried over $MgSO_4$ and solvent was removed under reduced pressure. Purification by column chromatography (SiO_2, MeOH/CH_2Cl_2 20:80) afforded **E23** (412 mg, 67%) as a colourless oil. ^{1}H NMR (400 MHz, $CDCl_3$): δ = 7.38 – 7.26 (m, 2H, H_b), 7.26 – 7.11 (m, 3H, $H_{a,c}$), 3.29 – 3.04 (m, 4H, $H_{f,g}$), 2.69 (t, J = 7.0 Hz, 2H, H_n), 2.62 (t, J = 8.0 Hz, 2H, H_d), 1.86 (apparent as dt, J = 12.0, 8.0 Hz, 2H, H_e), 1.57 – 1.37 (m, 13H, $H_{h,m,o}$), 1.37 – 1.20 (m, 8H, $H_{i,j,k,l}$). ^{13}C NMR (101 MHz, $CDCl_3$): δ = 155.63, 139.81, 128.37 (2C), 128.30 (2C), 125.86, 79.05, 47.15, 46.84, 42.27, 33.86, 33.30, 29.47, 29.37, 28.49 (3C), 26.83 (4C) $[M+H]^+$ $C_{22}H_{39}N_2O_2$, calc. 365.2911, found 365.3006.

Synthesis of (E24)

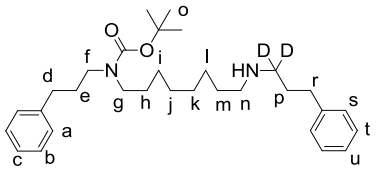

To a solution of **E23** (680 mg, 1.87 mmol, 1.0 equiv.) in dry EtOH (100 mL), 3-phenylpropionaldehyde-d_1 (203 mg, 1.50 mmol, 0.8 equiv.) was added in one portion. The reaction was stirred under N_2 for 72 h at room temperature. $NaBD_4$ (370 mg, 9.00 mmol, 6 equiv.) was then added in portions and reaction was kept stirring under N_2 for another 12 h. After this time H_2O (50 mL) was added to the reaction mixture and the product was extracted with CH_2Cl_2 (3 x 50 mL). The combined organic layers were washed with brine, dried over

$MgSO_4$ and the solvent was removed under reduced pressure. Column chromatography (SiO_2, MeOH/CH_2Cl_2 5:95) gave **E24** (430 mg, 47%) as a colourless oil. ^{1}H NMR (400 MHz, $CDCl_3$): δ = 7.32 – 7.24 (m, 4H, $H_{b,t}$), .23 – 7.14 (m, 6H, $H_{a,c,s,u}$), 3.35–2.98 (m, 4H, $H_{f,g}$), 2.65 (t, J = 8.0 Hz, 2H, H_d), 2.63 – 2.54 (m, 4H, $H_{n,r}$), 1.90 – 1.77 (m, 4H, $H_{e,p}$), 1.54 – 1.38 (m, 13H, $H_{h,m,o}$), 1.36–1.18 (s, 8H, $H_{i,j,k,l}$). ^{13}C NMR (101 MHz, $CDCl_3$): δ = 155.75, 142.50, 141.94, 128.48 (2C), 128.44, 128.42, 125.95, 125.87, 79.15, 50.09 (2C), 48.90 (p, J = 20.3 Hz C-D), 47.27, 46.96, 33.82, 33.41, 31.65, 30.27, 29.66, 29.46, 28.61 (3C), 27.45, 26.96 (2C). $[M+H]^+$ $C_{31}H_{47}D_2N_2O_2$, calc. 483.3914, found 483.3900.

Synthesis of (E25)

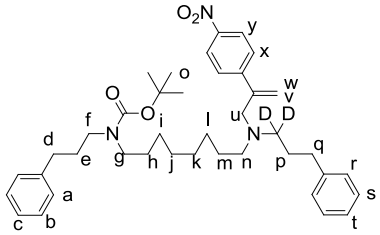

To a degassed solution of **E24** (400 mg, 0.82 mmol, 1 equiv.) in dry MeOH (50 mL), **W** (342 mg, 0.98 mmol, 1.2 equiv.) was added in one portion. The reaction mixture was stirred under N_2 at 50 °C for 72 h in the presence of ^{i}Pr$_2$NEt (420 µL, 2.46 mmol, 3 equiv.) After this time, the reaction was cooled to room temperature and H_2O (50 mL) was added. The mixture was extracted with CH_2Cl_2 (2 x 30 mL), dried over $MgSO_4$ and the solvents were removed under reduced pressure. Column chromatography (SiO_2, MeOH/CH_2Cl_2, 3:97) gave **E25** (400 mg, 76%) as an orange oil. ^{1}H NMR (400 MHz, $CDCl_3$): δ = 8.20 – 8.11 (m, 2H, H_y), 7.67 – 7.59 (m, 2H, H_x), 7.32 – 7.22 (m, 4H, $H_{b,s}$), 7.22 – 7.14 (m, 4H, $H_{a,c,t}$), 7.14 – 7.07(m, 2H, H_r), 5.53 (s, 1H, H_w), 5.40 (s, 1H, H_v), 3.42 (s, 2H, H_u), 3.31–3.02 (m, 4H, $H_{f,g}$), 2.60 (t, J = 7.8 Hz, 2H, H_d), 2.50 (t, J = 8.0 Hz, 2H, H_q), 2.39 (t, J = 7.4 Hz, 2H, H_n), 1.84 (apparent as dt, J = 15.3, 7.7 Hz, 2H, H_e), 1.71 (t, J = 8.0 Hz, 2H, H_p), 1.52 – 1.41 (m, 11H, $H_{h,o}$), 1.36 (apparent as dt, J = 14.3, 7.2 Hz, 2H, H_m), 1.30 – 1.09 (m, 8H, $H_{i,j,k,l}$). ^{13}C NMR (101 MHz, $CDCl_3$): δ = 155.63, 147.09, 146.98, 144.70, 142.33 (2C), 141.92, 128.37, 128.30 (2C), 127.34, 125.82, 125.73, 123.29, 118.30, 79.04, 59.06, 53.61, 47.15, 46.90, 33.63, 33.30, 29.72, 29.58 (2C), 29.44 (2C), 28.50, 28.46 (3C), 27.44, 26.89, 26.68 (C-D not observed). $[M+H]^+$ $C_{40}H_{54}D_2N_3O_4$, calc. 644.4391, found 644.4385.

Synthesis of (5).

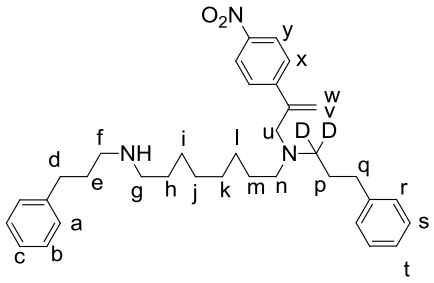

To a solution of **E25** (200 mg, 0.31 mmol, 1 equiv.) in CH_2Cl_2 (5 mL), trifluoroacetic acid (5 mL) was added dropwise. The reaction was left stirring open to air, at RT, and the disappearance of the substrate was monitored by ESI-MS. After 5 h, 5 mL of CH_2Cl_2 was added to the reaction mixture and the solution was carefully neutralised using $NaHCO_3$. The layers were separated and the aqueous layer was extracted with CH_2Cl_2 (10 mL). The combined organic layers were dried over $MgSO_4$ and the solvent removed under reduced pressure to give **5** (90 mg, 53%) as an orange oil. ^{1}H NMR (400 MHz, $CDCl_3$): δ = 8.22 – 8.14 (m, 2H, H_y), 7.68 – 7.61 (m, 2H, H_x), 7.32 – 7.25 (m, 4H, $H_{b,s}$), 7.24 – 7.16 (m, 2H, $H_{c,t}$), 7.16 – 7.10 (m, 4H, $H_{a,r}$), 5.55 (d, J = 0.9 Hz, 1H, H_w), 5.41 (d, J = 1.1 Hz, 1H, H_v), 3.44 (s, 2H, H_u), 2.91 (d, J = 7.7 Hz, 2H, H_d), 2.86 (d, J = 7.6 Hz, 2H, H_g), 2.65 (t, J = 7.5 Hz, 2H, H_f), 2.53 (t, J = 7.6 Hz, 2H, H_q), 2.41 (t, J = 7.4 Hz, 2H, H_n), 2.04 (apparent as dt, J = 15.6, 7.7 Hz, 2H, H_e), 1.74 (t, J = 7.7 Hz, 2H, H_p), 1.64 (apparent as dt, J = 14.0, 7.5 Hz, 2H, H_h), 1.43 – 1.36 (m, 2H, H_m), 1.35 – 1.14 (m, 8H, $H_{i,j,k,l}$). ^{13}C NMR (101 MHz, $CDCl_3$): δ = 147.06, 146.96, 144.56, 142.27, 139.79, 128.63, 128.30, 128.20, 127.35, 126.40, 125.75, 123.28, 118.42, 58.98, 53.53, 52.08 (apparent as broad, due to C-D coupling), 47.86, 47.25, 33.61, 32.59, 29.26, 28.94, 28.10, 27.39, 27.31, 26.66, 26.45, 25.83. $[M+H]^+$ $C_{35}H_{46}D_2N_3O_2$, calc 544.7863, found 544.7853.

Synthesis of (6)

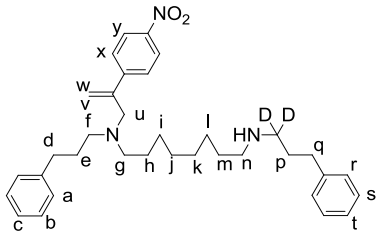

Compound **6** was synthesised according to Scheme E2.10. Experimental procedures are analogous to the ones described for the synthesis of compound **5**. Yields are shown in Scheme E2.10. ^{1}H NMR (500 MHz, $CDCl_3$): δ = 8.18 – 8.12 (m, 2H, H_y), 7.67 – 7.59 (m, 2H H_x), 7.31 – 7.22 (m, 4H, $H_{b,s}$), 7.22 – 7.14 (m, 4H, $H_{r,c,t}$), 7.14 – 7.08 (m, 2H, H_a), 5.53 (d, J

= 0.7 Hz, 1H, H_w), 5.39 (d, *J* = 1.0 Hz, 1H, H_v), 3.42 (s, 2H, H_u), 2.65 (t, *J* = 7.5 Hz, 2H, H_q), 2.60 (t, *J* = 7.3 Hz, 2H, H_n), 2.50 (t, *J* = 7.6 Hz, 2H, H_d), 2.44 (t, *J* = 7.1 Hz, 2H, H_f), 2.39 (t, *J* = 7.2 Hz, 2H, H_g), 1.84 (t, *J* = 7.8 Hz, 2H, H_p), 1.72 (apparent as dt, *J* = 15.1, 7.5 Hz, 2H, H_e), 1.47 (apparent as dt, *J* = 14.3, 7.4 Hz, 2H, H_m), 1.45 – 1.36 (m, 2H, H_h), 1.31 – 1.10 (m, 8H, $H_{i,j,k,l}$). ^{13}C NMR (126 MHz, $CDCl_3$): δ = 147.23, 147.11, 144.84, 142.46, 142.03, 128.51, 128.50, 128.44 (2C), 127.49, 125.98, 125.88, 123.43, 118.47, 59.29, 53.78, 53.24, 49.78, 46.21 (apparent as broad, due to C-D coupling), 33.82, 33.69, 31.06, 29.85, 29.81, 29.63, 29.60, 28.61, 27.57, 27.40, 26.85. $[M+H]^+$ $C_{35}H_{46}D_2N_3O_2$, calc 544.3867, found 544.3856.

Synthesis of MT

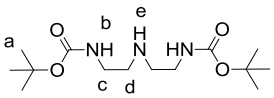

Synthesised according to a literature procedure [21]

Diethylenetriamine (1.00 g, 9.69 mmol) and Et_3N (2.94 g, 29.1 mmol) were dissolved in dry THF (50 mL) and cooled in an ice bath. 2-(Boc-oxyimino)-2-phenylacetonitrile (Boc-ON, 4.78 g, 19.4 mmol) dissolved in dry THF (20 mL) was then added dropwise and the reaction mixture was left to stir in the ice bath for 1 hour, and then at room temperature for a further 2 hours. After this time, the solvent was removed *in vacuo* and the residue was dissolved in CH_2Cl_2 and washed with 5 % $NaOH_{(aq)}$. The organic layer was dried over $MgSO_4$, and the solvent evaporated. The crude residue was purified by column chromatography using 9:1:0.1 CH_2Cl_2:MeOH:NH_4OH to give the pure product as a colourless oil (2.93 g, 99 %). ^{1}H NMR (400 MHz, $CDCl_3$): 4.93 (bs, 2H, H_b), 3.23 (m, 4H, H_c), 2.75 (t, *J* = 5.7 Hz, 4H, H_d), 1.47 (s, 18H, H_a). ^{13}C NMR (101 MHz, CDCl3) δ = 156.21, 79.29, 48.83, 40.30, 28.44.

Synthesis of (M-*1*Boc)

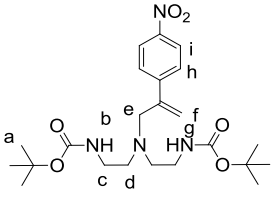

The Boc-protected amine **MT** (498 mg, 1.64 mmol), **W** (686 mg, 1.97 mmol) and ^{i}Pr$_2$NEt (424 mg, 3.29 mmol) were suspended in MeOH (20 mL) and heated at 50 ˚C for 4 days. After this time the reaction mixture was diluted with CH_2Cl_2 (50 mL), washed with water (30 mL), dried over $MgSO_4$ and the solvent removed *in vacuo*. The product was purified *via*

column chromatography using CH_2Cl_2 to 2% MeOH/CH_2Cl_2 as the eluent to give **M-***1*Boc as a pale yellow solid (630 mg, 83 %). ^{1}H NMR (400 MHz, $CDCl_3$) δ = 8.27 – 8.17 (m, 2H, H_i), 7.64 – 7.53 (m, 2H, H_h), 5.56 (s, 1H, H_f), 5.43 (s, 1H, H_g), 4.51 (s, 2H, H_b), 3.51 (s, 2H, H_e), 3.22 – 3.06 (m, 4H, H_c), 2.55 (t, J = 5.9 Hz, 4H, H_d), 1.40 (s, 18H, H_a). ^{13}C NMR (101 MHz, $CDCl_3$) δ = 156.09, 147.30, 146.57, 144.39, 127.51, 123.80, 119.35, 79.45, 59.17, 53.15, 38.09, 28.53 (6C). HRMS: $[M+H]^+$ $C_{23}H_{37}N_4O_6$, calc. 465.2713, found 465.2703.

Synthesis of M-*1*

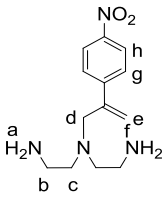

Compound **M-***1*Boc (40 mg, 0.086 mmol) was dissolved in CH_2Cl_2 (5 mL). Trifluoroacetic acid (0.5 mL) was added and the reaction stirred at room temperature for 1 hour. $NaHCO_3$ (sat.) was then added in portions to neutralise the acid, followed by water (10 mL). The CH_2Cl_2 layer was separated and discarded. The aqueous layer was then extracted with EtOAc (2 x 20 mL), and the combined organic layers were dried over $MgSO_4$ and the solvent removed to give the pure product as yellow oil (22 mg, quantitative). ^{1}H NMR (400 MHz, MeOD): δ = 8.13 (d, J = 8.9 Hz, 2H, H_h), 7.62 (d, J = 8.9 Hz, 2H, H_g), 5.59 (s, 1H, H_e), 5.47 (s, 1H, H_f), 3.60 (s, 2H, H_d), 3.21 (bs, 4H, H_a), 2.92 (apparent as bs, 4H, H_b), 2.70 (apparent as bs, 4H, H_c). ^{13}C NMR (101 MHz, $CDCl_3$) δ = 148.39, 147.13, 142.96, 128.38, 124.79, 122.60, 58.10, 51.28, 33.73. HRMS: $[M+H]^+$ $C_{13}H_{21}N_4O_2$ calc. 265.1665, found: 265.1651.

Full ^{1}H NMR spectra of selected compounds

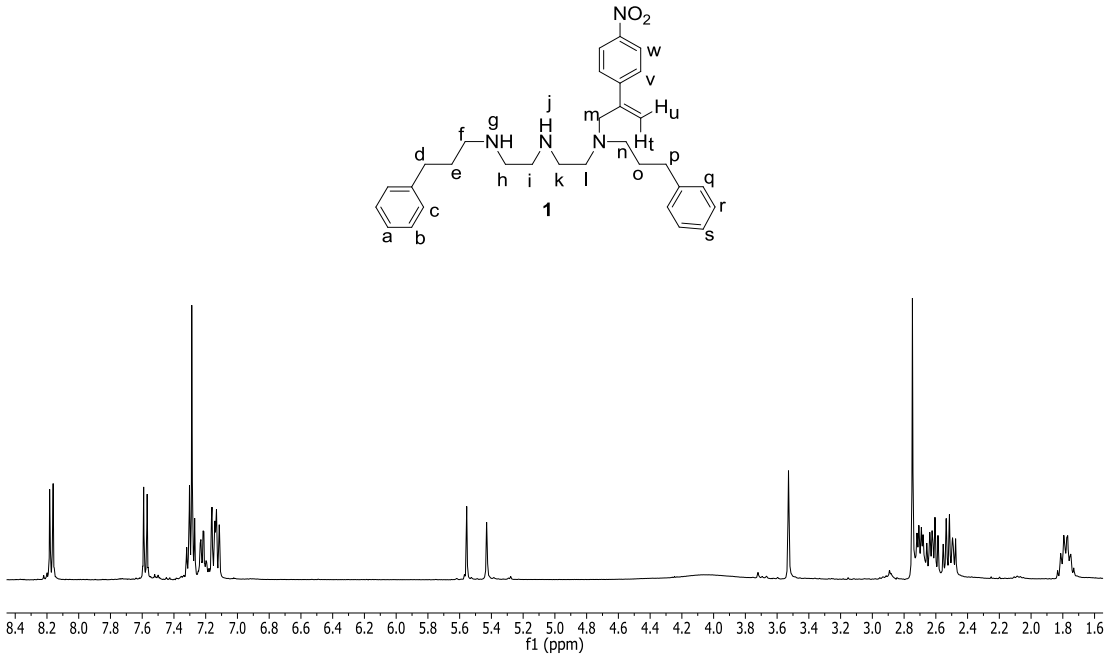

Figure E 2.1. ^{1}H NMR spectra (400 MHz, $CDCl_3$, 298 K) of compound **1**.

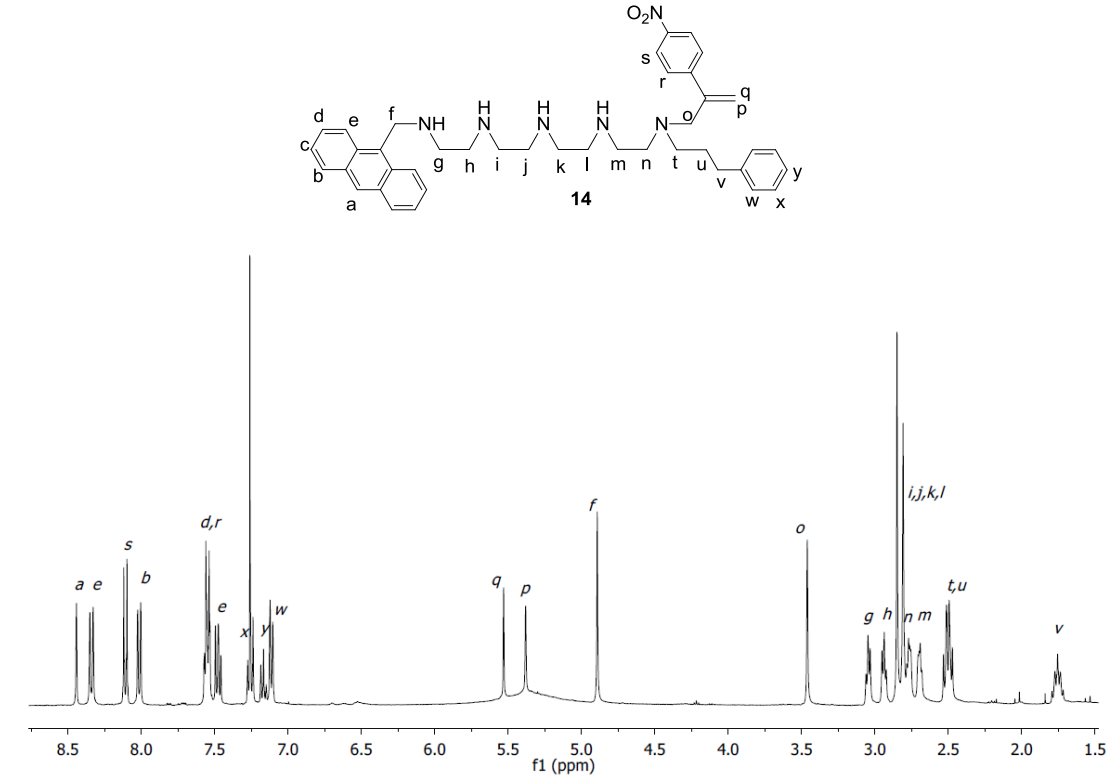

Figure E 2.2. ^{1}H NMR spectra (400 MHz, $CDCl_3$, 298 K) of compound **14**.

2.6 References

[1] a) *Molecular Motors* (Ed.: M. Schliwa), Wiley-VCH, Weinheim, **2003**; b) Vale, R. D. *Cell* **2003**, *112*, 467–480.

[2] a) von Delius, M.; Geertsema, E. M.; Leigh, D. A. *Nat. Chem.* **2010**, *2*, 96–101; b) Otto, S. *Nat. Chem.* **2010**, *2*, 75–76; c) von Delius, M.; Geertsema, E. M.; Leigh, D. A.; Tang, D.-T. D. *J. Am. Chem. Soc.* **2010**, *132*, 16134–16145; d) Barrell, M. J.; Campaña, A. G.; von Delius, M.; Geertsema, E. M.; Leigh, D. A. *Angew. Chem. Int. Ed.* **2011**, 50, 285–290.

[3] a) Yin, P.; Yan, H.; Daniell, X. G.; Turberfield, A. J.; Reif, J. H. *Angew. Chem. Int. Ed.* **2004**, *43*, 4906–4911; b) Bath, J.; Green, S. J.; Turberfield, A. J. *Angew. Chem. Int. Ed.* **2005**, *44*, 4358–4361; c) Tian, Y.; He, Y.; Chen, Y.; Yin, P.; Mao, C. *Angew. Chem. Int. Ed.* **2005**, *44*, 4355–4358; d) Yin, P.; Choi, H. M. T.; Calvert, C. R. ; Pierce, N. A. *Nature* **2008**, *451*, 318–322; e) Green, S. J.; Bath, J.; Turberfield, A. J. *Phys. Rev. Lett.* **2008**, *101*, 238101–238104; f) Omabegho, T.; Sha, R.; Seeman, N. C. *Science* **2009**, *324*, 67–71; g) Lund, K. *et al*. *Nature* **2010**, *465*, 206–210; h) Gu, H.; Xiao, S. J.; Seeman, N. C. *Nature* **2010**, *465*, 202–205; i) He, Y.; Liu, D. R. *Nat. Nanotechnol*. **2010**, *5*, 778–782; j) Wickham, S. F. J.; Endo, M.; Katsuda, Y.; Hidaka, K.; Bath, J.; Sugiyama, H.; Turberfield, A. J. *Nat. Nanotechnol*. **2011**, *6*, 166–169; k) Muscat, R. A.; Bath, J.; Turberfield, A. J. *Nano Lett.* **2011**, *11*, 982–987.

[4] For examples of molecular rearrangements, see: a) Kurti, L.; Czakó B. in *Strategic applications of named reactions in organic synthesis*, Elsevier, Oxford, **2005**. Successive Cope rearrangements: b) Ryan, J. P.; O'Connor, P. R. *J. Am. Chem. Soc.* **1952**, *74*, 5866–5869. Base-induced interconversion of bullvalone isomers: c) Lippert, A. R.; Kaeobamrung, J.; Bode, J. W. *J. Am. Chem. Soc.* **2006**, *128*, 14738–14739; d) Lippert, A. R.; Keleshian, V. L.; Bode, J. W. *Org. Biomol.Chem.* **2009**, *7*, 1529–1532; e) Lippert, A. R.; Nagawana, A.; Keleshian, V. L.; Bode, J. W. *J. Am. Chem. Soc.* **2010**, *132*, 15790–15799; f) He, M.; Bode, J. W. *Proc. Nat. Acad. Sci. U.S.A.* **2011**, *108*, 14752–14756. Processive crown ether migration along oligoamine scaffolds: g) Weimann, D. P.; Winkler, H. D. F.; Falenski, J. A.; Koksch, B.; Schalley, C. A. *Nat. Chem.* **2009**, *1*, 573–577; h) Winkler, H. D. F.; Weimann, D. P.; Springer, A.; Schalley, C. A. *Angew. Chem. Int. Ed.* **2009**, *48*, 7246–7250.

[5] von Delius, M.; Leigh, D. A. *Chem. Soc. Rev.* **2011**, *40*, 3656–3676.

[6] a) Mitra, S.; Lawton, R. G. *J. Am. Chem. Soc.* **1979**, *101*, 3097–3110; b) Brocchini, S. J.; Eberle, M.; Lawton, R. G. *J. Am. Chem. Soc.* **1988**, *110*, 5211–5212; c) Liberatore, F. A.; Comeau, R. D.; McKearin, J. M.; Pearson, D. A.; Belonga, B. Q.; Brocchini, S. J.; Kath, J.; Phillips,T.; Oswell, K.; Lawton, R. G. *Bioconjugate Chem.* **1990**, *1*, 36–50; d) del Rosario,

R. B.; Brocchini, S. J.; Lawton, R. G.; Wahl, R. L.; Smith, R. *Bioconjugate Chem.* **1990**, *1*, 51–59.

[7] Recently, structurally related three carbon bridges were used as disulfide-specific intercalators in proteins a) Balan, S.; Choi, J.; Godwin, A.; Teo, I.; Laborde, C. M.; Heidelberger, S.; Zloh, M.; Shaunak, S.; Brocchini, S. *Bioconjugate Chem*. **2007**, *18*, 61–76; and peptides: b) Pfisterer, A.; Eisele, K.; Chen, X.; Wagner, M.; Müllen, K.; Weil, T. *Chem. Eur. J*. **2011**, *35*, 9697–9707). Pfisterer *et al*. provide ^{1}H NMR evidence for the three-carbon-bridge formation through the addition–elimination mechanism originally proposed by Lawton *et al*. See: ref. [6a].

[8] Processivity is the tendency of the molecular fragment (*i.e*. the walker) to remain attached to the track during operation, *i.e*. to migrate along a molecular scaffold without detaching or exchanging with other molecules in the bulk. See ref. [5].

[9] Rannard, S. P.; Davis, N. J. *Org. Let.* **2000**, *2*, 2117–2120.

[10] The positional isomers of the walkers on the track are effectively the components of a dynamic combinatorial library: a) Corbett, P. T.; Leclaire, J.; Vial, L.; West, R.; Wietor, J. L.; Sanders, J. K. M.; Otto, S. *Chem. Rev*. **2006**, *106*, 3652–3711 and their interconversion a type of constitutional dynamic chemistry b) Lehn, J. -M. *Chem. Soc. Rev*. **2007**, *36*, 151–160.

[11] Although changing the spacer alters the conformation of the molecule, the distance between the outer footholds remains similar and the tracks are flexible.

[12] As $t_{1/2}$ = 1.5 h for the amine-exchange process, the average number of steps taken in 3 days is ~48.

[13] a) Vale, R. D.; Funatsu, T.; Pierce, D. W.; Romberg, L. ; Harada, Y.; Yanagida, T. *Nature* **1996**, *380*, 451–453; b) Case, R. B.; Pierce, D. W.; Hom-Booher, N. ; Hart, C. L.; Vale, R. D. *Cell* **1997**, *90*, 959–966.

[14] For structurally-related fluorophore-spacer-receptor systems, see: Bag, B.; Bharadwaj, P. K. *J. Phys. Chem. B* **2005**, *109*, 4377–4390.

[15] The fluorescence of anthrylmethylamines is quenched by intramolecular photoinduced electron transfer (PET) from the nitrogen lone pair to the anthracene moiety. a) Alves, S.; Pina, F.; Albelda, M. T.; España, E. G. *Eur. J. Inorg. Chem*. **2001**, 405–412; b) Soriano, C.; Luis, S. V.; Greiner, G.; Maier, I. *J. Chem. Soc. Perkin Trans*. **2002**, *2*, 1005–1011; c) Bradbury, A. J.; Lincoln, S. F.; Wainwright, K. P.; *New J. Chem*. **2008**, *32*, 1500–1508; d) Plush, S. E.; Lincoln, S. F.; Wainwright, K. P. *Inorg. Chim. Acta* **2009**, *362*, 3097–3103.

[16] Lakowicz, J. R. *Principles of Fluorescence Spectroscopy*, *3rd edition*, Springer. New York, **2006**.

[17] It was necessary to protonate samples before recording emission spectra in order to avoid folding of the molecule and prevent intramolecular PET from occurring. e) Nishimura, G.; Shiraishi, Y.; Hirai, T. *Chem. Commun*. **2005**, 5313–5315; f) Shiraishi, Y.; Tokitoh, Y.; Nishimura, G.; Hirai, T. *Org. Lett*. **2005**, *7*, 2611–2614. Experimental procedure: Compound **14** was dissolved in DMSO (spectrophotometric grade) at 7.14×10^{-5} M. Periodically, an aliquot (1.00 mL) was quenched with CF_3CO_2H (10.0 μL), diluted to 1.78×10^{-5} M, and the fluorescence spectrum recorded (λ_{ex} = 366 nm)

[18] A small amount (<5%) of additional signals attributed to decomposition of **14** began to be apparent in the ^{1}H NMR spectrum after 7.5 h.

[19] Kay, E. R.; Leigh, D. A.; Zerbetto, F. *Angew. Chem. Int. Ed.* **2007**, *46*, 72–191.

[20] Srinivasachari, S.; Liu, Y.; Zhang, G.; Prevette, L.; Reineke, T. M. *J. Am.Chem. Soc.* **2006**, *128*, 8176–8184.

[21] Rannard, S. P.; Davis, Nicola J. *Org. Let*. **2000**, *2*, 2117–2120.

Chapter III

One Dimensional Random Walk of a Synthetic Small Molecule Towards a Thermodynamic Sink

'One Dimensional Random Walk of a Synthetic Small Molecule Towards a Thermodynamic Sink', Campaña, A. G.; Leigh, D. A.; Lewandowska, U.,
J. Am. Chem. Soc., published online 14 May 2013, DOI: 10.1021/ja402382n

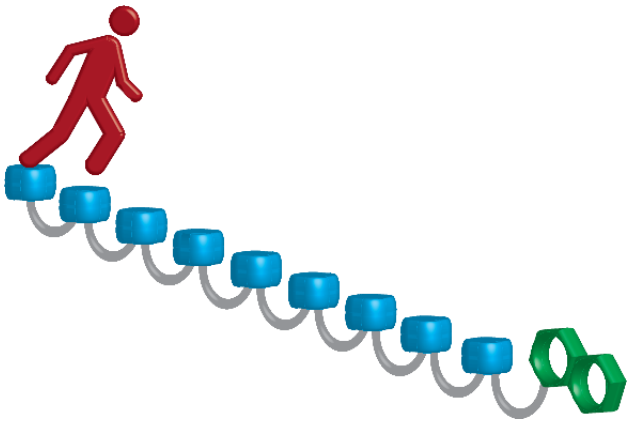

ACKNOWLEDGMENTS

Dr. Araceli G. Campaña if gratefully acknowledged for her contribution to this Chapter. The synthesis of compound ***5-1*** was performed by Dr. A. G. Campaña. Prof. Günter von Kiedrowski is kindly acknowledged for the generous gift of program SimFit and Dr. Craig. C. Robertson for many useful discussions and instructions while using SimFit program. Dr. Bartosz Lewandowski and Miriam R. Wilson are acknowledged for their assistance in acquiring ^{1}H NMR data for kinetic experiments.

Dr. Stephen Goldup is gratefully acknowledged for his input into the formalisation of intramolecular exchange as a random walk.

3.1 Synopsis

In this Chapter, a modified approach to synthesis of polyethyleneimine tracks of various lengths (number of amine footholds, n = 3, 5, 9) and the intramolecular, spontaneous migration of α-methylene-4-nitrostyrene from amine group to amine group, along those tracks, is described. Each track consists of n-1 secondary aliphatic footholds and features a naphthylmethyl amine as final foothold. In the presence of excess of base, the molecule preferentially 'walks' towards the favoured, final foothold and it is possible to monitor the population of each positional isomer in time (for n = 3, 5). Control over the rate of exchange is achieved by varying the amount of base added. The exchange along a 9 foothold track is also demonstrated and the molar fraction of walkers reaching the final foothold is determined quantitatively by ^{1}H NMR. The dynamic migration of this α-methylene-4-nitrostyrene upon the polyamine track is a diffusion process limited to one dimension and as such is additionally described using one dimensional random walk.

3.2 Introduction

Structural dynamics of small molecules are a subject of increasing interest in the scientific community. Shape shifting molecules like bullvalones, which undergo a series of sequential, spontaneous Cope rearrangements, forming large number of degenerate isomers, can be functionalised and the isomer distribution can be changed in response to a recognition event. [1] Dynamic Covalent Chemistry (DCC) [2] allowed for the development of new approaches in the design of artificial molecular transport systems, delivering the first examples of non-interlocked synthetic structures able to perform translational motion. [3] Supramolecular interactions have also been employed to study random and gradient driven migration of molecules. [4] In some cases however, the highly dynamic character of the migration mechanism, limits the control over direction or/and the degree of processivity. [5] At the interface of research avenues, α-methylene-4-nitrostyrene walking molecule[6] became an interesting example of combining the robustness of DCC and efficiency of sequential, reversible rearrangements. [7]

3.3 Results and Discussion

3.3.1 Modified Synthesis of Unsymmetrical Polyamine Tracks.

We investigated the unusual migration of α-methylene-4-nitrostyrene by a sequence of intramolecular Michael and retro-Michael reactions [8] between adjacent amine groups preferentially in one direction upon tracks of increasing lengths, towards the thermodynamically favoured distribution of walkers on the track. A series of unsymmetrical walker-track conjugates were synthesised. For the three-foothold track, the corresponding Boc protected diethylenetriamine **1** was desymmetrised via reductive amination with 1-naphthaldehyde, followed by a sequence of protection-deprotection reactions to yield free primary amine **2**, which after reductive amination with 3-phenylpropionaldehyde gave the desired track **3** featuring only one site for walker attachment (see Scheme 3.1). This way, the α-methylene-4-nitrostyrene walker unit **4** was introduced exclusively to the amine furthest from the naphthylmethyl group. Subsequent Boc deprotection gave compound **5**-*1* as a CF_3CO_2H salt, in which the walker was free to migrate along the track from its original position, but only when it was subjected to suitable walking conditions.

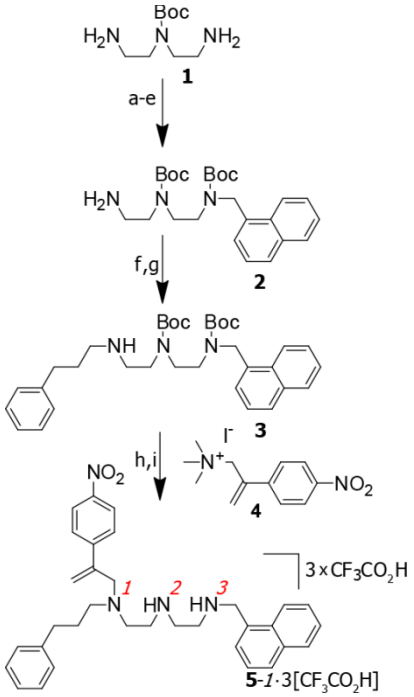

Scheme 3.1. Synthesis of walker-track conjugate **5**-1[3×CF_3CO_2H]. Reaction conditions: a) 1-naphthaldehyde, EtOH, RT, 16 h; b) $NaBH_4$, RT, 3 h, 34% (two steps); c) CF_3CO_2Et, CH_2Cl_2, 0 °C→RT, 16 h; d) Boc_2O, Et_3N, RT, 12 h; e) NaOH, MeOH/H_2O, RT, 5 h, 92% (three steps); f) 3-phenylpropionaldehyde, EtOH, RT, 16 h; g) $NaBH_4$, RT, 3 h, 27%, (two steps); h) **4**, $^{i}Pr_2NEt$, MeOH, 50 °C, 24 h, 54%; i) CF_3CO_2H, CH_2Cl_2, RT, 3 h, quant.

3.3.2 Probing the Reaction Conditions for the Intramolecular Migration Upon Three Foothold Tracks.

In order to find optimum walking conditions, the intramolecular exchange of **5**-*1*·3[CF_3CO_2H] was monitored in [D_6]DMSO (20 mM, 298 K) in the presence of 4, 3 and 2 equiv. of diisopropylethylamine ($^{i}Pr_2NEt$). Reactions were followed by ^{1}H NMR spectroscopy and evaluated using SimFit program.[9] When the exchange of **5**-*1*·3[CF_3CO_2H] was performed in the presence of 4 equiv. of $^{i}Pr_2NEt$, the disappearance of substrate and appearance of new sets of signals corresponding to new positional isomers was observed (Figure 3.1). Interestingly, the analysis of ^{1}H NMR spectra showed that the walker migrates predominantly through exchange between adjacent amine footholds. Only after the positional isomer **5**-*2* (blue coloured, see Figure 3.1 and Figure 3.2) was formed, signals corresponding to isomer **5**-*3* became apparent in the spectrum (green coloured, see Figure 3.1 and Figure 3.2), which confirms the results of our previous studies of over-stepping of footholds in polyethyleneimine tracks.[7] After 48 h of reaction, the majority of walker units (67%) populated the last foothold of the track (**5**-*3*, Figure 3.2b) and no further changes were observed in the ^{1}H NMR spectrum.

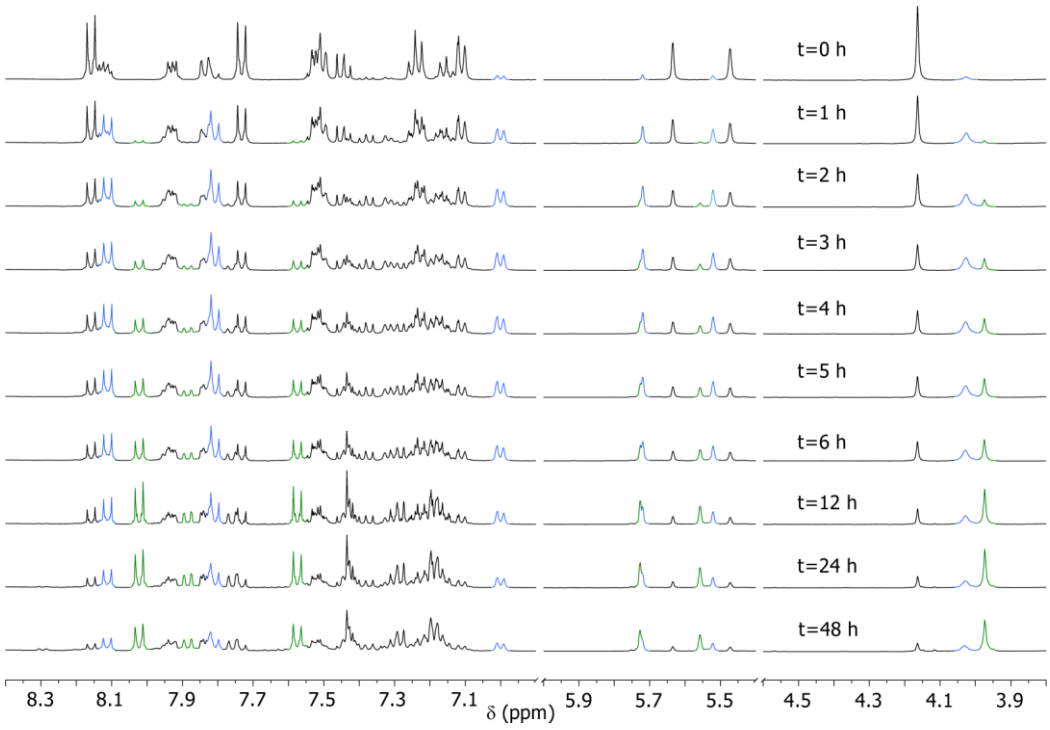

Figure 3.1. Partial ^{1}H NMR spectra (400 MHz, 20 mM, [D_6]DMSO, 298 K) monitoring the intramolecular exchange of **5**-*1*·3[CF_3CO_2H] (black resonances at t = 0 h) in the presence of 4 equiv. of $^{i}Pr_2NEt$, showing the consecutive formation of **5**-*2* (blue resonances) and **5**-*3* (green resonances) at given times.

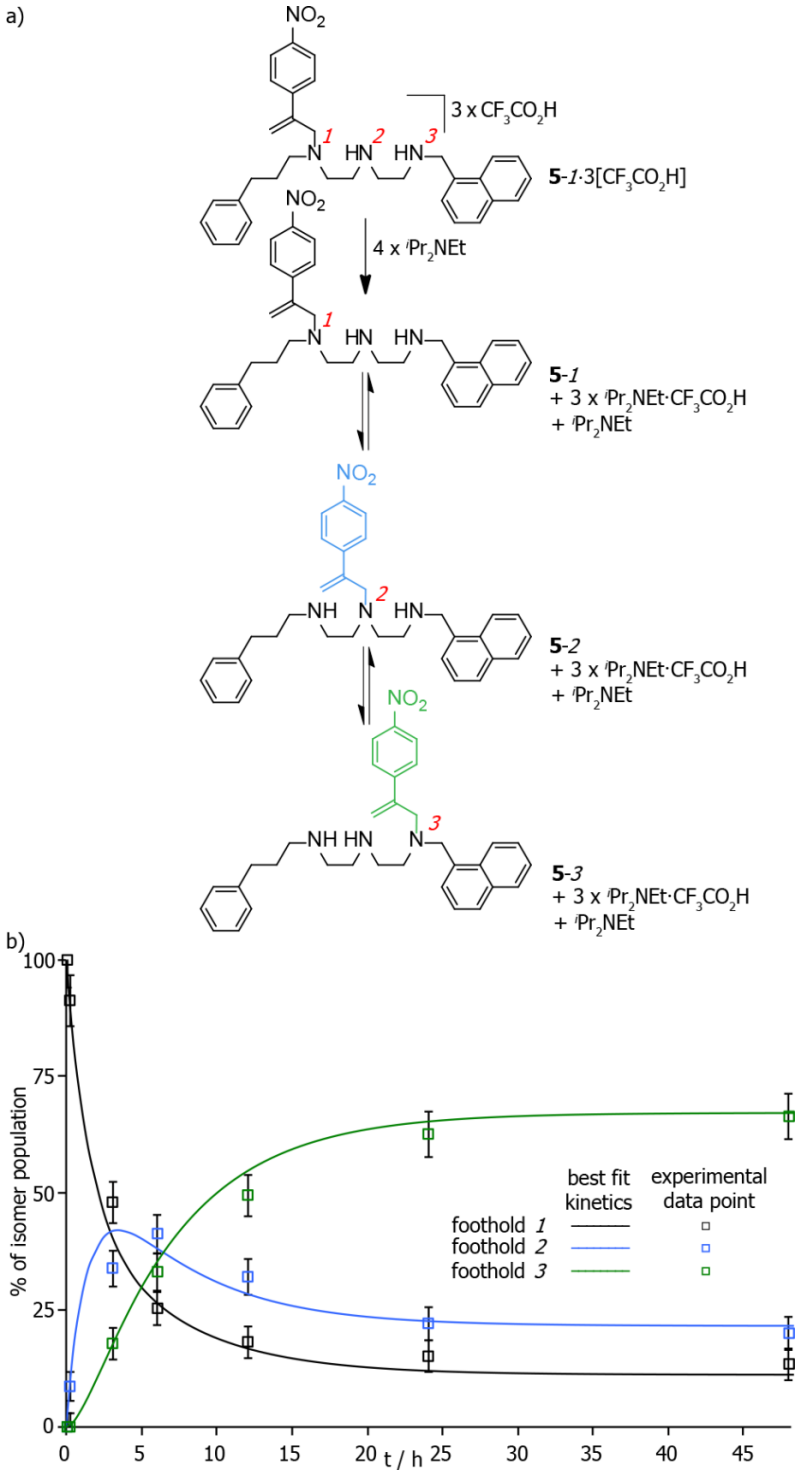

Figure 3.2. a) Intramolecular migration of **5**-*1*·3[CF_3CO_2H] in the presence of 4 equiv. of $^{i}Pr_2NEt$. Walker's stepwise migration towards the end of the track is the preferred process. b) Rate of formation or disappearance of isomers during the exchange process, based on ^{1}H NMR spectra at given times. After 48 h of exchange, 67% of walkers reach the final foothold of the track (isomer **5**-*3*). Continuous lines represent the best fit of the experimental data to the kinetics of the exchange between **5**-*1*, **5**-*2* and **5**-*3* using the SimFit program (see Experimental Section for details). Error bars represent the estimated ±3% error of ^{1}H NMR integration (the proton signals used for the integration are the equivalent ones in each positional isomer, see section 3.6.3.3).

When the exchange of **5**-*1*·3[CF_3CO_2H] was performed in the presence of 3 equiv. of $^{i}Pr_2NEt$, walker unit was also free to explore all three footholds in the track and it was possible to follow formation of each of the positional isomers (see Figure 3.3 and Figure 3.4). However, migration was significantly slower and after 48 h, 47% of walkers had reached the last foothold (Figure 3.4b).

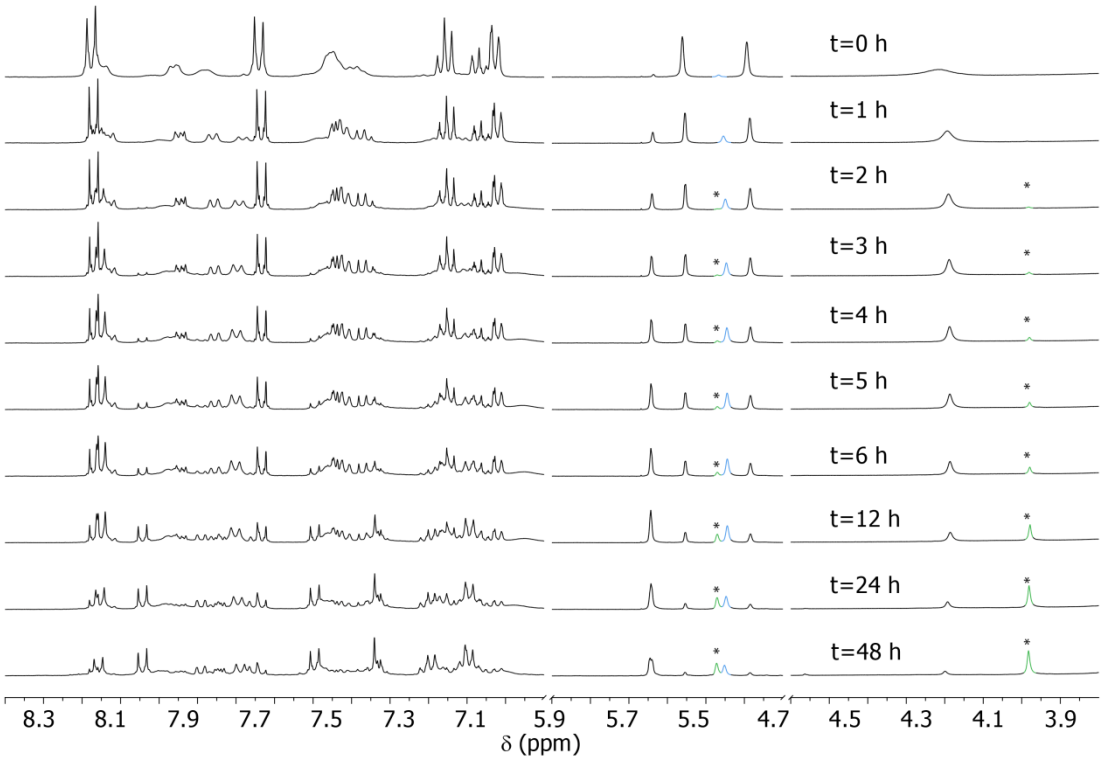

Figure 3.3. Partial ^{1}H NMR spectra (400 MHz, 20 mM, [D_6]DMSO, 298 K) monitoring the intramolecular exchange of **5**-*1*·3[CF_3CO_2H] (black resonances at t = 0 h) in the presence of 3 equiv. of $^{i}Pr_2NEt$, showing the consecutive formation of **5**-*2* (blue resonances) and **5**-*3* (green resonances, annotated with *) at given times.

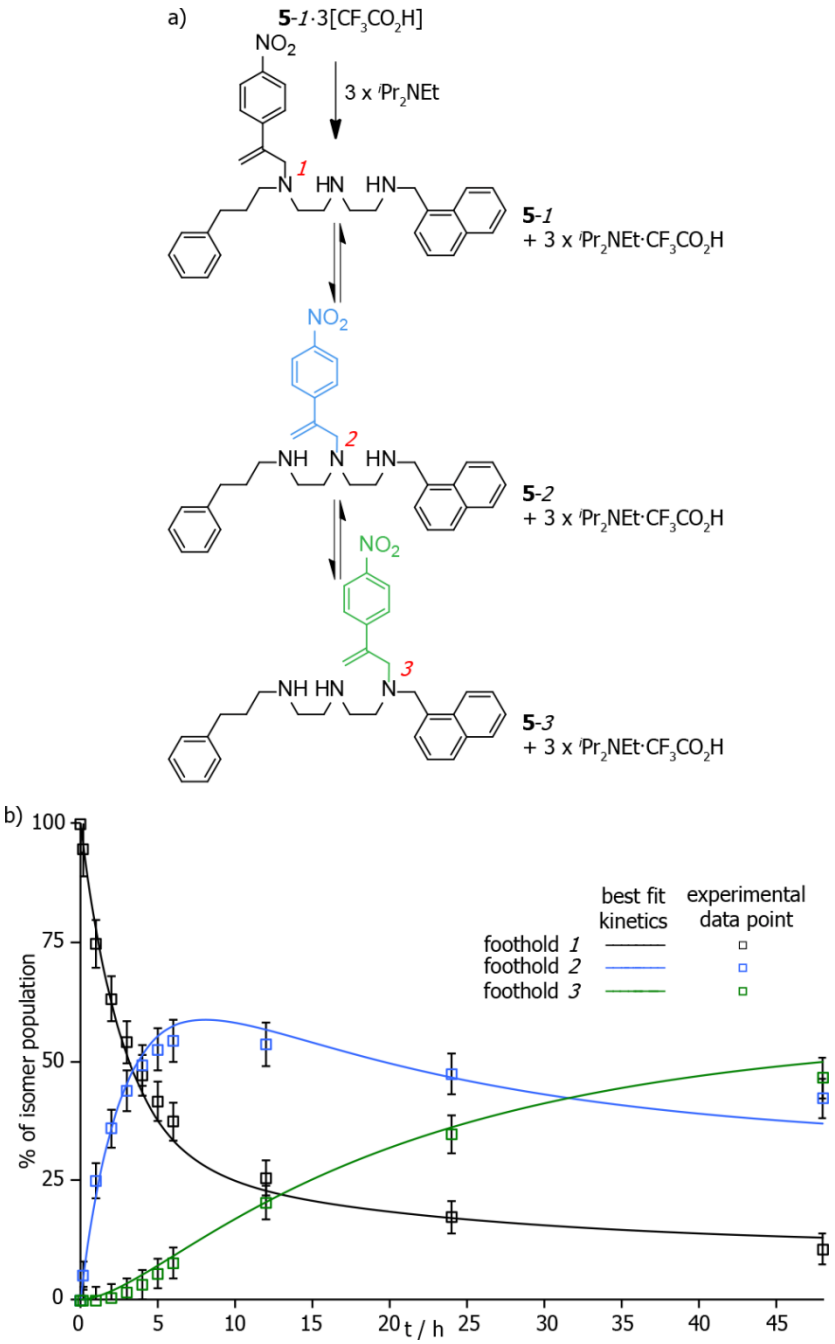

Figure 3.4. a) Intramolecular migration of **5**-*1*·3[CF_3CO_2H] in the presence of 3 equiv. $^{i}Pr_2NEt$. b) Rate of formation or disappearance of isomers during the exchange process, based on ^{1}H NMR spectra at given times. After 48 h of exchange, 47% of walker units occupy the final foothold of the track. Continuous lines represent the best fit of the experimental data to the kinetics of the exchange between **5**-*1*, **5**-*2* and **5**-*3* using the SimFit program (see Experimental Section for details). Error bars represent the estimated ±3% error of ^{1}H NMR integration (the proton signals used for the integration are the equivalent ones in each positional isomer, see section 3.6.3.3).

Interestingly, during the exchange of **5**-*1*·3[CF_3CO_2H] in the presence of 2 equiv. $^{i}Pr_2NEt$, after 48 h of reaction, **5**-*2* accounted for about 90% of the reaction mixture and formation of **5**-*3* accounted for only 4% of the reaction mixture (Figure 3.5 and Figure 3.6). These results suggest that the final foothold in **5**-*1*·3[CF_3CO_2H] is more basic than the central foothold in the polyethylenamines.[10] Therefore in the presence of only 2 equiv. of $^{i}Pr_2NEt$, the walker is mainly located on the second foothold of the track. The relatively mild basicity of $^{i}Pr_2NEt$ (pK_a ~10.5)[11] implies that an excess of base is needed to fully deprotonate those tracks which is in agreement with the experiment.

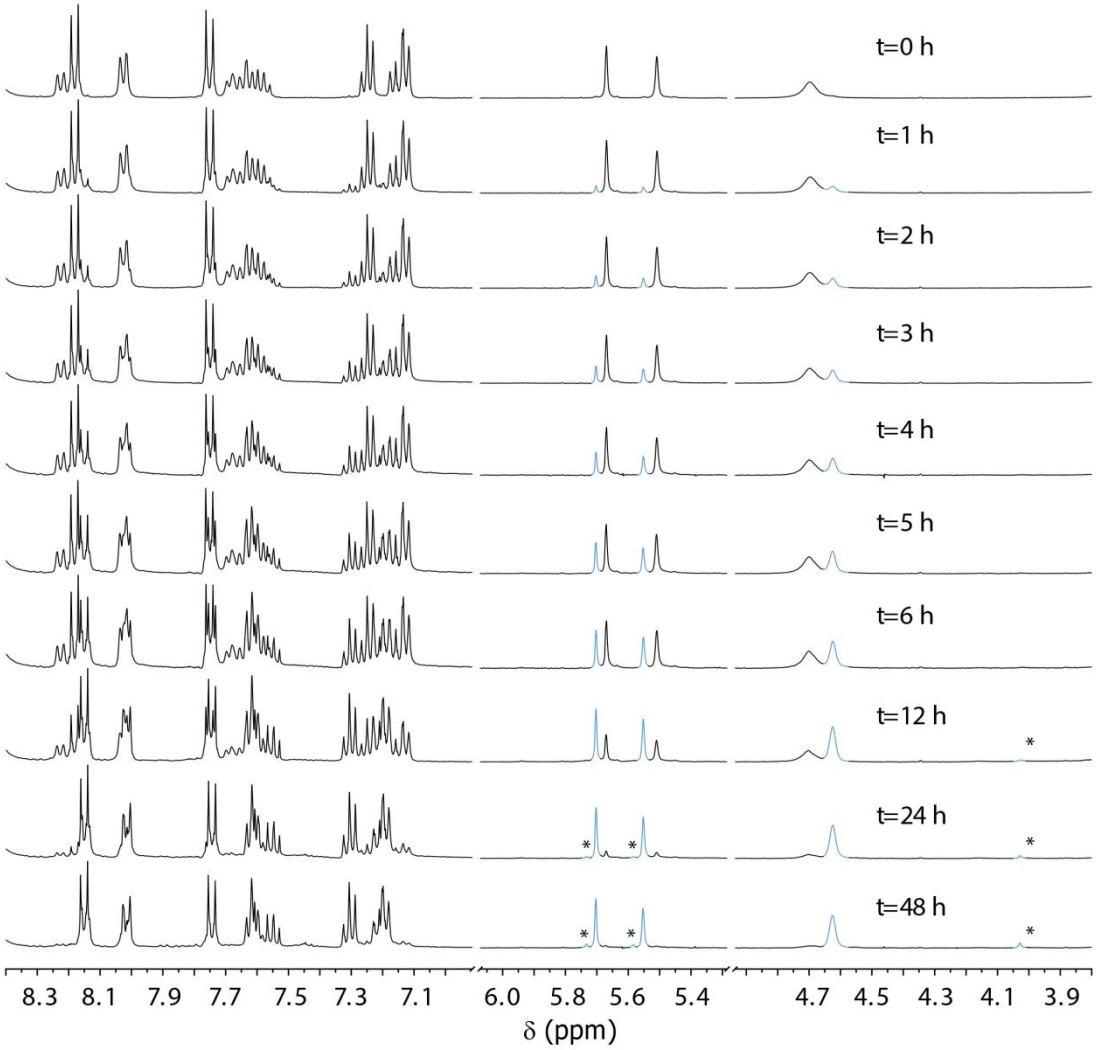

Figure 3.5. Partial ^{1}H NMR spectra (400 MHz, 20 mM, [D_6]DMSO, 298 K) monitoring the intramolecular exchange of **5**-*1*·3[CF_3CO_2H] (black resonances at t = 0 h) in the presence of 2 equiv. of $^{i}Pr_2NEt$, showing the consecutive formation of **5**-*2* (blue resonances) and **5**-*3* (green resonances, annotated with *) at given times.

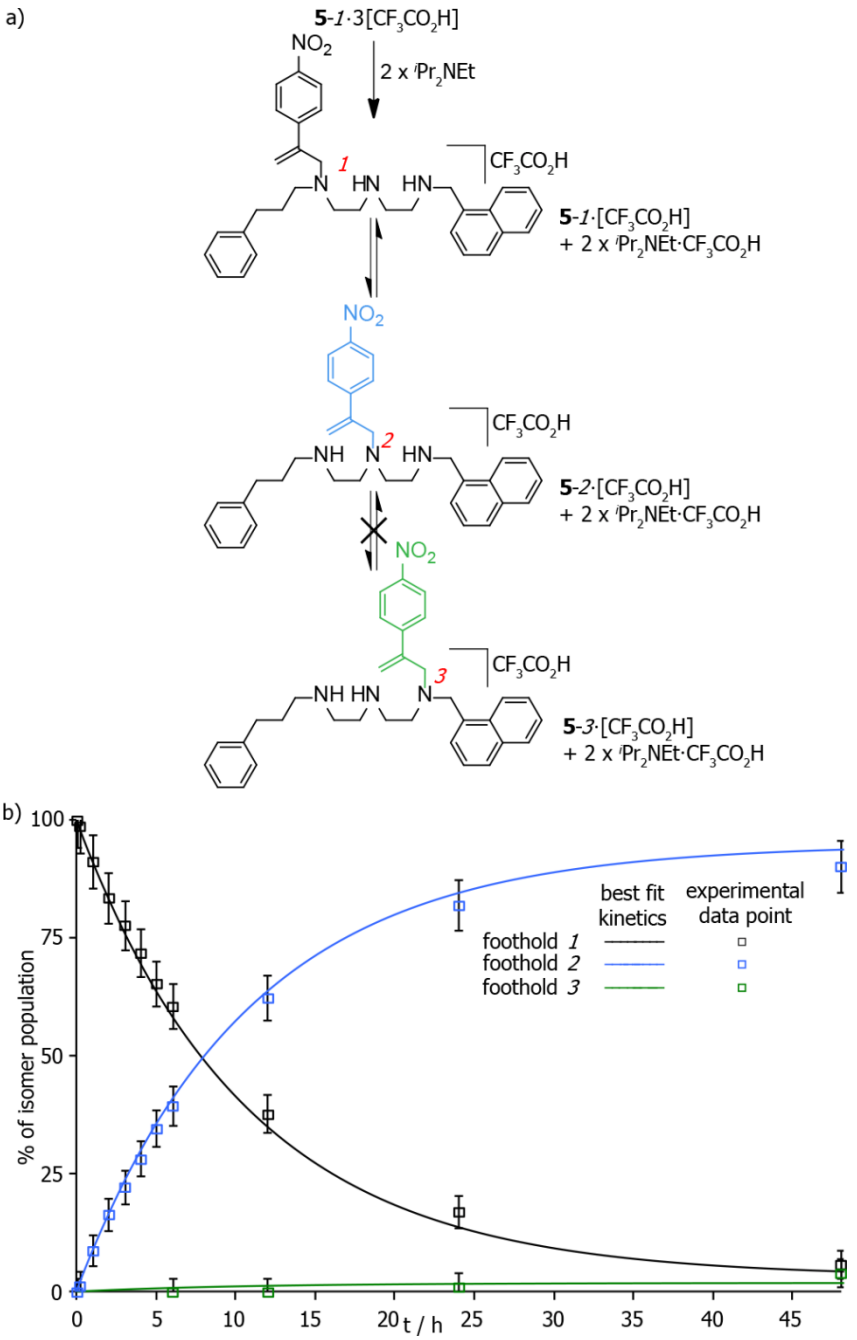

Figure 3.6. a) Intramolecular migration of **5**-*1*·3[CF_3CO_2H] in the presence of 2 equiv. $^{i}Pr_2NEt$. b) Rate of formation or disappearance of isomers during the exchange process, based on ^{1}H NMR spectra at given times. Benzylic foothold remains protonated and walker's migration towards the end of the track is not possible. Continuous lines represent the best fit of the experimental data to the kinetics of the exchange between **5**-*1*, **5**-*2* and **5**-*3* using the SimFit program (see Experimental Section for details). Error bars represent the estimated ±3% error of ^{1}H NMR integration (the proton signals used for the integration are the equivalent ones in each positional isomer, see section 3.6.3.3).

3.3.3 Walking Experiments in Optimised Conditions.

3.3.3.1 Walking upon five-foothold track

For walker-track conjugates isolated as CF_3CO_2H salts, [D_6]DMSO, with 1 equiv. of excess of $^{i}Pr_2NEt$ proved to be the conditions of choice for the intramolecular exchange as the deprotonation of all footholds in the track can be ensured. Under these conditions, preference towards the final, naphthylmethylamine is observed in the walking process.

Thus, we sought to demonstrate that the walker could travel further distances by moving towards the end of longer tracks. Firstly, five foothold walker-track conjugate **6**-*1*·5[CF_3CO_2H] was synthesised by analogy to compound **5**-*1*·3[CF_3CO_2H], using suitably protected tetraethylenepentaamine as a starting material (see Experimental Section for details).The product was then subjected to the optimised walking conditions (**6**-*1*·5[CF_3CO_2H] + 6 equiv. $^{i}Pr_2NEt$) and due to exceptionally good resolution of one of the walker's vinyl signals it was possible to identify each of the five possible positional isomers (Figure 3.7). Integration of each positional isomer was performed using deconvolution function of MestReNova programme.

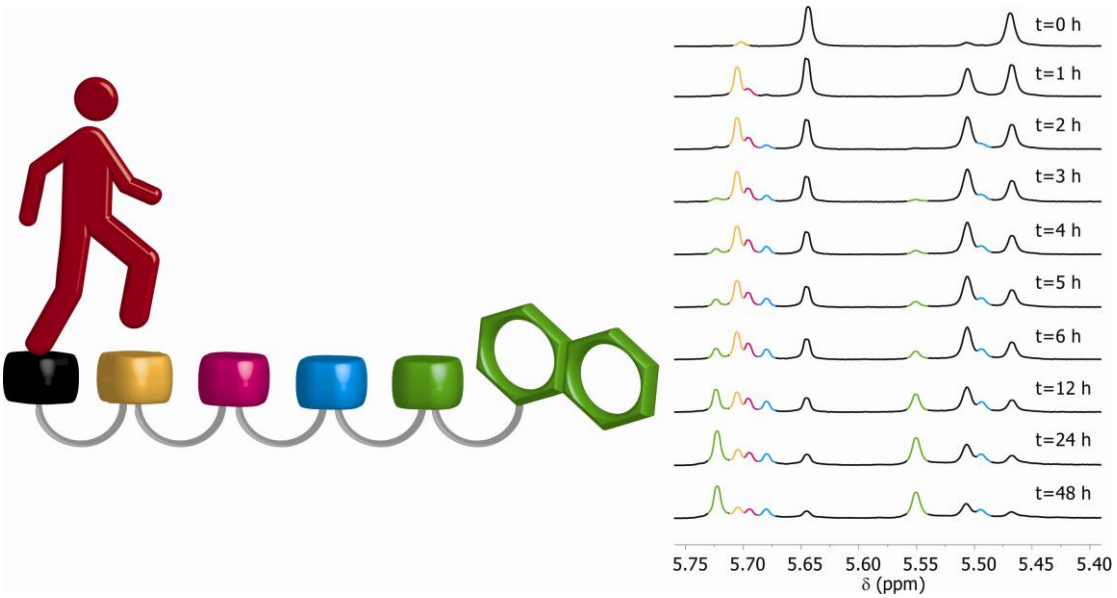

Figure 3.7. Partial ^{1}H NMR spectra of **6**-*1*·5[CF_3CO_2H] + 6 equiv. $^{i}Pr_2NEt$ (400 MHz, 20 mM, [D_6]DMSO, 298 K) showing consecutive formation of five possible positional isomers at given times (signal colouring corresponds to cartoon foothold colouring).

Aspects of processivity as well as overstepping were extensively covered in Chapter II for chemically similar systems in which α-methylene-4-nitrostyrene moiety is intramolecularly exchanging between adjacent secondary amine footholds. Based on these results, we know that overstepping accounts for less than 1% of the walking process and that intramolecular reactions in this system are ~530x more frequent than the corresponding

intermolecular events. As such, the walking process is taking place in a predominantly stepwise fashion and overstepping is not a preferred process, so the order in which signals become apparent in the spectrum corresponds to the sequence in which consecutive positional isomers are being formed (colouring in Figure 3.7 and Figure 3.9 corresponds to structure and graph colouring in Figure 3.10). After 48 h at room temperature, 46% of walkers have reached the final, fifth foothold of the track and no more changes were observed.

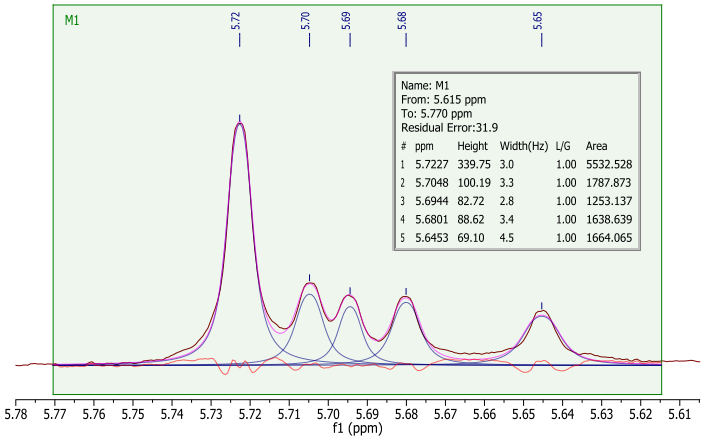

Figure3.8 Diagnostic region of ^{1}H NMR deconvoluted using MestReNova programme.

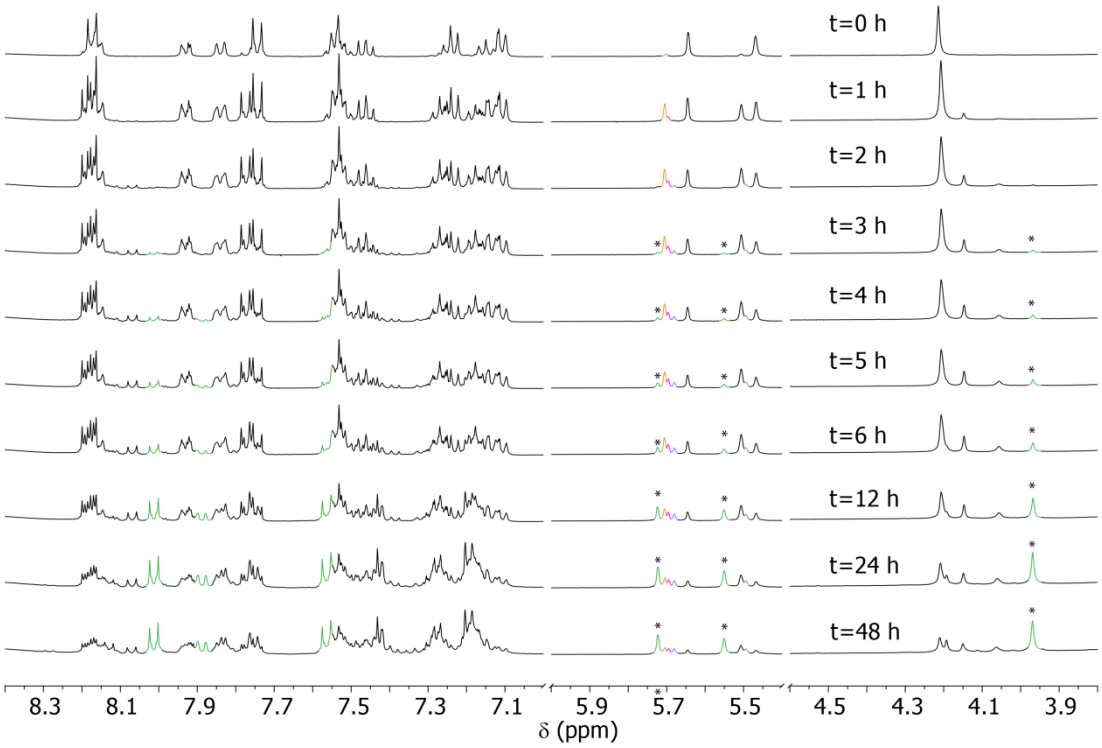

Figure 3.9. Partial ^{1}H NMR spectra (400 MHz, 20 mM, [D_6]DMSO, 298 K) monitoring the intramolecular exchange of **6**-*1*·5[CF_3CO_2H] (black resonances at t = 0 h) in the presence of 6 equiv. of $^{i}Pr_2NEt$, showing the consecutive formation of **6**-*1*, **6**-*2*, **6**-*3*, **6**-*4* and **6**-*5* (annotated with *) (signal; colouring corresponds to positional isomer colouring in Fig 3.9) at given times.

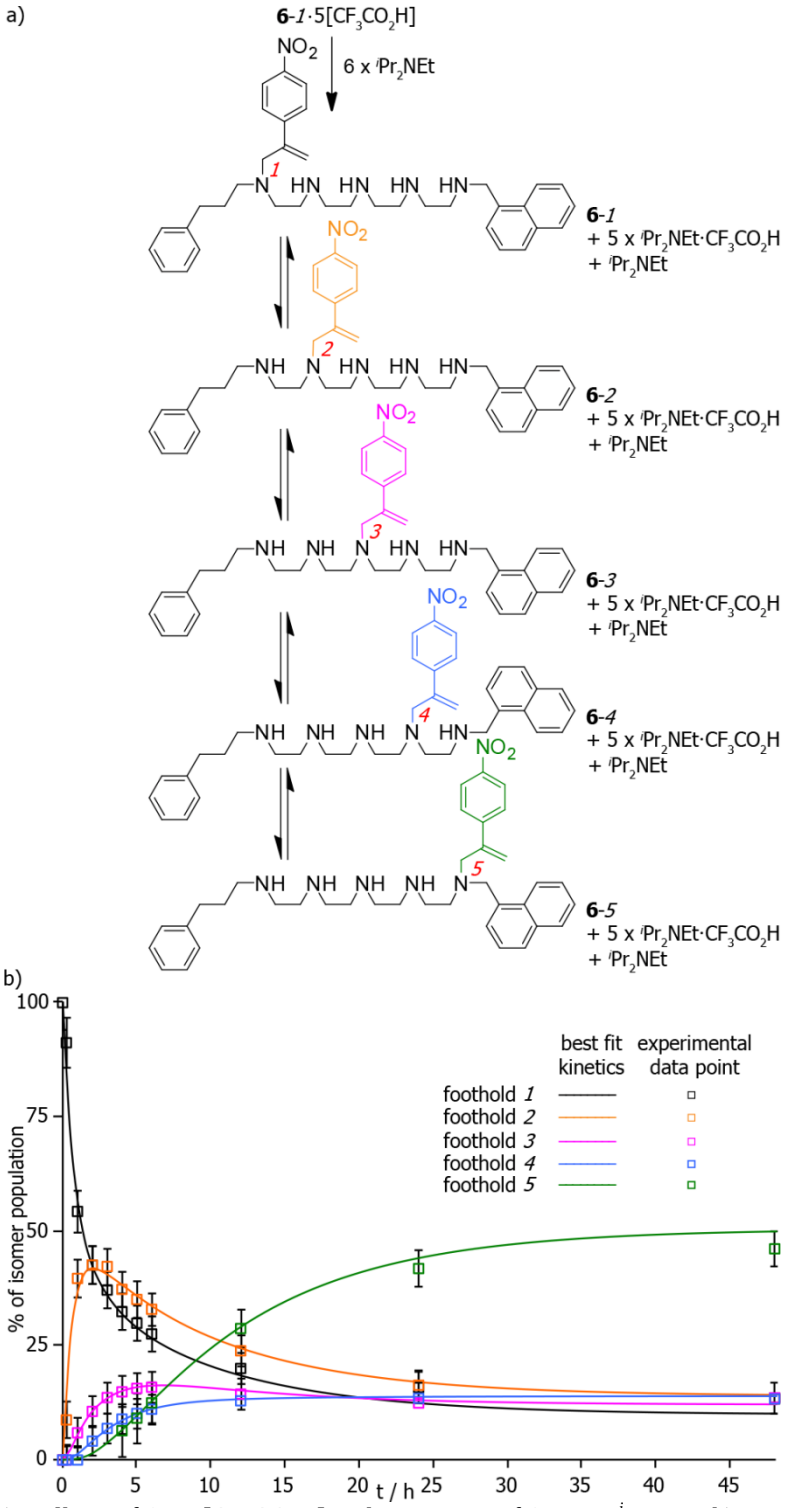

Figure 3.10. a) Walking of **6**-*1*·5[CF_3CO_2H] in the presence of 6 equiv. $^{i}Pr_2NEt$. b) Rate of formation or disappearance of isomers during the exchange process of **6**-*1*·5[CF_3CO_2H] the presence of 6 equiv. $^{i}Pr_2NEt$, based on ^{1}H NMR spectra at given times. After 48 h of experiment, 46% of walkers reach the final foothold of the track. Continuous lines represent the best fit of the experimental data to the kinetics of the exchange between **6**-*1*, **6**-*2*, **6**-*3*, **6**-*4* and **6**-*5* using the SimFit program (see experimental Section for details). Error bars represent the estimated ±3% error of ^{1}H NMR integration (the proton signals used for the integration are the equivalent ones in each positional isomer, see section 3.6.3.3).

3.3.3.1.1 MS Analysis of 6-*1* after walking

Chapter II provides the analysis which shows that intramolecular exchange is ~530 × more frequent than the corresponding intermolecular reactions in a system where α-methylene-4-nitrostyrene moiety is exchanging between adjacent secondary amine footholds. Chemically related systems studied in Chapter III also show an excellent level of intramolecular versus intermolecular reactivity (no additional peaks corresponding to two walkers on one track in ^{1}H NMR after 48 h, as example, see Figure 3.2).

In addition to ^{1}H NMR investigation, an ESI MS analysis of **6**-*1*·5[CF_3CO_2H] + 6 equiv. $^{i}Pr_2NEt$ mixture after 14 days of walking was performed. After two weeks of exchange, $[M+H]^+$ m/z = 609.36 in Figure 3.11, corresponding to an intact walker-track conjugate was the most intensive signal present in the MS spectrum. Minor signal of $[M\text{-walker}+H]^+$ m/z = 448.08, corresponding to the presence of walker-free track (and loss of processivity) accounted for less that 5 % of the relative abundance, which further confirms stability and good processivity in this system.

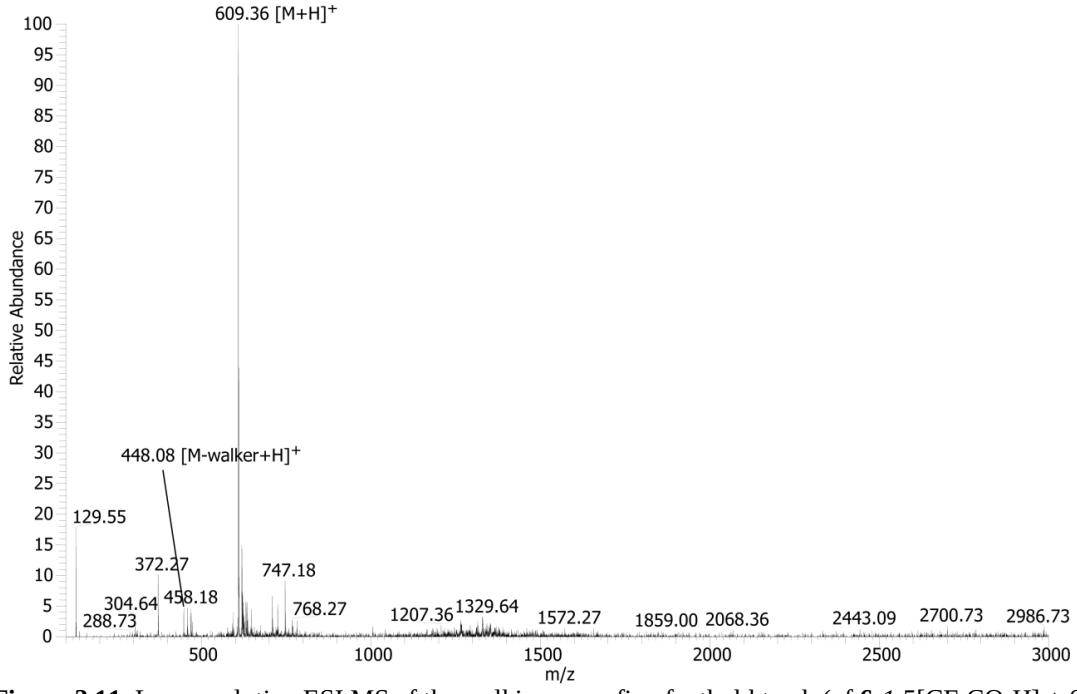

Figure 3.11. Low resolution ESI MS of the walking upon five foothold track (of **6**-*1*·5[CF_3CO_2H] + 6 equiv. $^{i}Pr_2NEt$) after 14 days of experiment ([D_6]DMSO, 20 mM, 298 K). Calculated peaks (m/z) 609.39 $[M+H]^+$, 448.34 $[M\text{-walker}+H]^+$.

3.3.3.2 Walking upon nine-foothold track

Having established that, in optimised conditions, the α-methylene-4-nitrostyrene walker unit can efficiently exchange between the footholds and migrate preferentially towards the end of a tri- and pentaamine track, we sought to demonstrate that the walker can migrate processively and preferentially in one direction along even longer track through the same mechanism.

A nine foothold walker-track conjugate **7**-*1*·9[CF_3CO_2H] was synthesised starting from the commercially available 2-(2-aminoethylamino)ethanol **8** which was subjected to a sequence of protection-deprotection reactions, to give **9** (see Scheme 3.2). Reductive amination of **9** with 3-phenylpropionaldehyde gave **10**. Subsequent Cbz protection and oxidation using Dess-Martin periodinane (DMP) yielded the aldehyde building block **11**. Second half of the track was synthesised, starting from the reductive amination of **8** with 1-naphthaldehyde, followed by selective Boc protection to give **12**. Primary alcohol was oxidised to aldehyde **13** using DMP and then subjected to reductive amination with a commercially available tetraethylenepentaamine.[12] Crude mixture was submitted to TFA protection of primary amine, followed by quadruple Boc protection of the remaining secondary amines to give **14**. Deprotection of the primary amine afforded **15** as a single product. Reductive amination using **11** and **15** as reaction partners furnished nine-foothold track featuring one 'free' secondary amine, which was then Boc-protected, to give **16** as a single compound. Finally, under conditions orthogonal to Boc deprotection, Cbz group was reductively cleaved, yielding nine-foothold track featuring a single secondary amine group. After walker (**4**) attachment, compound **17** was subjected to Boc-deprotection conditions to give the final product **7**-*1* as a CF_3CO_2H salt.

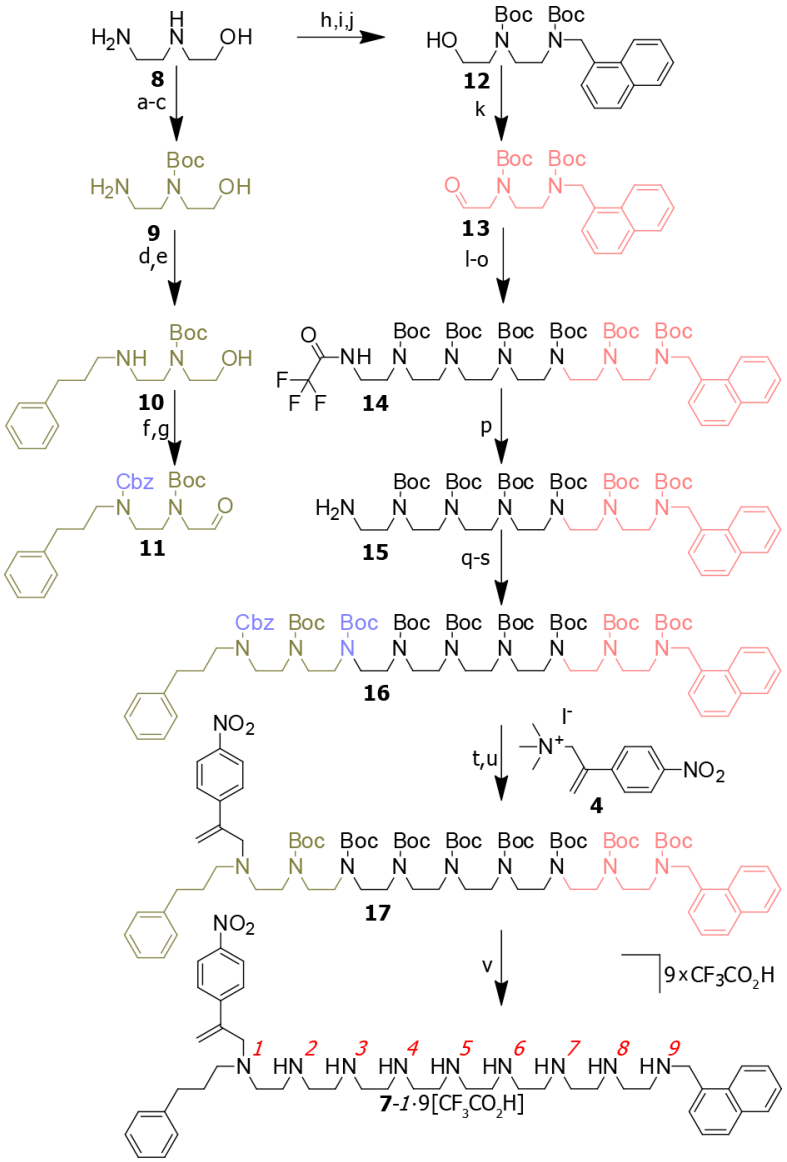

Scheme 3.2. Synthesis of a walker-track conjugate **7**-*1*·9[CF_3CO_2H]. Reaction conditions: a) CF_3CO_2Et, CH_2Cl_2, 0 °C→RT, 3 h; b) Boc_2O, Et_3N, RT, 12 h, 60% (two steps); c) NaOH, MeOH/H_2O, RT, 5 h, 73%; d) 3-phenylpropionaldehyde, EtOH, RT, 16 h; e) $NaBH_4$, RT, 3 h, 36% (two steps); f) CbzCl, Et_3N, CH_2Cl_2, RT, 4 h, 68%; g) DMP, CH_2Cl_2, RT, 12 h, 81%, h) 1-naphthaldehyde, EtOH, RT, 16 h, i) $NaBH_4$, RT, 3 h; j) Boc_2O, MeCN, RT, 12 h, 64% (three steps); k) DMP, CH_2Cl_2, RT, 12 h, 68%; l) tetraethylenepentaamine, EtOH, RT, 16 h; m) $NaBH_4$, RT, 3 h; n) CF_3CO_2Et, CH_2Cl_2, 0 °C→RT, 16 h; o) Boc_2O, Et_3N, RT, 12 h, p) NaOH, MeOH/H_2O, RT, 5 h, 20% (five steps); q) **11**, EtOH, RT, 16 h; r) $NaBH_4$, RT, 3 h; s) Boc_2O, Et_3N, RT, 12 h, 30% (three steps); t) Pd(C), H_2, THF, RT, 20 h, 50%; u) **4**, MeOH, $^{i}Pr_2NEt$ 50 °C, 48 h, 50%; v) CF_3CO_2H, CH_2Cl_2, RT, 7 h, quant.

In order to investigate the walking process, compound **7**-*1* was subjected to walking conditions (10 mM, [D_6]DMSO, **7**-*1*·9[CF_3CO_2H] + 10 equiv. $^{i}Pr_2NEt$) and the reaction was monitored by ^{1}H NMR spectroscopy. Due to the large number of structurally similar positional isomers, overlapping of signals occurred. Analysis of ^{1}H NMR spectra showed the gradual disappearance of starting material **7**-*1* and a number of sets of signals, corresponding to new positional isomers **7**-*2*–**7**-*8* being formed (Figure 3.12). Reaction was monitored periodically and after 15 h of exchange, signals corresponding to **7**-*9* (walker molecule reaching the last foothold of the track) appeared (green coloured resonances, Figure 3.12 and Figure 3.13b). Gradual increase in intensity of **7**-*9* signals was observed and after 90 h 19% of walkers had reached the last, ninth foothold.

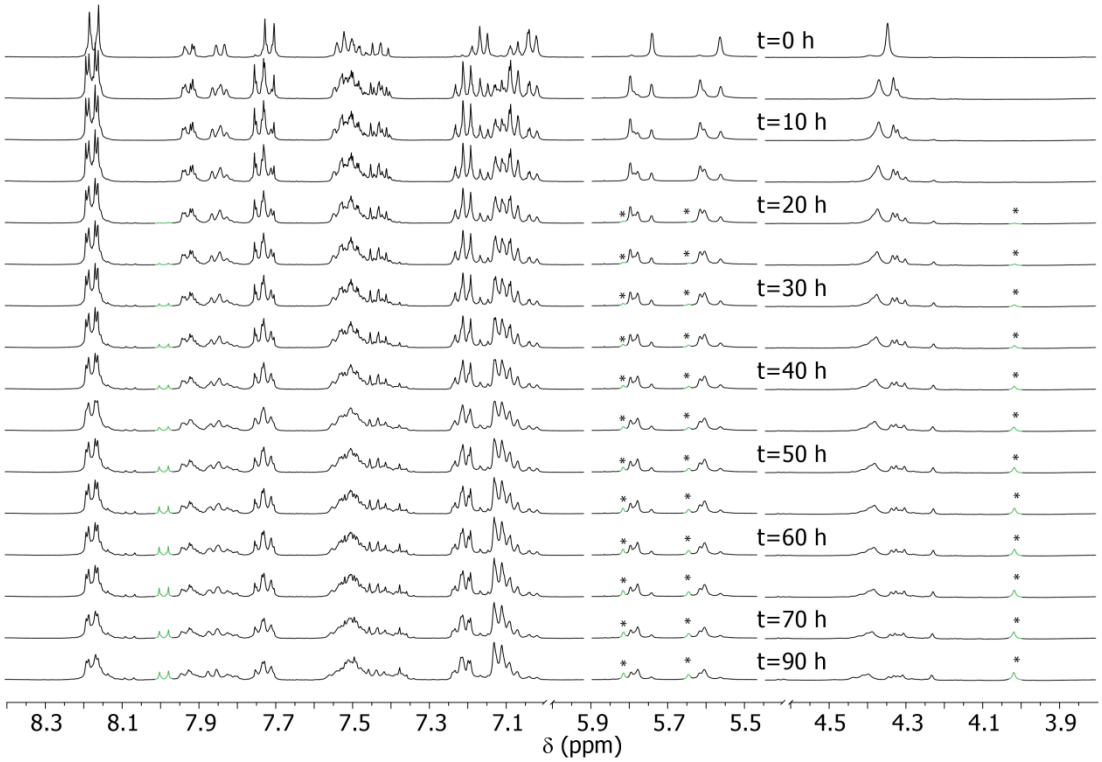

Figure 3.12. Partial ^{1}H NMR spectra (400 MHz, 10 mM, [D_6]DMSO, 298 K) monitoring the intramolecular exchange of **7**-*1*·9[CF_3CO_2H] (black resonances at t = 0 h) in the presence of 10 equiv. . $^{i}Pr_2NEt$, showing the disappearance of **7**-*1* and formation of indistinguishable isomers **7**-*2* – **7**-*8* at given times. Resonances corresponding to gradual formation of **7**-*9* are highlighted in green and annotated with *.

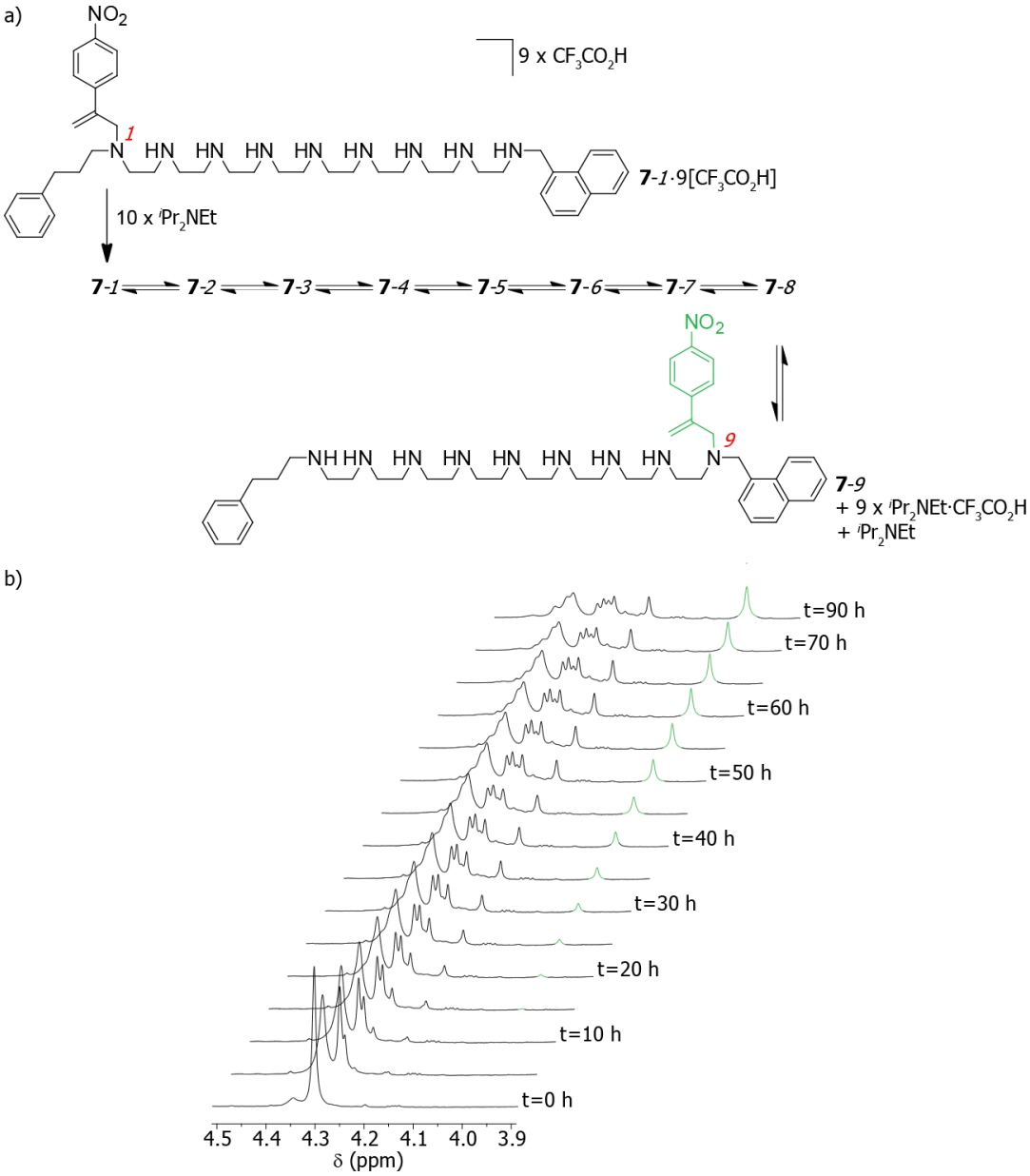

Figure 3.13. a) Walking of **7**-*1*[9×CF_3COOH] in the presence of 10 equiv. $^{i}Pr_2NEt$. b) Partial ^{1}H NMR spectra (400 MHz, 10 mM, [D_6]DMSO, 298 K) of the reaction mixture at given times. Migration towards the end of the track is the preferred process. After 90 h of exchange, 19% of walkers reach the final, 9th foothold of the track. Green coloured resonances correspond to **7**-*9*.

3.3.3.2.1 MS Analysis of 7-*1* after walking

According to the analysis provided in Chapter II and previous results presented in Chapter III, the walking process in all similar, chemically related systems is predominantly intramolecular (no additional peaks corresponding to two walkers on one track in ^{1}H NMR after 48 h, as example, see Figure 3.2).

In addition to ^{1}H NMR investigation, an ESI MS analysis of **7**-*1*·5[CF_3CO_2H] + 10 equiv. $^{i}Pr_2NEt$ mixture after 7 days of walking was also performed. After one week of exchange, $[M+H]^+$ m/z = 781.92 in Figure 3.12, corresponding to an intact **7**-*1* was the most intensive signal present in the MS spectrum. Minor signal of $[M\text{-walker}+H]^+$ m/z = 620.92, corresponding to the presence of walker-free track (and loss of processivity) accounted for less that 5 % of the relative abundance which further confirms stability and good processivity in this system.

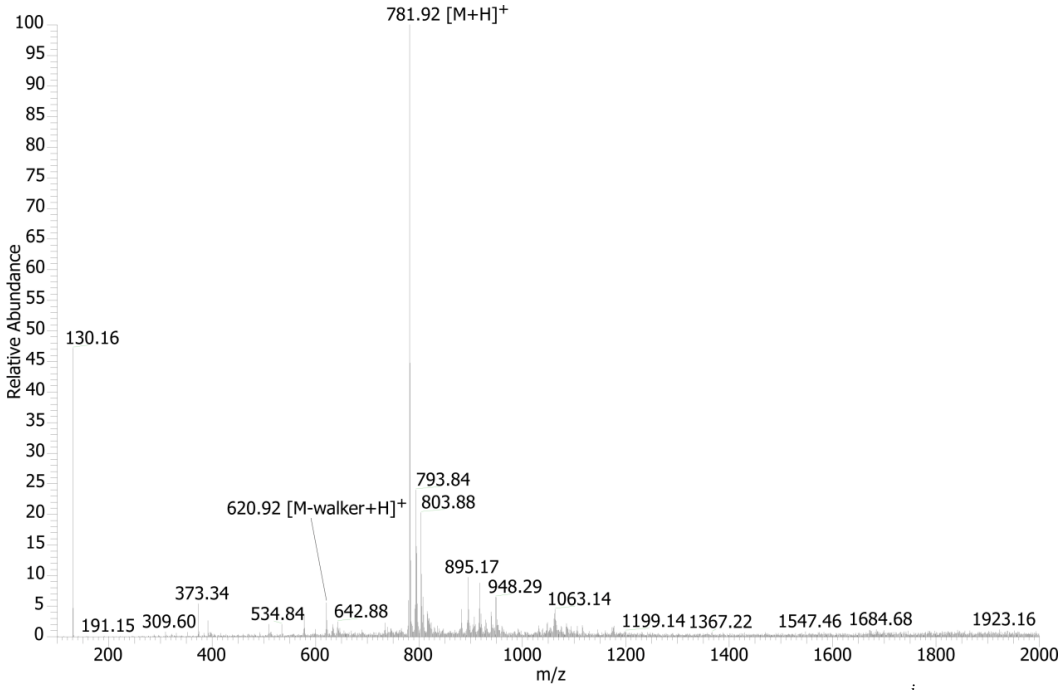

Figure 3.14. ESI MS of the walking upon nine foothold (**7**-*1*·9[CF_3CO_2H] + 10 equiv. $^{i}Pr_2NEt$) after 7 days of experiment ([D_6]DMSO, 10 mM, 298 K). Calculated peaks (m/z) 781.56 $[M+H]^+$, 620.51 $[M\text{-walker}+H]^+$.

3.3.4 Experimental Data Fitting using von Kiedrowski SimFit Program.

The experimental data set (molar fraction of positional isomers appearing or disappearing determined by ^{1}H NMR) was analysed according to empirical rate equations of von Kiedrowski using the SimFit program. An appropriate kinetic model for studied compounds is presented in Figure 3.15.

Analyses show significant influence of experimental conditions (the amount of $^{i}Pr_2NEt$ added) on K_{final} for migration in **5**-*1* which is in agreement with the experiment (see Table 3.1). Also, for two of the studied walker-track conjugates (**5**-*1*, **6**-*1*) in optimised walking conditions (*i.e.* in the presence of 1 equiv. of excess $^{i}Pr_2NEt$) $K_{final} \approx 3$ which shows that in both cases the walking unit moves preferentially towards the last foothold.

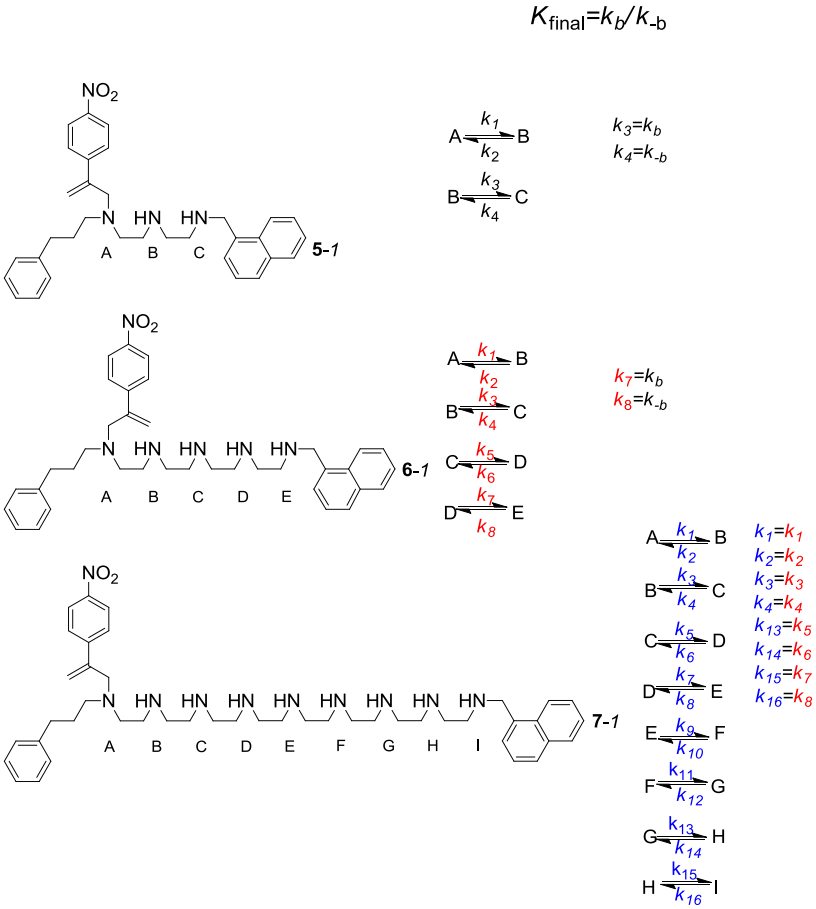

Figure 3.15. Model of reversible stepping along polyethyleneimine tracks used for experimental data fitting using SimFit program and then used in the simulation of population of positional isomers of **7**-*1*.

Table 3.1. Reaction rate constants based on experimental data, calculated using SimFit program for **5**-*1* and **6**-*1*.

Number of footholds in the track(*n*)	conditions	k_b/s^{-1}	k_{-b}/s^{-1}	K_{final}	Fitting error / %
3	acidic	2.83×10^{-5}	1.40×10^{-3}	0.02	2.58
3	neutral	1.07×10^{-5}	6.21×10^{-6}	1.73	4.77
3	basic	5.35×10^{-5}	1.71×10^{-5}	3.12	6.88
5	basic	1.31×10^{-5}	3.88×10^{-5}	3.38	9.13

Rate constants obtained for **6**-*1* were used in the kinetic model for fitting of experimental data for **7**-*1* (input file is presented in the Experimental Procedures section) and the rates of reactions obtained were then used to simulate the population of all 9 positional isomers in time (Figure 3.16). Experimental values obtained from ^{1}H NMR spectra at given times (black and green squares), clearly follow the simulated curves (black and green solid lines in Figure 3.16).

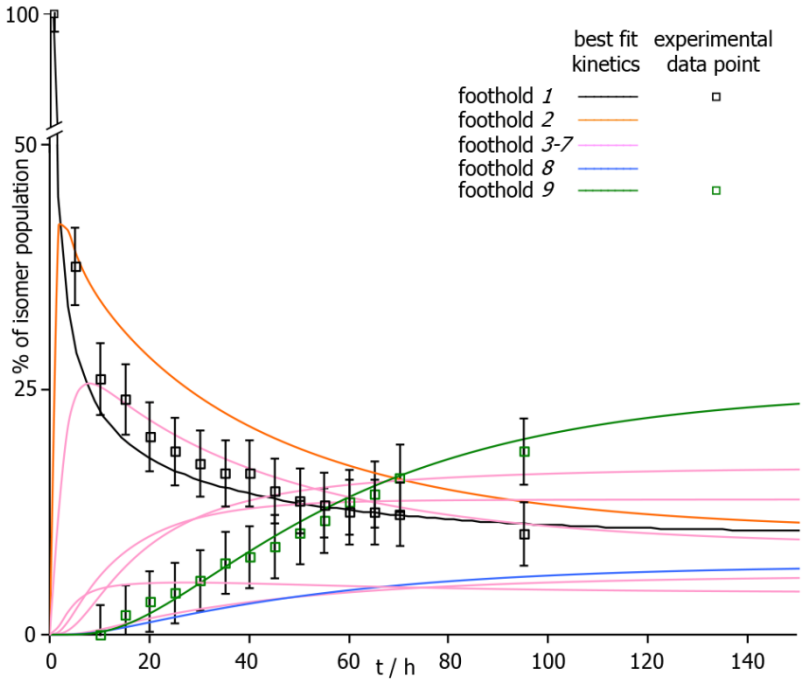

Figure 3.16. The simulated rate of formation or disappearance of isomers during the exchange process of **7**-*1*·9[CF_3CO_2H] in the presence of 10 equiv. ^{i}Pr$_2$NEt calculated using SimFit program (see Experimental Section for details) (continuous lines) superimposed with experimental data points. Error bars represent the estimated ±3% error of ^{1}H NMR integration (the proton signals used for the integration are the equivalent ones in each positional isomer, see section 3.6.3.3).

3.3.5 Intramolecular Migration as a Diffusion Process.

The α-methylene-4-nitrostyrene molecule migrates between footholds in a series of small steps which allow the molecule to move away from its initial position. Such an intuitive picture is usually proposed to explain particle diffusion phenomena and can be successfully applied to the calculation of the mean distance travelled by α-methylene-4-nitrostyrene molecule along a molecular track. At any given time, the mean distance travelled by all particles <*n*> is a sum of the displacement of each particle along a track, weighted by the probability of its occurrence at a given position. Therefore <*n*> varies as the square root of the elapsed time (see Equation 1a, *t* –time, *D* – diffusion coefficient).

At equilibrium, the molar fraction of each positional isomer $[x_0, x_1, x_2 \ldots, x_n]$, determined using SimFit program was multiplied by the number of steps that each positional isomer has travelled $[s_0, s_1, s_2 \ldots, s_n]$ to obtain the net displacement of walker units along a track at equilibrium <*n*>(t_{eq}) (t_{eq} – time needed to reach equilibrium based on SimFit calculations). For experiments performed in the presence of excess base, the net displacement of molecules along their tracks was analysed (Equation 1b) using data calculated with SimFit programme. The net distance walked upon tracks of different lengths was calculated based on the data from SimFit programme, plotted in Figure 3. **17** and summarised in Table 3.2. The graph plotted in Figure 3.18 shows the great slowness of diffusion with length of the track and confirms that the net distance walked varies as the square root of the elapsed time.[13]

Equation 1. Net displacement of walker units in time.

$$a) \quad \langle n \rangle = 2(Dt/\pi)^{1/2}$$

$$b) \quad \langle n \rangle(t_0) = \sum_{i=1}^{n} x_0 s_0(t_0) + x_1 s_1(t_0) + x_2 s_2(t_0) \ldots, x_n s_n(t_0)$$

$$\langle n \rangle(t_1) = \sum_{i=1}^{n} x_0 s_0(t_1) + x_1 s_1(t_1) + x_2 s_2(t_1) \ldots, x_n s_n(t_1)$$

$$\vdots$$

$$\langle n \rangle(t_{eq}) = \sum_{i=1}^{n} x_0 s_0(t_{eq}) + x_1 s_1(t_{eq}) + x_2 s_2(t_{eq}) \ldots, x_n s_n(t_{eq})$$

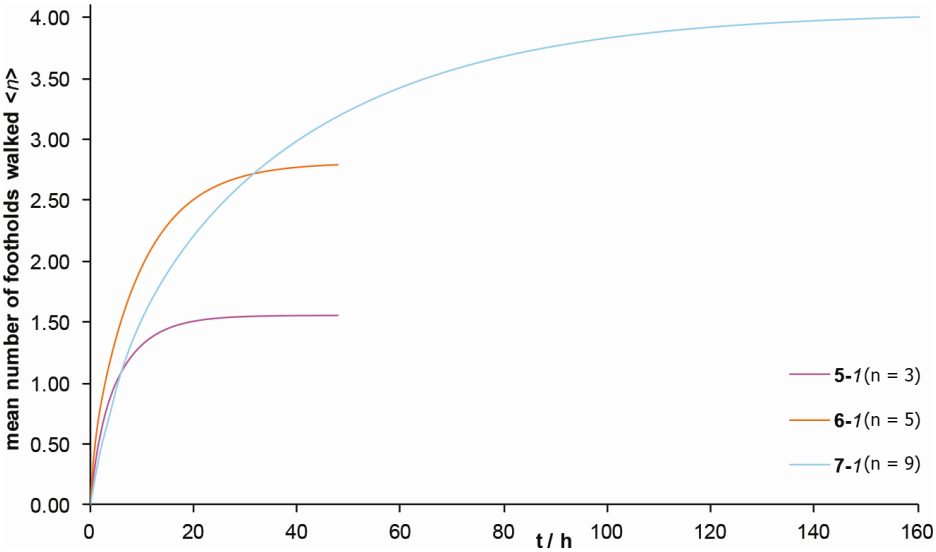

Figure 3. 17 Net distance walked by α-methylene-4-nitrostyrene in molecules **5**-*1*, **6**-*1*, **7**-*1* based on SimFit program.

Table 3.2. SimFit calculated net distance travelled in time along linear tracks of different length.

n	**<*n*>**	**% of walkers on final foothold at equilibrium (calc. in SimFit)**	**t_{eq} / h**	**log (*t* / s)**
3	1.56	67	24	4.94
5	2.79	49	45	5.24
9	4.00	24	160	5.76

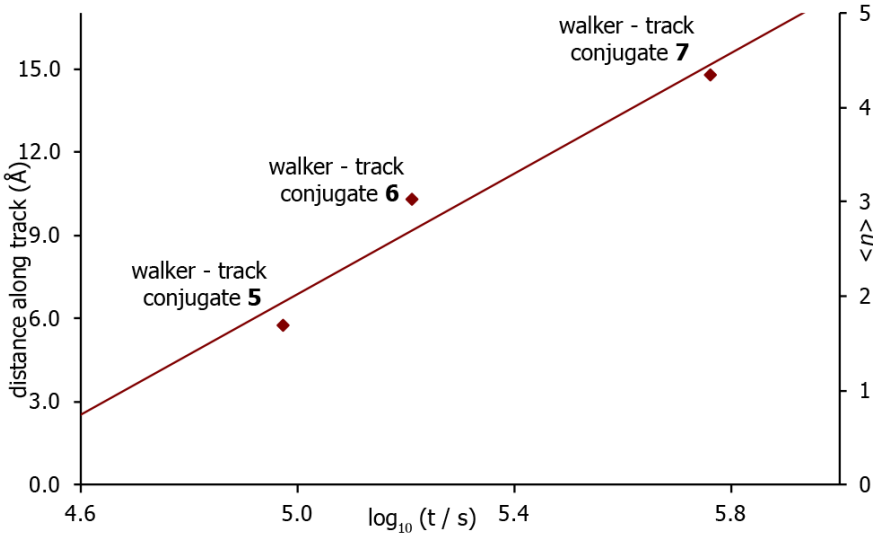

Figure 3.18. Calculated net displacement (distance along the vector of the track (Å, left-hand axis; an average number of footholds travelled [<*n*>], right-hand axis) of α-methylene-4-nitrostyrene walker as a function of time.

3.3.6 Intramolecular Migration as one Dimensional Random Walk.[14]

The walker unit can only take forward and backward steps of equal distance (due to the track's architecture) and therefore its migration can in principle be described using one dimensional random walk. Random walks consider an equal probability of stepping forward and backwards[15] and can be used to determine the probability (*P*) of finding the molecule at the end of studied tracks (*n* = 3, 5, 9). Using a binary diagram (Figure 3.19) the number of right (N_R) and left (N_L) steps necessary for the walker to reach the end of studied tracks can be calculated (number of footholds in the track, N_R and N_L indicated in pink, green and red, respectively). The net distance travelled (*d*) and total number of steps (*N*) could then be determined using relation (1) and (2), respectively. Finally, *P* of finding the molecule at the end of track of given (*n*) could be calculated using first (3) and then (4).[13]

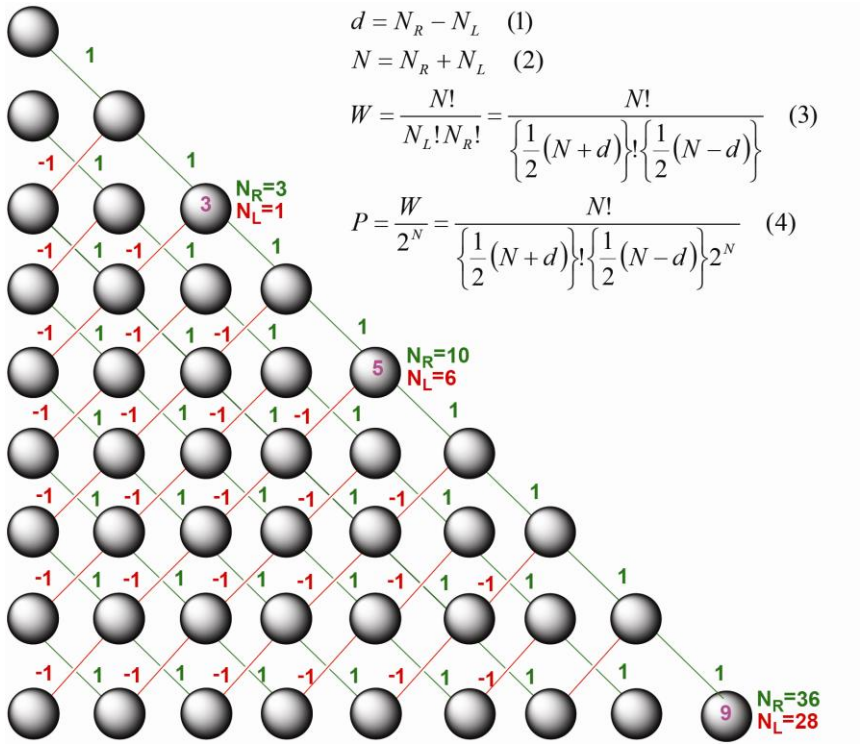

Figure 3.19. Diagram representing simple random walk with equal probability of left and right steps.

In order to model migration of α-methylene-4-nitrostyrene molecule along nine-foothold track as a simple random walk with the equal probability of stepping back and forth between all footholds (equivalent rate constants for forward and backward walking), changes in the distribution of walker along the track were expressed using the probability of molecule appearing or disappearing from its position along the track.

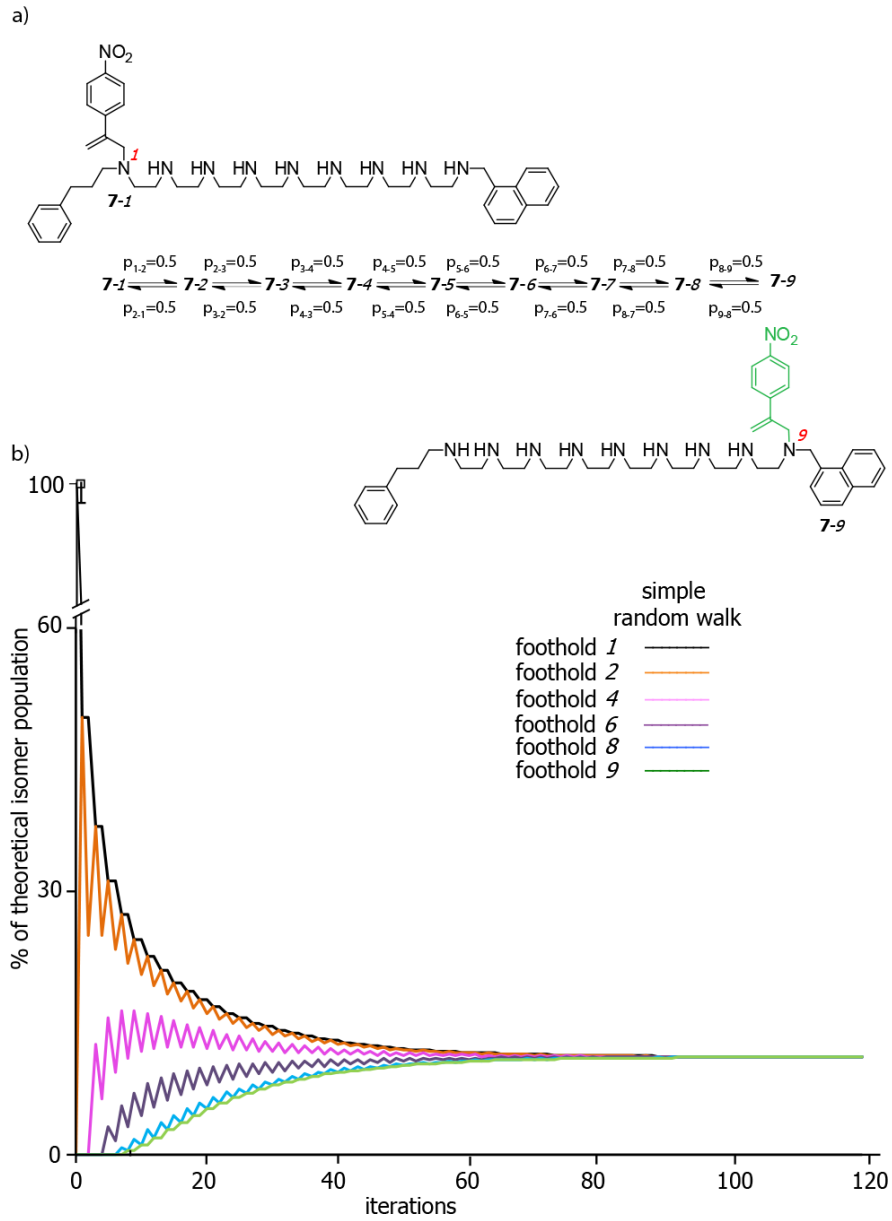

Figure 3.20 The theoretical rates of formation or disappearance of positional isomers during the intramolecular migration of α-methylene-4-nitrostyrene in **7**-*1* according to simple random walk (the probability of $p = 0.5$ for each forward and backward stepping process). Walker's stepwise migration between each of the footholds is equally probable. Continuous lines represent the population of selected positional isomers formed. For clarity reasons, rates of formation or disappearance of positional isomers **7**-3, **7**-*5* and **7**-*7* (summarized in Table 3.4) were not included in the graph.

Before the first iteration, population of **7**-1_0 = 100 % and it can only be altered if walker steps onto the second foothold with the probability of $p_{1\text{-}2}$ or if **7**-2_0 steps onto the first foothold with probability of $p_{2\text{-}1}$. After first iteration, the population of **7**-1_1 will be described as:

$$\mathbf{7}\text{-}1_1 = \mathbf{7}\text{-}1_0 - (\mathbf{7}\text{-}1_0 \times p_{1\text{-}2}) + (\mathbf{7}\text{-}2_0 \times p_{2\text{-}1})$$

and as **7**-2_0 = 0, we obtain **7**-1_1 = 50 %. Using this model we can calculate an unbiased random walk and plot changes in the distribution of walker molecules which after over 100 iterations reach a steady population of 11.1 % of positional isomers **7**-*1* – **7**-*9* evenly distributed along a 9 foothold track (see Figure 3.20 and Table 3.4 in 3.6.4.3 section for detailed distribution of positional isomers).

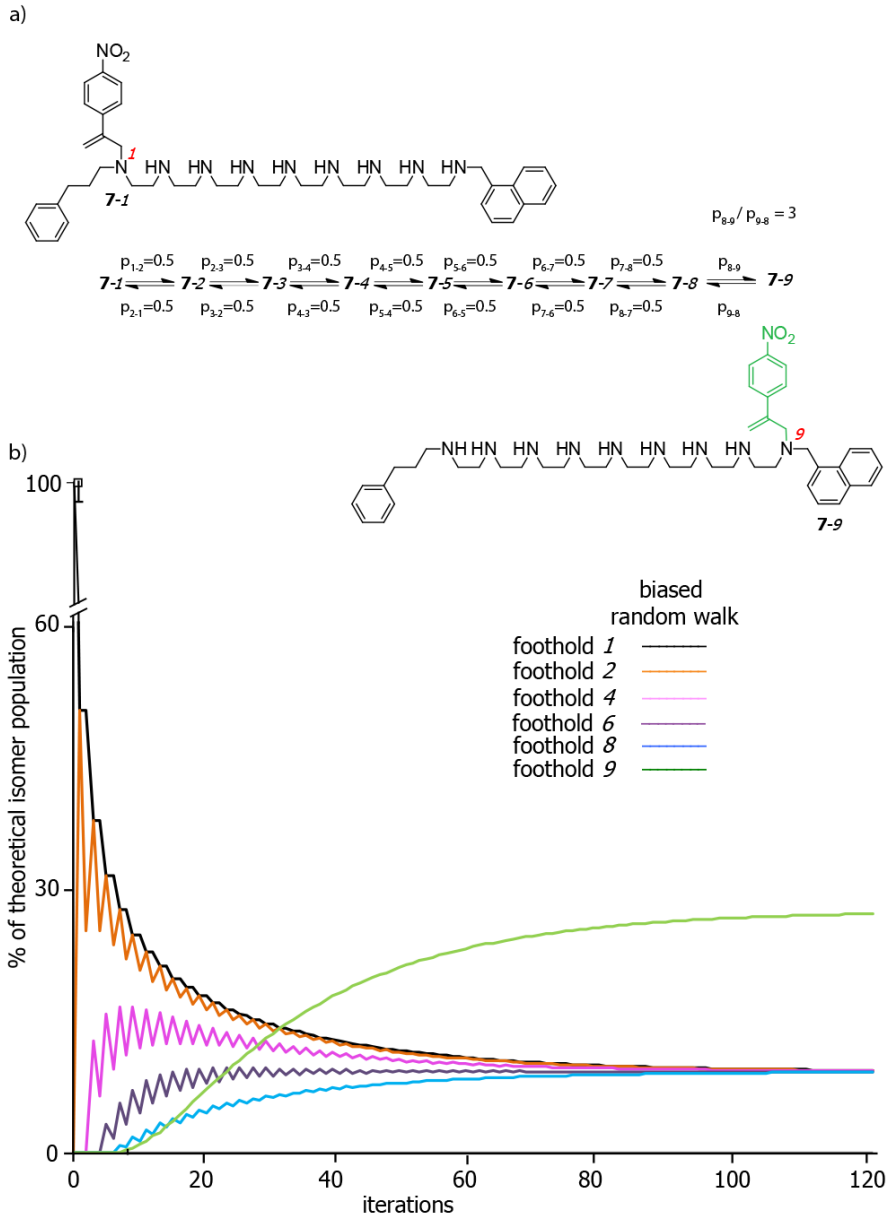

Figure 3.21 The theoretical rates of formation or disappearance of positional isomers during the intramolecular migration of α-methylene-4-nitrostyrene in **7**-*1* according to biased random walk (the probability of p = 0.5 for each forward and backward stepping process, except for the final step, where $p_{8\text{-}9}$ / $p_{9\text{-}8}$ = 3). Walker's stepwise migration towards the end of the track is the preferred process. Continuous lines represent the population of selected positional isomers formed. For clarity reasons, rates of formation or disappearance of positional isomers **7**-*3*, **7**-*5* and **7**-*7* (summarized in Table 3.5) were not included in the graph.

In order to examine the influence of the thermodynamic sink present at the end of the track on the population of walker molecules, the ratio of probabilities of stepping onto the last foothold ($p_{8\text{-}9}$ / $p_{9\text{-}8}$) must be fixed and reflect value of $K_{final} \approx 3$, (determined for the three and five foothold walker-track conjugates using SimFit, see Table 3.1) while keeping probabilities of taking other steps equal (see Figure 3.21). Using these assumptions, we can model random walk along 9 foothold track with only one, final step being biased. The final distribution of walker molecules reaches a steady population of 9.1 % of positional isomers **7**-*1* – **7**-*8* and 27.3 % of **7**-9 after over 100 iterations (see Figure 3.21 and Table 3.5 in 3.6.4.3 section for detailed distribution of positional isomers).

Population of isomer **7**-*9* (27 %) calculated using biased random walk is in good agreement with the value obtained from fitting of experimental results (**7**-*1*•9[CF_3CO_2H] walking in the presence of 10 equiv. $_{i}Pr_2Net$) using SimFit program (24 % of **7**-*9* at the steady state, see Table 3.2) and therefore the intramolecular exchange of α-methylene-4-nitrostyrene molecule between consecutive footholds of a 9 foothold track can be successfully described using one dimensional random walk.

3.4 Conclusions

We have described a system in which a high degree of control over processive, spontaneous migration of α-methylene-4-nitrostyrene preferentially in one direction along synthetic tracks of increasing lengths is achieved (n = 3, 5, 9). Varying the walking conditions was crucial for controlling the rate of intramolecular exchange.

It was possible to switch the character of the final, benzylic foothold in the track from unfavoured (when protonated) to preferred. This was achieved due to the walker's preference towards final, secondary, naphthylmethylamine over internal aliphatic footholds, as well as the high processivity of walking. In the optimised conditions we could monitor formation of each individual positional isomer for several walker-track conjugates (n = 3, 5).

Preferential migration in one direction upon the 9-foothold track was also demonstrated. In this case monitoring of two positional isomers was possible and distribution of each individual isomer could be simulated using SimFit program.

We have also demonstrated that the walking of α-methylene-4-nitrostyrene along polyethyleneimine tracks is a diffusion limited process in one dimension. Additionally, as the distance between footholds is equal, the molecule's migration can be described using one dimensional random walk.

3.5 Future Work

The walker-track systems presented in Chapters II and III represent a significant advance in the development of synthetic molecules able to perform translational motion without external intervention. The most important and unique property of this bipedal walker is high processivity of its stepwise migration *via* reversible Michael/retro Michael reaction which proceeds with remarkable efficiency and therefore can be successfully executed on tracks of extended lengths and used to perform a simple task, namely quenching of the fluorescence of an anthracene unit incorporated into the track's architecture.

The primary drawback of the presented systems stems from the limited possibility of coupling the walking process to fuel consumption and as a result driving the distribution of walkers upon the track away from its thermodynamic minimum. Also, as both of the walker's feet are identical (double bond conjugated with *p*-nitrobenzene) it is difficult to imagine how one could achieve directionality in the system (*i.e.* asymmetry in the stepping mechanism) by functionalisation of the walker unit.

Projects are currently being pursued in the Leigh group in which α-methylene-4-nitrostyrene walkers could migrate upon branched tracks or simultaneously to perform a simple reaction to unblock the foothold in front of it. The potential functionalisation of the walker unit with a long polyethylene glycol (PEG) chain for direct monitoring of walker migration by AFM is currently being investigated in collaboration.

3.6 Experimental Section

3.6.1 General Remarks on Experimental Data

Unless otherwise stated, all reagents were purchased from commercial sources and used without further purification. Dry CH_2Cl_2, $CHCl_3$ and THF were obtained by passing the solvent (HPLC grade) through an activated alumina column on a PureSolv™ solvent purification system (InnovativeTechnologies, Inc., MA). Dry DMF, EtOH and MeOH were purchased from Sigma-Aldrich. Flash column chromatography was carried out using Kieselgel C60 (Merck, Germany) as the stationary phase. Analytical TLC was performed on precoated silica gel plates (0.25 mm thick, 60 F254, Merck, Germany) and observed under UV light or visualised using ninhydrin dip/heating. All ^{1}H and ^{13}C NMR spectra were recorded on Bruker AV 400, AV 500 (cryoprobe), at a constant temperature of 298 K. Chemical shifts are reported in parts per million and referenced to residual solvent. Coupling constants (*J*) are reported in Hertz (Hz). Standard abbreviations indicating multiplicity were used as follows: m = multiplet, p = pentet, q = quartet, t = triplet, d = doublet, s = singlet, b = broad. Assignment of the ^{1}H NMR signals was accomplished by two-dimensional NMR spectroscopy (COSY, NOESY, HSQC). All melting points were determined using a Sanyo Gallenkamp apparatus. Mass spectrometric analysis was carried out by the mass spectrometry services at the University of Edinburgh and by the EPSRC National Centre at the University of Wales, Swansea.

The extended lengths of synthesized track molecules and the presence of many NBoc groups, connected by short, ethylene spacers, for which restricted rotation around the C–N bond is active on the ^{1}H NMR timescale, causes peak broadening in several instances. Therefore where it was not possible to report the chemical shifts in a meaningful way spectra are displayed next to relevant experimental procedure without assignment. For a similar case reported previously, see ref. 12.

3.6.2 Synthesis Overview.

a) Synthesis of three foothold walker-track conjugate **5**-*1*·3[CF_3CO_2H].

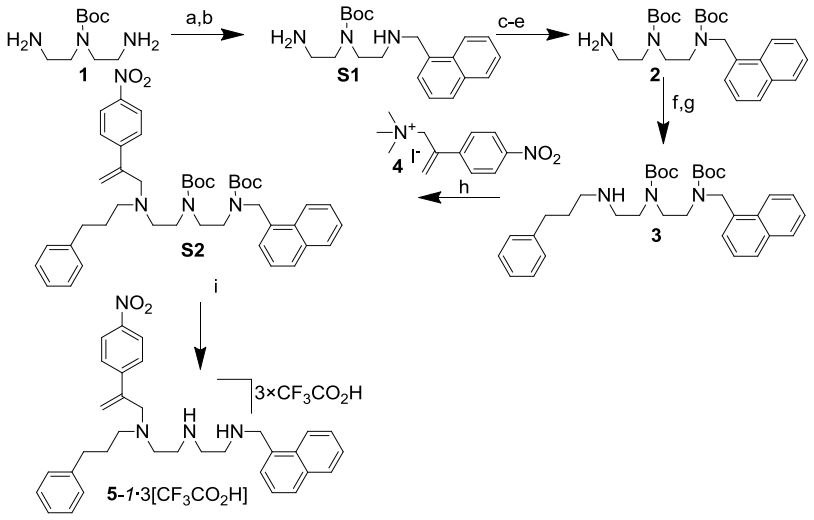

Scheme E3.1. a) 1-naphthaldehyde, EtOH, RT, 16 h; b) $NaBH_4$, RT, 3 h, 34% (two steps); c) CF_3CO_2Et, CH_2Cl_2, 0 °C→RT, 16 h; d) Boc_2O, Et_3N, RT, 12 h; e) NaOH, MeOH/H_2O, RT, 5 h 92% (three steps); f) 3- phenylpropionaldehyde, EtOH, RT, 16 h; g) $NaBH_4$, RT, 3 h 27%, (two steps); h) **4** (walker unit), $^{i}Pr_2NEt$, MeOH, 50 °C, 24 h 54%; i) CF_3CO_2H, CH_2Cl_2, RT, 3 h, quant.

b) Synthesis of five foothold walker-track conjugate **6**-*1*·5[CF_3CO_2H].

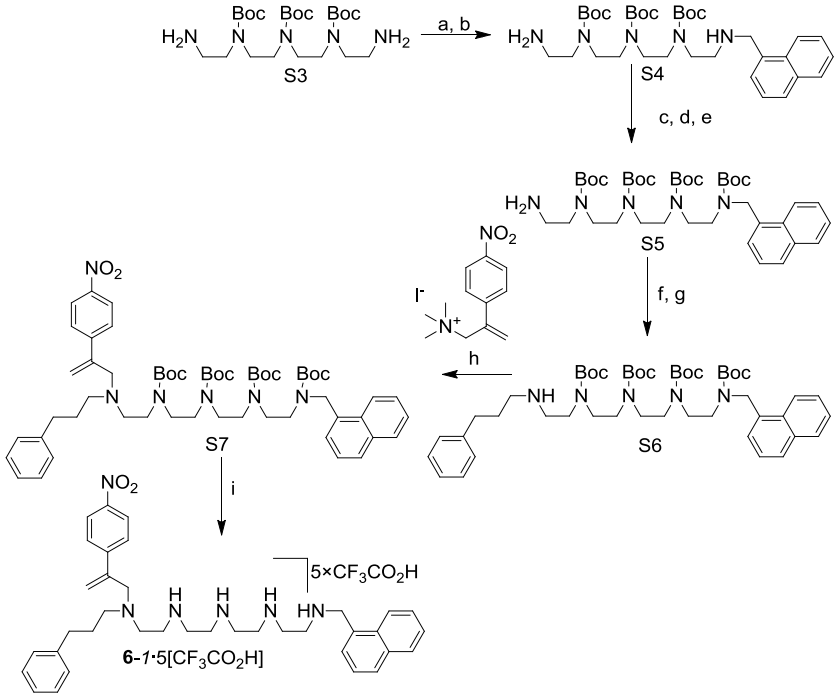

Scheme E3.2. a) 1-naphthaldehyde, EtOH, RT, 16 h; b) $NaBH_4$, RT, 3 h, 34% (two steps) c) CF_3CO_2Et, CH_2Cl_2, 0 °C→RT, 16 h; d) Boc_2O, Et_3N, RT, 12 h; e) NaOH, MeOH/H_2O, RT, 5 h 74% (three steps); f) 3- phenylpropionaldehyde, EtOH, RT, 16 h; g) $NaBH_4$, RT, 3 h 35%, (two steps); h) **4** (walker unit), $^{i}Pr_2NEt$, MeOH, 50 °C, 24 h 49%; i) CF_3CO_2H, CH_2Cl_2, RT, 3 h, quant.

c) Synthesis of 9 foothold walker-track conjugate **7**-*1*·9[CF_3CO_2H].

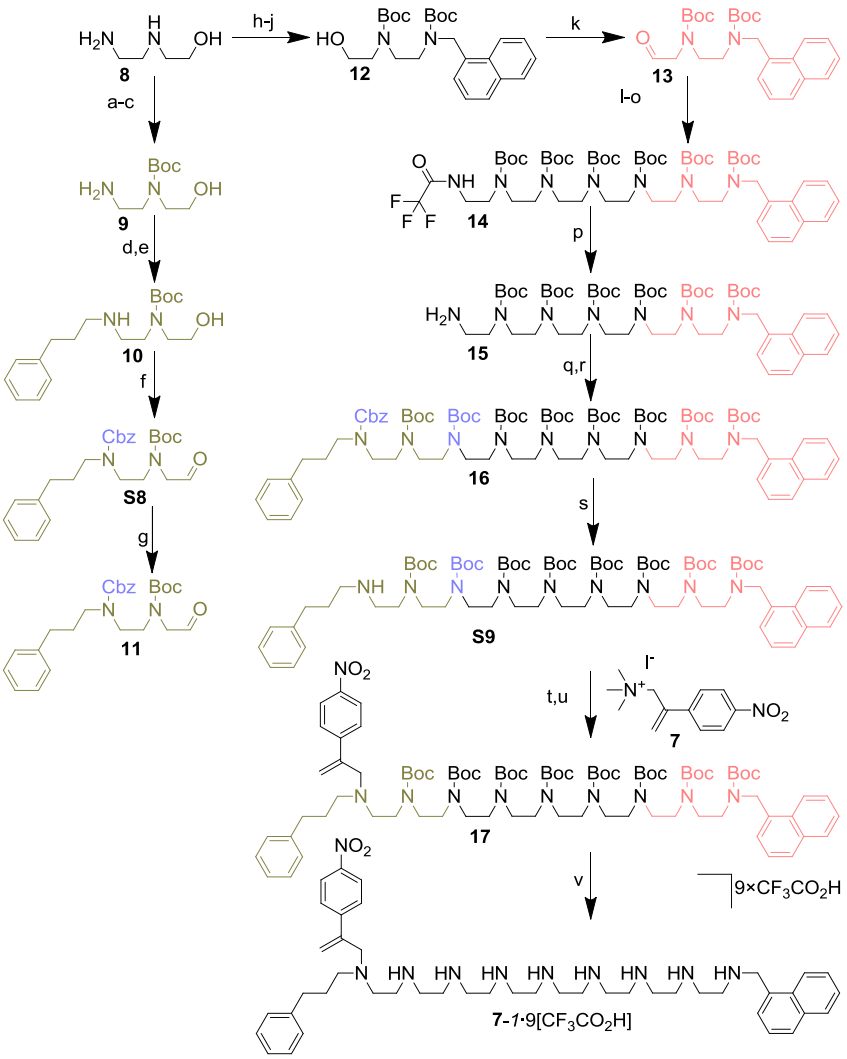

Scheme E3.3. a) CF_3CO_2Et, CH_2Cl_2, 0 °C→RT, 3 h; b) Boc_2O, Et_3N, RT, 12 h, 60% (two steps); c) NaOH, MeOH/H_2O, RT, 5 h, 73%; d) 3-phenylpropionaldehyde, EtOH, RT, 16 h; e) $NaBH_4$, RT, 3 h, 36% (two steps); f) CbzCl, Et_3N, CH_2Cl_2, RT, 4 h, 68%; g) DMP, CH_2Cl_2, RT, 12 h, 81%, h) 1-naphthaldehyde, EtOH, RT, 16 h, i) $NaBH_4$, RT, 3 h,; j) Boc_2O, MeCN, RT, 12 h, 64% (three steps); k) DMP, CH_2Cl_2, RT, 12 h, 68%; l) tetraethylenepentaamine, EtOH, RT, 16 h; m) $NaBH_4$, RT, 3 h; n) CF_3CO_2Et, CH_2Cl_2, 0 °C→RT, 16 h; o) Boc_2O, Et_3N, RT, 12 h, p) NaOH, MeOH/H_2O, RT, 5 h, 20.2% (five steps); q) **12**, EtOH, RT, 16 h; r) $NaBH_4$, RT, 3 h,; s) Boc_2O, Et_3N, RT, 12 h, 30% (three steps); t) Pd(C), H_2, THF, RT, 20 h, 50%; u) **4**, MeOH, $^{i}Pr_2NEt$, 50 °C, 48 h, 50%; v) CF_3CO_2H, CH_2Cl_2, RT, 7 h, quant.

3.6.3 Synthetic Procedures and Characterization Data

Synthesis of 1

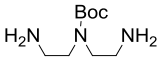

Synthesised according to a literature procedure.[16]

Synthesis of S1

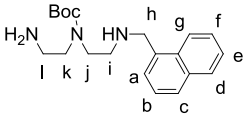

To a stirred solution of **1** (1.05 g, 5.19 mmol, 1.0 equiv.) in dry EtOH (100 mL), 1-naphthaldehyde (0.71 mL, 5.19 mmol, 1.0 equiv.) was added in one portion. The reaction was stirred under N_2 for 16 h at room temperature. $NaBH_4$ (590 mg, 15.6 mmol, 3 equiv.) was then added in portions and reaction was kept stirring under N_2 for another 3 h. After this time H_2O (100 mL) was added to the reaction mixture and product was extracted with CH_2Cl_2 (3 x 100 mL). The combined organic layers were repeatedly washed with water (4 x 100 mL), brine, dried over $MgSO_4$ and the solvent was removed under reduced pressure. Column chromatography (SiO_2, MeOH:CH_2Cl_2:NH_4OH 10:90:2) gave **S1** (619 mg, 34%) as an yellow oil. ^{1}H NMR (500 MHz, $CDCl_3$) δ = 8.11 (d, *J* = 8.2 Hz, 1H, H_c), 7.85 (d, *J* = 7.7 Hz, 1H, H_d), 7.76 (d, *J* = 8.1 Hz, 1H, H_g), 7.54 – 7.38 (m, 4H, $H_{a,b,e,f}$), 4.25 (s, 2H, H_h), 3.51 – 3.15 (m, 4H, $H_{j,k}$), 2.96 – 2.85 (m, 2H, H_i), 2.79 (t, *J* = 6.5 Hz, 2H, H_l), 1.42 (s, 9H, H_{Boc}). ^{13}C NMR (126 MHz, $CDCl_3$) δ = 156.11, 135.88, 133.98, 131.86, 128.81, 127.90, 126.19, 126.07, 125.74, 125.47, 123.76, 79.75, 51.57, 51.00, 48.32, 47.86, 40.91, 28.53. HRMS: $[M+H]^+$ $C_{20}H_{30}N_3O_2$ calc. 344.2333, found 344.2335.

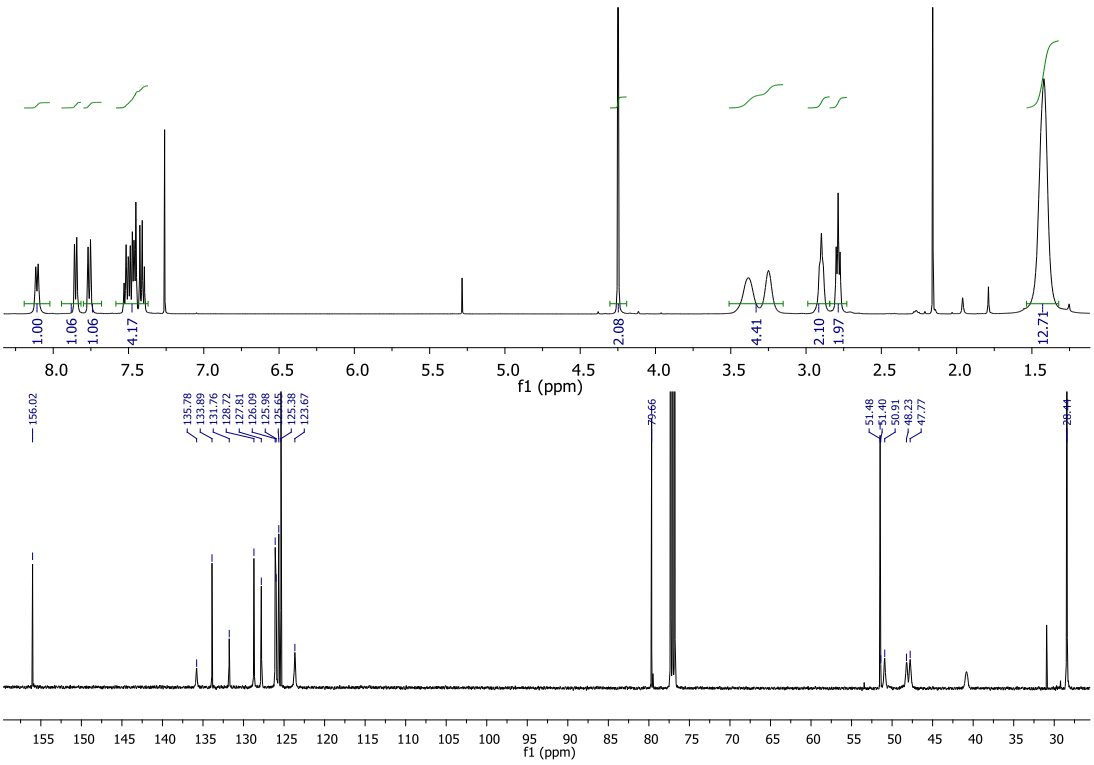

Synthesis of 2

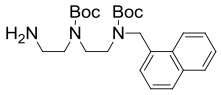

Under N_2, **S1** (600 mg, 1.75 mmol, 1 equiv.) was dissolved in CH_2Cl_2 (25 mL) and cooled to 0 °C. Ethyl trifluoroacetate (0.250 mL, 2.10 mmol, 1.2 equiv.) was added dropwise over 30 min to protect the primary amine. This mixture was then stirred for 30 min at 0 °C and at room temperature for additional 1 h. To the resulting mixture, a solution of Boc_2O (763 mg, 3.5 mmol, 2 equiv.) in CH_2Cl_2 (5 mL) was added dropwise. Dry Et_3N (0.490 mL, 3.50 mmol, 2 equiv.) was then added and the solution was stirred for 12 h at RT. The reaction mixture was then washed with $NaHCO_3$. The organic layer was separated, washed with water, dried over Na_2SO_4 and evaporated.

Crude product was then dissolved in MeOH (15 mL), NaOH (295 mg, 8.75 mmol, 5 equiv.) in H_2O (7 mL) was added. The reaction mixture was stirred at RT for 5 h. After this time the solvent was removed under reduced pressure, the residue was dissolved in H_2O, and extracted with CH_2Cl_2 (4 x 20 mL). The combined organic layers were dried over $MgSO_4$ and solvent was removed under reduced pressure. Purification by column chromatography (SiO_2, MeOH/CH_2Cl_2 20:80) afforded **2** (720 mg, 92%) as a yellow oil. HRMS: $[M+H]^+$ $C_{25}H_{38}N_3O_4$ calc. 444.2857, found 444.2853

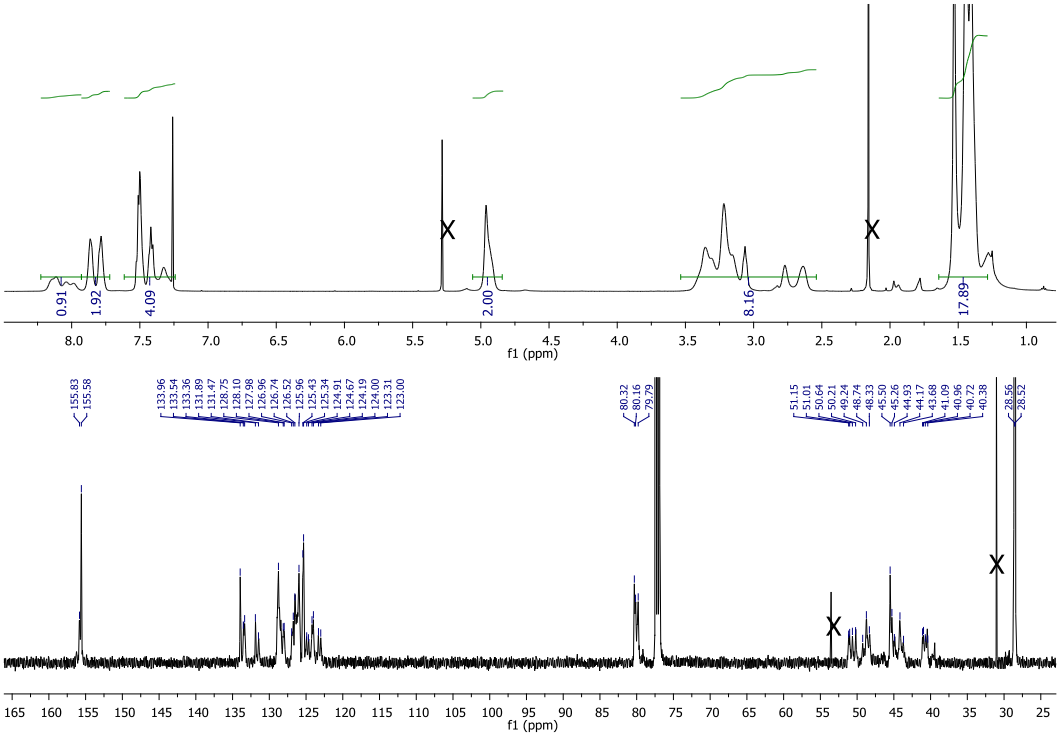

Synthesis of 3

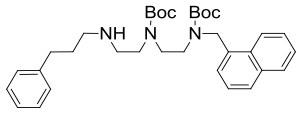

To a solution of **2** (690 mg, 1.56 mmol, 1.0 equiv.) in dry EtOH (100 mL), 3-phenylpropionaldehyde (0.205 mL, 1.56 mmol, 1.0 equiv.) was added in one portion. The reaction was stirred under N_2 for 16 h at room temperature. $NaBH_4$ (177 mg, 4.68 mmol, 3 equiv.) was then added in portions and reaction was kept stirring under N_2 for another 3 h. After this time H_2O (50 mL) was added to the reaction mixture and the product was extracted with CH_2Cl_2 (3 x 50 mL). The combined organic layers were washed with brine, dried over $MgSO_4$ and the solvent was removed under reduced pressure. Column chromatography (SiO_2, MeOH/CH_2Cl_2 3:98) gave **3** (234 mg, 27%) as a yellow oil. HRMS: $[M+H]^+$ $C_{34}H_{48}N_3O_4$ calc. 562.3639, found 562.3640.

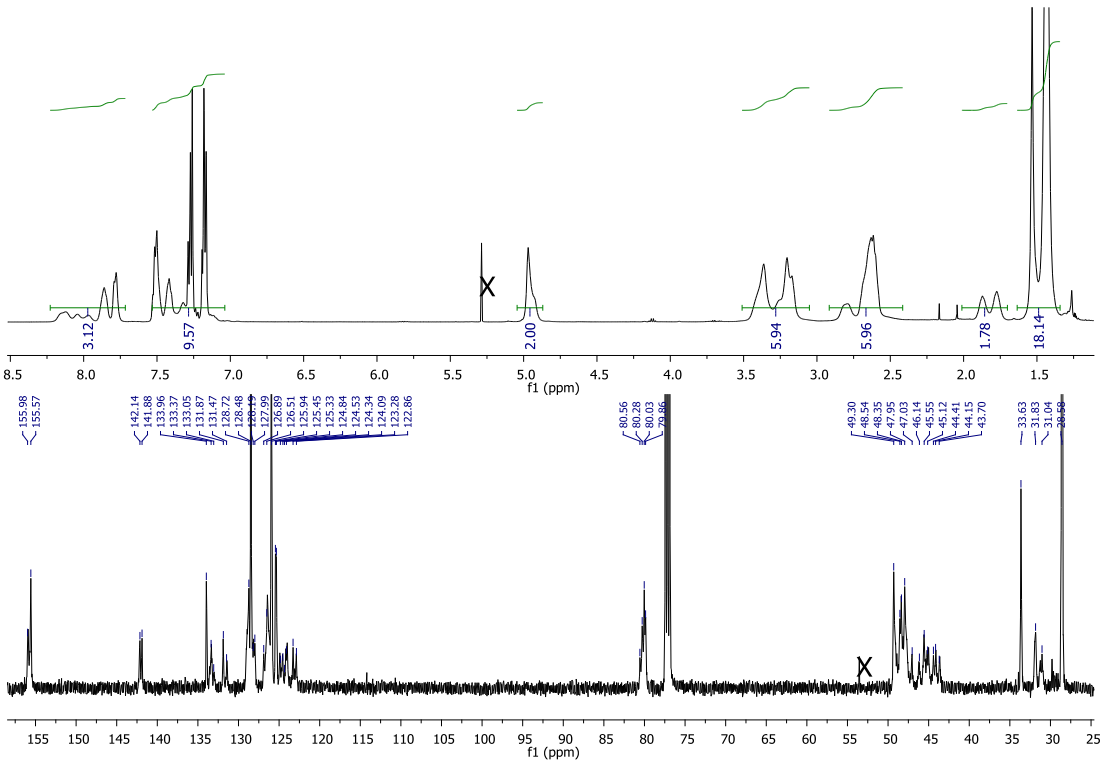

Synthesis of 4

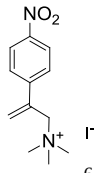

Synthesised according to the literature procedure.[6]

Synthesis of S2

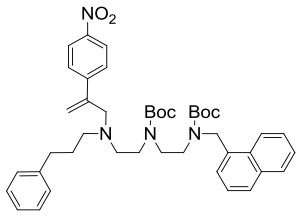

To a degassed solution of **3** (200 mg, 0.36 mmol, 1.0 equiv.) in dry MeOH (30 mL), **4** (149 mg, 0.43 mmol, 1.2 equiv.) was added in one portion. The reaction mixture was kept stirring under N_2 at 65 °C for 24 h in the presence of $^{i}Pr_2NEt$ (186 µL, 1.07 mmol, 3.0 equiv.) After this time, the reaction was cooled to room temperature and H_2O (30 mL) was added. The mixture was extracted with CH_2Cl_2 (3 x 30 mL), dried over $MgSO_4$, and the solvent removed under reduced pressure. Column chromatography (SiO_2, MeOH:CH_2Cl_2 1:99) gave **S2** (140 mg, 54%) as an orange oil. HRMS: $[M+H]^+$ $C_{43}H_{55}N_4O_6$ calc. 723.4116, found 723.4108.

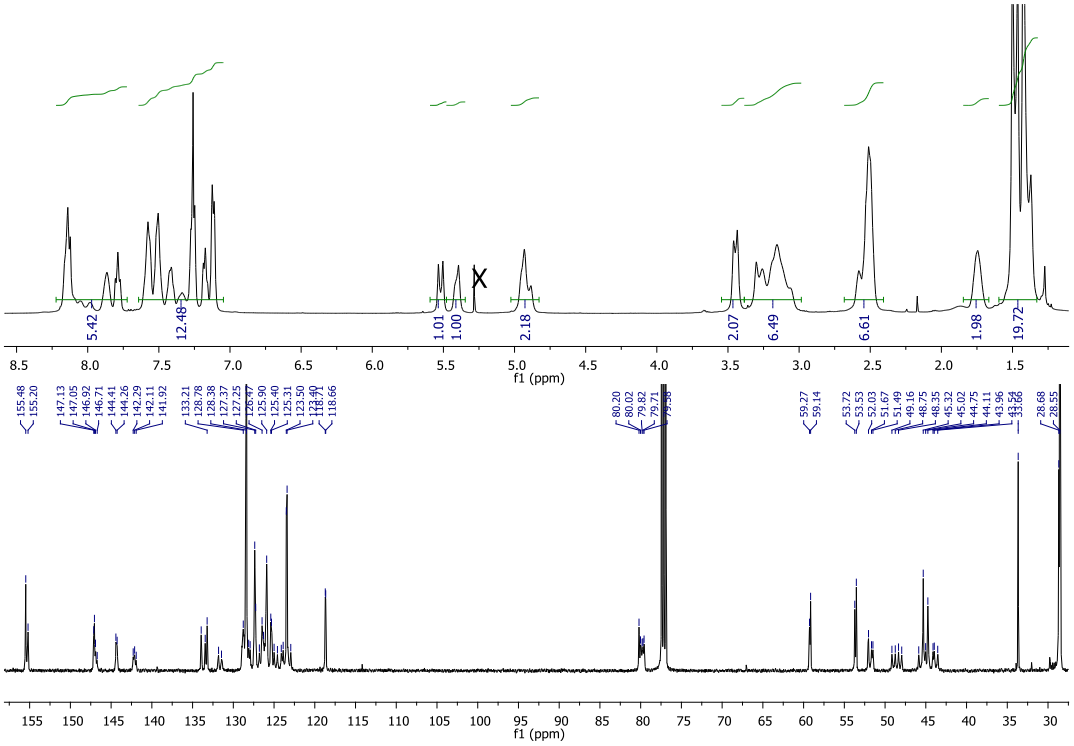

Synthesis of 5-*1*·3[CF_3CO_2H].

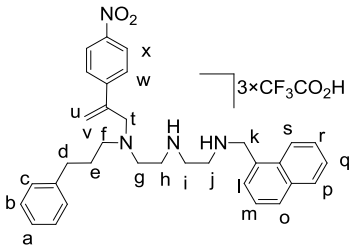

To a solution of **S2** (10 mg, 0.14 µmol, 1.0 equiv.) in CH_2Cl_2 (3 mL), trifluoroacetic acid (0.75 mL) was added dropwise. The reaction was left stirring open to air, at RT, and the disappearance of the substrate was monitored by ESI-MS. After 3 h, solvents were removed and product dried using high vacuum pump to afford the product **5**-*1*·3[CF_3CO_2H] (12 mg, quant.). ^{1}H NMR (500 MHz, CD_3CN) δ = 8.20 – 8.15 (m, 3H, $H_{x,o}$), 8.07 – 7.99 (m, 2H, $H_{p,s}$), 7.73 (d, J = 6.6 Hz, 1H, H_l), 7.70 – 7.60 (m, 4H, $H_{m,r,w}$), 7.58 (dd, J = 8.2, 7.2 Hz, 1H, H_q), 7.36 – 7.29 (m 2H, H_b), 7.28 – 7.23 (m, 1H, H_a), 7.20 – 7.14 (m, 2H, H_c), 5.87 (s, 1H, H_u), 5.82 (s, 1H, H_v), 4.73 (s, 2H, H_k), 4.30 (s, 2H, H_t), 3.62 – 3.53 (m, 4H, $H_{g,j}$), 3.50 – 3.36 (m, 4H, $H_{h,i}$), 3.12 – 3.03 (m, 2H, H_f), 2.58 (t, J = 7.5 Hz, 2H, H_d), 2.05 – 1.99 (m, 2H, H_e). ^{13}C NMR (126 MHz, CD_3CN) δ = 148.00, 144.17, 140.16, 136.71, 133.81, 131.20, 130.34, 129.09, 128.89, 128.56, 128.35, 127.93, 127.89, 127.12, 126.73, 126.49, 126.37, 125.36, 123.92, 123.04, 56.74, 52.45, 49.93, 48.65, 44.74, 44.50, 42.88, 31.85, 24.12. HRMS: $[M+H]^+$ $C_{33}H_{39}N_4O_2$ calc. 523.3068, found 523.3058.

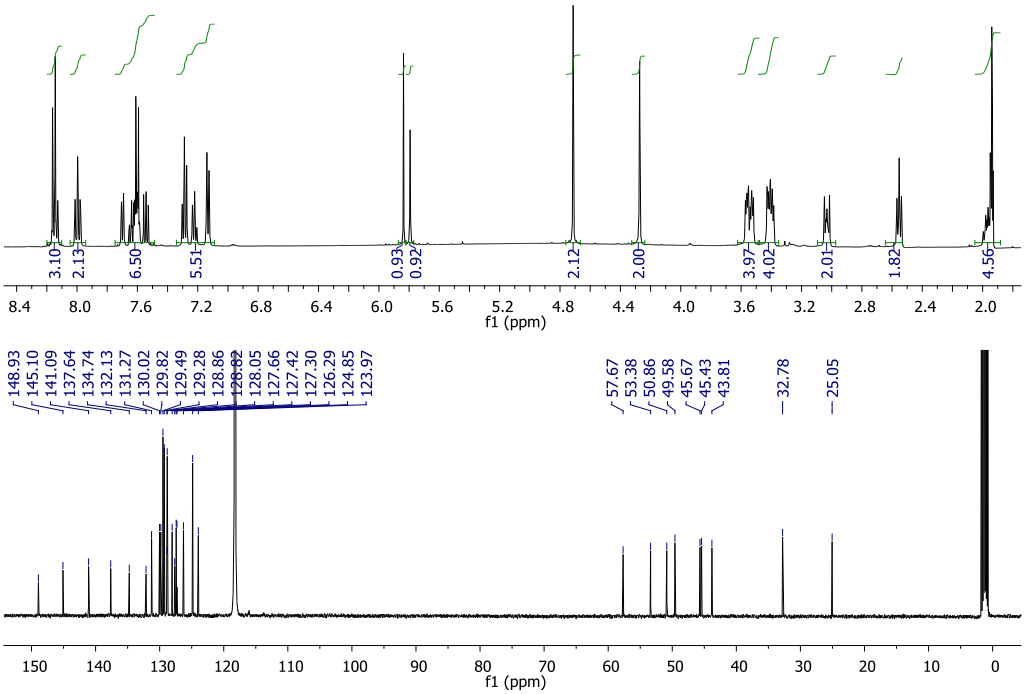
3.10
2.13
6.50
5.51
0.93
0.92
2.12
2.00
3.97
4.02
2.01
1.82
4.56
f1 (ppm)
148.93
145.10
141.09
137.64
134.74
132.13
131.27
130.02
129.82
129.49
129.28
128.86
128.82
128.05
127.66
127.42
127.30
126.29
124.85
123.97
57.67
53.38
50.86
49.58
45.67
45.43
43.81
32.78
25.05
f1 (ppm)

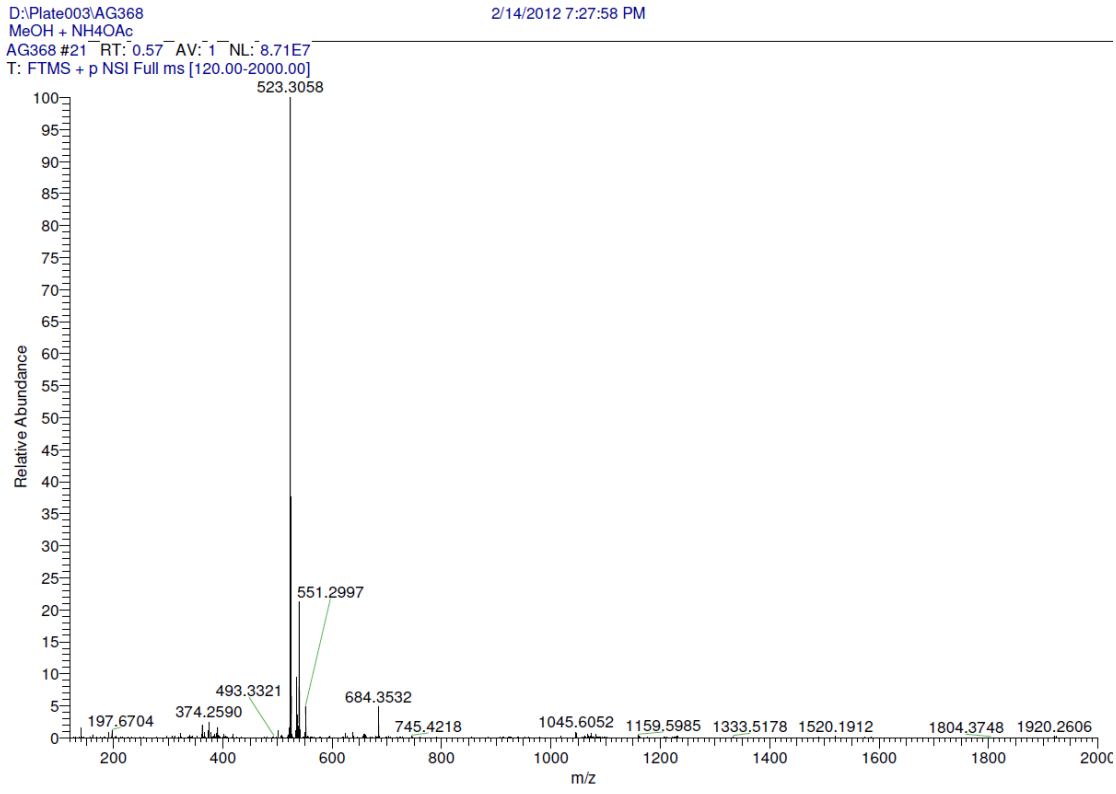
D:\Plate003\AG368
MeOH + NH4OAc
2/14/2012 7:27:58 PM
AG368 #21 RT: 0.57 AV: 1 NL: 8.71E7
T: FTMS + p NSI Full ms [120.00-2000.00]
523.3058
551.2997
493.3321
684.3532
374.2590
197.6704
745.4218
1045.6052
1159.5985
1333.5178
1520.1912
1804.3748
1920.2606
Relative Abundance
m/z

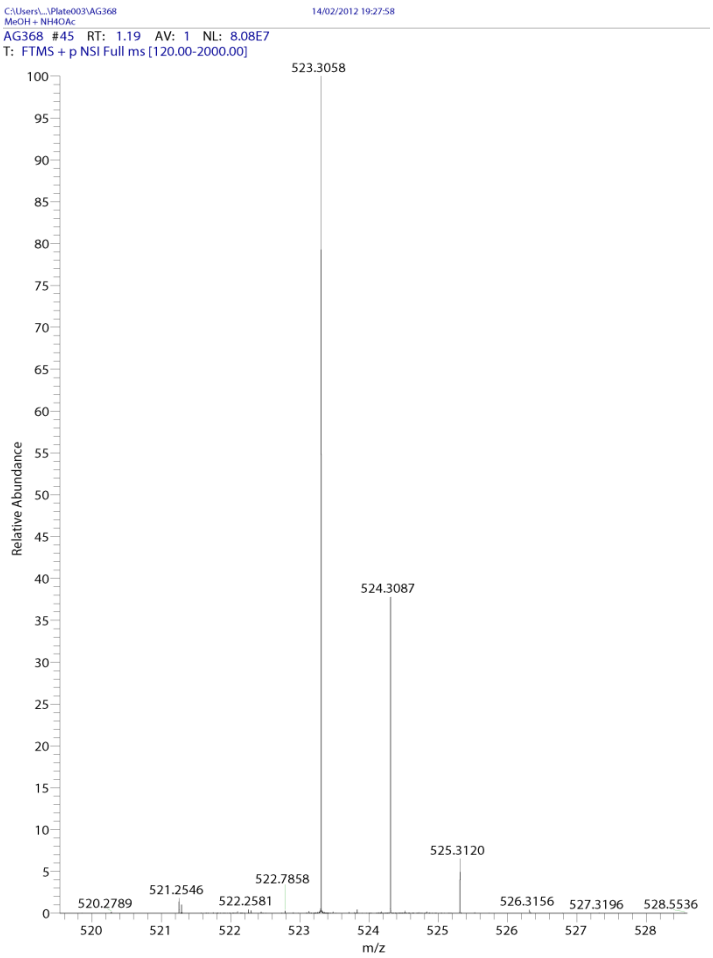

Synthesis of S3

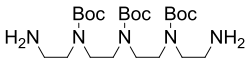

Synthesised according to the literature procedure.[17,6]

Synthesis of S4

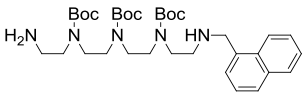

Synthesised according to the procedure described for **S1** (based on 156 mg of 1-naphthaldehyde), 466 mg (34%) of **S4** isolated as an yellow oil after purification by column chromatography (SiO_2, MeOH:CH_2Cl_2:Et_3N 7.5:92.5:1). HRMS: $[M+H]^+$ $C_{34}H_{56}N_5O_6^+$ calc. 630.4231, found 630.4197.

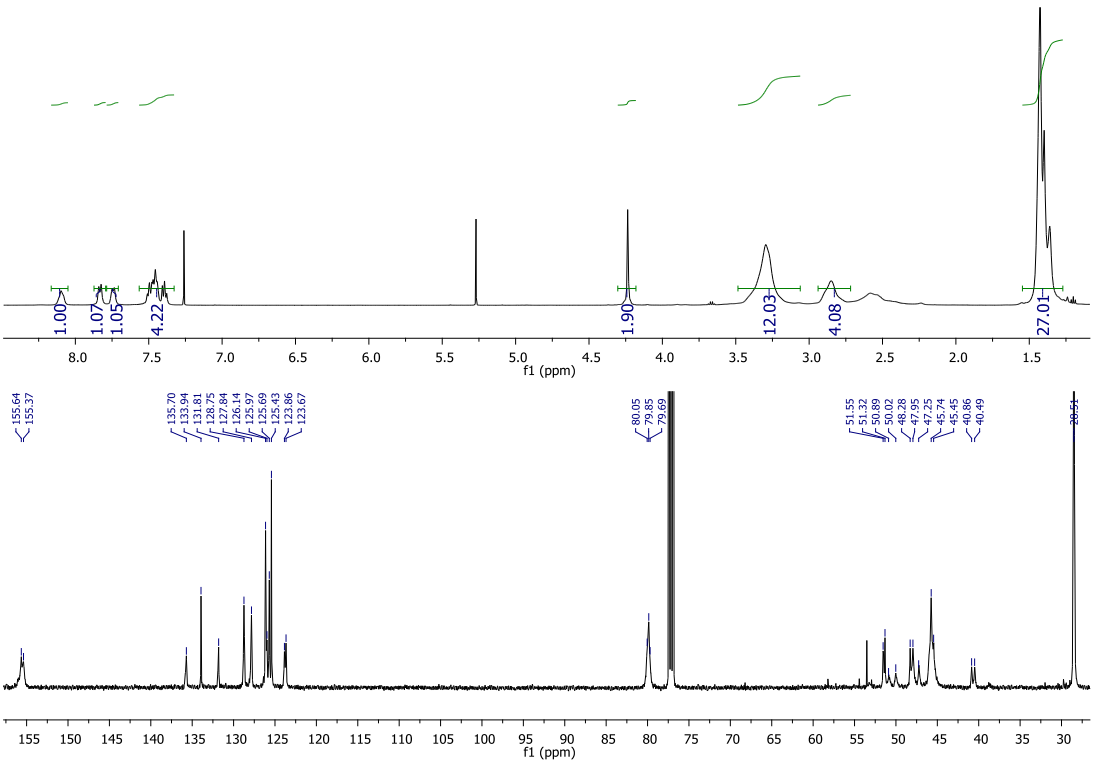

Synthesis of S5

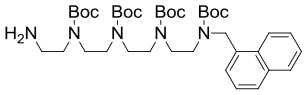

Synthesised according to the procedure described for **2** (based on 400 mg of **S4**), 345 mg (74%) of **S5** was isolated as a white solid after purification by column chromatography (SiO_2, MeOH:CH_2Cl_2:Et_3N 5:95:1). HRMS: $[M+H]^+$ $C_{39}H_{64}N_5O_8^+$ calc. 730.4755 found 730.4707, $[2M+H^+]$ $C_{78}H_{127}N_{10}O_{16}^+$ Calc. 1459.9432 found 1459.9339. Mp. 53-55 °C.

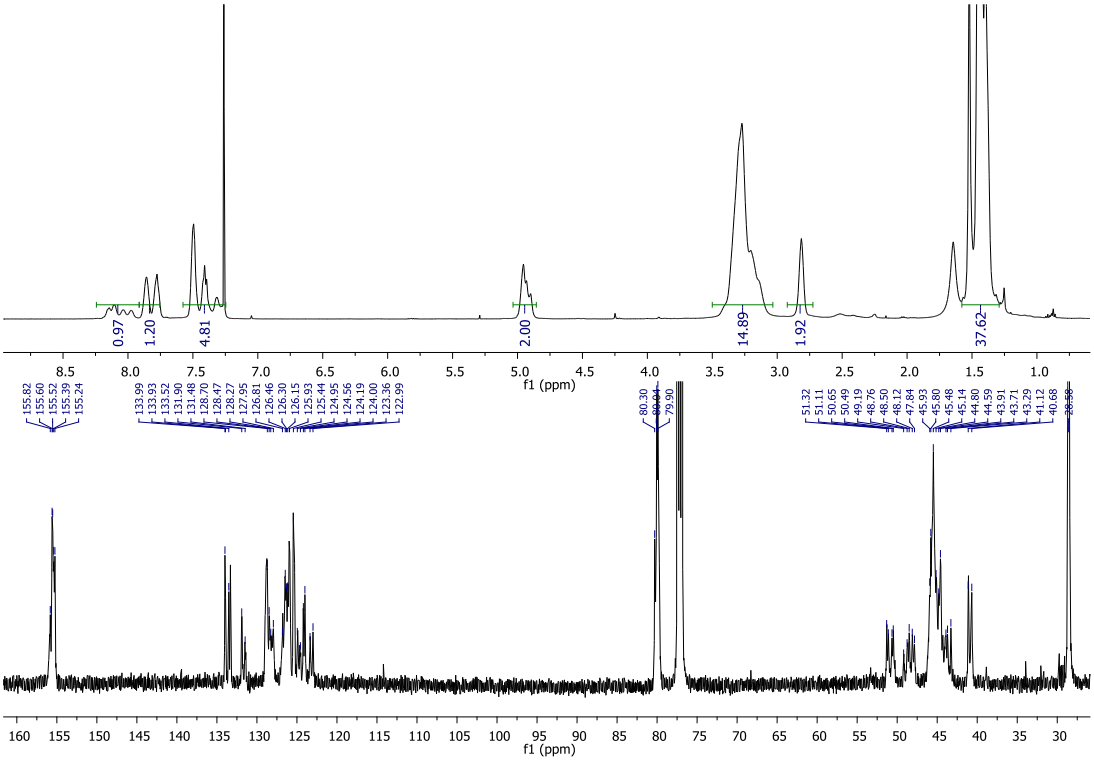

Synthesis of S6

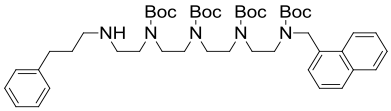

Synthesised according to the procedure described for **3** (based on 246 mg of **S5**), 100 mg (35%) of **S6** was isolated as a white solid after purification by column chromatography (SiO_2, MeOH:CH_2Cl_2 5:95). Mp. 44-45°C.

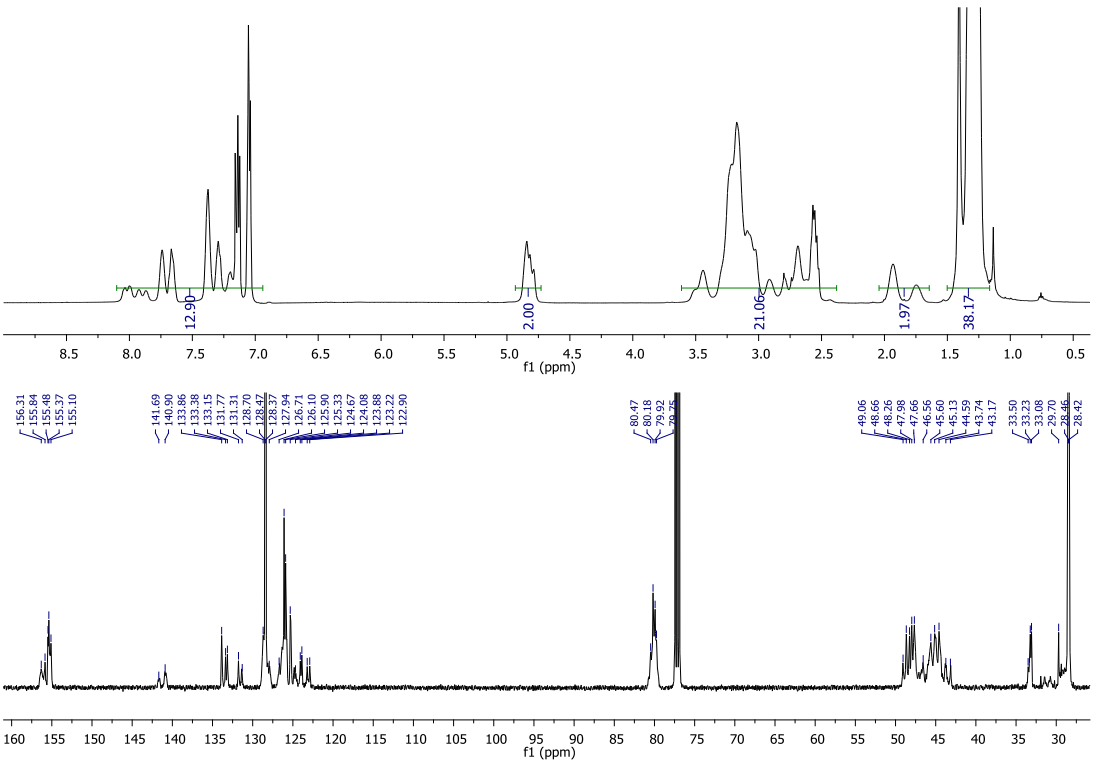

Synthesis of S7

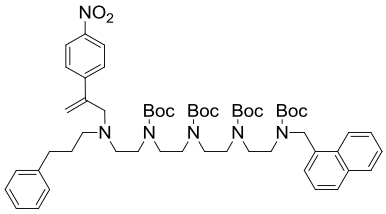

Synthesised according to the procedure described for **S2** (based on 100 mg of **S6**), 58 mg (49%) of **S7** was isolated after purification by column chromatography (SiO_2, petroleum:EtOAc 80:20) as a yellow oil. HRMS: $[M+H]^+$ $C_{57}H_{81}N_6O_{10}^+$ calc. 1009.6014, found 1009.5979.

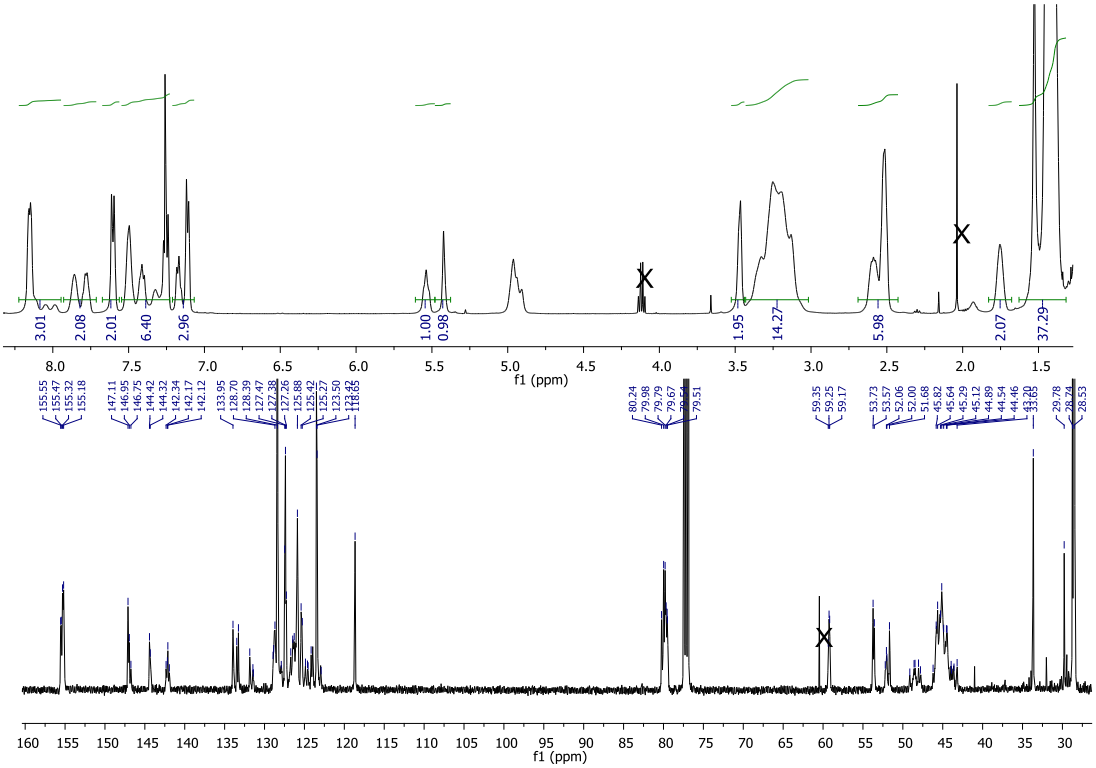

Synthesis of 6-*1*·5[CF_3CO_2H].

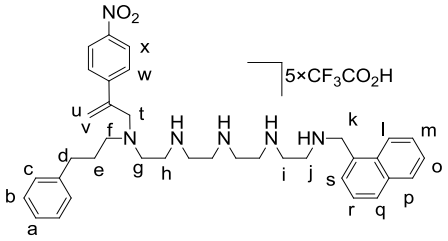

Synthesised according to the procedure described for **5**-*1*·3[CF_3CO_2H] (based on 15 mg of **S7**) 18 mg (quant.) of **6**-*1*·5[CF_3CO_2H] was isolated as a yellow oil. ^{1}H NMR (500 MHz, CD_3CN) δ = 8.24 – 8.18 (m, 2H, H_x) 8.15 (d, J = 8.4 Hz, 2H, H_q), 8.07 – 8.00 (m, 2H, $H_{p,l}$), 7.72 (d, J = 6.8 Hz, 1H, H_s), 7.70 – 7.60 (m, 4H, $H_{m,r,w}$), 7.58 (dd, J = 8.1, 7.3 Hz, 1H, H_o), 7.36 – 7.30 (m, 2H, H_b), 7.29 – 7.23 (m, 1H, H_a), 7.19 – 7.13 (m, 2H, H_c), 5.83 (s, 1H, H_u), 5.76 (s, 1H, H_v), 4.71 (s, 2H, H_k), 4.25 (s, 2H, H_t), 3.59 – 3.51 (m, 2H, H_j), 3.50 – 3.34 (m, 14H, $H_{g,h,i,}$ + 4×CH_2), 3.05 – 2.98 (m, 2H, H_f), 2.52 (t, J = 7.5 Hz, 2H, H_d), 1.97 – 1.92 (m, 2H, H_e). ^{13}C NMR (126 MHz, CD_3CN) δ = 148.06, 143.92, 140.00, 136.31, 133.83, 131.11, 130.50, 129.19, 128.94, 128.57, 128.33, 128.25, 127.85, 127.20, 126.55, 126.41, 126.37, 125.37, 124.01, 122.88, 56.82, 52.57, 49.61, 48.89, 44.88, 44.86, 44.75, 44.67, 44.54, 42.71, 31.76, 30.20, 24.12. In addition, 159.16 (q, J = 38.6 Hz) and 115.55 (q, J = 287.8 Hz) for C-F of the counteranion are present. HRMS: $[M+H]^+$ $C_{71}H_{107}N_8O_{14}^+$ $C_{37}H_{49}N_6O_2$ calc. 609.3912, found 609.3908.

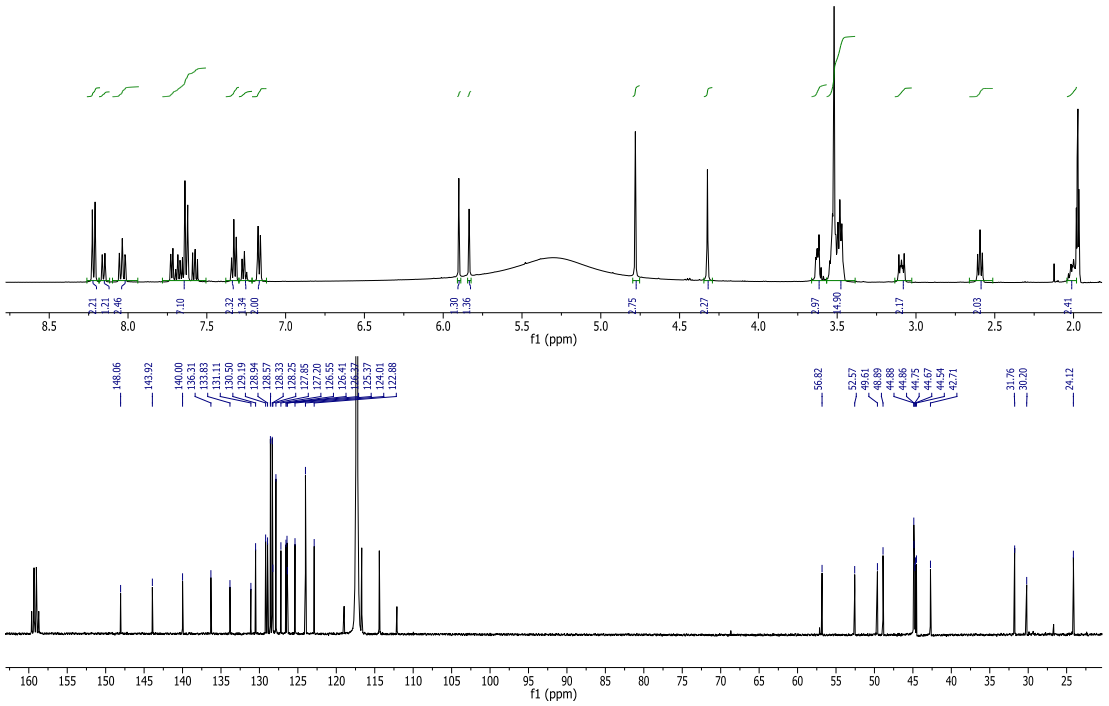
f1 (ppm)
f1 (ppm)

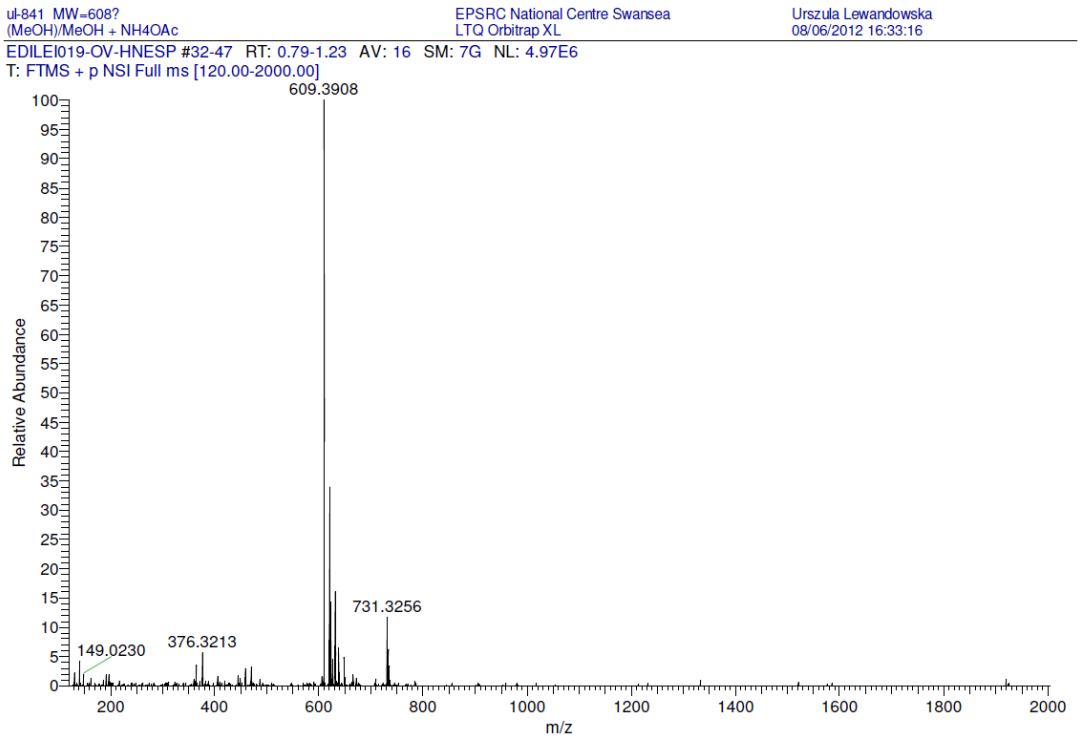
ul-841 MW=608?
(MeOH)/MeOH + NH4OAc
EPSRC National Centre Swansea
LTQ Orbitrap XL
Urszula Lewandowska
08/06/2012 16:33:16
EDILEI019-OV-HNESP #32-47 RT: 0.79-1.23 AV: 16 SM: 7G NL: 4.97E6
T: FTMS + p NSI Full ms [120.00-2000.00]
609.3908
731.3256
376.3213
149.0230
Relative Abundance
m/z

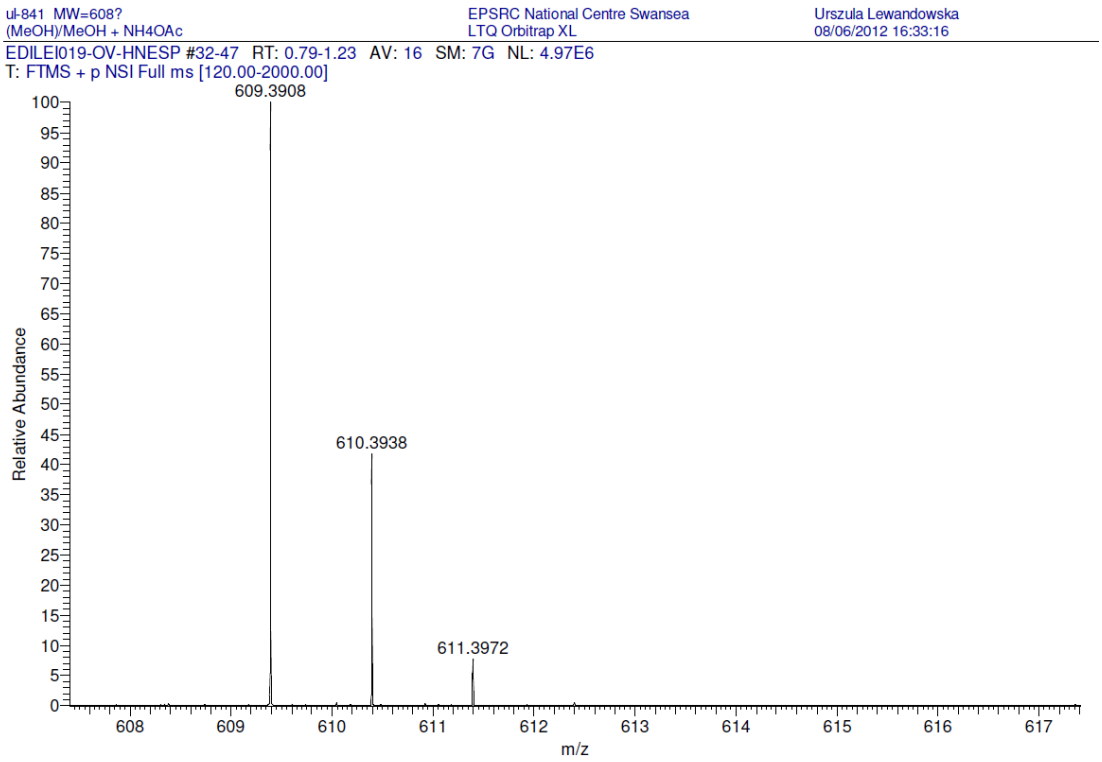

Synthesis of 9

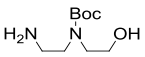

Synthesised according to a modified literature procedure.[17]

Under N_2, **8** (4.85 mL, 48.0 mmol, 1 equiv.) was dissolved in CH_2Cl_2 (25 mL) and cooled to 0 °C. Ethyl trifluoroacetate (6.2 mL, 52.8 mmol, 1.1 equiv.) was added dropwise over 30 min to protect the primary amine. This mixture was then stirred for 30 min at 0 °C and at room temperature for additional 1 h. To the resulting mixture, a solution of Boc_2O (12.5 g, 57.3 mmol, 1.2 equiv.) was added in portions. Dry Et_3N (10 mL, 72.0 mmol, 2 equiv.) was then added and the solution was stirred for 12 h at RT. The reaction mixture was then washed with $NaHCO_3$. The organic layer was separated, washed with water, dried over Na_2SO_4 and evaporated.

Crude product was dissolved in MeOH (165 mL), NaOH (14.1 g, 0.352 mol, 7.3 equiv.) in H_2O (82.6 mL) was added. The reaction mixture was stirred at RT for 5 h. After this time the solvent was removed under reduced pressure, the residue was dissolved in H_2O, and extracted with CH_2Cl_2 (4 x 20 mL). The combined organic layers were dried over $MgSO_4$ and solvent was removed under reduced pressure. Isolated colourless oil **9** (4.24 g, 92%) was pure by ^1H NMR and was used without further purification.

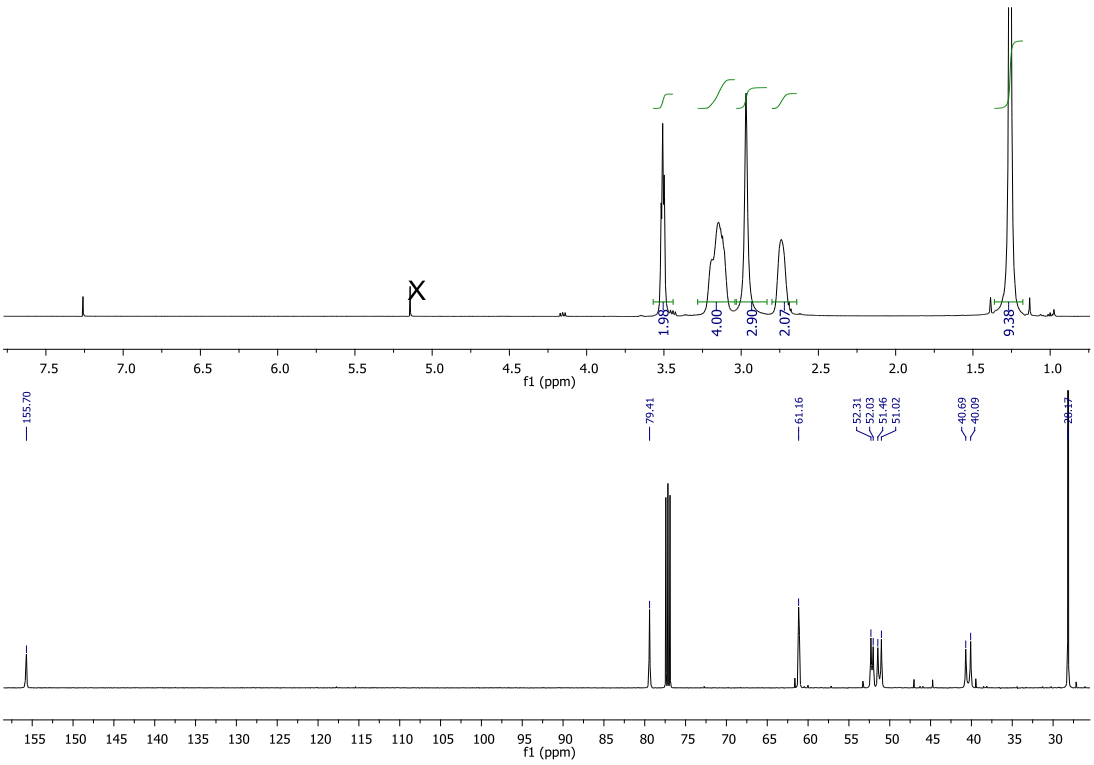

Synthesis of 10

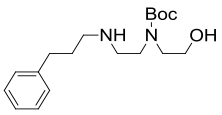

Synthesised according to the procedure described for **S6** (based on 4 g of **9**). 2 g (36%) of **10** were isolated as a colourless oil after purification by column chromatography (SiO_2, MeOH:CH_2Cl_2:Et_3N 2:98:1). HRMS: $[M+H]^+$ $C_{18}H_{31}N_2O_3^+$ calc. 323.2335 found 323.2318.

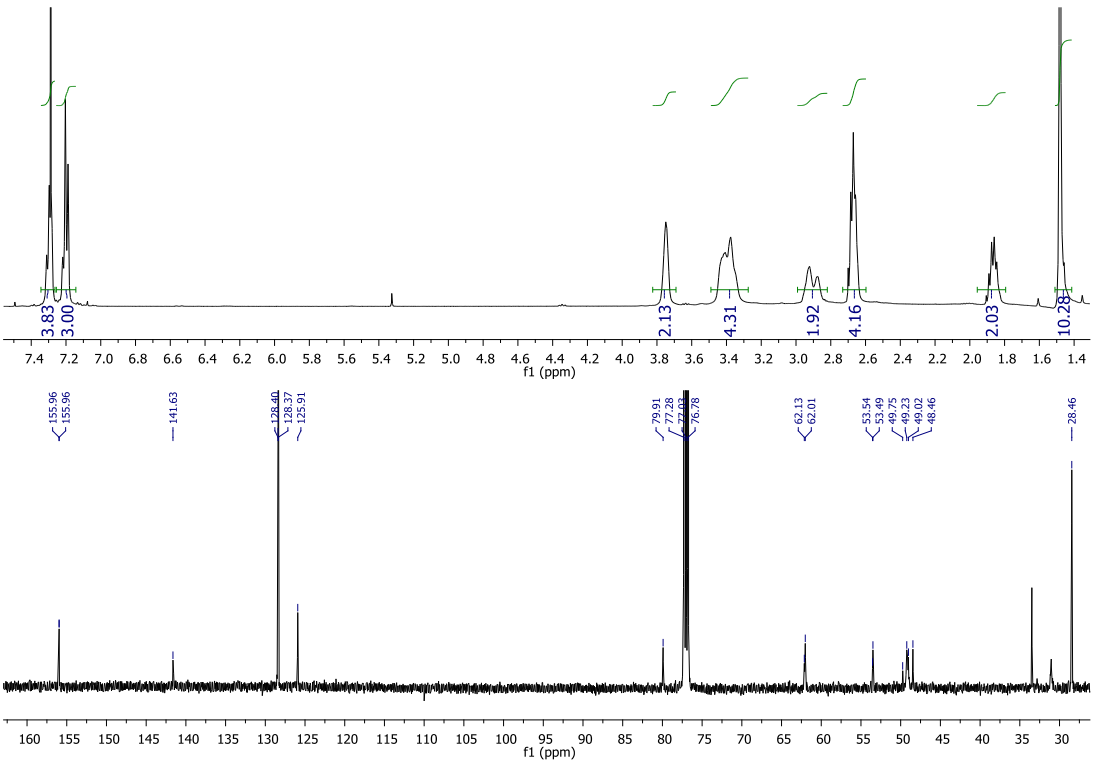

Synthesis of S8

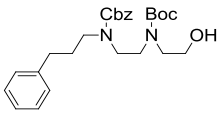

Under N_2, **10** (810 mg, 2.5 mmol, 1 equiv.) was dissolved in CH_2Cl_2 (30 mL) and cooled to 0 °C. CbzCl (0.57 mL, 4.0 mmol, 1.6 equiv.) was added dropwise over 30 min to protect the secondary amine. This mixture was then stirred for 30 min at 0 °C and at room temperature for additional 12 h. The reaction mixture was then washed with $NaHCO_3$. The organic layer was separated, washed with water, dried over Na_2SO_4 and evaporated. Column chromatography (SiO_2, MeOH:CH_2Cl_2 2:98) afforded **S8** (800 mg, 61%) as colourless oil. HRMS: $[M+H]^+$ $C_{26}H_{37}N_2O_5^+$ calc. 457.2702, found 457.3053.

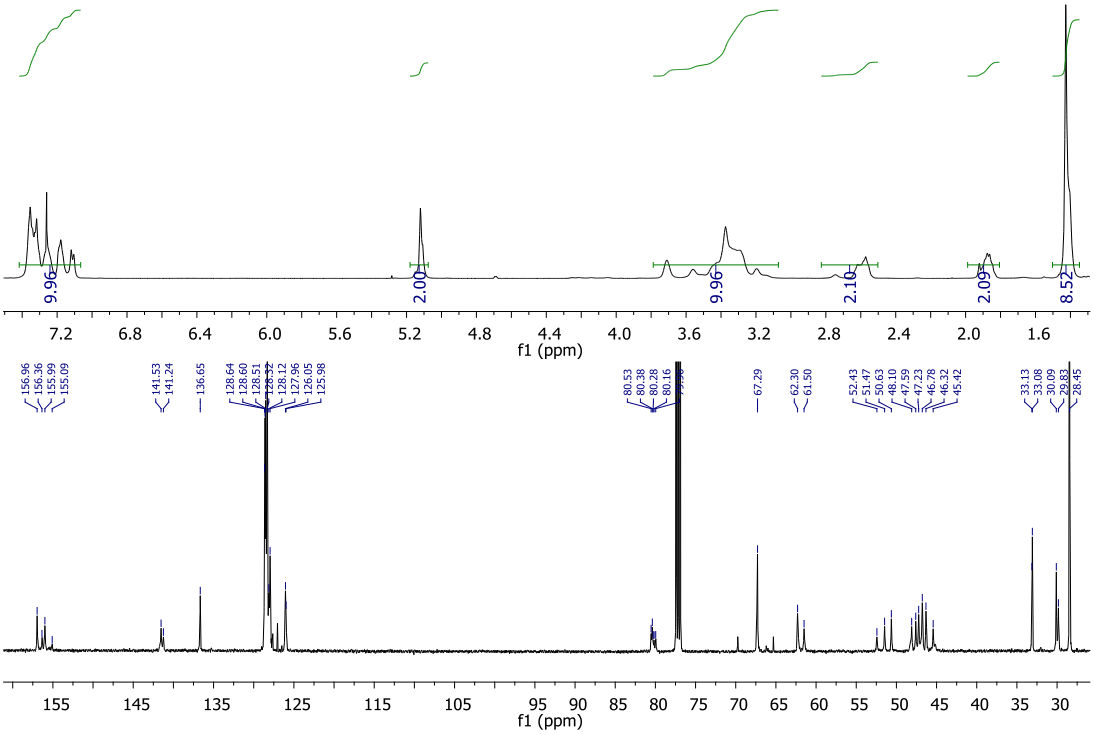

Synthesis of 11

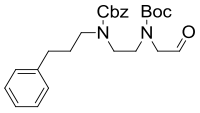

Cbz protected **S8** (700 mg 1.53 mmol, 1 equiv.) was dissolved in CH_2Cl_2 (10 mL). Dess-Martin periodinane (DMP) (780 mg, 1.84 mmol, 1.2 equiv.) was added and the reaction was stirred for 12 h at room temperature. The reaction mixture was filtered, and a 15% solution of $Na_2S_2O_3$ in $NaHCO_3$ was added to the filtrate to decompose remaining DMP. The organic layer was separated after 20 min, washed with water, dried over Na_2SO_4 and the solvent removed under reduced pressure. Column chromatography (SiO_2, CH_2Cl_2:MeOH 99:1) gave **11** (568 mg, 81%) as a colourless oil. HRMS: [M-Boc+H^+] $C_{21}H_{27}N_2O_3^+$ calc. 355.2022 found 355.2014

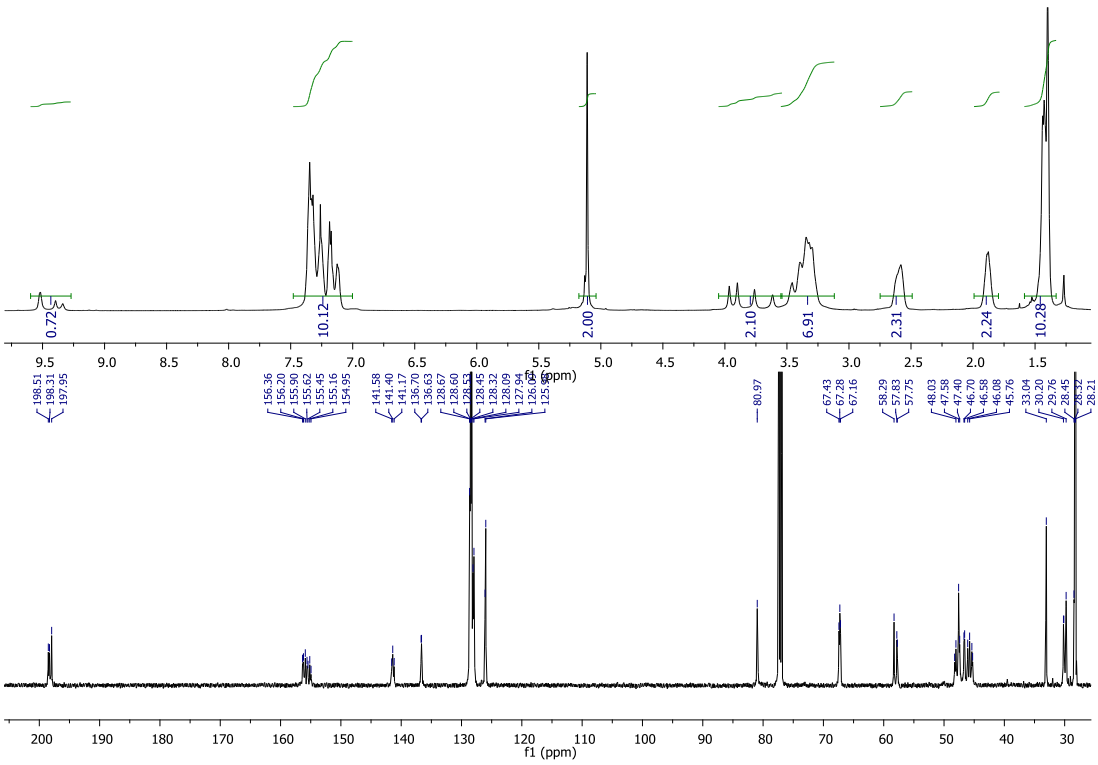

Synthesis of 12

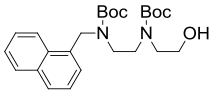

To a stirred solution of **8** (3.51 mL, 34.6 mmol, 1.0 equiv.) in dry EtOH (100 mL), 1-naphthaldehyde (4.70 mL, 34.6 mmol, 1.0 equiv.) was added in one portion. The reaction was stirred under N_2 for 16 h at room temperature. $NaBH_4$ (2.56 g, 69.2 mmol, 2 equiv.) was then added in portions and reaction was kept stirring under N_2 for another 3 h. After this time reaction was concentrated and residue taken up in H_2O (60 mL) and product was extracted with EtOAc (3 x 100 mL). The combined organic phases were washed with water and brine, dried over $MgSO_4$ and the solvent was removed under reduced pressure.

The crude mixture was dissolved in MeCN (15 mL). Boc_2O (16.6 g, 76.1 mmol, 2.2 equiv.) in CH_2Cl_2 (2 mL) was added in portions to selectively protect the secondary amine. This mixture was stirred for 12 h after which solvent was removed under reduced pressure. Column chromatography (SiO_2, CH_2Cl_2:MeOH 97:3) afforded **13** (9.8 g, 64%) as an yellow oil. HRMS: $[M+H]^+$ $C_{25}H_{37}N_2O_5^+$ calc. 445.2702 found 445.2680

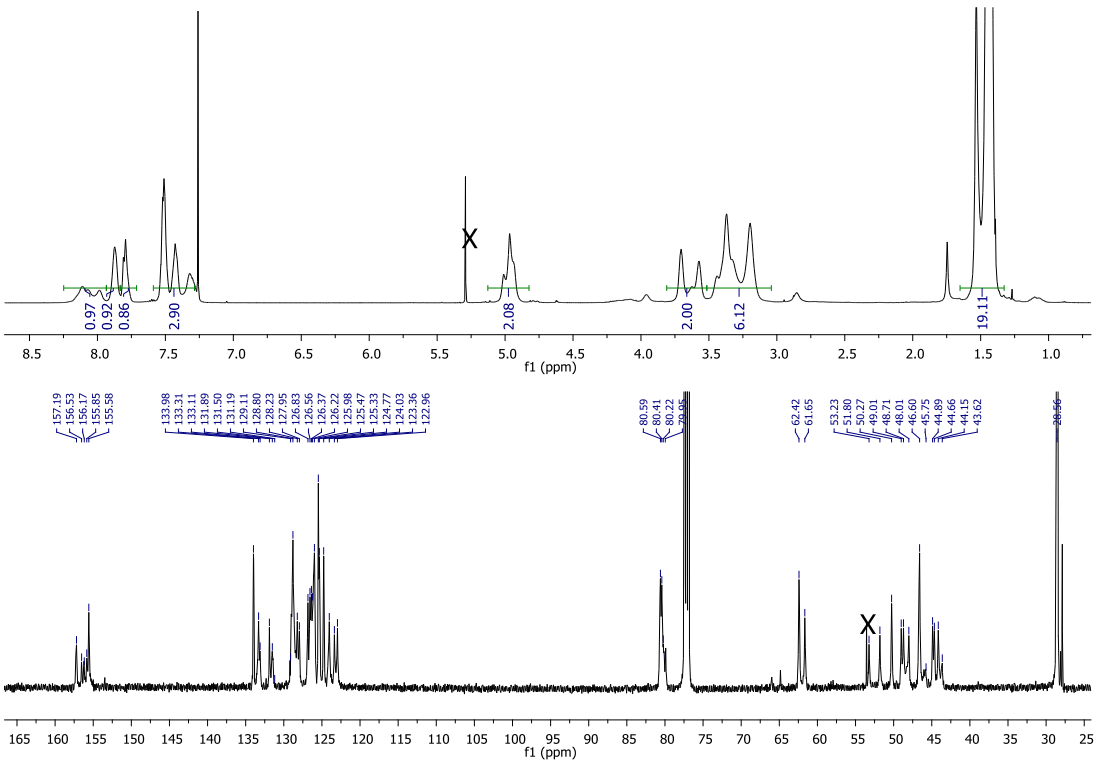

Synthesis of 13

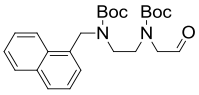

Synthesised according to the procedure described for **11** (based on 3 g of **12**), 2 g (68%) of **13** were isolated as an yellow oil after purification by column chromatography (SiO_2, MeOH:CH_2Cl_2 1:99). HRMS: $[M+H]^+$ $C_{25}H_{35}N_2O_5^+$ calc. 443.2546, found 443.2535.

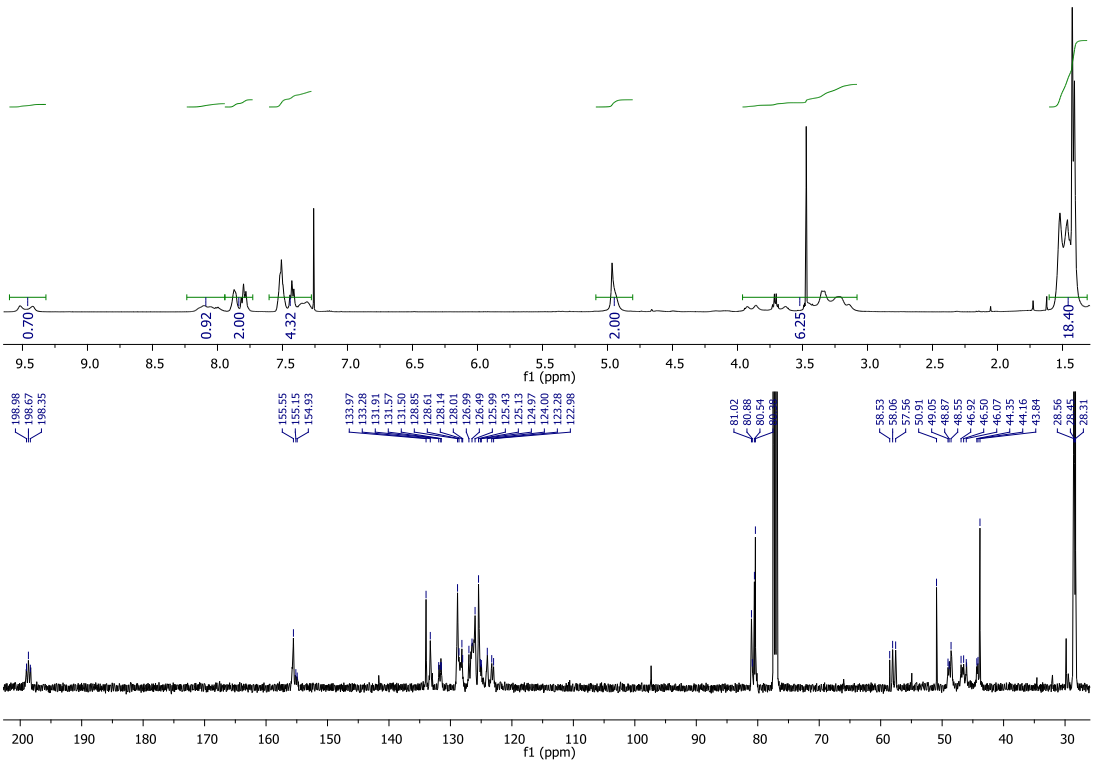

Synthesis of 15

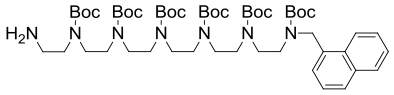

To a solution of tetraethylenepentaamine (1.64 mL, 8.5 mmol, 2.0 equiv.) in dry EtOH (50 mL), **13** (1.9 g, 4.2 mmol, 1.0 equiv.) was added as a solution in EtOH (5 mL). The reaction was stirred under N_2 for 16 h at room temperature. $NaBH_4$ (1 g, 26.5 mmol, 3 equiv.) was then added in portions and reaction was kept stirring under N_2 for another 3 h. After this time H_2O (50 mL) was added to the reaction mixture and the product was extracted with EtOAc (3 x 50 mL). The combined organic layers were washed with water, brine, dried over $MgSO_4$ and the solvent was removed under reduced pressure.

Under N_2, crude mixture was dissolved in CH_2Cl_2 (100 mL) and cooled to 0 °C. Ethyl trifluoroacetate (0.61 mL, 5.14 mmol, 1.2 equiv.) was added dropwise to protect the primary amine. This mixture was then stirred for 30 min at 0 °C and at room temperature for additional 1 h. To the resulting mixture, Boc_2O (7.32 g, 33.6 mmol, 8.0 equiv.) was added in portions. Dry Et_3N (6.4 mL, 46.2 mmol, 11.0 equiv.) was then added and the solution was stirred for 12 h at RT. The reaction mixture was then washed with $NaHCO_3$. The organic layer was separated, washed with water, dried over Na_2SO_4 and evaporated. After purification by column chromatography (SiO_2, gradient MeOH:CH_2Cl_2 1→2:99→98) 320 mg of partially purified compound was isolated.

Partially purified **14** (1.8 g) was dissolved in MeOH (12 mL), NaOH (860 mg, 21.0 mmol) in H_2O (6 mL) was added. The reaction mixture was stirred at RT for 5 h. After this time the solvent was removed under reduced pressure, the residue was dissolved in H_2O, and extracted with CH_2Cl_2 (3 x 50 mL). The combined organic layers were dried over $MgSO_4$ and solvent was removed under reduced pressure. Purification by column chromatography (SiO_2, first MeOH:CH_2Cl_2 1:99, followed by MeOH:CH_2Cl_2:Et_3N 1:99:1) afforded **15** (885 mg, 20.2%) as a white solid. ES-MS: $[M+H]^+$ $C_{53}H_{90}N_7O_{12}^+$ calc. 1016.66 found 1016.66 Mp. 43-45°C.

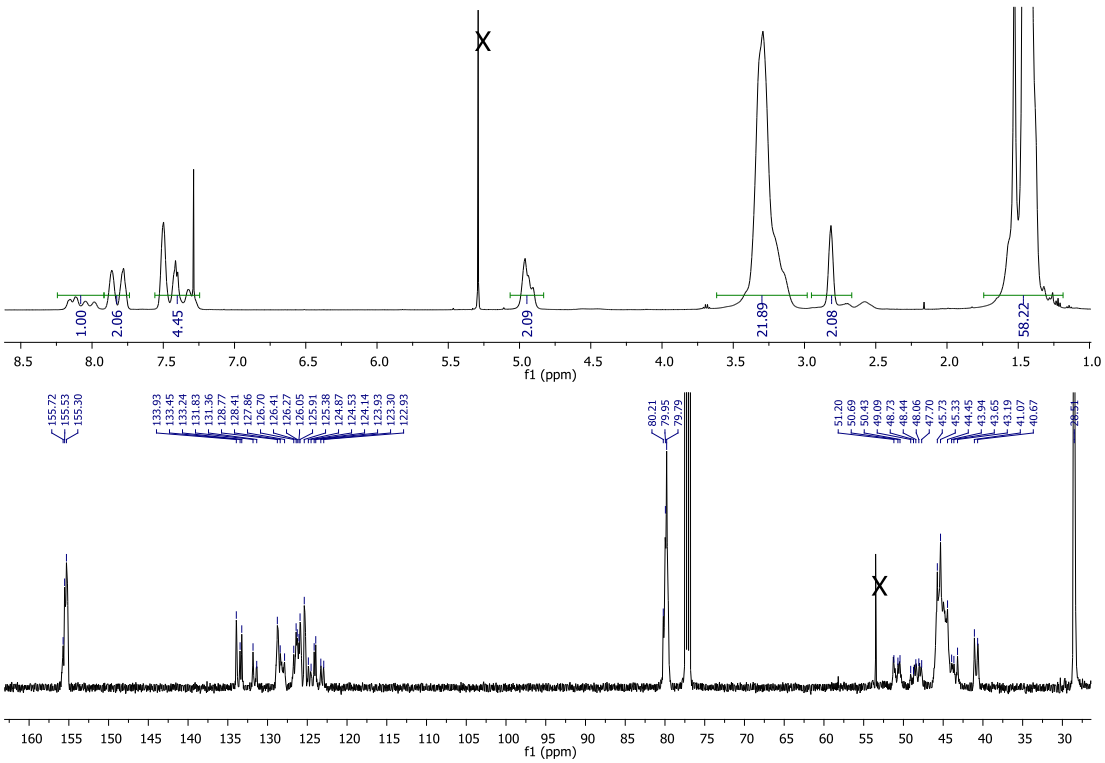

Synthesis of 16

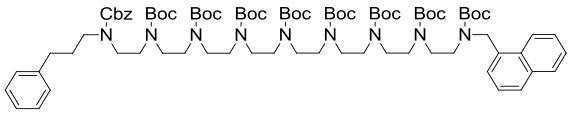

15 (470 mg, 0.46 mmol, 1.0 equiv.) and **11** (250 mg, 0.55 mmol, 1.2 equiv.) were dissolved in dry EtOH (10 mL). The reaction was stirred under N_2 for 16 h at room temperature. $NaBH_4$ (70 mg, 1.8 mmol, 4 equiv.) was then added in portion and reaction was kept stirring under N_2 for another 3 h. After this time H_2O (50 mL) was added to the reaction mixture and the product was extracted with EtOAc (3 x 10 mL). The combined organic layers were washed with water, brine, dried over $MgSO_4$ and the solvent was removed under reduced pressure. After purification by column chromatography (SiO_2, MeOH:CH_2Cl_2 5:95) 226 mg

of product (HRMS: $[M+H]^+$ $C_{79}H_{124}N_9O_{16}^+$ calc 1454.9166, found 1454.9099) which was then dissolved in CH_2Cl_2 (10 mL). Boc_2O (37 mg, 171 µmol, 1.1 equiv.) and dry Et_3N (32 µL, 233 µmol, 1.5 equiv.) was then added and the solution was stirred for 12 h at RT. The reaction mixture was then washed with $NaHCO_3$. The organic layer was separated, washed with water, dried over Na_2SO_4 and evaporated. After purification by column chromatography (SiO_2, MeOH:CH_2Cl_2 3:97) compound **16** (220 mg, 30%) was isolated as a white solid. ESI-MS: $[M+Na]^+$ $C_{84}H_{131}N_9NaO_{18}^+$ calc. 1576.95, found 1576.94. Mp. 106-108 °C.

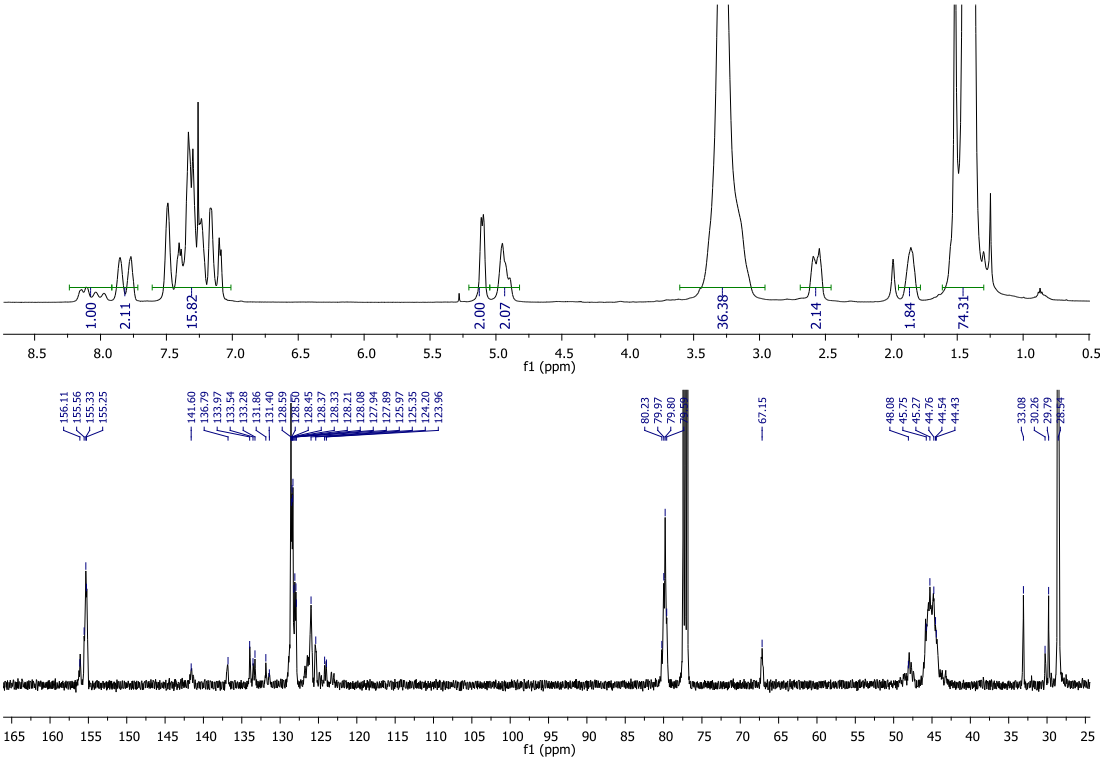

Synthesis of S9

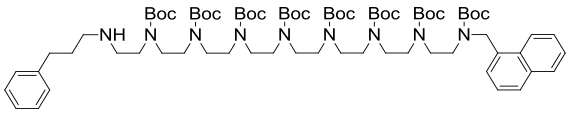

To a solution of **16** (100 mg, 64 µmol) in THF (2 mL) 10%$_{wt}$ of Pd(C) was added in one portion. Air was evacuated from the flask and H_2 gas was bubbled through the solvent for 5 h. Reaction was left stirring overnight in the H_2 atmosphere at RT. After this time, conversion of starting material was complete. Reaction was filtered, solvent was removed under reduced pressure and crude product was purified by column chromatography (SiO_2, MeOH:CH_2Cl_2 5:95) to afford **S9** (46 mg, 50%) as a yellow oil. ESI-MS: $[M+H]^+$ $C_{76}H_{125}N_9O_{16}$ calc. 1420.93 found 1420.92.

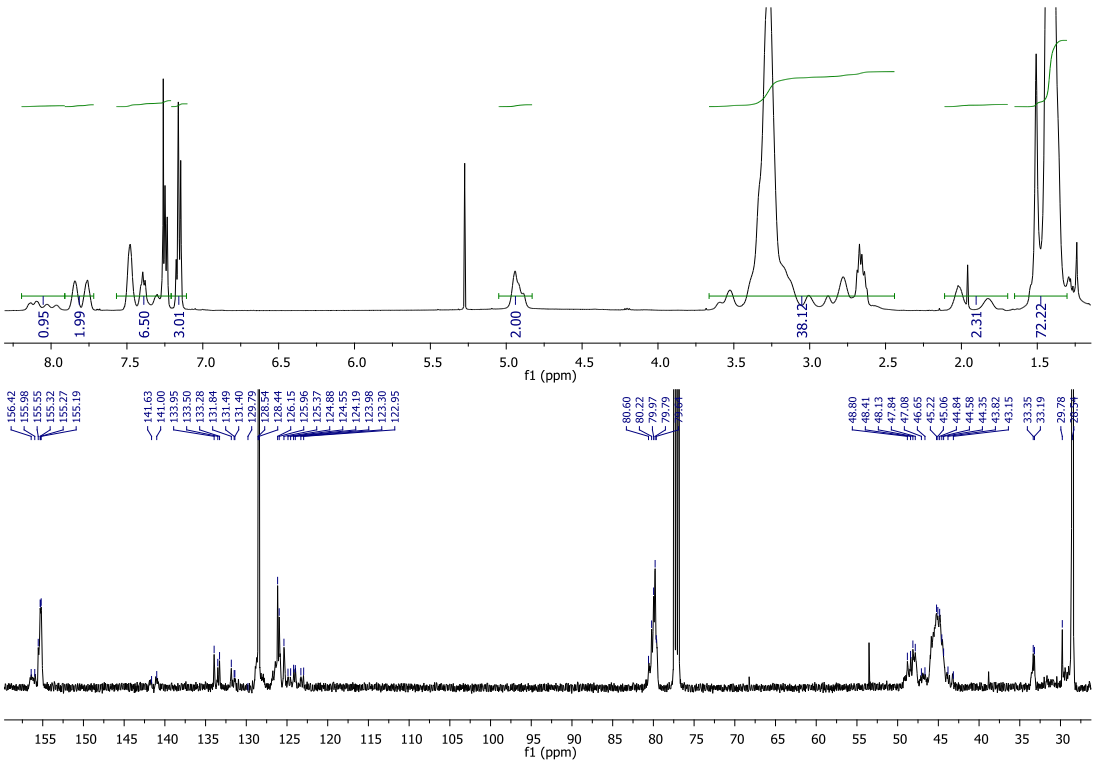

Synthesis of 17

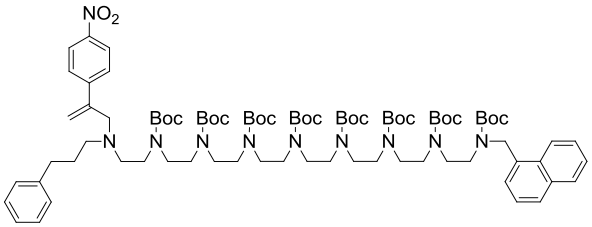

Synthesised according to the procedure described for **S2** and **S7** (based on 46 mg of **S9**), 25 mg (50%) of **17** was isolated as an yellow oil after purification by column chromatography (SiO_2, gradient Petroleum:EtOAc 75→80:25→20). ESI-MS: $[M+Na]^+$calc. $C_{85}H_{132}N_{10}NaO_{18}^+$ calc.: 1603.96 found 1603.95.

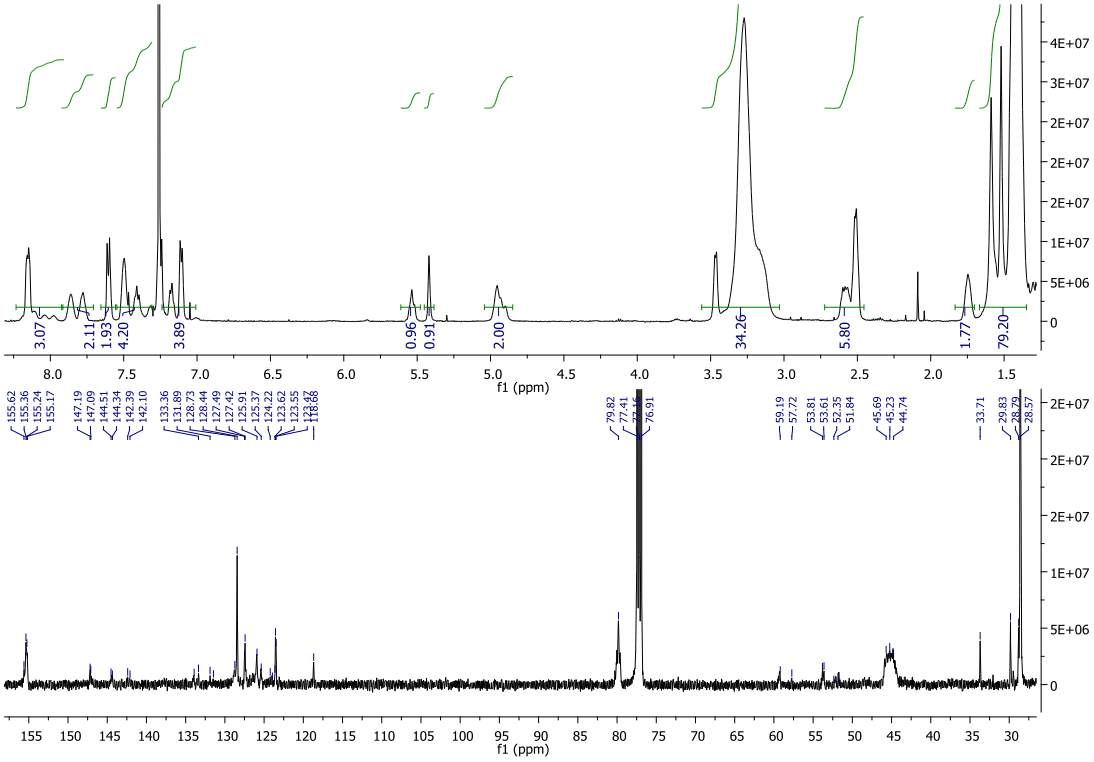

Synthesis of 7-*1*·9[CF_3CO_2H]

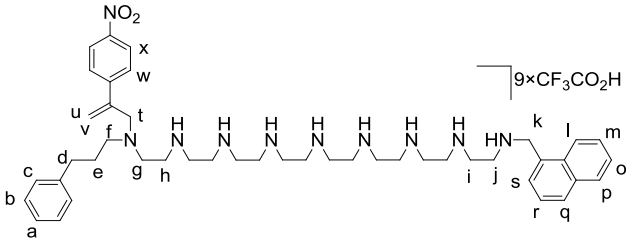

Synthesised according to the procedure described for **5**-*1*·3[CF_3CO_2H] and **6**-*1*·5[CF_3CO_2H] (based on 15 mg of **17**) 17 mg (quant.) of **7**-*1*·9[CF_3CO_2H] was isolated as an yellow oil. ^{1}H NMR (400 MHz, CD_3CN) δ = 8.26 – 8.18 (m, 2H H_x), 8.16 (d, *J* = 8.4 Hz, 1H, H_q), 8.08 – 7.98 (m 2H, $H_{p,l}$), 7.72 (d, *J* = 6.5 Hz, 1H, H_s), 7.70 – 7.60 (m, 4H, $H_{m,r,w}$), 7.57 (dd, *J* = 8.3, 7.1 Hz, 1H, H_o), 7.36 – 7.29 (m, 2H, H_b), 7.29 – 7.23 (m, 1H, H_a), 7.20 – 7.13 (m, 2H, H_c), 5.83 (s, 1H, H_u), 5.77 (s, 1H, H_v), 4.71 (s, 2H, H_k), 4.26 (s, 2H, H_t), 3.59 – 3.53 (m, 2H, H_j), 3.53 – 3.35 (m, 30H, $H_{g,h,i}$+12×CH_2), 3.06 – 2.97 (m, 2H, H_f), 2.52 (t, *J* = 7.5 Hz, 2H, H_d), 1.99 – 1.92 (m, 2H, H_e). ^{13}C NMR (126 MHz, CD_3CN) *δ* = 149.06, 145.03, 141.05, 137.38, 134.84, 132.14, 131.47, 130.17, 129.95, 129.59, 129.35, 129.26, 128.88, 128.21, 127.55 (2C), 127.42, 126.39, 125.02 (2C), 57.78, 53.56, 50.75, 49.86, (45.86 – 45.60)-14C, 43.78, 30.91, 26.25. In addition, 159.78 (q, *J* = 39.4, Hz) and 115.81 (q, *J* = 288.8 Hz) for C-F of countof the eranion are present, HRMS: $[M+H]^+$ $C_{45}H_{69}N_{10}O_2$ calc. 781.5599 found 781.5588.

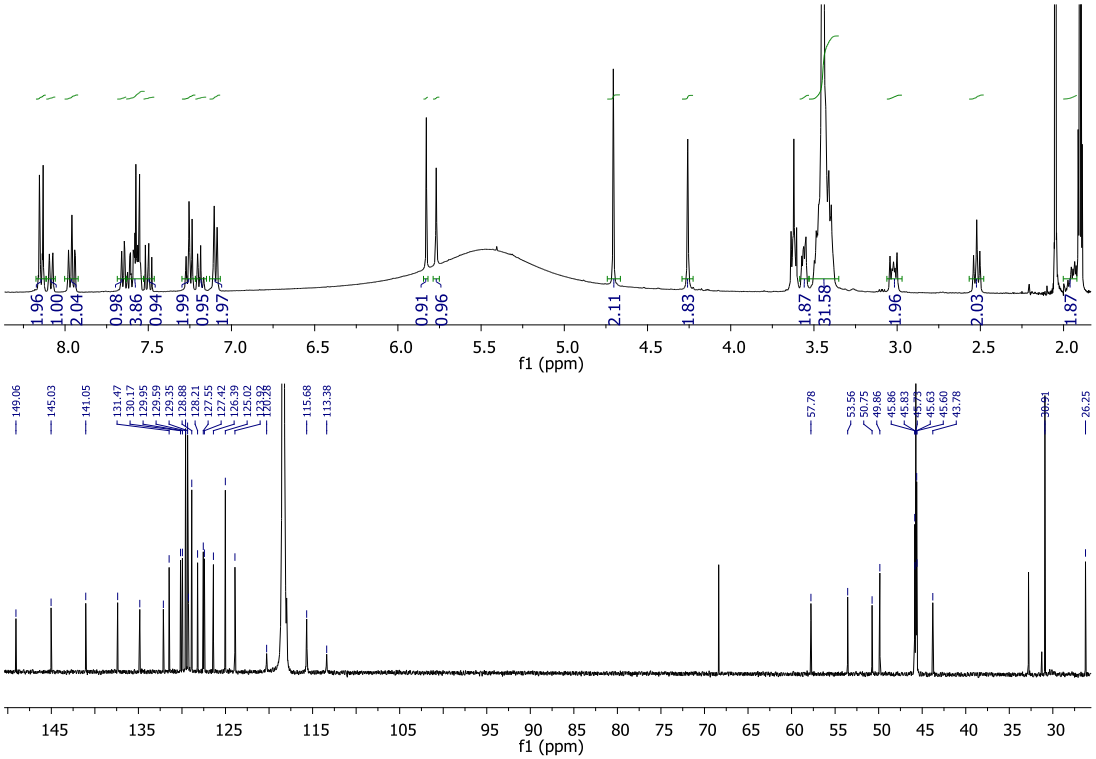
1.96
1.00
2.04
0.98
3.86
0.94
1.99
0.95
1.97
0.91
0.96
2.11
1.83
1.87
31.58
1.96
2.03
1.87
f1 (ppm)
149.06
145.03
141.05
131.47
130.17
129.95
129.59
129.35
128.88
128.21
127.51
127.42
126.39
125.02
115.68
113.38
57.78
53.56
50.75
49.86
45.86
45.83
45.73
45.63
45.60
43.78
30.91
26.25
f1 (ppm)

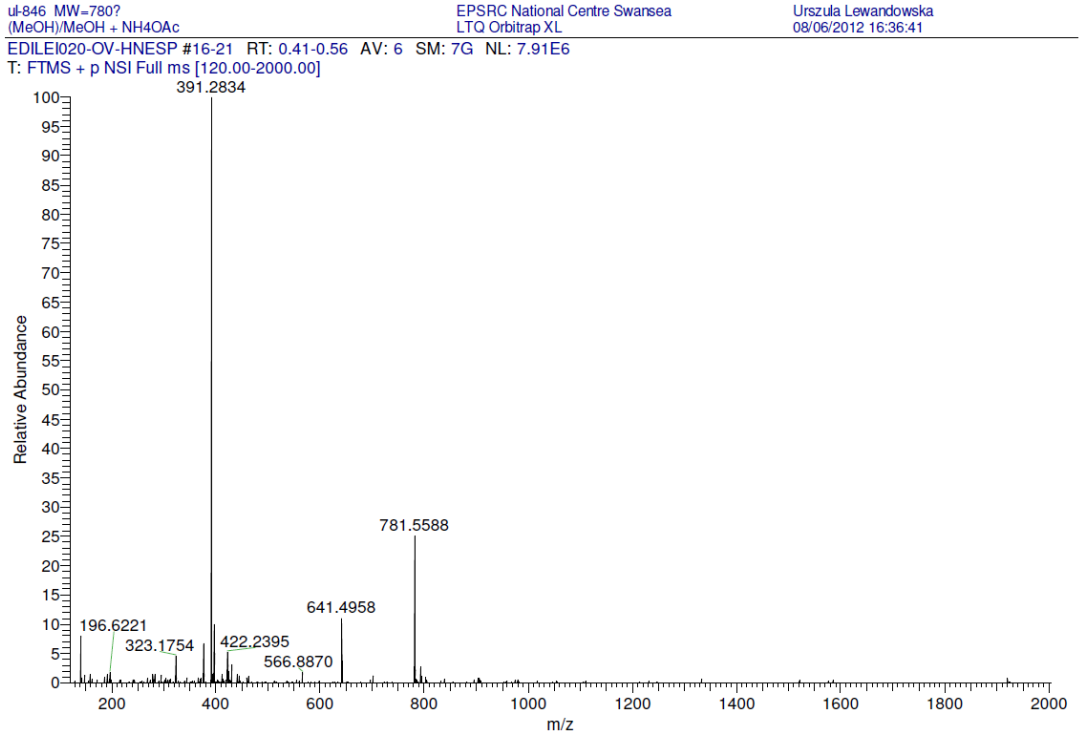
ul-846 MW=780?
(MeOH)/MeOH + NH4OAc
EPSRC National Centre Swansea
LTQ Orbitrap XL
Urszula Lewandowska
08/06/2012 16:36:41
EDILEI020-OV-HNESP #16-21 RT: 0.41-0.56 AV: 6 SM: 7G NL: 7.91E6
T: FTMS + p NSI Full ms [120.00-2000.00]
391.2834
781.5588
641.4958
196.6221
323.1754
422.2395
566.8870
Relative Abundance
m/z

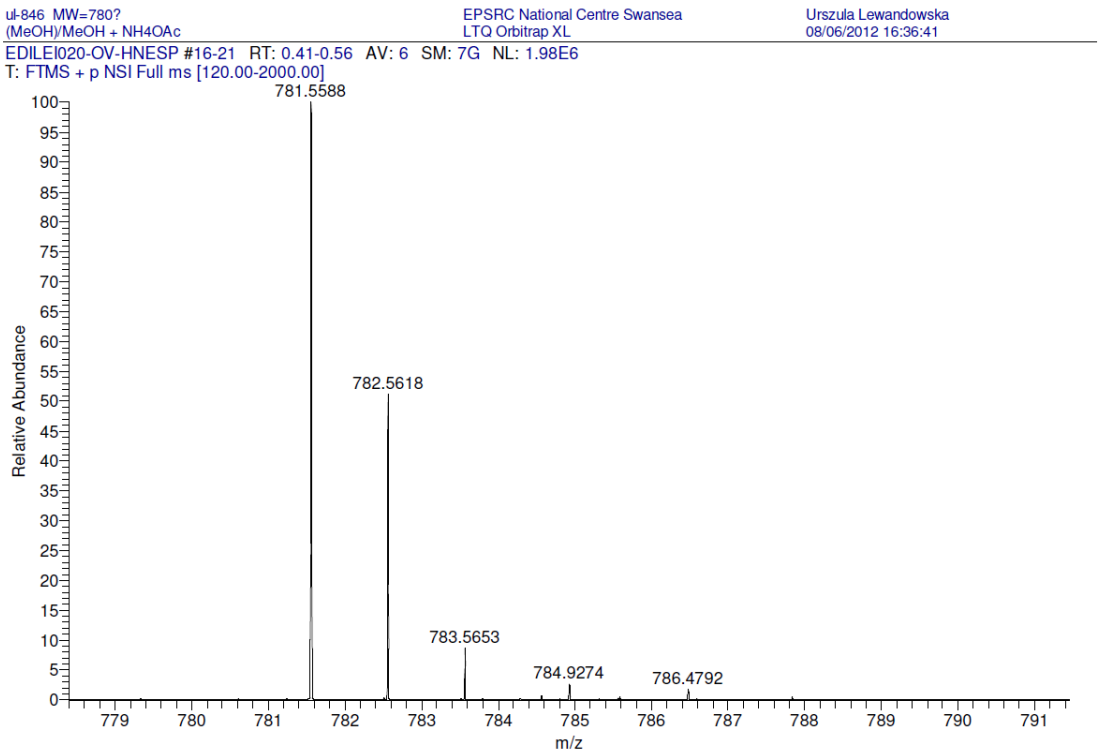

3.6.3.1 An Input File for Fitting of Walking Experiment of Compound 7-*1*·9[CF_3CO_2H] Using SimFit Program.

REACTION (A --> B) CONSTANT (1, 2.3381E-4, 0)
REACTION (B --> A) CONSTANT (2, 1.6680E-4, 0)
REACTION (B --> C) CONSTANT (3, 8.4212E-5, 0)
REACTION (C --> B) CONSTANT (4, 9.8027E-5, 0)

values obtained from fitting of data from the walking of 6-*1* (Figure 3.14)

REACTION (C --> D) CONSTANT (5, 8.4212E-5, 1, 1, 100)
REACTION (D --> C) CONSTANT (6, 9.8027E-5, 2, 1, 100)
REACTION (D --> E) CONSTANT (7, 8.4212E-5, 3, 1, 100)
REACTION (E --> D) CONSTANT (8, 9.8027E-5, 4, 1, 100)
REACTION (E --> F) CONSTANT (9, 8.4212E-5, 5, 1, 100)
REACTION (F --> E) CONSTANT (10, 9.8027E-5, 6, 1, 100)
REACTION (F --> G) CONSTANT (11, 8.4212E-5, 7, 1, 100)
REACTION (G --> F) CONSTANT (12, 9.8027E-5, 8, 1, 100)

variable values

REACTION (G --> H) CONSTANT (13, 1.7614E-4, 0)
REACTION (H --> G) CONSTANT (14, 1.5062E-4, 0)
REACTION (H --> I) CONSTANT (15, 1.1630E-4, 0)
REACTION (I --> H) CONSTANT (16, 3.2390E-5, 0)

values obtained from fitting of data from the walking of 6-*1* (Figure 3.14)

REACTION (COMPILE)

REACTION (SHOW)
CONSTANT (SHOW)
DEFINE (1, A, P, 1) SCALE (3,1)
DEFINE (2, B, P, 2) SCALE (3,1)
DEFINE (3, C, P, 3) SCALE (3,1)
DEFINE (4, D, P, 4) SCALE (3,1)
DEFINE (5, E, P, 5) SCALE (3,1)
DEFINE (6, F, P, 6) SCALE (3,1)
DEFINE (7, G, P, 7) SCALE (3,1)
DEFINE (8, H, P, 8) SCALE (3,1)
DEFINE (9, I, P, 9) SCALE (3,1)

SELECT (A, I)

```
READ (ULA9.txt)

REACTION (DOC)
CONSTANT (DOC)

TIME (SEC)

WIN (0, 648000, 25000, 200, 0, 20e-3, 5e-3, 3e-5)

DIM (8)

ASSIGN (OBS, A = A)
ASSIGN (OBS, B = B)
ASSIGN (OBS, C = C)
ASSIGN (OBS, D = D)
ASSIGN (OBS, E = E)
ASSIGN (OBS, F = F)
ASSIGN (OBS, G = G)
ASSIGN (OBS, H = H)
ASSIGN (OBS, I = I)

ASSIGN (SPEC, A = #20e-3 )
ASSIGN (SPEC, B = #00e-3 )
ASSIGN (SPEC, C = #00e-3 )
ASSIGN (SPEC, D = #00e-3 )
ASSIGN (SPEC, E = #00e-3 )
ASSIGN (SPEC, F = #00e-3 )
ASSIGN (SPEC, G = #00e-3 )
ASSIGN (SPEC, H = #00e-3 )
ASSIGN (SPEC, I = #00e-3 )

CHOOSE (EXP1)

INTEG (STIFF, 1E-9, 1, 0.075, 100, 50)

PLOT (OBS, RES)

* Optimise rate constants using simplex

SIMPLEX (PLOT)
SIMPLEX (PLOT)
SIMPLEX (PLOT)
SIMPLEX (PLOT)
SIMPLEX (PLOT)
SIMPLEX (PLOT)
SIMPLEX (PLOT)
SIMPLEX (PLOT)
SIMPLEX (PLOT)
SIMPLEX (PLOT)

PLOT (OBS, RES)
PLOT (FILE)
```

3.6.3.2 Relative error estimation for ^{1}H NMR integration of 6-*1*.

The error of integration based on equivalent proton signal in the ^{1}H NMR spectrum was estimated at ± 3% level, (absolute error of 0.03 when integral is equal 1). In all discussed experiments, vinyl signal is the diagnostic one, therefore in the calculation of relative uncertainty of integration in compounds **6**-*1* – **6**-*5* the worst case was taken into the account, where the measured signal intensity was underestimated at the same time as the overall integration of the vinyl region was overestimated. So for the outlined entry in Table 3.3:

maximum intergral value for **6**-*2* (*t* = 4 h) = (0.37+0.03)/(1-0.03) = 0.41

minimum integral value for **6**-*2* (*t* = 4 h) = (0.37-0.03)/(1+0.03) = 0.33,

therefore the integral of **6**-*2* (*t* = 4 h) = 0.37 ± 0.04.

By analogy, the relative error was estimated for the ^{1}H NMR integration of **5**-*1*, **5**-*2*, **5**-*3*, **7**-*1* and **7**-*9* in Chapter III as well as for integration of compound **2**, presented in Figure 2.22 in Chapter II.

Table 3.3 Table summarizing relative errors in ^{1}H NMR integration of **6**-*1* – **6**-*5* positional isomers.

t / h	6-*1*	error 6-*1*	6-*2*	error 6-*2*	6-*3*	error 6-*3*	6-*4*	error 6-*4*	6-*5*	error 6-*5*
0	1.00	0.06	-	-	-	-	-	-	-	-
0.25	0.91	0.06	0.09	0.03	-	-	-	-	-	-
1	0.54	0.04	0.40	0.04	0.06	0.03	0.00	-	-	-
2	0.43	0.04	0.43	0.04	0.11	0.03	0.04	0.03	-	-
3	0.37	0.04	0.42	0.04	0.14	0.03	0.07	0.03	-	-
4	0.32	0.04	0.37	0.04	0.15	0.03	0.09	0.03	0.06	0.03
5	0.30	0.04	0.35	0.04	0.16	0.03	0.10	0.03	0.09	0.03
6	0.28	0.04	0.33	0.04	0.16	0.03	0.11	0.03	0.12	0.03
12	0.20	0.03	0.24	0.04	0.14	0.03	0.13	0.03	0.29	0.04
24	0.16	0.03	0.16	0.03	0.12	0.03	0.13	0.03	0.42	0.04
48	0.14	0.03	0.13	0.03	0.14	0.03	0.13	0.03	0.46	0.04

3.6.3.3 Distribution of Positional Isomers of 7-*1* Based on Simple and Biased Random Walk.

Table 3.4 and Table 3.5 summarise the distribution of **7**-*1* – **7**-*9* positional isomers upon iterations of simple and biased random walk, respectively. First ten as well as the last four iterations, leading to the steady distribution are included.

Table 3.4. The theoretical formation or disappearance of isomers based on simple random walk for 7-*1*, where $p = 0.5$ for each forward and backward stepping process (See Figure 3.20).

step number	foothold number								
/iteration	1	2	3	4	5	6	7	8	9
0	100.0	0.0	0.0	0.0	0.0	0.0	0.0	0.0	0.0
1	50.0	50.0	0.0	0.0	0.0	0.0	0.0	0.0	0.0
2	50.0	25.0	25.0	0.0	0.0	0.0	0.0	0.0	0.0
3	37.5	37.5	12.5	12.5	0.0	0.0	0.0	0.0	0.0
4	37.5	25.0	25.0	6.3	6.3	0.0	0.0	0.0	0.0
5	31.3	31.3	15.6	15.6	3.1	3.1	0.0	0.0	0.0
6	31.3	23.4	23.4	9.4	9.4	1.6	1.6	0.0	0.0
7	27.3	27.3	16.4	16.4	5.5	5.5	0.8	0.8	0.0
8	27.3	21.9	21.9	10.9	10.9	3.1	3.1	0.4	0.4
9	24.6	24.6	16.4	16.4	7.0	7.0	1.8	1.8	0.4
10	24.6	20.5	20.5	11.7	11.7	4.4	4.4	1.1	1.1
:	:	:	:	:	:	:	:	:	:
:	:	:	:	:	:	:	:	:	:
100	11.2	11.1	11.1	11.1	11.1	11.1	11.1	11.1	11.1
101	11.2	11.2	11.1	11.1	11.1	11.1	11.1	11.1	11.1
102	11.2	11.1	11.1	11.1	11.1	11.1	11.1	11.1	11.1
103	11.1	11.1	11.1	11.1	11.1	11.1	11.1	11.1	11.1

Table 3.5. The theoretical formation or disappearance of isomers based on biased random walk for **7**-*1*, where $p = 0.5$ for each forward and backward stepping process, except for the final step, where $p_{8\text{-}9} / p_{9\text{-}8} = 3$ (See Figure 3.21).

step number	foothold number								
/iteration	1	2	3	4	5	6	7	8	9
0	100.0	0.0	0.0	0.0	0.0	0.0	0.0	0.0	0.0
1	50.0	50.0	0.0	0.0	0.0	0.0	0.0	0.0	0.0
2	50.0	25.0	25.0	0.0	0.0	0.0	0.0	0.0	0.0
3	37.5	37.5	12.5	12.5	0.0	0.0	0.0	0.0	0.0
4	37.5	25.0	25.0	6.3	6.3	0.0	0.0	0.0	0.0
5	31.3	31.3	15.6	15.6	3.1	3.1	0.0	0.0	0.0
6	31.3	23.4	23.4	9.4	9.4	1.6	1.6	0.0	0.0
7	27.3	27.3	16.4	16.4	5.5	5.5	0.8	0.8	0.0
8	27.3	21.9	21.9	10.9	10.9	3.1	3.1	0.3	0.5
9	24.6	24.6	16.4	16.4	7.0	7.0	1.7	1.6	0.6
10	24.6	20.5	20.5	11.7	11.7	4.4	4.3	0.8	1.4
:	:	:	:	:	:	:	:	:	:
:	:	:	:	:	:	:	:	:	:
136	9.2	9.2	9.1	9.1	9.1	9.1	9.1	9.1	27.1
137	9.2	9.1	9.1	9.1	9.1	9.1	9.1	9.1	27.1
138	9.2	9.1	9.1	9.1	9.1	9.1	9.1	9.1	27.1
139	9.1	9.1	9.1	9.1	9.1	9.1	9.1	9.1	27.1

3.7 References

[1] a) Lippert, A. R.; Kaeobamrung, J.; Bode, J. W. *J. Am. Chem. Soc*. **2006**, *128*, 14738–14739; b) Lippert, A. R.; Keleshian, V. L.; Bode, J. W. *Org. Biomol. Chem*. **2009**, *7*, 1529–1532; c) Lippert, A. R.; Nagawana, A.; Keleshian, V. L.; Bode, J. W. *J. Am. Chem. Soc*. **2010**, *132*, 15790–15799. (d) He, M.; Bode, J. W. *Proc. Nat. Acad. Sci. U. S. A.* **2011**, *108*, 14752–14756; e) Larson, K. K.; He, M.; Teichert, J. F.; Naganawa, A.; Bode, J. W. *Chem. Sci.* **2012**, *3*, 1825–1828.

[2] a) Corbett, P. T.; Leclaire, J.; Vial, L.; West, R.; Wietor, J. L.; Sanders, J. K. M.; Otto, S. *Chem. Rev*. **2006**, *106*, 3652–3711; b) Lehn, J. -M. *Chem. Soc. Rev.* **2007**, *36*, 151–160.

[3] a) von Delius, M.; Geertsema, E. M.; Leigh, D. A. *Nat. Chem.* **2010**, *2*, 96–99; b) von Delius, M.; Geertsema, E. M.; Leigh, D. A.; Tang, D. -T. D. *J. Am. Chem. Soc*. **2010**, *132*, 16134–16145; c) Barrell, M. -J.; Campaña, A. G.; von Delius, M.; Geertsema, E. M.; Leigh, D. A. *Angew. Chem. Int. Ed*. **2011**, 50, 285–290; d) von Delius, M.; Leigh, D. A. *Chem. Soc. Rev*. **2011**, *40*, 3656–3676; e) Belowich, M. E.; Stoddart, J. F. *Chem. Soc. Rev*. **2012**, *41*, 2003–2024; f) Kovaříček, P.; Lehn, J. -M. *J. Am. Chem. Soc*. **2012**, *134*, 9446–9455.

[4] a) Weimann, D. P.; Winkler, H. D. F.; Falenski, J. A.; Koksch, B.; Schalley, C. A. *Nat. Chem.* **2009**, *1*, 573–577; b) Winkler, H. D. F.; Weimann, D. P.; Springer, A.; Schalley, C. A. *Angew. Chem. Int. Ed*. **2009**, *48*, 7246–7250; c) Perl, A.; Gomez-Casado, A.; Thompson, D.; Dam, H. H.; Jonkheijm, P.; Reinhoudt, D. N.; Huskens, J. *Nat. Chem.* **2011**, *3*, 317–322.

[5] Processivity is the tendency of a molecular fragment (for example the walker unit) to remain attached to the track during operation, *i.e.* to migrate along a molecular scaffold without detaching or exchanging with other molecules in the bulk. See ref. (3a–d).

[6] Campaña, A. G.; Carlone, A.; Chen, K.; Dryden, D. T. F.; Leigh, D. A.; Lewandowska, U.; Mullen, K. M. *Angew. Chem. Int. Ed.* **2012**, *51*, 5480–5483.

[7] For an interesting example of isomerization of an internal alkyne into a terminal alkyne using 1,3-diaminopropanide (known as an alkyne zipper reaction), see: a) Brown, C. A.; Yamashita, A. J. Am. Chem. Soc., **1975**, *97*, 891–892. For examples of molecular rearrangements, see: b) Kurti, L.; Czakó, B. in *Strategic applications of named reactions in organic synthesis*, Elsevier, Oxford, **2005**. Successive Cope rearrangements: c) Ryan, J. P.; O'Connor, P. R. *J. Am. Chem. Soc.* **1952**, *74*, 5866–5869.

[8] For an example of reversible Michael addition of thiols, see: a) Shi, B.; Greaney, M. F.; *Chem. Commun*. **2005**, 886–888; b) Shi, B.; Stevenson, R.; Campopiano, D. J.; Greaney, M. F. *J. Am. Chem. Soc.* **2006**, *128*, 8459–8467.

[9] a) Hayden, E. J.; von Kiedrowski, G.; Lehman, N. *Angew. Chem. Int. Ed.* **2008**, *47*, 8424–8428; b) Stahl, I.; von Kiedrowski, G. *J. Am. Chem. Soc.* **2006**, *128*, 14014–14015; c) Schöneborn, H.; Bülle, J.; von Kiedrowski, G. *ChemBioChem* **2001**, *2*, 922–927.

[10] This is in agreement with the previously reported studies on the protonation of polyamine chains bearing an ethylene or naphtalene unit: a) Albelda, M. T.; Aguilar, J.; Alves, S.; Aucejo, R.; Diaz, P.; Lodeiro, C.; Lima, J. C.; Garcia-Espana, E.; Pina, F.; Soriano, C. *Helv. Chim. Acta* **2003**, *86*, 3118–3135; b) Del Piero, S.; Ghezzi, L.; Melchior, A.; Tine, M.R.; Tolazzi, M. *Helv. Chim. Acta* **2005**, *88*, 839–853.

[11] Comparable literature pK_a values of DIPEA (see: Blanchette, M. A.; Choy, W.; Davis, J. T.; Essenfeld, A. P.; Masamune, S.; Roush, W. R.; Sakai. T. *Tetrahedron Lett.* **1984**, *25*, 2183–2186) and structurally related polyamines (see: Greiner, G.; Maier, I. *J. Chem. Soc., Perkin Trans. 2*, **2002**, 1005–1011 and ref. 11 suggest that an excess of $^{i}Pr_2NEt$ is needed to deprotonate all footholds in the track.

[12] Belowich, M. E.; Valente, C.; Smaldone, R. A.; Friedman, D. C.; Thiel, J.; Cronin, L.; Stoddart, J. F. *J. Am. Chem. Soc.* **2012**, *134*, 5243–5261.

[13] Atkins, P. W.; *Physical Chemistry, 6th edition*. Oxford University Press. Oxford, **1998**

[14] Random walks are used throughout sciences, also as a simplified model of Brownian motion. For an example of biased random walk, see: Macnab, R. M.; Koshland, D. E. Jr. *Proc. Natl. Acad. Sci. U. S. A.* **1972**, *69*, 2509–2512. For a DNA mobile junction migration (known as Holliday junction) modelled as an unbiased and biased random walk, see: Bruist, M. F.; Myers, E. *J. Theor. Biol.* **2003**, *220*, 139–156. See also Weiss, G. H. *Aspects and applications of the random walk*, North Holland Press, **1994**.

[15]Smoluchowski, M. *Annalen der Physik* **1906**, *326*, 756–780.

[16] Srinivasachari, S.; Liu, Y.; Zhang, G.; Prevette, L.; Reineke, T. M. *J. Am.Chem. Soc.* **2006**, *128*, 8176–8184.

[17] **NitroMed, Inc. Patent:** *US6297260 B1*, **2001** ;

Appendix

Published Papers

'A Small Molecule that Walks Non-Directionally Along a Track Without External Intervention', Campaña, A. G.; Carlone, A.; Chen, K.; Dryden, D. T. F.; Leigh, D. A.; Lewandowska, U.; Mullen, K. M. *Angew. Chem. Int. Ed.* **2012**, *51*, 5480–5483.

'One Dimensional Random Walk of a Synthetic Small Molecule Towards a Thermodynamic Sink', Campaña, A. G.; Leigh, D. A.; Lewandowska, U., *J. Am. Chem. Soc., published online 14 May 2013, DOI: 10.1021/ja402382n*

Molecular Walkers

DOI: 10.1002/anie.201200822

A Small Molecule that Walks Non-Directionally Along a Track Without External Intervention**

Araceli G. Campaña, Armando Carlone, Kai Chen, David T. F. Dryden, David A. Leigh, Urszula Lewandowska, and Kathleen M. Mullen*

Kinesin, dynein, and some myosin motor proteins transport cargoes within the cell by "walking" along polymeric filaments, that is carrying out successive, repetitive, mostly directional changes of their point of contact with the molecular track without completely detaching from it.[1] These extraordinary biomolecules are inspiring scientists to mimic aspects of their dynamics to create artificial molecular transport systems.[2,3] Recently, the first small molecules that are able to walk down short molecular tracks were described.[2] However, external intervention (the addition of chemical reagents and/or irradiation with light) are required to mediate each step taken by the walker units in the non-DNA systems reported to date. Although migrations of submolecular fragments occur in many different types of chemical reaction,[4] few systems appear to offer the potential for multiple successive and cumulative transport necessary for developing small-molecule walkers.[5] An interesting exception are the so-called equilibrium transfer alkylating cross-linking (ETAC) reagents introduced in the 1970s by Lawton and co-workers for the dynamic cross-linking of biomolecules.[6,7] These reagents reversibly form covalent bonds between pairs of accessible nucleophilic sites on proteins through a series of inter- and intramolecular Michael and retro-Michael reactions until the most thermodynamically stable crosslink is located (Scheme 1 a).[6a] We wondered whether it would be possible to apply a similar concept, focusing instead on chemistry where the cross-linked products are less stable than those attached by a single covalent bond, to make synthetic small molecules that migrate with a high degree of processivity[8] along a linear molecular track.

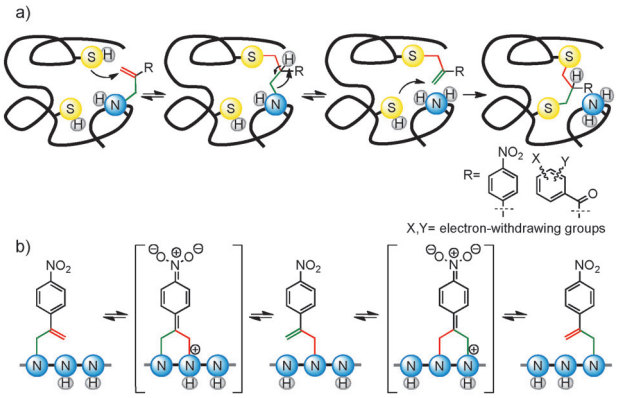

Scheme 1. a) The migration of an ETAC[6] reagent between nucleophilic sites of a protein by Michael/retro-Michael reactions towards the most thermodynamically stable cross-linked product. b) Processive (intramolecular) migration of α-methylene-4-nitrostyrene along a polyamine track. Michael addition of a track amine group to the olefin of the "two-legged walker" results in a bridged intermediate (both "feet" attached to the track, shown in square brackets) that can subsequently undergo a retro-Michael reaction to either side, unmasking the double bond and leaving the walker attached to the track through a single covalent bond.

Herein we describe the attachment of α-methylene-4-nitrostyrene to oligoethylenimine tracks and the dynamics of its subsequent migration from amine group to amine group without fully detaching by a sequence of intramolecular Michael and retro-Michael reactions. In this way the α-methylene-4-nitrostyrene units move towards the most thermodynamically favored distribution of walkers on oligoamine tracks (Scheme 1 b).[9]

A model walker-track conjugate, **1**, was synthesized in which α-methylene-4-nitrostyrene was attached to an outer amine group of a triamine track and then allowed to exchange between the secondary amine footholds (Scheme 2 a; see the Supporting Information for experimental procedures and characterization data). The reaction was followed by ^{1}H NMR spectroscopy through the different chemical shift of vinyl protons ($H_{c/c'}$ and $H_{d/d'}$) of isomers **1** and **2** (Figure 1).

The kinetics of the amine-to-amine migration of the α-methylene-4-nitrostyrene unit ("walking") is highly solvent-dependent. Starting from pristine **1** (5 mM), no formation of **2** was observed in $CDCl_3$ or CD_2Cl_2 over 15 h at room temperature and the reaction only proceeded slowly in CD_3OD (< 10% conversion over 15 h) or CD_3CN (< 25% conversion over 15 h). However, the interconversion of **1** with **2** reached a close-to-1:1 steady-state ratio of **1**:**2** over 15 h in [D_7]DMF or 4.5 h in [D_6]DMSO (298 K, 5 mM). Increasing

[*] Dr. A. G. Campaña, Dr. A. Carlone, Dr. K. Chen, Dr. D. T. F. Dryden, Prof. D. A. Leigh, U. Lewandowska, Dr. K. M. Mullen[+]
School of Chemistry, University of Edinburgh
The King's Buildings, West Mains Road, Edinburgh EH9 3JJ (UK)
Prof. D. A. Leigh
School of Chemistry, University of Manchester
Oxford Road, Manchester M13 9PL (UK)
E-mail: david.leigh@manchester.ac.uk
Homepage: http://www.catenane.net
[+] Current address: Science and Engineering Faculty, Queensland University of Technology
GPO Box 2434, Brisbane, 4001 (Australia)

[**] We thank Prof. Richard Lawton (University of Michigan) for many useful discussions and the EPSRC National Mass Spectrometry Service Centre (Swansea (UK)) for high resolution mass spectrometry. This research was funded by the ERC. A.G.C. thanks the Fundación Ramón Areces (Spain) for a postdoctoral fellowship.
Supporting information for this article is available on the WWW under http://dx.doi.org/10.1002/anie.201200822.

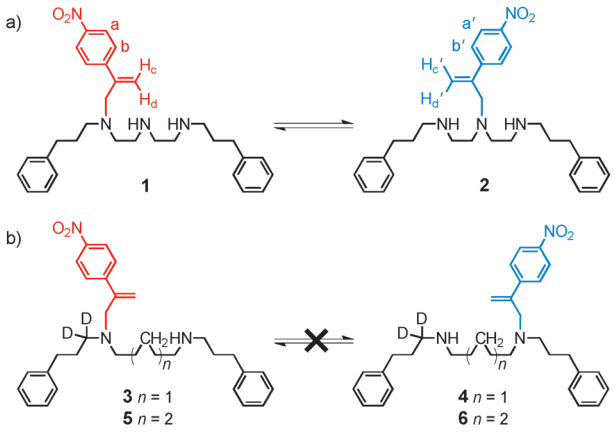

Scheme 2. Transfer of α-methylene-4-nitrostyrene between secondary amine groups through a) 1,4-*N*,*N*-migration and b) possible 1,7- or 1,10-*N*,*N*-migration. The experimental results show that under conditions ([D$_6$]DMSO, 298 K, 5 mM) where $t_{1/2} = 1.5$ h for (a), the double (1,7-) and triple (1,10-) "over-stepping" shown in (b) is not detectable over 48 h, suggesting that they would be rare events during walker migration along a poly(ethylenimine) track.

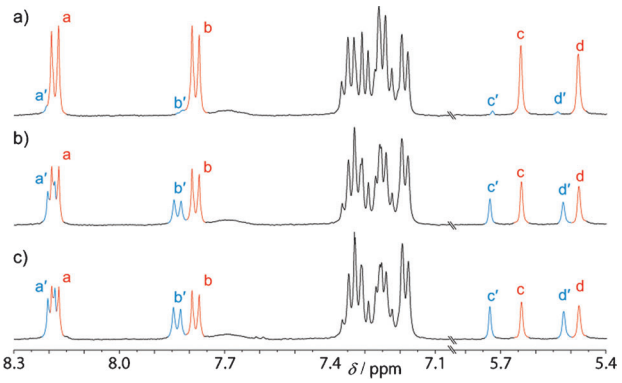

Figure 1. Partial ^{1}H NMR spectra (400 MHz, [D$_6$]DMSO, 5 mM, 298 K) of exchange between **1** and **2** at: a) $t = 5$ min, **1**:**2** ratio 1:0.06; b) $t = 2$ h, **1**:**2** ratio 1:0.6; c) $t = 15$ h, **1**:**2** ratio 1:0.9. The lettering corresponds to the proton labeling shown in Scheme 2.

the concentration of the starting material tenfold (to 50 mM **1**) gave no change in the rate constant of the reaction or the **1**:**2** isomer ratio. Partial ^{1}H NMR spectra of the exchange between **1** and **2** in [D$_6$]DMSO (298 K, 5 mM) are shown in Figure 1. A half-life $t_{1/2} = 1.5$ h was determined for the stepping process (see the Supporting Information).[10]

To determine the processivity of the migration reaction (in other words, the degree to which the reaction is intramolecular or intermolecular),[8] the exchange between **1** and **2** (Scheme 2a) was performed in the presence of a different walker-free track and the intermolecular migration monitored by mass spectrometry (see the Supporting Information for details). After 3 days, less than 6% of the walkers had detached from the original track or transferred to the different track. Accordingly, under these conditions, each α-methylene-4-nitrostyrene unit takes an average of 530 "steps" between amine groups before completely detaching from its track, which is several times the processivity of most wild-type kinesin motor proteins (typically mean step number 75–175).[11]

To determine how likely the walker is to take a double (1,7-) or triple (1,10-) step while migrating along the track, we prepared diamine tracks with five (**3**) or eight (**5**) methylene groups between the secondary amine sites (Scheme 2b).[12] The initial site of attachment of the α-methylene-4-nitrostyrene was deuterium-labeled to distinguish the walker position (that is, **3** or **4**; **5** or **6**) by ^{1}H NMR spectroscopy. Under conditions where single (1,4-) stepping occurs for **1**/**2** with a $t_{1/2} = 1.5$ h, no reaction was observed for either **3** or **5** over 48 h (see the Supporting Information). This suggests that on a longer polyamine track the walker should migrate predominantly through exchange between adjacent amine footholds. The large number of steps that the α-methylene-4-nitrostyrene walker takes on average before competing reactions occur (that is, over-stepping, completely detaching, or exchange with other tracks) is presumably a consequence of the relatively low-energy seven-membered-ring transition state for 1,4-N,N-migration.

Having established that an α-methylene-4-nitrostyrene walker can exchange between the amino groups of a di- or triamine track in a stepwise fashion with a high degree of processivity, we sought to demonstrate that the walker could migrate along a longer track through this mechanism and perform an observable task. A five-foothold walker–track conjugate **7**, incorporating an anthracene group situated at the far end of the pentaethylenimine track from the initial site of attachment of the walker, was prepared as shown in Scheme 3. Pentamine **8** was desymmetrized by reductive amination with 3-phenylpropionaldehyde and subsequent reaction with 9-anthraldehyde to give **9**. The α-methylene-4-nitrostyrene walker unit (**10**) was introduced exclusively to

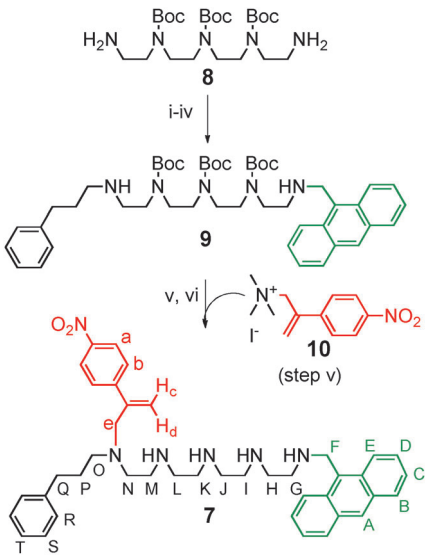

Scheme 3. Synthesis of five-foothold walker–track conjugate **7**. i) 3-phenylpropionaldehyde, EtOH, RT, 72 h; ii) $NaBH_4$, RT, 24 h, 60% (two steps); iii) 9-anthraldehyde, EtOH, RT, 72 h; iv) $NaBH_4$, RT, 24 h, 55% (two steps); v) MeOH, *N*,*N*-diisopropylethylamine (DIPEA), 50°C, 72 h, 30%; vi) CH_2Cl_2, CF_3CO_2H, 5 h, quantitative. See the Supporting Information for details.

the amine furthest from the anthracene group. Subsequent deprotection gave compound **7** in which the walker was free to migrate along the five-foothold track from its original position.

Model compounds showed that the distance between the α-methylene-4-nitrostyrene unit and the anthrylmethyl moiety in the track influences its fluorescence.[13] Fluorescence lifetime measurements showed that static quenching by the nitrostyrene group quenches the anthracene fluorescence (see the Supporting Information). Dilution experiments confirmed that the quenching observed was from an intramolecular mechanism.

Molecular walker–track conjugate **7** was submitted to walking conditions (DMSO, 7.14×10^{-5} M, 298 K) and its fluorescence emission spectrum recorded periodically.[14] The fluorescence intensity diminished by 54% over 6.5 h, after which time the fluorescence intensity became almost invariant (Figure 2a).

The walker migration in **7** was also monitored by ^{1}H NMR spectroscopy, albeit under more concentrated conditions to give a suitable signal-to-noise ratio ([D_6]DMSO, 20 mM, 298 K, Figure 2b). The reaction was monitored every 0.5 h and, after 3 h, signals indicating that a proportion of the walker units had reached the fifth foothold of the track were observed (Figure 2b). After 6.5 h, no further changes were observed in the ^{1}H NMR spectrum until signals attributed to degradation of the anthracene moiety started to appear.[15] Accordingly, both ^{1}H NMR and fluorescence measurements (Figure 2) indicate that the walking of the α-methylene-4-nitrostyrene unit proceeds back and forth along the pentaethylenimine track, producing a steady distribution of walkers over the five-foothold track after 6.5 h.

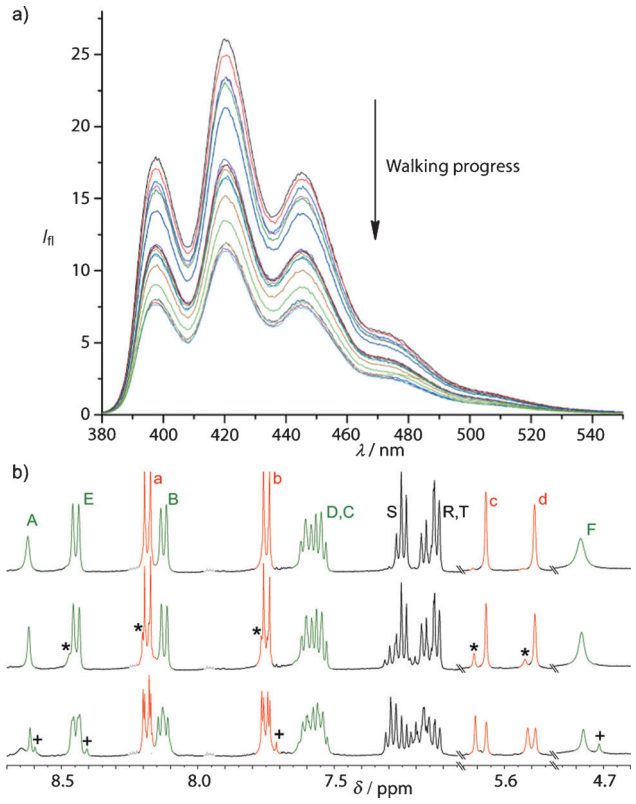

Figure 2. a) Fluorescence quenching ($\lambda_{exc}=366$ nm, $\lambda_{em}=413$ nm) in **7** (DMSO + 0.25% CF_3CO_2H, 1.78×10^{-5} M) as a result of migration of α-methylene-4-nitrostyrene along the oligoamine track. b) Partial ^{1}H NMR spectra (400 MHz, [D_6]DMSO, 20 mM, 298 K) of the reaction mixture at: $t=5$ min (top); $t=1$ h (middle); $t=6.5$ h (bottom). ⋆ Walkers attached to the inner three amine footholds, + walkers attached to the anthrylmethylamine group. The lettering and coloring corresponds to the proton labeling shown in Scheme 3.

In conclusion, we have described a system in which a small synthetic molecular walker migrates along oligoamine tracks without external intervention, moving towards an equilibrium distribution of walkers over all possible positions on the track. In terms of synthetic molecular machine properties, this walker–track system is reminiscent of a rotaxane-based molecular shuttle with degenerate stations:[16] The walker–track system uses a transferable covalent linkage between the α-methylene-4-nitrostyrene and the oligoethylenimine to ensure processivity and determine the preferred positions of the substrate on the track; in a rotaxane-based molecular shuttle a mechanical linkage confers the former property and attractive non-covalent interactions between a macrocycle and specific sites on the thread can be used to achieve the latter.

The small-molecule walking process is processive and takes place predominantly in a stepwise fashion by a Michael–retro-Michael addition mechanism between adjacent amines. The position of the walker can be precisely determined on short tracks by ^{1}H NMR spectroscopy, and on longer tracks the progress of walker migration can be inferred by performance of a simple task: quenching of the fluorescence of an anthracene group at one end of the track by the walker. Work towards developing walkers that consume a fuel to move directionally, and which carry cargoes along extended and branched tracks, is currently ongoing in our laboratory.

Received: January 31, 2012
Published online: April 5, 2012

Keywords: anthracene · fluorescence quenching · Michael addition · molecular devices · molecular walkers

[1] a) *Molecular Motors* (Ed.: M. Schliwa), Wiley-VCH, Weinheim, **2003**; b) R. D. Vale, *Cell* **2003**, *112*, 467–480.
[2] a) M. von Delius, E. M. Geertsema, D. A. Leigh, *Nat. Chem.* **2010**, *2*, 96–101; b) S. Otto, *Nat. Chem.* **2010**, *2*, 75–76; c) M. von Delius, E. M. Geertsema, D. A. Leigh, D.-T. D. Tang, *J. Am. Chem. Soc.* **2010**, *132*, 16134–16145; d) M. J. Barrell, A. G. Campaña, M. von Delius, E. M. Geertsema, D. A. Leigh, *Angew. Chem.* **2011**, *123*, 299–304; *Angew. Chem. Int. Ed.* **2011**, *50*, 285–290.
[3] a) P. Yin, H. Yan, X. G. Daniell, A. J. Turberfield, J. H. Reif, *Angew. Chem.* **2004**, *116*, 5014–5019; *Angew. Chem. Int. Ed.* **2004**, *43*, 4906–4911; b) J. Bath, S. J. Green, A. J. Turberfield, *Angew. Chem.* **2005**, *117*, 4432–4435; *Angew. Chem. Int. Ed.* **2005**, *44*, 4358–4361; c) Y. Tian, Y. He, Y. Chen, P. Yin, C. Mao, *Angew. Chem.* **2005**, *117*, 4429–4432; *Angew. Chem. Int. Ed.* **2005**, *44*, 4355–4358; d) P. Yin, H. M. T. Choi, C. R. Calvert, N. A. Pierce, *Nature* **2008**, *451*, 318–322; e) S. J. Green, J. Bath, A. J. Turberfield, *Phys. Rev. Lett.* **2008**, *101*, 238101; f) T.

Omabegho, R. Sha, N. C. Seeman, *Science* **2009**, *324*, 67 – 71; g) K. Lund, et al., *Nature* **2010**, *465*, 206 – 210; h) H. Gu, S. J. Xiao, N. C. Seeman, *Nature* **2010**, *465*, 202 – 205; i) Y. He, D. R. Liu, *Nat. Nanotechnol.* **2010**, *5*, 778 – 782; j) S. F. J. Wickham, M. Endo, Y. Katsuda, K. Hidaka, J. Bath, H. Sugiyama, A. J. Turberfield, *Nat. Nanotechnol.* **2011**, *6*, 166 – 169; k) R. A. Muscat, J. Bath, A. J. Turberfield, *Nano Lett.* **2011**, *11*, 982 – 987.

[4] For examples of molecular rearrangements, see: a) L. Kurti, B. Czakó in *Strategic Applications of Named Reactions in Organic Synthesis*, Elsevier, Oxford, **2005**; successive Cope rearrangements: b) J. P. Ryan, P. R. O'Connor, *J. Am. Chem. Soc.* **1952**, *74*, 5866 – 5869; base-induced interconversion of bullvalone isomers: c) A. R. Lippert, J. Kaeobamrung, J. W. Bode, *J. Am. Chem. Soc.* **2006**, *128*, 14738 – 14739; d) A. R. Lippert, V. L. Keleshian, J. W. Bode, *Org. Biomol. Chem.* **2009**, *7*, 1529 – 1532; e) A. R. Lippert, A. Nagawana, V. L. Keleshian, J. W. Bode, *J. Am. Chem. Soc.* **2010**, *132*, 15790 – 15799; f) M. He, J. W. Bode, *Proc. Natl. Acad. Sci. USA* **2011**, *108*, 14752 – 14756; processive crown ether migration along oligoamine scaffolds: g) D. P. Weimann, H. D. F. Winkler, J. A. Falenski, B. Koksch, C. A. Schalley, *Nat. Chem.* **2009**, *1*, 573 – 577; h) H. D. F. Winkler, D. P. Weimann, A. Springer, C. A. Schalley, *Angew. Chem.* **2009**, *121*, 7382 – 7386; *Angew. Chem. Int. Ed.* **2009**, *48*, 7246 – 7250.

[5] M. von Delius, D. A. Leigh, *Chem. Soc. Rev.* **2011**, *40*, 3656 – 3676.

[6] a) S. Mitra, R. G. Lawton, *J. Am. Chem. Soc.* **1979**, *101*, 3097 – 3110; b) S. J. Brocchini, M. Eberle, R. G. Lawton, *J. Am. Chem. Soc.* **1988**, *110*, 5211 – 5212; c) F. A. Liberatore, R. D. Comeau, J. M. McKearin, D. A. Pearson, B. Q. Belonga, S. J. Brocchini, J. Kath, T. Phillips, K. Oswell, R. G. Lawton, *Bioconjugate Chem.* **1990**, *1*, 36 – 50; d) R. B. del Rosario, S. J. Brocchini, R. G. Lawton, R. L. Wahl, R. Smith, *Bioconjugate Chem.* **1990**, *1*, 51 – 59; e) R. B. del Rosario, L. A. Baron, R. G. Lawton R. L. Wahl, *Nucl. Med. Biol.* **1992**, *19*, 417 – 421.

[7] Recently, structurally related three-carbon bridges were used as disulfide-specific intercalators in proteins: a) S. Balan, J. Choi, A. Godwin, I. Teo, C. M. Laborde, S. Heidelberger, M. Zloh, S. Shaunak, S. Brocchini, *Bioconjugate Chem.* **2007**, *18*, 61 – 76 and peptides: b) A. Pfisterer, K. Eisele, X. Chen, M. Wagner, K. Müllen, T. Weil, *Chem. Eur. J.* **2011**, *17*, 9697 – 9707. Pfisterer et al. provide ^{1}H NMR evidence for the three-carbon-bridge formed through the addition – elimination mechanism originally proposed by Lawton et al.; see Ref. [6a].

[8] Processivity is the tendency of the molecular fragment (that is, the walker) to remain attached to the track during operation; in other words, to migrate along a molecular scaffold without detaching or exchanging with other molecules in the bulk. See Ref. [5].

[9] The positional isomers of the walkers on the track are effectively the components of a dynamic combinatorial library: a) P. T. Corbett, J. Leclaire, L. Vial, K. R. West, J.-L. Wietor, J. K. M. Sanders, S. Otto, *Chem. Rev.* **2006**, *106*, 3652 – 3711; their interconversion is a type of constitutional dynamic chemistry: b) J.-M. Lehn, *Chem. Soc. Rev.* **2007**, *36*, 151 – 160.

[10] As $t_{1/2} = 1.5$ h for the amine-exchange process, the average number of steps taken in 3 days is about 48.

[11] a) R. D. Vale, T. Funatsu, D. W. Pierce, L. Romberg, Y. Harada, T. Yanagida, *Nature* **1996**, *380*, 451 – 453; b) R. B. Case, D. W. Pierce, N. Hom-Booher, C. L. Hart, R. D. Vale, *Cell* **1997**, *90*, 959 – 966.

[12] Although changing the spacer varies the conformation of the molecule, the distance between the outer footholds is similar and the tracks are flexible.

[13] For structurally related fluorophore – spacer – receptor systems, see: B. Bag, P. K. Bharadwaj, *J. Phys. Chem. B* **2005**, *109*, 4377 – 4390.

[14] The fluorescence of anthrylmethylamines is quenched by intramolecular photoinduced electron transfer (PET) from the nitrogen lone pair to the anthracene moiety: a) S. Alves, F. Pina, M. T. Albelda, E. G. España, *Eur. J. Inorg. Chem.* **2001**, 405 – 412; b) C. Soriano, S. V. Luis, G. Greiner, I. Maier, *J. Chem. Soc. Perkin Trans. 2* **2002**, 1005 – 1011; c) A. J. Bradbury, S. F. Lincoln, K. P. Wainwright, *New J. Chem.* **2008**, *32*, 1500 – 1508; d) S. E. Plush, S. F. Lincoln, K. P. Wainwright, *Inorg. Chim. Acta* **2009**, *362*, 3097 – 3103; for this reason it was necessary to protonate samples before recording emission spectra to avoid folding of the molecule and prevent intramolecular PET from occurring: e) G. Nishimura, Y. Shiraishi, T. Hirai, *Chem. Commun.* **2005**, 5313 – 5315; f) Y. Shiraishi, Y. Tokitoh, G. Nishimura, T. Hirai, *Org. Lett.* **2005**, *7*, 2611 – 2614. Experimental procedure: Compound **7** was dissolved in DMSO (spectrophotometric grade) at 7.14×10^{-5} M. Periodically, an aliquot (1.00 mL) was quenched with CF_3CO_2H (10.0 μL), diluted to 1.78×10^{-5} M, and the fluorescence spectrum recorded ($\lambda_{ex} =$ 366 nm).

[15] A small amount (< 5 %) of additional signals attributed to decomposition of **7** began to be apparent in the ^{1}H NMR spectrum after 7.5 h.

[16] E. R. Kay, D. A. Leigh, F. Zerbetto, *Angew. Chem.* **2007**, *119*, 72 – 196; *Angew. Chem. Int. Ed.* **2007**, *46*, 72 – 191.

A Journal of the Gesellschaft Deutscher Chemiker

Angewandte Chemie

International Edition

GDCh

www.angewandte.org

2012–51/22

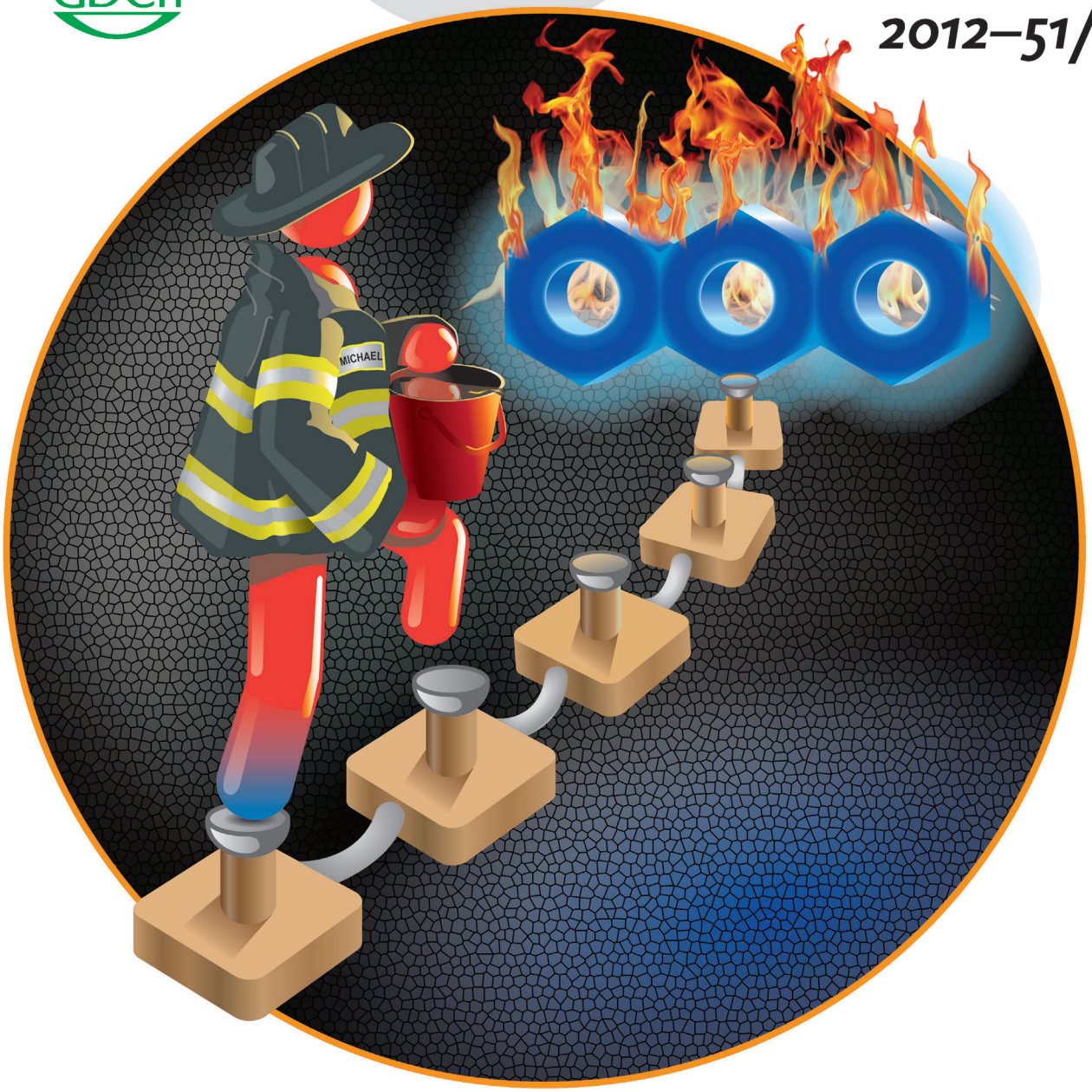

Walking along a track ...

… is no problem for a small molecule, as described by D. A. Leigh et al. in their Communication on page 5480 ff. The synthetic small molecule walks through successive Michael/retro-Michael reactions and ultimately performs a task, namely quenching the fluorescence of an anthracene group at one end of the track.

WILEY-VCH

Article

One Dimensional Random Walk of a Synthetic Small Molecule Towards a Thermodynamic Sink

Araceli G. Campaña, David A. Leigh, and Urszula Lewandowska

J. Am. Chem. Soc., **Just Accepted Manuscript** • DOI: 10.1021/ja402382n • Publication Date (Web): 14 May 2013

One Dimensional Random Walk of a Synthetic Small Molecule Towards a Thermodynamic Sink

Araceli G. Campaña†, David A. Leigh*†‡ and Urszula Lewandowska‡

† School of Chemistry, University of Edinburgh, The King's Buildings, West Mains Road, Edinburgh EH9 3JJ, United Kingdom

‡ School of Chemistry, University of Manchester, Oxford Road, Manchester M13 9PL, United Kingdom

molecular machines, molecular walkers, dynamic covalent chemistry, Michael addition, one dimensional random walk

Supporting Information Placeholder

ABSTRACT: We report on the spontaneous intramolecular migration of α-methylene-4-nitrostyrene from amine group to amine group along oligoethyleneimine tracks up to eight repeat units in length (number of amine footholds, *n*, = 3, 5, 9). Each track consists of *n*-1 aliphatic secondary amine footholds plus a naphthylmethylamine group foothold situated at one end of the track. Under basic conditions the α-methylene-4-nitrostyrene unit undergoes a series of reversible intramolecular Michael-retro-Michael reactions between adjacent amine groups that move it up and down the track. For *n* = 3 and 5 it is possible to monitor the population of every positional isomer on the track by ^{1}H NMR spectroscopy. On the longest track (*n* = 9) the fraction of walkers on each end-foothold can be quantified with respect to those on the inner footholds. In all cases the naphthylmethylamine foothold acts as a thermodynamic sink with the steady-state distribution significantly biased in favor of the walker at that site. The dynamics of the walker migration is well described by the random walk of a Brownian particle in one dimension.

INTRODUCTION

Various motor proteins from the myosin, dynein and kinesin superfamilies move along filaments and microtubules in the cell, transporting cargos such as membranous organelles, protein complexes and messenger RNA.[1] These remarkable biological molecular machines are inspiring the invention of artificial systems that may one day be able to migrate along polymer tracks and perform similarly useful tasks.[2] In the last few years small molecules that are able to 'walk' down short molecular tracks have been described.[3,4] However, many of these systems require intervention in the form of the sequential addition of reagents (and in some cases irradiation with light) for the 'walker' to take each 'step'. Our group[4a] and that of Lehn[4b] recently reported conceptually related model compounds in which a molecular fragment can be transferred intramolecularly between adjacent amine groups on a short track without the need for the sequential addition of reagents or other forms of intervention.[4] Both systems involve dynamic covalent chemistry[5] of nitrogen-containing functional groups: the Lehn approach is based upon transimination reactions (the reversible formation of C=N bonds)[6]; ours utilizes the reversible Michael addition of secondary amines to an α-methylene-4-nitrostyrene unit, chemistry based on the equilibrium transfer alkylating cross-linking (ETAC) reagents introduced by Lawton in the 1970s for the cross-linking of proteins under thermodynamic control.[7]

The preliminary publications from both groups focused on establishing the reversibility and intramolecular nature of the 'stepping' dynamics on model systems, demonstrating that the small-molecule fragment is randomly exchanged between adjacent amines on short (up to three or four repeat units) oligoethyleneimine tracks. Here we describe the extension of the Michael-retro-Michael walker concept to long (up to nine foothold) tracks and investigate the effect of acid and base on migration. Moreover, we show that under basic conditions a naphthylmethylamine foothold introduced at one end of the oligoethyleneimine track acts as a thermodynamic sink for the walker. Although the steps taken on the internal regions of the track proceed at the same rate in either direction, the rate that the walker departs from the naphthylmethylamine site is significantly slower than from the other footholds meaning that the walker distribution is biased towards this site generating net directional transport from one end of the track to the other even on long (up to nine-foothold) tracks. The α-methylene-4-nitrostyrene walker migrates from one end of a nine-foothold track to the other under dynamics that correspond well to the theoretical description of a one dimensional random walk of a Brownian particle.[8]

RESULTS AND DISCUSSION

Influence of acid and base on Michael and retro-Michael reactions of α-methylene-4-nitrostyrene on a diethylenetriamine track. We previously investigated the migration of α-methylene-4-nitrostyrene walker unit between adjacent amine groups of short oligoethyleneimine tracks under neutral conditions. To probe the effect of acid and base on these reactions a three-foothold walker-track conjugate **5**-*1* was synthesized as the *tris*-trifluoroacetic acid salt (Scheme 1). Boc-protected diethylenetriamine **1** was desymmetrized through reductive amination with 1-naphthaldehyde (Scheme 1 a,b), followed by a sequence of Boc-protection-deprotection reactions (Scheme 1 c-e) to yield free primary amine **2**, which after reductive amination

with 3-phenylpropionaldehyde (Scheme 1 f,g) afforded track **3** featuring a single site for walker attachment. The α-methylene-4-nitrostyrene walker unit **4** was subsequently introduced exclusively at foothold 1 (Scheme 1 h). Removal of the Boc group gave compound **5**-*1* as the *tris*-trifluoroacetic acid salt. With all of the amine groups of the track protonated, the α-methylene-4-nitrostyrene group does not migrate away from its original position.

Scheme 1. Synthesis of walker-track conjugate 5-*1*·3[CF_3CO_2H][a].

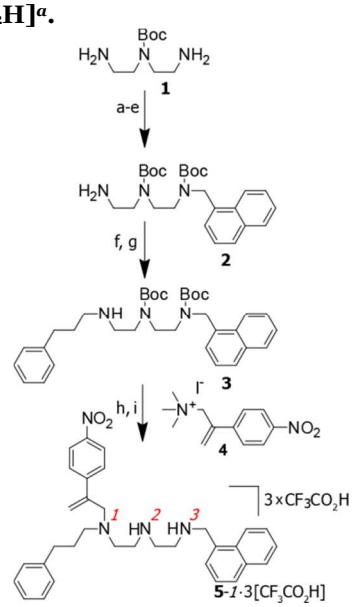

[a] Reaction conditions: a) 1-naphthaldehyde, EtOH, RT, 16 h; b) $NaBH_4$, RT, 3 h, 34% (two steps); c) CF_3CO_2Et, CH_2Cl_2, 0 °C→RT, 16 h; d) Boc_2O, Et_3N, RT, 12 h; e) NaOH, MeOH/H_2O, RT, 5 h, 92% (three steps); f) 3-phenylpropionaldehyde, EtOH, RT, 16 h; g) $NaBH_4$, RT, 3 h, 27%, (two steps); h) **4**, MeOH, ^{i}Pr$_2$NEt, 50 °C, 24 h, 54%; i) CF_3CO_2H, CH_2Cl_2, RT, 3 h, quant.

Walker migration on a diethylenetriamine track in the presence of one equiv. excess base. Treatment of **5**-*1*·3[CF_3CO_2H] in DMSO-d_6 (20 mM, 298 K) with four equiv. of diisopropylethylamine (^{i}Pr$_2$NEt), i.e. one molar excess of base, led to spontaneous migration of the α-methylene-4-nitrostyrene unit along the track (Figures 1 and 2). The reaction was monitored by ^{1}H NMR spectroscopy (Figure 2). Under these conditions the initial migration from foothold 1 to foothold 2 is fast, with more than half of the walkers having left foothold 1 after 4 h (Figures 1 and 2). The steady-state is reached after 24-48 h, with 67±3% of walkers ultimately located at the naphthylmethylamine foothold (foothold 3). The dynamics of the exchange of the positional isomers was simulated using the SimFit program[9] (Figure 1b; see Supporting Information for details).

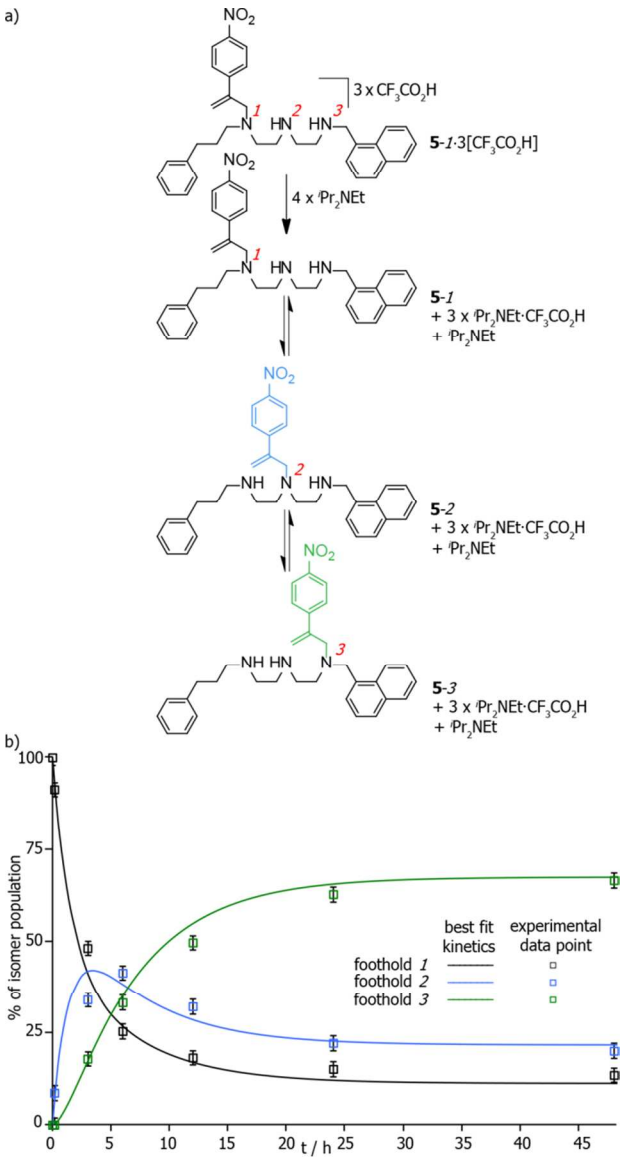

Figure 1. a) Intramolecular migration of the α-methylene-4-nitrostyrene unit of **5**-*1*·3[CF_3CO_2H] in the presence of four equiv. of ^{i}Pr$_2$NEt. b) Population of isomers (^{1}H NMR integration; see Figure 2). After 48 h, 67±3% of walkers are positioned on foothold 3 of the track (isomer **5**-*3*). Lines show the best fit of the experimental data to the kinetics of exchange between **5**-*1*, **5**-*2* and **5**-*3* using SimFit[9] (see Supporting Information for details). Error bars are indicative of the error associated with ^{1}H NMR integration using equivalent protons in each positional isomer.

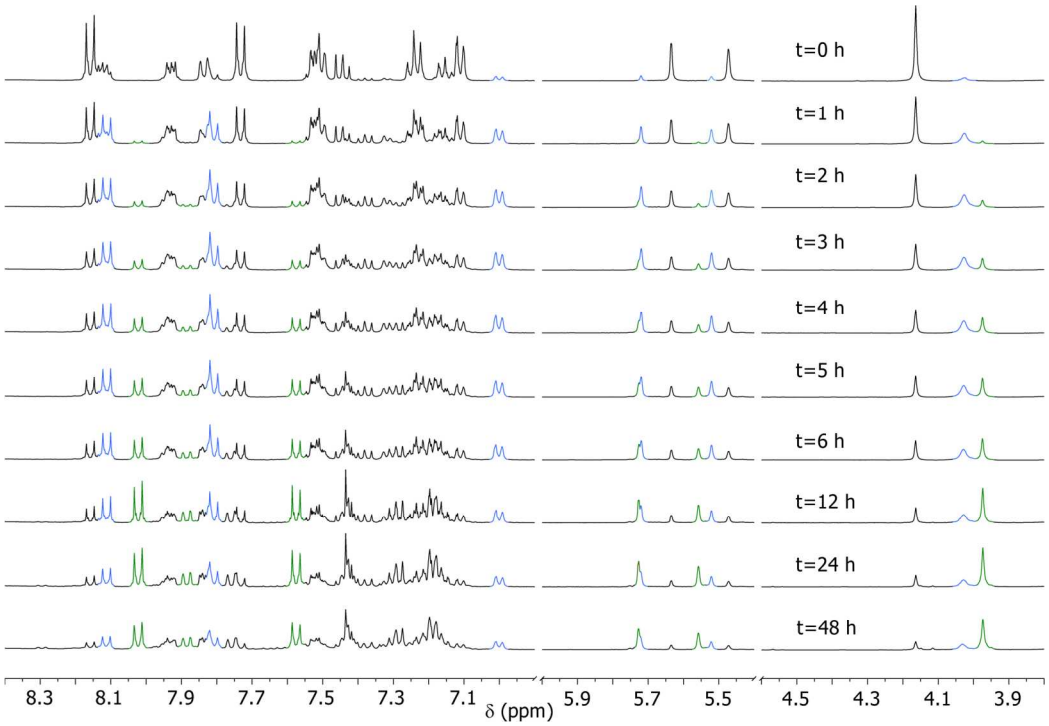

Figure 2. Partial ^{1}H NMR spectra (400 MHz, 20 mM, DMSO-d_6, 298 K) of **5**-*1*•3[CF_3CO_2H] + 4 equiv. of ^{i}Pr$_2$NEt, showing the interconversion of **5**-*1* (black resonances), **5**-*2* (blue resonances) and **5**-*3* (green resonances) over 48 h.

Walker migration on a diethylenetriamine track under neutral conditions. Treatment of **5**-*1*·3[CF_3CO_2H] in DMSO-d_6 (20 mM, 298 K) with three equiv. of ^{i}Pr$_2$NEt, i.e. just sufficient to deprotonate all of the ammonium groups of the track, also led to spontaneous migration of the α-methylene-4-nitrostyrene unit along the track (Figure 3). Initial migration away from foothold 1 occurs at a similar rate to that in the presence of excess base, but at the steady-state footholds 2 and 3 are populated to a comparable extent (43±3% and 47±3%, respectively).

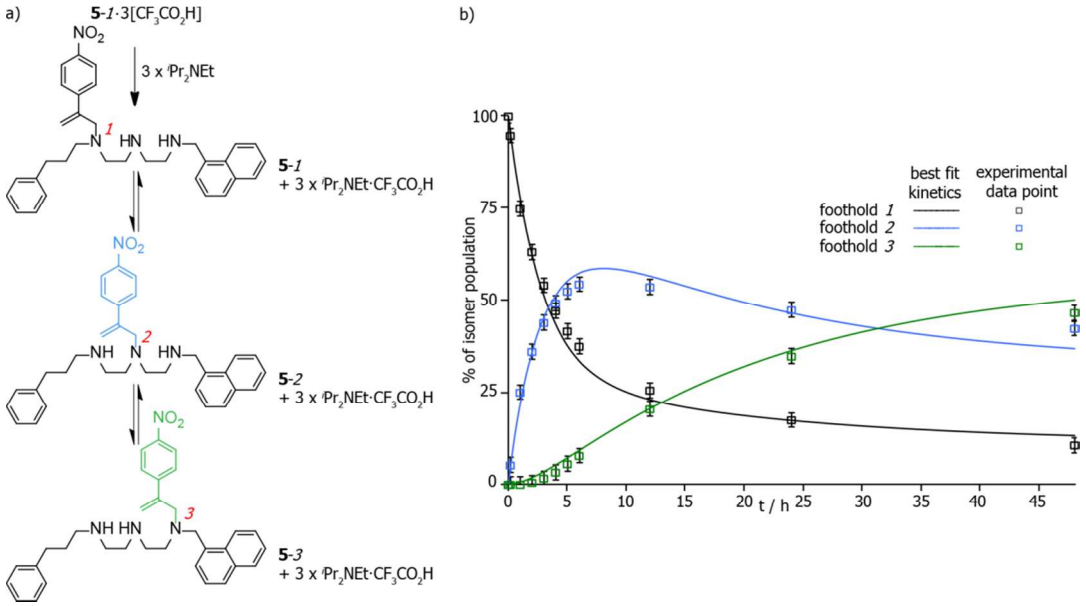

Figure 3. a) Intramolecular migration of the α-methylene-4-nitrostyrene unit of **5**-*1*·3[CF_3CO_2H] in the presence of three equiv. of ^{i}Pr$_2$NEt. b) Population of isomers (^{1}H NMR integration). After 48 h, 47±3% of walkers are positioned on foothold 3 of the track (isomer **5**-*3*) and 43±3% on position 2 (isomer **5**-*2*). Lines show the best fit of the experimental data to the kinetics of the exchange between **5**-*1*, **5**-*2* and **5**-*3* using SimFit[9] (see Supporting Information for details). Error bars are indicative of the error associated with ^{1}H NMR integration using equivalent protons in each positional isomer.

Walker migration on a diethylenetriamine track in the presence of one equiv. excess acid. When **5**-*1*·3[CF_3CO_2H] was treated with two equiv. of $^{i}Pr_2NEt$, i.e. only sufficient to deprotonate two of the three ammonium groups of the track, the dynamic behavior of the walker was very different to that under neutral or basic conditions (Figure 4). The kinetics of the initial migration from foothold 1 to foothold 2 is significantly slower: after 4 h only ~30% of walkers had left foothold 1. Furthermore, even after 48 h only a trace of walker units (<3%) could be detected on foothold 3 with the majority (88±3%) situated on foothold 2. This is presumably a result of the relative basicity of the three amine groups of the track, with the most basic naphthylmethylene secondary amine[10] remaining protonated and thus unavailable to take part in Michael reactions.

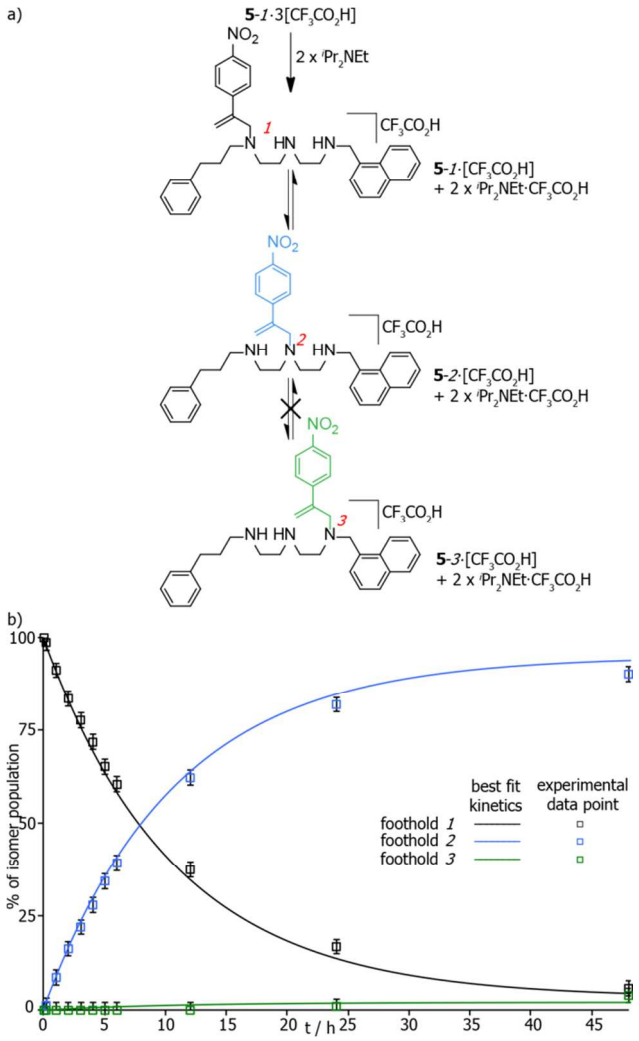

Figure 4. a) Intramolecular migration of the α-methylene-4-nitrostyrene unit of **5**-*1*·3[CF_3CO_2H] in the presence of two equiv. of $^{i}Pr_2NEt$. b) Population of isomers (^{1}H NMR integration). After 48 h, 90±3% of walkers are positioned on foothold 2 of the track (isomer **5**-*2*). Lines show the best fit of the experimental data to the kinetics of the exchange between **5**-*1*, **5**-*2* and **5**-*3* using SimFit[9] (see Supporting Information for details). Error bars are indicative of the error associated with ^{1}H NMR integration using equivalent protons in each positional isomer.

Walker migration on a tetraethylenepentamine track.
Given the ability of the naphthylmethylamine foothold to act as a thermodynamic sink for the α-methylene-4-nitrostyrene walker on a three-foothold track in the presence of excess base (Figure 1), we investigated the walker's behavior on longer, five- and nine-, foothold tracks (Figures 6-9). A walker-five-foothold-track conjugate was prepared as the penta-trifluoroacetic acid salt, **6**-*1*[5×CF_3CO_2H], according to Scheme 2 (see Supporting Information). Upon treatment with six equiv. $^{i}Pr_2NEt$ in DMSO-d_6 (20 mM, 298 K) the walker processively[11] migrated along the track. ^{1}H NMR signals diagnostic for each positional isomer could be identified (Figure 5b) and thus the population of each positional isomer monitored over time (Figure 6). After 48 h the steady-state had been reached with 46±3% of the walkers having taken a net four steps directionally along the track to be positioned on the naphthylmethylamine foothold.

Scheme 2. Synthesis of a walker-track conjugate 6-*1*.[a]

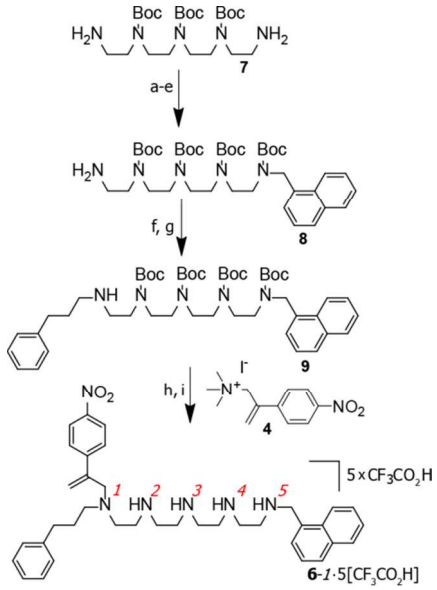

[a] Reaction conditions: a) 1-naphtaldehyde, EtOH, RT, 16 h; b) $NaBH_4$, RT, 3 h, 34% (two steps) c) CF_3CO_2Et, CH_2Cl_2, 0 °C→RT, 16 h; d) Boc_2O, Et_3N, RT, 12 h; e) NaOH, MeOH/H_2O, RT, 5 h, 74% (three steps); f) 3- phenylpropionaldehyde, EtOH, RT, 16 h; g) $NaBH_4$, RT, 3 h, 35%, (two steps); h) **4**, MeOH, $^{i}Pr_2NEt$, 50 °C, 24 h, 49%; i) CF_3CO_2H, CH_2Cl_2, RT, 3 h, quant.

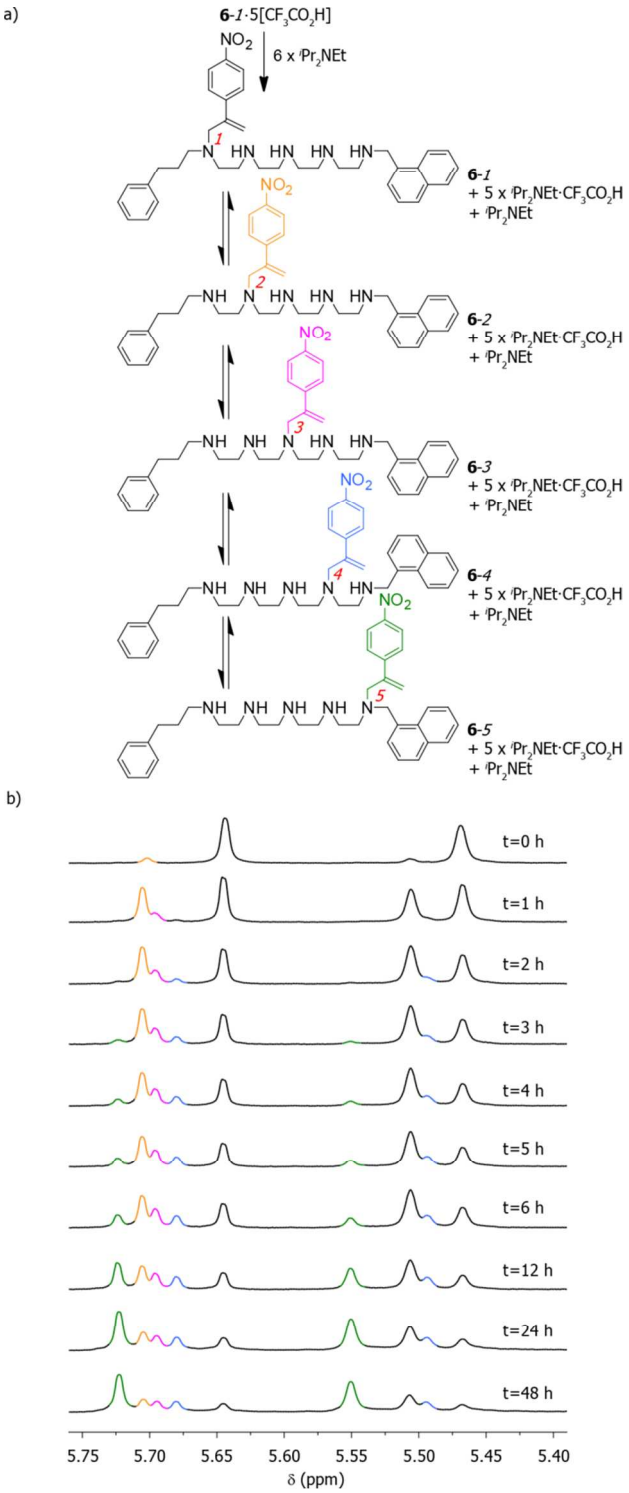

Figure 5. a) Walking of **6**-*1*•5[CF_3CO_2H] in the presence of 6 equiv. ^{i}Pr$_2$NEt. b) Partial ^{1}H NMR spectra of of **6**-*1*•5[CF_3CO_2H] + 6 equiv. ^{i}Pr$_2$NEt (400 MHz, 20 mM, DMSO-d_6, 298 K) showing the successive formation of the five positional isomers (the colors of the signals corresponds to the structures shown in part (a)).

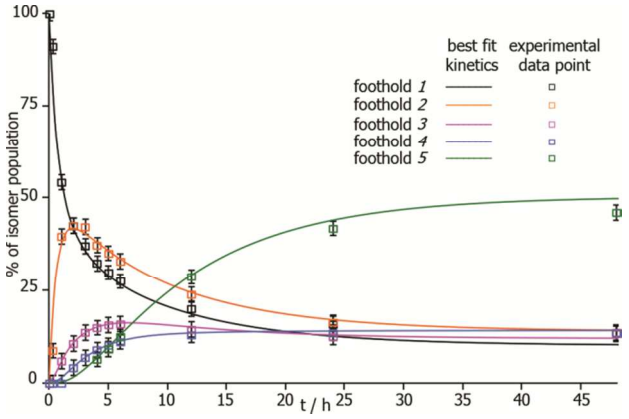

Figure 6. Intramolecular migration of the α-methylene-4-nitrostyrene unit of **6**-*1*•5[CF_3CO_2H] in the presence of six equiv. of ^{i}Pr$_2$NEt. Population of isomers (^{1}H NMR integration). After 48 h, 46±3% of walkers are positioned on foothold 5 of the track (isomer **6**-*5*). Lines show the best fit of the experimental data to the kinetics of the exchange between **6**-*1*, **6**-*2*, **6**-*3*, **6**-*4* and **6**-*5* using SimFit[9] (see Supporting Information for details). Error bars are indicative of the error associated with ^{1}H NMR integration using equivalent protons in each positional isomer.

Walker migration on an octaethylenenonamine track.

A nine-foothold walker-track conjugate **10** was synthesized starting from commercially available 2-(2-aminoethylamino)ethanol (**11**), which was subjected to a sequence of protection-deprotection reactions (Scheme 3 a-c) to give **12**. Reductive amination of **12** with 3-phenylpropionaldehyde afforded **13** (Scheme 3 d,e). Subsequent Cbz protection and oxidation using Dess-Martin periodinane (DMP) yielded the aldehyde building block **14** (Scheme 3 f,g). The second half of the track was synthesized, starting from the reductive amination of **11** with 1-naphthaldehyde (Scheme 3 h,i) followed by selective Boc protection to give **15** (Scheme 3 j). The primary alcohol was oxidized to aldehyde **16** (Scheme 3 k) and then subjected to reductive amination with commercially available tetraethylenepentaamine (Scheme 3 l,m). The primary amine was protected as the trifluoroacetate, followed by quadruple Boc protection of the remaining secondary amines to give **17** (Scheme 3 n, o). Deprotection of the primary amine (Scheme 3 p) afforded **18** and reductive amination with **14** furnished the nine-foothold track with one 'free' secondary amine (Scheme 3 q,r), which was subsequently Boc-protected to give **19** (Scheme 3 s). The Cbz group was reductively cleaved (Scheme 3 t), and the walker attached and the protecting groups removed (Scheme 3 u,v) to give **10**-*1*•9[CF_3CO_2H] (see Supporting Information for experimental procedures and characterization data).

In order to investigate the processive[11] walking process on the nine-foothold track, **10**-*1*•9[CF_3CO_2H] was treated with ten equiv. ^{i}Pr$_2$NEt in DMSO-d_6 (10 mM, 298 K) and the reaction monitored by ^{1}H NMR spectroscopy (Figure 7 and 8). Although the assignment of each of the nine positional isomers is not possible, we

were able to quantify the amount of walkers on each of the terminal footholds (i.e. **10**-*1* and **10**-*9*) and compare each of those to the number sited on the internal footholds (i.e. **10**-*2*–**10**-*8*). After 15 h, signals corresponding to **10**-*9* (the walker molecule reaching the last foothold of the track) were apparent (green resonances, Fig. 7 and 8b) and gradually increased in intensity until after 90 h (Fig. 8b) 19±3% of the walker units were present on the last foothold.

Scheme 3. Synthesis of a walker-track conjugate 7-*1*.[a]

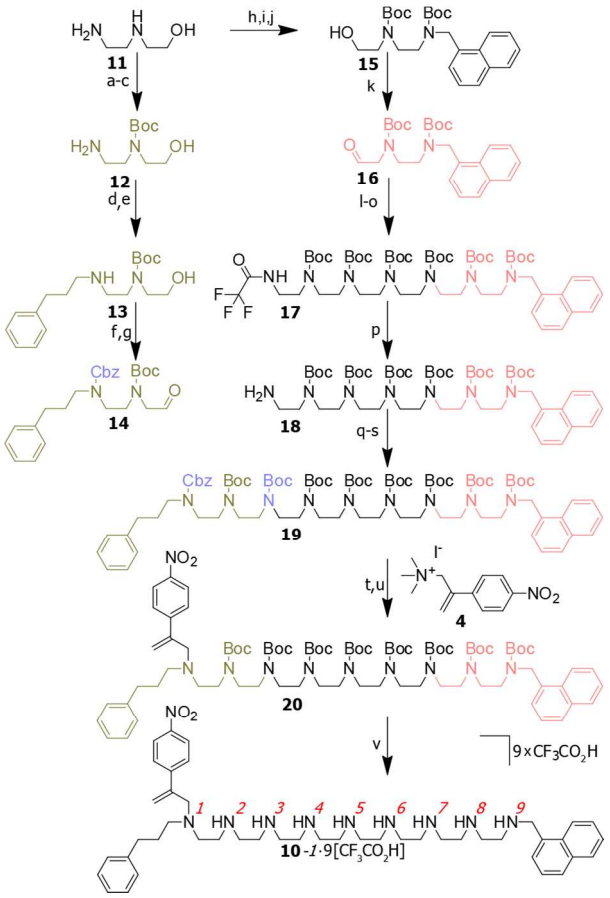

[a] Reaction conditions: a) CF_3CO_2Et, CH_2Cl_2, 0 °C→RT, 3 h; b) Boc_2O, Et_3N, RT, 12 h, 60% (two steps); c) NaOH, $MeOH/H_2O$, RT, 5 h, 73%; d) 3-phenylpropionaldehyde, EtOH, RT, 16 h; e) $NaBH_4$, RT, 3 h, 36% (two steps); f) CbzCl, Et_3N, CH_2Cl_2, RT, 4 h, 68%; g) DMP, CH_2Cl_2, RT, 12 h, 81%, h) 1-naphthaldehyde, EtOH, RT, 16 h, i) $NaBH_4$, RT, 3 h,; j) Boc_2O, MeCN, RT, 12 h, 64% (three steps); k) DMP, CH_2Cl_2, RT, 12 h, 68%; l) tetraethylenepentaamine, EtOH, RT, 16 h; m) $NaBH_4$, RT, 3 h; n) CF_3CO_2Et, CH_2Cl_2, 0 °C→RT, 16 h; o) Boc_2O, Et_3N, RT, 12 h, p) NaOH, $MeOH/H_2O$, RT, 5 h, 20% (five steps); q) **14**, EtOH, RT, 16 h; r) $NaBH_4$, RT, 3 h; s) Boc_2O, Et_3N, RT, 12 h, 30% (three steps); t) Pd/C, H_2, THF, RT, 20 h, 50%; u) **4**, MeOH, $^{i}Pr_2NEt$, 50 °C, 48 h, 50%; v) CF_3CO_2H, CH_2Cl_2, RT, 7 h, quant.

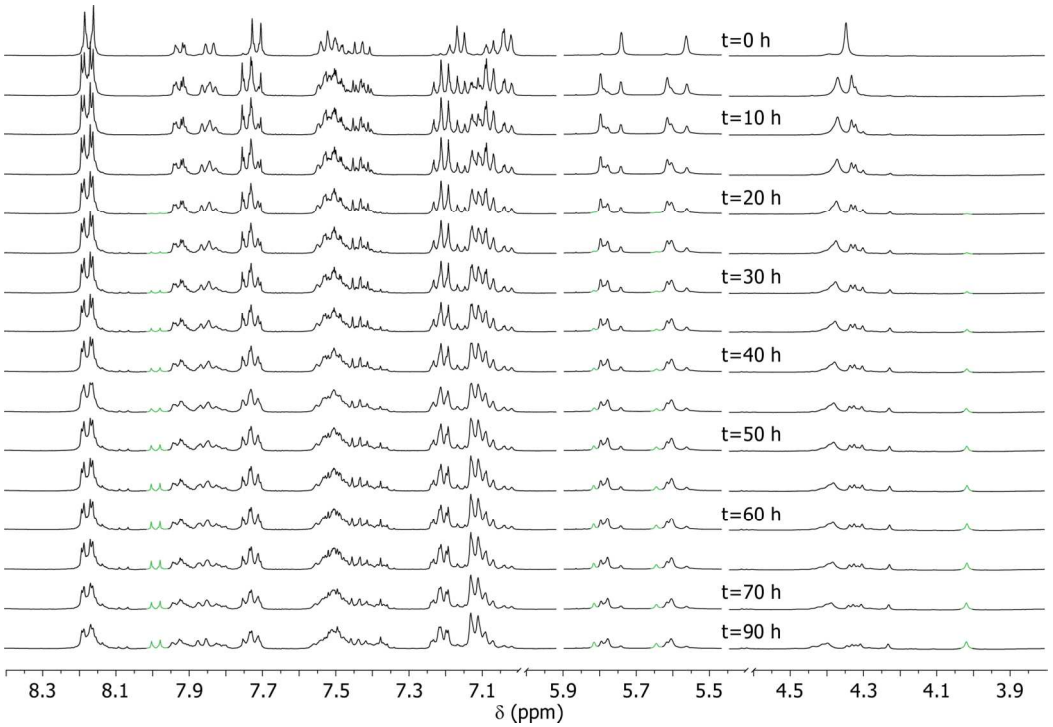

Figure 7. Partial ^{1}H NMR spectra (400 MHz, 10 mM, DMSO-d_6, 298 K) monitoring the intramolecular exchange of **10**-*1*•9[CF_3CO_2H] (black resonances at t = 0 h) in the presence of 10 equiv. ^{i}Pr$_2$NEt, showing the disappearance of **10**-*1* and formation of positional isomers **10**-*2*–**10**-*8*. Resonances corresponding to **10**-*9* are shown in green.

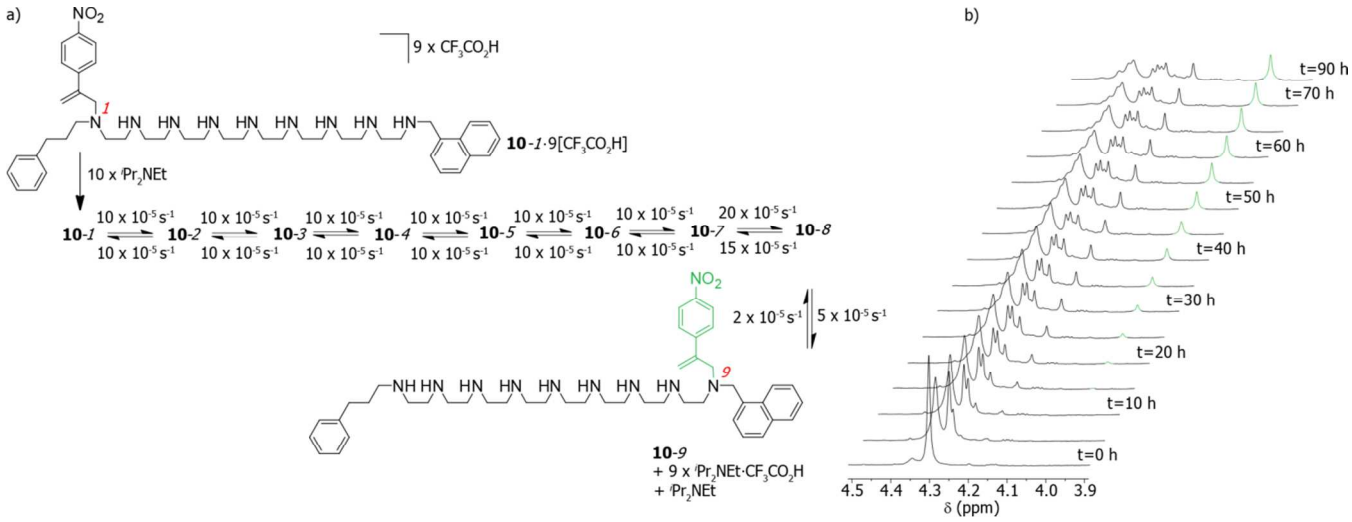

Figure 8. a) Walking of **10**-*1*•9[CF_3CO_2H] in the presence of 10 equiv. ^{i}Pr$_2$NEt. b) Partial ^{1}H NMR spectra (400 MHz, 10 mM, DMSO-d_6, 298 K) of the reaction mixture over time. After 90 h of exchange, 19±3% of walkers are positioned on the 9th foothold of the track (**10**-*9*). Green resonances correspond to **10**-*9*. Rate constants obtained from the fitting of the experimental values to a kinetic model using SimFit[9] (see Figure 9 and Supporting Information for details).

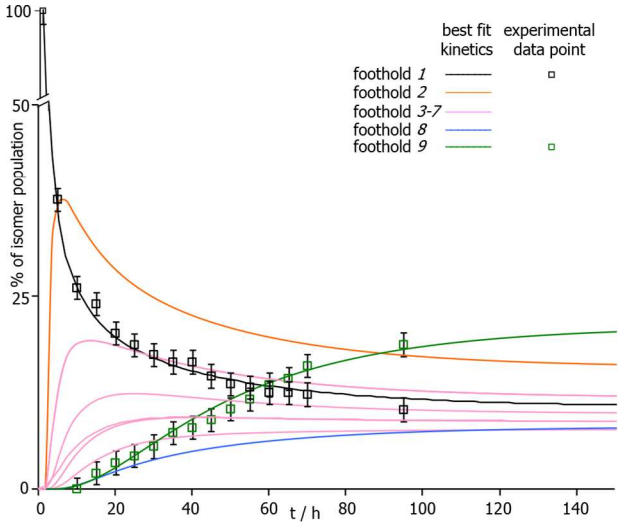

Figure 9. Intramolecular migration of the α-methylene-4-nitrostyrene unit of **10**-*1*•9[CF_3CO_2H] in the presence of ten equiv. of $^{i}Pr_2NEt$. Population of isomers (^{1}H NMR integration). After 90 h, 19±3% of walkers are positioned on foothold *9* of the track (isomer **10**-*9*). Lines show the best fit of the experimental data to the kinetics of the exchange between **10**-*1*, **10**-*2*, **10**-*3*, **10**-*4*, **10**-*5*, **10**-*6*, **10**-*7*, **10**-*8* and **10**-*9* using SimFit[9] (see Supporting Information for details). Error bars are indicative of the error associated with ^{1}H NMR integration using equivalent protons in each positional isomer. Error of fit ±10 %.

Intramolecular migration as a one dimensional random walk towards a thermodynamic sink. Figure 10 shows the rate of diffusion of the walker along the various length tracks (compounds **5**, **6** and **10**) and confirms that the net distance varies as the square root of the elapsed time.[12] The rate constants for the interconversion of adjacent positional isomers (e.g. between **10**-*3* and **10**-*2* and **10**-*4*) suggested by SimFit are similar for almost all exchanges between amine groups on the internal positions of the track (Figure 8a). Although the influence of the naphthylmethylamine group is diminished in the presence of eight alternative amine footholds there is still a significant bias for the site, resulting in net directional walking of the α-methylene-4-nitrostyrene unit along the track. Interesting, however, the preference for the walker to spend more time towards one end of the track appears to be a result of kinetics associated with foothold 8, the amine adjacent to the naphthylamine group, as well as the naphthylamine foothold itself. Due to the track's architecture, the walker unit can only take forward and backward steps of equal distance and therefore the migration is well described as a one dimensional random walk towards a modest thermodynamic sink.[8,12]

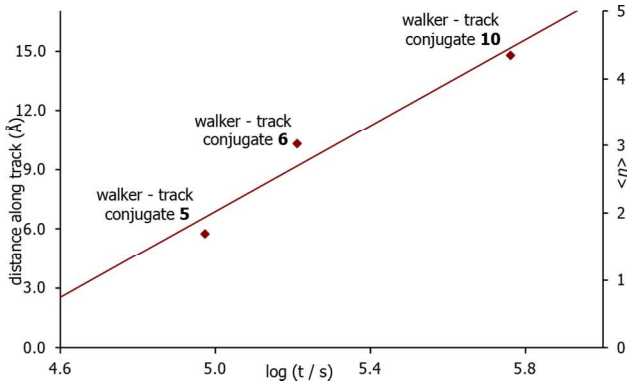

Figure 10. Calculated net displacement (distance along the vector of the track, Å, left-hand axis; average number of footholds travelled, <*n*>, right-hand axis) of α-methylene-4-nitrostyrene walker as a function of time.

CONCLUSIONS

We have shown that the migration of α-methylene-4-nitrostyrene along oligoethyleneimine tracks by Michael-retro-Michael reactions is hindered in the presence of acid but occurs readily under neutral and basic conditions. The intramolecular transfer from amine group to adjacent amine group is not limited to short model systems but also occurs on extended tracks up to nine footholds long. Moreover, under basic conditions a naphthylmethylamine foothold can act as a thermodynamic sink, leading to net directional migration of the walker even in the presence of eight other amine footholds. Directional movement along tracks over significant distances may enable synthetic small-molecule systems to transport cargoes and perform other useful tasks[13] at the molecular level.

ASSOCIATED CONTENT

Experimental procedures, synthesis and characterization data, processivity experiments, kinetic measurements and rate constant determinations. This material is available free of charge via the internet at http://pubs.acs.org.

AUTHOR INFORMATION

Corresponding Author

David.Leigh@manchester.ac.uk

Funding Sources

We thank the EPSRC National Mass Spectrometry Service Centre (Swansea, UK) for high resolution mass spectrometry. This research was funded by the ERC. A.G.C. thanks the Fundación Ramón Areces (Spain) for a postdoctoral fellowship.

Notes

The authors declare no competing financial interest.

ACKNOWLEDGMENT

The authors thank Prof Dr G. von Kiedrowski for the use of the program SimFit, Dr C. C. Robertson for useful discussions, and Dr B. Lewandowski and M. R. Wilson for their assistance in acquiring ^{1}H NMR data for the kinetic experiments.

REFERENCES

(1) (a) *Molecular Motors* (Ed.: Schliwa, M.), Wiley-VCH, Weinheim, 2003. (b) Vale, R. D. *Cell* **2003**, *112*, 467–480. (c) Hirokawa, N. *Science* **1998**, *279*, 519–526. (d) Vale, R. D.; Milligan, R. A. *Science* **2000**, *288*, 88–95. (e) Schliwa, M.; Woehlke, G. *Nature* **2003**, *422*, 759–765. (f) Mallik, R.; Gross, S. P. *Curr. Biol.* **2004**, *14*, 971–982. (g) Amos, L. A. *Cell. Mol. Life Sci.* **2008**, *65*, 509–515.

(2) (a) von Delius, M.; Leigh, D. A. *Chem. Soc. Rev.* **2011**, *40*, 3656–3676. (b) Muscat, R. A.; Bath, J.; Turberfield, A. J. *Nano Lett.* **2011**, *11*, 982–987. (c) Wickham, S. F.; Endo, M.; Katsuda, Y.; Hidaka, K.; Bath, J.; Sugiyama, H.; Turberfield, A. J. *Nat. Nanotechnol.* **2011**, *6*, 166–169. (d) Ando, T. *Nanotechnol.* **2012**, *23*, 062001. (e) You, M.; Chen, Y.; Zhang, X.; Liu, H.; Wang, R.; Wang, K.; Williams, K. R.; Tan,W. *Angew. Chem. Int. Ed* **2012**, *51*, 2457–2460. (f) You, M.; Huang, F.; Chen, Z.; Wang, R.; Tan, W. *ACS Nano* **2012**, *6*, 7935–7941. For diffusion driven walking events, see: (g) Kwon, K.- Y.; Wong, K. L.; Pawin, G.; Bartels, L.; Stolbov, S.; Rahman, T. S. *Phys. Rev. Lett.* **2005**, *95*, 166101. (h) Wong, K. L.; Pawin, G.; Wong, K.-Y.; Lin, X.; Jiao, T.; Solanki, U.; Fawcett, R. H. J.; Bartels, L.; Stolbov, S.; Rahman, T. S. *Science* **2007**, *315*, 1391–1393. (i) Cheng, Z.; Chu, E. S.; Sun, D.; Kim, D.; Luo, M.; Pawin, G.; Wong, K. L.; Carp, R.; Marsella, M.; Bartels, L. *J. Am. Chem. Soc.* **2010**, *132*, 13578–13581. (j) Perl, A.; Gomez-Casado, A.; Dam, H. H.; Jonkheijm, P.; Reinhoudt, D. N.; Huskens, J. *Nat. Chem.* **2011**, *3*, 317–322.

(3) (a) von Delius, M.; Geertsema, E. M.; Leigh, D. A. *Nat. Chem.* **2010**, *2*, 96–99. (b) von Delius, M.; Geertsema, E. M.; Leigh, D. A.; Tang, D.-T. D. *J. Am. Chem. Soc.* **2010**, *132*, 16134–16145. (c) Barrell, M. J.; Campaña, A. G.; von Delius, M.; Geertsema, E. M.; Leigh, D. A. *Angew. Chem. Int. Ed.* **2011**, 50, 285–290.

(4) (a) Campaña, A. G.; Carlone, A.; Chen, K.; Dryden, D. T. F.; Leigh, D. A.; Lewandowska, U.; Mullen, K. M. *Angew. Chem. Int. Ed.* **2012**, *51*, 5480–5483. (b) Kovaříček, P.; Lehn, J.-M. *J. Am. Chem. Soc.* **2012**, *134*, 9446–9455. (c) Lehn, J.-M. *Angew. Chem. Int. Ed.* **2013**, *52*, 2836–2850.

(5) (a) Lehn, J.-M. *Chem. Eur. J.* **1999**, *5*, 2455–2463. (b) Rowan, S. J.; Cantrill, S. J.; Cousins, G. R. L.; Sanders, J. K. M.; Stoddart, J. F. *Angew. Chem. Int. Ed.* **2002**, *41*, 898–952. (c) Corbett, P. T.; Leclaire, J.; Vial, L.; West, K. R.; Wietor, J.-L.; Sanders, J. K. M.; Otto, S. *Chem. Rev.* **2006**, *106*, 3652–3711. (d) Lehn, J.-M. *Chem. Soc. Rev.* **2007**, *36*, 151–160. (e) Hunt, R. A. R.; Otto, S. *Chem. Commun.* **2011**, *47*, 847–858. (f) Cougnon, F. B. L.; Jenkins, N. A.; Pantoş, D. G.; Sanders, J. K. M. *Angew. Chem. Int. Ed.* **2012**, *51*, 1443–1447. (g) Ponnuswamy, N.; Cougnon, F. B. L.; Clough, J. M.; Pantoş, G. D.; Sanders, J. K. M. *Science* **2012**, *338*, 783–785.

(6) Belowich, M. E.; Stoddart, J. F. *Chem. Soc. Rev.* **2012**, *41*, 2003–2024.

(7) (a) Mitra, S.; Lawton, R. G. *J. Am. Chem. Soc.* **1979**, *101*, 3097–3110. (b) Brocchini, S. J.; Eberle, M.; Lawton, R. G. *J. Am. Chem. Soc.* **1988**, *110*, 5211–5212; (c) Liberatore, F. A.; Comeau, R. D.; McKearin, J. M.; Pearson, D. A.; Belonga, B. Q.; Brocchini, S. J.; Kath, J.; Phillips, T.; Oswell, K.; Lawton, R. G. *Bioconjugate Chem.* **1990**, *1*, 36–50; (d) del Rosario, R. B.; Brocchini, S. J.; Lawton, R. G.; Wahl, R. L.; Smith, R. *Bioconjugate Chem.* **1990**, *1*, 51–59; (e) del Rosario, R. B.; Baron, L. A.; Lawton, R. G.; Wahl, R. L. *Nucl. Med. Biol.* **1992**, *19*, 417–421.

(8) Weiss, G. H. *Aspects and applications of the random walk*, North Holland Press, **1994**.

(9) (a) Hayden, E. J.; von Kiedrowski, G.; Lehman, N. *Angew. Chem. Int. Ed.* **2008**, *47*, 8424–8428. (b) Stahl, I.; von Kiedrowski, G. *J. Am. Chem. Soc.* **2006**, *128*, 14014–14015. (c) Schöneborn, H.; Bülle, J.; von Kiedrowski, G. *ChemBioChem* **2001**, *2*, 922–927.

(10) (a) Albelda, M. T.; Aguilar, J.; Alves, S.; Aucejo, R.; Diaz, P.; Lodeiro, C.; Lima, J. C.; Garcia-Espana, E.; Pina, F.; Soriano, C. *Helv. Chim. Acta* **2003**, *86*, 3118–3135. (b) Del Piero, S.; Ghezzi, L.; Melchior, A.; Tine, M.R.; Tolazzi, M. *Helv. Chim. Acta* **2005**, *88*, 839–853.

(11) Processivity is the tendency of the molecular fragment (i.e. the walker) to remain attached to the track during operation, i.e. to migrate along a molecular scaffold without detaching or exchanging with other molecules in the bulk (ref 2a). We previously reported (ref 3a) that α-methylene-4-nitrostyrene takes on average 530 steps between adjacent amines on model (up to four repeat units) oligoethyleneimine tracks before detaching. Mass spectrometry was used to confirm high processivity during migration on the longer tracks used in this paper in the presence of excess base (see Supporting Information).

(12) Atkins, P. W.; *Physical Chemistry, 6th edition*. Oxford University Press. Oxford, **1998**.

(13) Lewandowski, B.; De Bo, G.; Ward, J. W.; Papmeyer, M.; Kuschel, S.; Aldegunde, M. J.; Gramlich, P. M. E.; Heckmann, D.; Goldup, S. M.; D'Souza, D. M.; Fernandes, A. E.; Leigh, D. A. *Science* **2013**, *339*, 189–193.

TOC Graphic